Durham University

Durham E-Theses

Studies on main group and transition metal compounds containing a sterically demanding, electron-withdrawing ligand

L.J. Sequeira

How to cite:

Sequeira, L.J. (1996) Studies on main group and transition metal compounds containing a sterically demanding, electron-withdrawing ligand. Doctoral thesis, Durham University.

Use policy

The full-text may be used and/or reproduced, and given to third parties in any format or medium, without prior permission or charge, for personal research or study, educational, or not-for-profit purposes provided that:

- a full bibliographic reference is made to the original source
- a https://etheses.durham.ac.uk/id/eprint/5396/ is made to the metadata record in Durham E-Theses
- the full-text is not changed in any way

The full-text must not be sold in any format or medium without the formal permission of the copyright holders.

Please consult the full Durham E-Theses policy for further details.

Academic Support Office, The Palatine Centre, Durham University, Stockton Road, Durham, DH1 3LE
e-mail: e-theses.admin@durham.ac.uk Tel: +44 0191 334 6107
https://etheses.durham.ac.uk

Studies on Main Group and Transition Metal Compounds Containing a Sterically Demanding, Electron-Withdrawing Ligand

by

L.J. Sequeira B.Sc.(Dunelm)

Graduate Society

A thesis submitted for the degree of Doctor of Philosophy

at the University of Durham.

April 1996

The copyright of this thesis rests with the author.
No quotation from it should be published without
his prior written consent and information derived
from it should be acknowledged.

4 JUL 1996

STATEMENT OF COPYRIGHT

The copyright of this thesis rests with the author. No quotation from it should be published without her prior written consent and information derived from it should be acknowledged.

DECLARATION

The work described in this thesis was carried out in the Department of Chemistry of the University of Durham between October 1992 and September 1995. All the work is my own, unless stated to the contrary, and it has not been submitted previously for a degree at this or any other University.

For my Family

Acknowledgements

I would like to thank my supervisors Prof. Vernon Gibson and Dr. Keith Dillon for the initial inspiration to undertake this thesis and for their constant support and encouragement during the three years.

I would also like to thank a number of people in Durham: Alan, Julia, Jarka, Lara, Chris Drury for rescuing me so often from disasters on the Bruker, Dave Hunter for all his help with the high pressure facilities and Ray and Gordon for inspired glassblowing and mending. I am also grateful to Prof. J.A.K. Howard and the crystallographers at Durham, Jing Wen Yao and Dr. A.S. Batsanov for structural determinations, and to Prof. W. Clegg and Dr. M.R.J Elsegood for the structural determinations carried out in Newcastle. Thanks also go to the Durham University Chemistry Department for funding.

I am greatly indebted to Prof. F.G.N. Cloke at Sussex University for letting me loose on his most prized possession, the MVS machine, to Dr P. Scott for his help with the voltammetry studies, and to everyone in Lab 9, especially Polly, David, Ralph, Kevin and Julie.

To all the people who have put up so uncomplainingly with the decibel level which seems to follow me wherever I go: Lab 19; Phil, Matt Jolly, Mike, Martyn, Brenda, Chris, Gaz, Brian and Matt Giles, and Lab 104; Penny, Lynn, Marky R, Patrick, Gavin, Hugh, Wendy and Brian Hall; I hope you are all enjoying the peace now. To all my housemates during the last three years: Reena, Helen, Martyn, Sarah P, Bev and Fiona, who all have first-hand experience of the strange landlord phenomenon which occurred whenever I moved into a house, I apologise.

Most importantly, I would like to thank my family for all their love and care, and Ed, who may always have been there with the fire extinguisher, but for whom there will always be a fire burning in my heart.

Abstract

Studies on Main Group and Transition Metal Compounds Containing a Sterically Demanding, Electron-Withdrawing Ligand

The studies described herein relate to the co-ordination chemistry of 1,3,5-tris(trifluoromethyl)benzene, Ar^FH. The unique combination of steric bulk and a highly electron-withdrawing nature found in the σ-bound Ar^F ligand has already been exploited to stabilise a variety of unusual main group compounds including the surprisingly air- and moisture-stable diphosphene $Ar^FP{=}PAr^F$. Other examples are discussed in the introductory chapter, as is the increasingly active area of diphosphene research.

Chapter 2 describes the synthesis and structural characterisation of six early σ-Ar^F transition metal complexes, $Mo(N^tBu)_2(Ar^F)_2$, $Cr(NAd)_2(Ar^F)_2$, $[Mo(NAr)_2(Ar^F)Cl{\cdot}LiCl(dme)]_2$, $V(Ar^F)_2Cl(thf)$, $V(Ar^F)_3$-O-$Li(thf)_3$ and $Cr(Ar^F)_2(PMe_3)_2$. The first five of these compounds exhibit the rare phenomenon of weak metal-fluorine interactions, which is discussed in terms of several structural factors such as tilting of the aryl ring towards the direction of the M···F interaction

The co-ordination chemistry of the diphosphenes $Ar^FP{=}PAr^F$, Ar*P=PAr* and $Ar^*P{=}PAr^F$ (Ar* = 2,4,6-$^tBuC_6H_3$) is reported in chapter 3. $Ar^FP{=}PAr^F$ is shown to displace olefins from a bis(imido)molybdenum centre to generate complexes such as $Mo(NR)_2(PMe_3)(\eta^2\text{-}Ar^FP{=}PAr^F)$ (R = ^tBu, 2,6-$^iPr_2C_6H_3$). The crystal structure of $Mo(N^tBu)_2(PMe)_3(\eta^2$-$Ar^FP{=}PAr^F)$ has been elucidated. Related investigations have focused on the co-ordination mode of the diphosphenes Ar*P=PAr* and $Ar^*P{=}PAr^F$ with $[Pt(PEt_3)Cl_2]_2$, and a variety of η^1-complexes has been spectroscopically observed.

The development of phosphorus based analogue of the industrially important olefin metathesis reaction is detailed in chapter 4. The reaction of $ArPCl_2$, [Ar = Ar^F, Ar* and 2,6-$(CF_3)_2$-C_6H_3 ($Ar^{F'}$)] with the halide abstractor $W(PMe_3)_6$ leads to the generation of ArP=PAr via a postulated [W]=PAr phosphinidene intermediate. The unsymmetrical diphosphene $Ar^FP{=}PAr^*$ has been synthesised analogously from a mixture of Ar^FPCl_2 and Ar^*PCl_2 with $W(PMe_3)_6$. When Ar is small (2,4,6-$^iPr_3C_6H_2$, 2,4,6-$Me_3C_6H_2$), $ArPCl_2$ reacts with $W(PMe_3)_6$ to give three-membered tricyclophosphanes, $[ArP]_3$.

π-bound complexes of the Ar^FH ligand have been synthesised *via* metal vapour synthesis experiments, carried out in collaboration with Prof. F.G.N. Cloke at Sussex University. Chapter 5 describes the preparation of the bis-arene complexes $M(\eta^6\text{-}Ar^FH)_2$ (M=Cr, V, Nb) and $Ru(\eta^6\text{-}Ar^FH)(\eta^4\text{-}Ar^FH)$.

Full experimental details and characterising data for chapters 2-5 are collected in chapter 6.

Leela Josephine Sequeira (April 1996)

Abbreviations

Ad	Adamantyl
Ar* (supermes)	2,4,6-tris(^{t}butyl)phenyl
Ar^F	2,4,6-tris(trifluoromethyl)phenyl
$Ar^{F'}$	2,6-bis(trifluoromethyl)phenyl
Cp	cyclopentadienyl ligand (C_5H_5)
Cp*	pentamethylcyclopentadienyl ligand (C_5Me_5)
CV	cyclic voltammetry
DBU	1,8-diazobicyclo[5,4,0]undec-7-ene
DME	1,2-dimethoxyethane
EPR	electron paramagnetic resonance
L	General 2-electron donor ligand
LUMO	lowest unoccupied molecular orbital
mes (mesityl)	2,4,6-trimethylphenyl
MVS	metal vapour synthesis
NAr	2,6-diisopropylarylimido
N_3N	$(Me_3SiN(CH_2)_2)_3N$).
NMR	nuclear magnetic resonance
NCE	calomel electrode, 1 molar KCl
SCE	calomel electrode, saturated KCl
THF	tetrahydrofuran
TMP	2,2,6,6-tetramethylpiperidenyl
trip	2,4,6-triisopropylphenyl
VdW	Van der Waals radius
R	General alkyl ligand

Contents Page

Chapter One

Introduction

1.1 Bulky and electron-withdrawing ligands

1.1.1 The chemistry of the Ar^F ligand

The 2,4,6-tris(trifluoromethyl)phenyl substituent, (Ar^F), is unique amongst all other sterically demanding ligands used so far in the stabilisation of low co-ordinate main group derivatives.[1,2] A combination of stabilising factors contribute to the unusual properties of Ar^F derivatives. Sterically, this ligand is not significantly more bulky than 2,4,6-trimethylphenyl (mesityl) and is certainly less bulky than 2,4,6-tri(^{t}butyl)phenyl (supermesityl, Ar*). In contrast to most other sterically demanding ligands, however, Ar^F is a strongly electron-withdrawing substituent, and therefore should be able to stabilise low oxidation states and consequently low co-ordination number complexes. Equally important is the potential of the *ortho*-CF_3 groups to form weak interactions with the main group atom, thus blocking possible co-ordination sites and hence reducing any tendency for the formation of high nuclearity species. This is witnessed by the unusually high stability often encountered in main group Ar^F derivatives.[3]

The discovery of Ar^FH dates back to 1947 when McBee and Leech described its preparation by chlorination of mesitylene followed by fluorination of the intermediate 1,3,5-tris(trichloromethyl)benzene.[4] This two-step synthetic route is somewhat laborious and the overall yield is only 49%. Today's synthesis of Ar^FH involves treatment of commercially available trimesic acid (benzene-1,3,5-tri-carboxylic acid) with excess sulfur tetrafluoride. SF_4 is a well established reagent for the conversion of -COOH functional groups into - CF_3 units. Initially described by Chambers *et al.*, the method was reported to afford a 33% yield of Ar^FH.[5] A major boost to Ar^F chemistry came from the discovery by Edelmann *et al.* that the yield could be increased dramatically by changing the reaction conditions.

Prolonged heating of trimesic acid with excess SF_4 in a Monel cylinder at 170°C for 48 hours routinely produced Ar^FH in 90-95% yield (equation 1.1).[6]

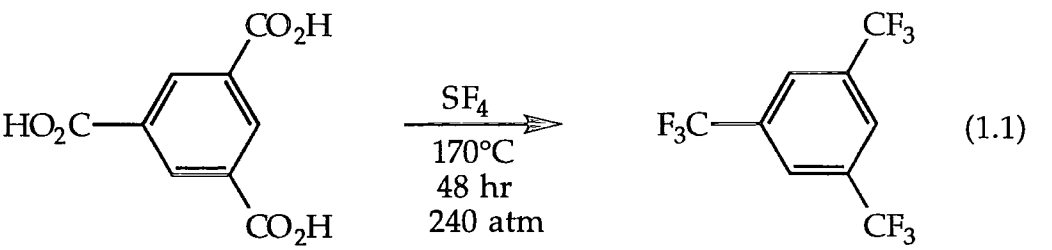

(1.1)

The ready availability of the parent fluorocarbon in large quantities has resulted in the rapid development of its derivative chemistry. Ar^FH can be lithiated by treatment with n-butyllithium in diethylether (equation 1.2).[5,6] The product, 2,4,6-tris(trifluoromethyl)phenyllithium (Ar^FLi), is the key precursor to other main group compounds containing Ar^F substituents.

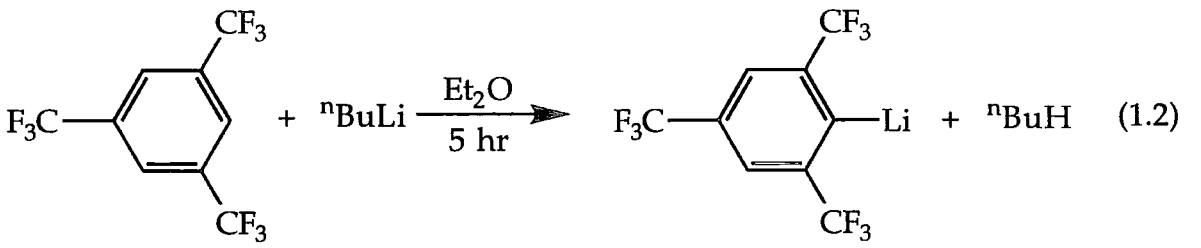

(1.2)

Solid Ar^FLi should only be handled with extreme care and in small quantities as occasional explosions have been reported for this material.[7] Exposure to excess alkyllithium reagents has also afforded violent decomposition.[7] In general Ar^FLi should therefore be prepared in solution and used *in situ* for subsequent reactions. Metathetical reaction with main group halides has allowed the synthesis of a variety of main group compounds of the Ar^F ligand (figure 1.1).[8-13]

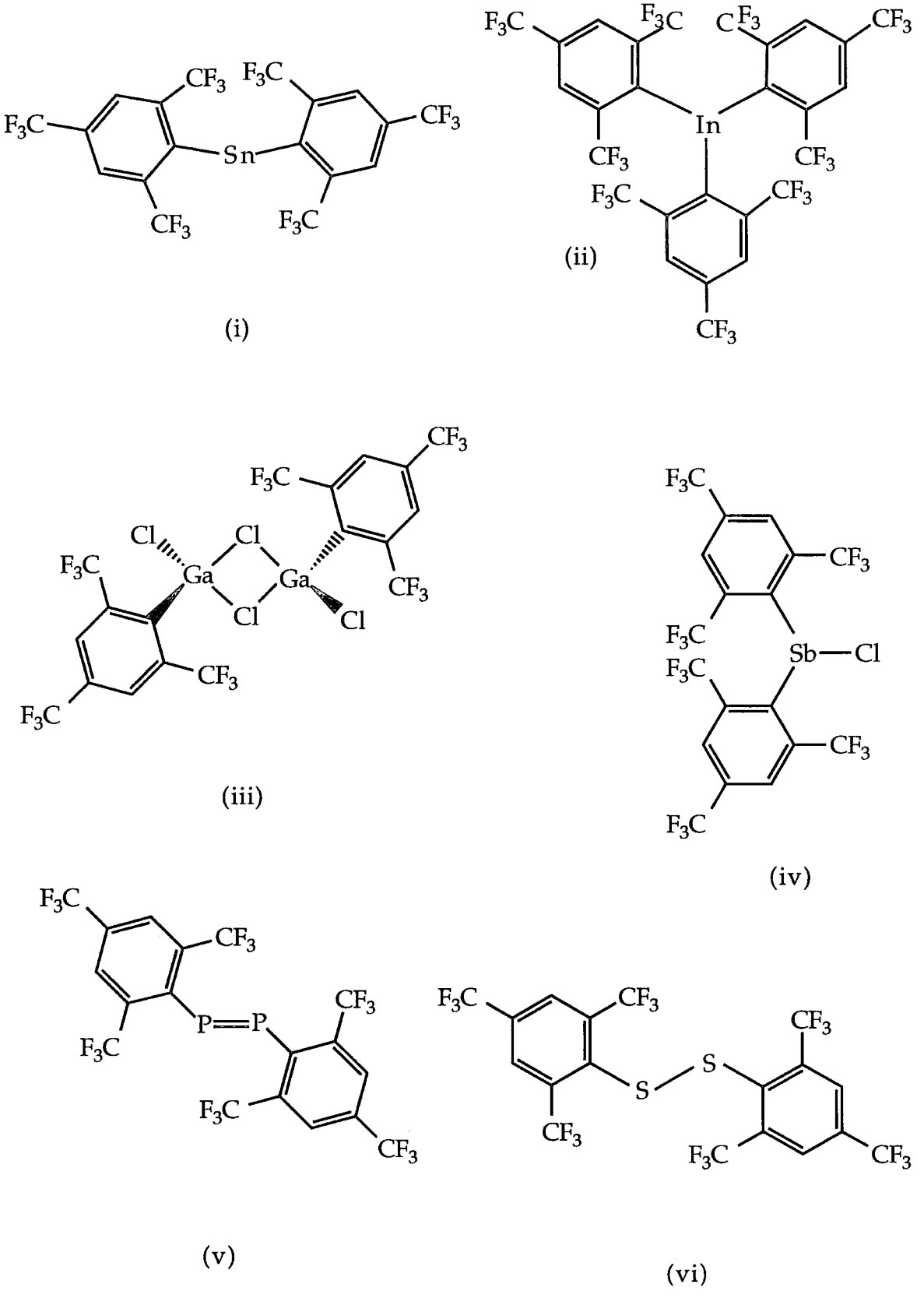

Figure 1.1: *Examples of Main Group Compounds bearing the σ-Bound Ar^F Ligand*

In most of the Ar^F main group compounds, structural analysis has shown that the M-C bond distance is longer than in the mesityl analogues, reflecting the larger steric demands of the Ar^F substituent. However, in some cases it could also be due to electrostatic ligand-ligand repulsions which appear to lead to a lengthening of bonds rather than a widening of angles. The lengthening could also, as in $Sn(Ar^F)_2$, be due to repulsive interactions between the electropositive tin atom and the *ipso* carbon, which has also been made electropositive due to the electron-withdrawing CF_3 groups.[8]

Interactions between the metalloid atom and the *ortho* fluorines have also been proposed as a stabilising factor in complexes containing this ligand.[8] Evidence for these interactions stems from M-F distances, which lie between the sum of the Van der Waals radii and the covalent distance for the M-F bond. These interactions can sometimes play a role in the conformational preference. For example, in $In(Ar^F)_3$ the twist angles range from 49-54°, whereas in $In(mes)_3$ one of the rings is almost perpendicular to the InC_3 plane. [9]

Evidence for the existence of M···F interactions can sometimes be provided by NMR spectroscopy. For instance, in $Sn(Ar^F)_2$ fluorine coupling can be observed in the ^{119}Sn NMR spectrum with the tin resonance split into 13 lines by coupling to the *ortho* fluorine atoms ($^1J_{Sn-F}$ 239.5Hz).[8] Furthermore, in toluene, temperature-dependent couplings of the fluorine nuclei with ^{117}Sn and ^{119}Sn were detected. These couplings, 239.5Hz (^{119}Sn) and 228.5Hz (^{117}Sn), increase linearly about 1.4Hz for every 10° as the sample is cooled. Such an effect is not observed in diethylether, however, presumably due to solvent co-ordination.

In $Bi(Ar^F)_3$ only one signal is seen for all of the fluorine atoms in the *ortho*-CF_3 groups at room temperature.[14] On cooling to -90° two signals are observed, indicating that rotation about the Bi-C bond is frozen out at this

temperature. At the coalescence temperature a barrier to rotation of 38.5 $kJmol^{-1}$ has been calculated.

The potential for forming weak M···F interactions means that the Ar^F group is also capable of inhibiting oligomerisation, as exemplified by its role in stabilising the first monomeric diaryl stannylene.[8] Although sterically the ligand lies between mesityl and triisopropylphenyl, neither of these ligands is capable of inhibiting such oligomerisation. This stabilising effect is therefore only partly due to steric shielding. The electron donating ability *via* the lone pairs at the fluorine atoms, albeit weak, is probably the most important factor inhibiting oligo- or polymerisation.

1.1.2 Fluorocarbon transition metal complexes

The co-ordination and activation of fluorocarbons by transition metal complexes is an area that has recently attracted the attention of both inorganic and organometallic chemists.[15-17] Substantial progress was made in the 1970's and 1980's concerning the co-ordination and activation of halocarbons, and this vast body of work has been the subject of several reviews.[17-19]

Fluorine is the most electronegative element and forms the strongest single bond with carbon. The replacement of hydrogen with fluorine results in a marked change in the physical and chemical properties of hydrocarbons. Fluorocarbons are more resistant to chemical attack, demonstrate high thermal stability[20-24] and are reluctant to co-ordinate to metal centres.[17,25]

However, when they can be prepared, fluorocarbon-transition metal complexes are extremely robust compared to hydrocarbon-transition metal complexes.[26-28] This improved thermal stability is thought to be due in part to the contraction of the metal orbitals by the electronegative fluorocarbon group, thus allowing greater overlap with the carbon atomic orbital.[29] This is aptly demonstrated by the metal-carbon bond distance which is usually

shorter in metal-fluorocarbon complexes than in the corresponding hydrocarbon-metal complexes.

1.1.3 Transition metal mesityl complexes

The hydrocarbon analogue of Ar^FH, the 2,4,6-trimethylphenyl ligand (mesityl) has a wide and varied chemistry. Both its main group and transition metal chemistry have been intensively explored. Many σ- and π-bound homoleptic complexes have been synthesised as well as many mixed ligand systems. A few of the more unusual compounds are briefly discussed below.

Tetramesityltitanium has been prepared by the reaction of titanium trichloride with four equivalents of mesityllithium, and subsequent oxidation of the product, $LiTi(mes)_4$, in air.[30] In contrast to the extreme air- and water-sensitivity of other Ti(IV) alkyls and aryls, $Ti(mes)_4$ is stable in air but is still light-sensitive. Indeed, the mesityl ligand has been employed to particular effect in the stabilisation of neutral homoleptic complexes of many transition metals.[31]

The π-bound mesityl complex $(CpV)_2mes$ was one of the first sandwich compounds with a bridging arene group [Figure 1.2(a)].[32] The formally unsaturated 26 electron complex violates the 30 and 34 electron rule[33] for triple decker complexes. $Cr_2(mes)_3$ has been synthesised using metal vapour techniques and was the first homoleptic triple decker complex containing only aryl ligands [Figure 1.2(b)].[34]

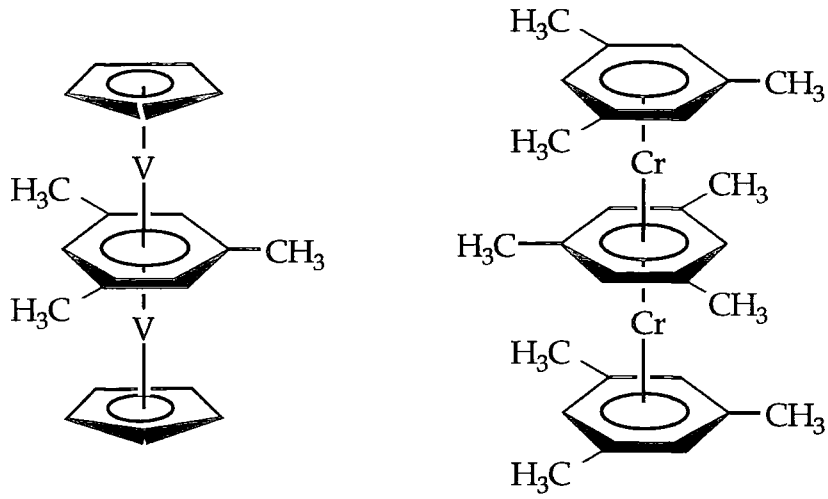

(a) (b)

Figure 1.2: *π-Bound Mesityl Complexes of Vanadium and Chromium*

The first σ-organochromium (VI) compound to be isolated, $Cr(N^tBu)_2(mes)_2$ was prepared from $Cr(N^tBu)_2(OSiMe_3)_2$ by Wilkinson and co-workers in 1986 (Figure 1.3).[35] The presence of the *o*-methyl groups on the phenyl rings undoubtedly contributes to the air and thermal stability of the compound. The analogous compounds could not be isolated when $Cr(N^tBu)_2(OSiMe_3)_2$ was treated with *o*-tolyl- or phenyl-magnesium bromide or when phenylzinc was used.

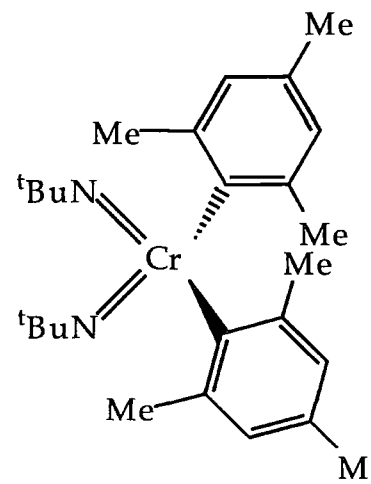

Figure 1.3: *$Cr(N^tBu)_2(mes)_2$*

In view of these results, it was anticipated that the transition metal chemistry of the Ar^F ligand would be worthy of study. Chapter 2 of this thesis discusses the synthesis of several σ-bound transition metal analogues and chapter 5 describes attempts to isolate π-bound Ar^FH complexes using metal vapour synthesis techniques. Furthermore, the co-ordination chemistry of the Ar^F substituted diphosphene, $Ar^FP{=}PAr^F$ [Figure1.1(v)] has also been investigated and is described in chapter 3.

1.2 Diphosphenes

1.2.1 Synthesis of symmetrical and unsymmetrical diphosphenes

According to the so-called "classical double bond rule",[36] stable molecules featuring multiple bonding should only be possible with elements of the first long period of the periodic table. This statement was rationalised by long bond distances and concomitantly inefficient π-bonding for the second and third periods. This rule must have arisen as a result of numerous thwarted attempts to prepare compounds with double bonds between elements of the second period such as two phosphorus or silicon atoms.

Early reports by Köhler and Michaelis (1877) claimed that the condensation reaction of $PhPCl_2$ and $PhPH_2$ gave the doubly bonded "Ph-P=P-Ph" (phosphabenzene).[37] However, eighty-one years later, Kuchen showed that this condensation product was a mixture of oligomers of phosphabenzene.[38] This was later confirmed by X-ray structure analysis of pentaphenylcyclopentaphosphane $[(PhP)_5]$ and hexaphenylcyclohexa phosphane $[(PhP)_6]$.[39,40]

In 1981, the first diphosphene was reported by Yoshifuji, who showed that the reduction of Ar^*PCl_2 with elemental magnesium in THF led to the isolation of the orange red crystalline diphosphene $Ar^*P{=}PAr^*$. (equation 1.3)[41]

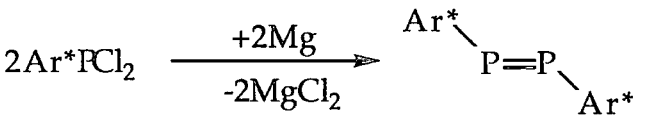

(1.3)

This kinetic stabilisation of reactive multiple bonds by very bulky substituents provided the breakthrough to molecules with P=P, P=As and As=As double bonds.

Due to the fact that carbon and phosphorus are diagonally related in the periodic table, it would not be unreasonable to expect some similarity in the formation of C=C, C=P and P=P double bonds. Therefore, by comparison with the hydrocarbon system, one should expect base-induced 1,2-hydrogen halide elimination from halogenated diphosphanes HRP-PR'X to give diphosphenes (equation 1.4).

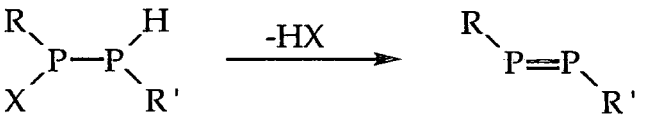

(1.4)

However, in contrast to the purely organic precursors, in phosphorus chemistry the respective educts for the elimination process, the halo-functionalised diphosphanes, are often not easily available as stable compounds, but have to be prepared by the *in situ* formation of the P-P single bond before the elimination.

In cases where the chlorophosphane is stable, Escudié has shown that dehydrohalogenation can be achieved by reaction with DBU. For example, using this method Ar*PHCl was transformed almost quantitatively into Ar*P=PAr* (equation 1.5).[42,43]

$$2Ar^*PHCl \xrightarrow[-2DBU.HCl]{2DBU} Ar^*P{=}PAr^* \qquad (1.5)$$

Chlorophosphanes are only sufficiently stable with bulky substituents. However, the easily available (trichlorogermyl)phosphanes, (RHP-$GeCl_3$), can be utilised as *in situ* reagents for these species. They are conveniently accessible by the treatment of a primary phosphane with $GeCl_4$, and the subsequent removal of $GeCl_2$ can be achieved with DBU.[44]

The strategy of intermolecular dehydrochlorination can also be used to access diphosphenes. For example, reaction of Ar^FPCl_2 with Ar^FPH_2 in the presence of DBU generated the extremely stable $Ar^FP{=}PAr^F$, which was isolated as a pale yellow solid.[12]

The conversion of organodihalophosphanes, such as Ar^*PCl_2, to diphosphenes has also been accomplished by a number of reducing agents, such as magnesium metal, sodium naphthalenide, organolithium species, bis(trimethylsilyl)mercury, divalent germanium and tin compounds or electron-rich olefins such as bisimidazolidine.[45]

The reaction of dichlorophosphane $(Me_3Si)_3CPCl_2$ with sodium naphthalenide afforded the first dialkyl diphosphene $(Me_3Si)_3CP{=}PC(SiMe_3)_3$.[44,46] When the sodium naphthalenide reduction was carried out with equimolar amounts of Ar^*PCl_2 and $(Me_3Si)_3CPCl_2$ the predominant formation of the symmetrical diphosphenes Ar*P=PAr* and $(Me_3Si)_3CP{=}PC(SiMe_3)_3$ was observed. In addition the unsymmetrical diphosphene $(Me_3Si)_3CP{=}PAr^*$ was produced in 20% yield (equation 1.6).[47]

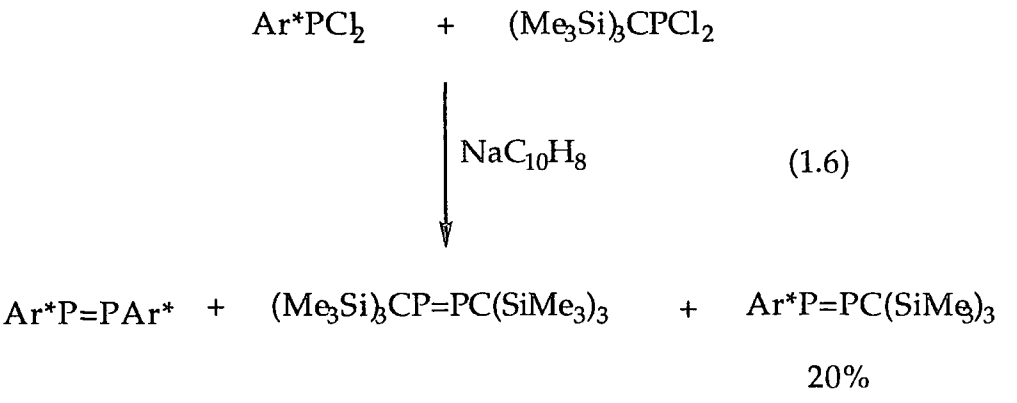

Reaction of Ar^*PH_2 with aryldichlorophosphanes in the presence of DBU provided a clean approach to symmetrical and unsymmetrical diphosphenes.[48] It was pointed out by Yoshifuji that although the unsymmetrical phenylsupermesityldiphosphene was observable by ^{31}P NMR, it could not be isolated without decomposition.[48]

When the DBU induced elimination was carried out with a mixture of $Ar^*PH\text{-}GeCl_3$ and $Ar^{F'}PH\text{-}GeCl_3$ a 60% yield of the unsymmetrical diphosphene was obtained [$Ar^{F'}$=2,6-bis(trifluoromethyl)phenyl]. The symmetrical diphosphenes $Ar^*P=PAr^*$ and $Ar^{F'}P=PAr^{F'}$ were also observed in 30% and 10% yield respectively (equation 1.7).[43]

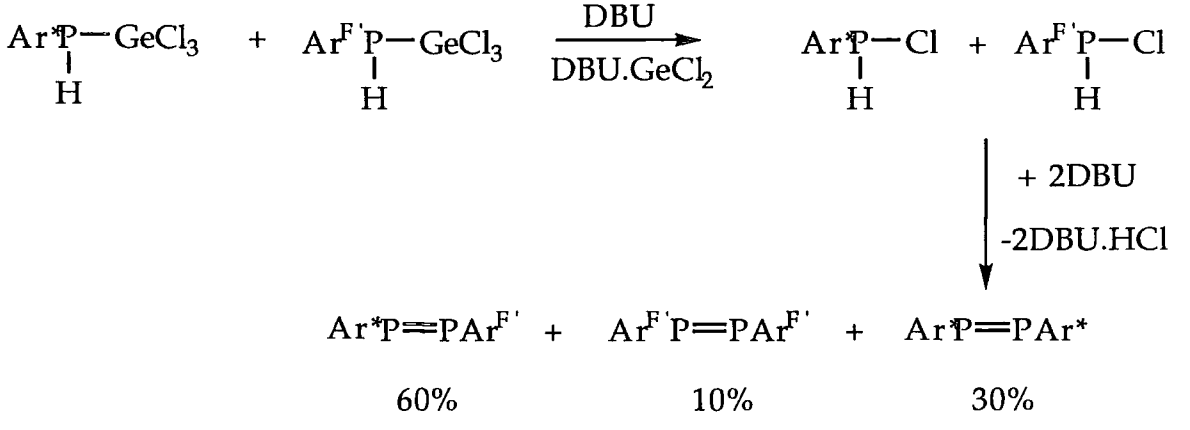

(equation 1.7)

Niecke has succeeded in the synthesis of a number of stable unsymmetrical diphosphenes containing substituents derived from nitrogen, phosphorus and oxygen atoms.[49] These compounds are of particular interest because amongst their number exist rare examples of (Z)-configuration diphosphenes (*vide infra*). Most of these diphosphenes are orange to red crystalline solids although some were isolated as orange to red oils.

1.2.2 Structure of diphosphenes

The molecular structures of several diphosphenes have been elucidated by X-ray crystallography. Their most notable feature is a short P=P double bond which typically ranges between 2.00 and 2.05Å.[45] Theoretical calculations on HP=PH predict a P=P bond length of 2.004Å,[50] which is in good agreement with the sum of the double bond covalent radii (2.00Å).[51] The P=P bond distances of diphosphenes relative to those in diphosphanes (ca. 2.22Å)[52] also merit some comment. Generally it is accepted that a double bond in main group compounds involves both a σ- and a π-bond component. The difference in length between double and single bonds is therefore due to π-overlap and also to a change in hybridisation in the σ-bonding orbitals. For C=C double bonds the shortening due to (p-p) π-overlap typically amounts to 70-75%, whereas 25-30% can be attributed to the change in hybridisation from sp^3-sp^2.[51] In an elegant study, Power *et al* showed that in the case of diphosphenes the bond shortening is about equally divided between (p-p) π-overlap and rehybridisation of the σ-orbitals.[53] Theoretical calculations on HP=PH propose a valence angle of 96.0°, well below the expected angle for an sp^2 hybridised phosphorus.[52] In reality, angles of up to 110° have been observed as a consequence of the steric bulk of the phosphorus substituents.[45]

In most cases the *E*-configuration of the ligands at the double bond is favoured. In all of these diphosphenes X-Ray analysis has shown that the

atoms directly attached to the P=P unit are located in approximately the same plane (XP-PY torsion angles range from 172.2° to 180.0°).[45] In *E*-diphosphenes with Ar* substituents the aryl rings are usually in an orthogonal orientation to the plane defined by the atoms X, P_1, P_2 and Y. The same holds for the diphosphene $(^iPr_2N)_2PP{=}PN(SiMe_2{}^tBu)_2$[49] and is in sharp contrast to $(^iPr_2N)_2P{=}PTMP$,[49] $Ar^*P{=}PN(^iPr)_2$[54] and Ar*P=PTMP[54] (TMP = 2,2,6,6-tetramethylpiperidenyl), where the lone pair at the nitrogen atom is in conjugation with the P=P double bond, thus establishing a 3-centre four-electron system, as is well known for the allylic anion. In accord with this, these diphosphenes display PN bonds [1.666(3), 1.685(4) and 1.691(4)Å respectively] which are significantly shortened in comparison to the corresponding distance in $(^iPr_2N)_2PP{=}PN(SiMe_2{}^tBu)_2$ (1.736(2)Å).[49]

In the only two Z-configuration diphosphenes $Ar^*P{=}PNH{}^tBu$[55] and Ar*P=PNH(1-Ad)[55] fully characterised by X-ray analyses the atoms N, P_1 and P_2 and the *ipso* carbon of the aryl substituent are located in the same plane. The aryl ring is directed orthogonally to the plane defined by N, P_1, P_2 and the *ipso* C atom, thus rendering it possible that the hydrogen atom of the amino group points to the centre of the arene ring. The attractive interaction resulting from this was invoked to explain the stability of the rare Z-arrangement.

1.2.3 NMR spectroscopy of diphosphenes

Chemical shifts for diphosphenes are amongst the lowest field shifts known in ^{31}P NMR spectroscopy. They essentially range from 450 to 670 ppm.[45] These characteristically low field shifts are due to a significant increase in the paramagnetic shielding term caused by the existence of low-lying excited states. This is a dominant effect in multiply bonded compounds.[56]

1.2.4 Co-ordination chemistry of diphosphenes

The rapid development of the chemistry of diphosphenes has also included a study of their properties as ligands to transition metals. At least seven modes of co-ordination have been encountered to date (Figure 1.4).[57]

In compounds of type A the diphosphene acts as an η^1 ligand toward the metal centre. Theoretical calculations on the model compound [$Cr(\eta^1$-$P_2H_2)(CO)_5$] revealed that a realistic description of the ligand metal interaction involves delocalised σ-donation from the HOMO of the ligand and π-back donation of a filled metal orbital into the empty LUMO (the π* orbital) of the ligand. The extent of the back donation is quite large and comprises 0.30 electrons. [58]

The second type of co-ordination (B) comprises an η^2-interaction of the P=P π system with the metal atom. As in olefin complexes, donation from the filled π-orbital to an empty metal orbital transfers electron density from the ligand to the metal. π-Back donation operates between filled metal orbitals and the LUMO (π*) orbital of the diphosphene.

In the co-ordination modes C-E a diphosphene bridges two independent metal complex fragments. In C this is achieved by two η^1 interactions, whereas in types D and E co-ordination is a combination of η^1 and η^2 modes.

In type F the diphosphene is incorporated into a butterfly molecule, whereas G is a representative of a cluster compound with a diphosphene building block. Other types of complexes with such a bonding situation are conceivable.

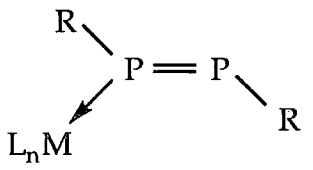

A (η^1)

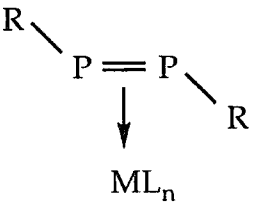

B (η^2)

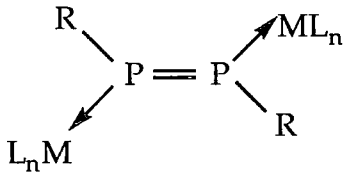

C (η^1, η^1)

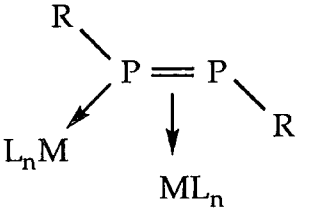

D (η^1, η^2)

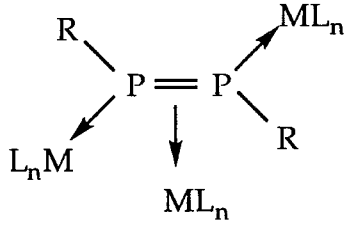

E (η^1, η^1, η^2)

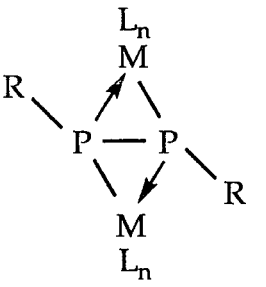

F (μ_2 (η^2, η^2)

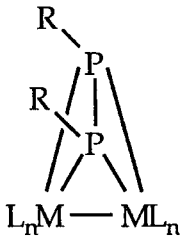

G (μ_2 (η^2, η^2)(M-M)

Figure 1.4: *Co-ordination Modes of Diphosphene Ligands*

There are two main synthetic pathways which lead to diphosphene complexation. Firstly, a diphosphene ligand can be added to a co-ordinatively unsaturated complex or may replace labile ligands in suitable co-ordination compounds. Secondly, the diphosphene ligand may be constructed from easily available and stable precursors in the co-ordination sphere of an organometallic complex. This method implies that the stability of the free diphosphene is not a prerequisite for its existence as a ligand in stable complexes.

1.3 References

1 F.T. Edelmann, *Comments Inorg. Chem.*, 1992, **12**, 259.

2 M. Witt and H.W. Roesky, *Progr. Inorg. Chem.*, 1992, **40**, 353.

3 F.T. Edelmann, *Main Group Metal Chemistry*, 1994, 17, 67 and references therein.

4 E.T. McBee and R.E. Leech, *Ind. Eng. Chem.*, 1947, **39**, 393.

5 G.E. Carr, R.D. Chambers, T.F. Holmes and D.G. Parker, *J. Organomet. Chem.*, 1987, **325**, 13.

6 M. Scholz, H.W. Roesky, D. Stalke, K. Keller and F.T. Edelmann, J. *Organomet. Chem.*, 1989, **366**, 73.

7 H.P. Goodwin, *Ph.D Thesis*, University of Durham, 1990.

8 $Sn(Ar^F)_2$: H. Grützmacher, H. Pritzkow and F.T. Edelmann, *Organometallics*, 1991, **10**, 23.

9 $In(Ar^F)_3$: R.D. Schluter, A.H. Cowley, D.A. Atwood, R.A. Jones, M.R. Bond and C.J. Carrano, *J. Am. Chem. Soc.*, 1993, **115**, 2070.

10 $Ga(Ar^F)Cl_2$ dimer: R.D. Schluter, H.S. Isom, A.H. Cowley, D.A. Atwood, R.A. Jones, F. Olbrich, S. Corbelin and R.A. Lagow, *Organometallics*, 1994, **13**, 4058.

11 $Sb(Ar^F)_2Cl$: K.B. Dillon, H.P. Goodwin, T.A. Straw and R.D. Chambers, *Proc. Euchem.*, PSIBLOCS Conf. Paris,1988

12 $Ar^FP{=}PAr^F$: See ref 11, also; M. Scholz, H.W. Roesky, D. Stalke and F.T. Edelmann, *J. Organomet. Chem.*, 1989, **366**, 73;

13 $Ar^FS\text{-}SAr^F$: A Edelmann, S. Brooker, N. Bertel, M. Noltemeyer, H.W. Roesky, G.M. Sheldrick and F.T. Edelmann, *Z. Naturforsch*, 1992, **47**, 305.

14 K.H. Whitmire, D. Labahn, H.W. Roesky, M. Noltemeyer and G.M. Sheldrick, *J. Organomet. Chem.*, 1991, **402**, 55.

15 R. Hughes, *Adv. Organomet. Chem.*, 1990, **31**, 183.

16 N.M. Doherty and N.W. Hoffman, *Chem. Rev.*, 1991, **91**, 553.

17 R.J. Kulaweic and R.H. Crabtree, *Coord. Chem. Rev.*, 1990, **99**, 89.

18 J.K. Stille and S.Y.L. Kriesler, *Acc. Chem. Res.*, 1977, **10**, 434.

19 J.K. Kochi, *Organometallic Mechanisms and Catalysis*; Academic Press; New York, 1978, 156.

20 M. Hudlicky, *Chemistry of Organic Fluorine Compounds*; Macmillan; New York, 1961.

21 R.D. Chambers, *Fluorine in Organic Chemistry*; Wiley; New York, 1973.

22 W.A. Sheppard and C.M. Sharts, *Organic Fluorine Chemistry*; Benjamin; New York, 1969.

23 *Fluorocarbon and Related Chemistry*, R.E. Banks and M.G. Barlow, Eds.; The Chemical Society; London, 1974 (Vols I and II).

24 B.E. Smart, *The Chemistry of Functional Groups, Supplement D*, S. Pattai and Z. Rappoport, Eds., Wiley; New York; 1983.

25 S.H. Strauss, *Chem. Rev.*, 1993, **93**, 927.

26 R. Cramer and G.W. Parshall, *J. Am. Chem. Soc.*, 1965, **87**, 1392.

27 R.D. Chambers and T. Chivers, *Organomet. Chem. Rev.*, 1966, **1**, 279.

28 P.M. Treichel and F.G.A. Stone, *Adv. Organomet. Chem.*, 1964, **1**, 143.

29 S.C. Cohen and A.G. Massey, *Advances in Fluorine Chemistry*, J.C. Tatlow, R.D. Peacock, H.H. Hyman, M. Stacey, Eds.; Butterworths; London, 1970, Vol 8, 235.

30 W. Seidel and I. Bürger, *Z. Chem.*, 1977, **17**, 185.

31 S.U. Koschmieder and G. Wilkinson, *Polyhedron*, 1991, **10**, 135.

32 A.W. Duff, K. Jonas, R. Goddard, H-J. Kraus and C. Kruger, *J. Am. Chem. Soc.*, 1983, **105**, 5479.

33 M. Elian, R. Hoffmann, J.W. Lauher and R.H. Summerville, *J. Am. Chem. Soc.*, 1976, **98**, 3219.

34 W.M. Lamanna, W.B. Gleason and D. Britton, *Organometallics*, 1987, **6**, 1583.

35 M.B. Hursthouse, M. Motevalli, A.C. Sullivan and G.Wilkinson, *J. Chem. Soc., Chem. Commun.*, 1986, 1398.

36 L.E. Gusel'nikov and N.S. Nametkin, *Chem. Rev.*, 1979, 529 and references therein.

37 H. Köhler and A. Michaelis, *Ber. Dtsch. Chem. Ges.*, 1877, **10**, 807.

38 W. Kuchen, H. Buchwald, *Chem. Ber.*, 1958, **91**, 2296.

39 J.J. Daly and L. Maier, *Nature*, 1964, **203**, 1167; J.J. Daly, *J. Chem. Soc.*, 1964, 6147

40 J.J. Daly and L. Maier, *Nature*, 1965, **208**, 383; J.J. Daly, *J. Chem. Soc.*, 1965, 4789

41 M. Yoshifuji, I. Shima, N. Inamoto, K. Hirotsu and T. Higuchi, *J. Am Chem. Soc.*, 1981, **103**, 4587

42 J. Escudié, C. Couret, H. Ranaivonjatovo and J. Satgé, *J. Chem, Soc, Chem, Commun.*, 1984, 1621; C. Couret, J. Escudié, H. Ranaivonjatovo and J. Satgé, *Organometallics*, 1986, **5**, 113; J. Satgé, J. Escudié, C. Couret, H. Ranaivonjatovo and M. Adrianarison, *Phosphorus and Sulfur*, 1986, **27**, 65.

43 J. Escudié, C. Couret and H. Ranaivonjatovo, M. Lazraq, J. Satgé, *Phosphorus and Sulfur*, 1987, **31** ,27.

44 A.H. Cowley, J.E. Kilduff, J.G. Lasch, S..K. Mehrotra, N.C. Norman, M. Pakulski, B.R. Whittlesey, J.L. Atwood and W.E. Hunter, *Inorg Chem*, 1984, **23**, 2582.

45 L. Weber, *Chem. Rev.*, 1992, **92**, 1839 and references therein.

46 A.H. Cowley, J.E. Kilduff, T.H. Newman and M. Pakulski, *J. Am. Chem. Soc.*, 1982, **104**, 5820.

47 A.H. Cowley, J.E. Kilduff, M. Pakulski and C. A. Stewart, *J. Am. Chem. Soc.*, 1983, **105**, 1655.

48 M. Yoshifuji, K. Shibayama, N. Inamoto, T. Matsushita and K. Nishimoto, *J. Am. Chem. Soc.*, 1983, **105**, 2495.

49 T. Busch, W.W. Schoeller, E. Niecke, M. Nieger and H. Westerman, *Inorg. Chem.*, 1989, **28**, 4334.

50 T.L. Allen, A.C. Scheiner, Y. Yamaguchi and H.F. Schaefer III, *J. Am. Chem. Soc.*, 1986, **108**, 7579.

51 L. Pauling, *The Nature of the Chemical Bond*, 3rd Edition, Cornell University Press, New York, 1960.

52 K.F. Tebbe, *Z. Anorg. Allg. Chem.*, 1980, **468**, 202.

53 D.C. Pestana and P.P. Power, *J. Am. Chem. Soc.*, 1989, **111**, 6887; D.C. Pestana and P.P. Power, *Inorg. Chem.*, 1991, **30**, 528.

54 L.N. Markovski, V.D. Romanenko and A.V. Ruban, *Chemistry of Acyclic Compounds of Two-coordinated Phosphorus*, Naukova Dumka, Kiev, 1988, p199.

55 E. Niecke, B. Kramer and M. Nieger, *Angew. Chem., Int. Ed. Engl*, 1991, **30**, 1136.

56 A.H. Cowley, *Polyhedron*, 1984, **3**, 389.

57 A-M. Caminade, J.P. Majoral, R. Mathieu, *Chem. Rev.*, 1991, **91**, 575; and O.J. Scherer, *Angew. Chem., Int. Ed. Engl.*, 1985, **24**, 924.

58 K.A. Schugart and R.F. Fenske, *J. Am. Chem. Soc.*, 1985, **107**, 3384.

Chapter 2

Transition Metal Complexes Containing the σ-Bound 2,4,6-Tris(trifluoromethyl)phenyl Ligand

2.1 Introduction

In recent years there has been considerable and growing interest in the bulky, highly electron withdrawing 2,4,6-tris(trifluoromethyl)phenyl ligand for its ability to stabilise low valent, low co-ordinate main group compounds, examples of which include compounds of metalloid elements such as Ga,[1] Sn,[2] Pb,[3] Bi,[4] As[5] and Sb.[6] Other p-block compounds of this ligand include $(Ar^F)_2SiCl_2$,[6] $B(Ar^F)_3$,[7] Ar^FPCl_2,[7] Ar^FPF_2,[7], Ar^FPH_2[7] and the remarkably air- and moisture-stable diphosphene $Ar^FP{=}PAr^F$.[8] By contrast, transition metal compounds containing this ligand remain rare, presently being restricted to d^{10} species such as $M(Ar^F)_2$ (M=Zn,[9] Hg[10]) and $Cu(Ar^F)$[10] and the homoleptic Ni d^8 and Co d^7 complexes $M(Ar^F)_2$;[11] to date, there have been no structural data reported on a transition metal Ar^F derivative.

The main reasons for studying transition metal complexes of the Ar^F ligand arise from its established ability to stabilise unusual co-ordination and oxidation states of main group elements. Recently, Cowley *et al* have synthesised various compounds of indium[12] and gallium[12] bearing between one and three Ar^F groups, thus showing the versatiliy of the bulky electron-withdrawing group in stabilising a variety of unusually co-ordinated main group species. In main group systems it has also been found that the Ar^F ligand is able to inhibit oligomerization. For example, it is the first ligand to stabilise a monomeric diaryl stannylene.[2] Although sterically the ligand lies between mesityl and 2,4,6-tri-*iso*-propylphenyl neither of these ligands is capable of inhibiting oligomerisation.[6] This stabilising effect is therefore only partly due to steric shielding. Despite the electron-withdrawing character of the CF_3 group through the σ-bond framework and negative hyperconjugation, the ability of the fluorine substituents to donate a lone

pair of electrons to a metal, thereby occupying a co-ordination site is probably the most important factor inhibiting oligo- or polymerisation.[2,13]

Thus, bulky electron-withdrawing substituents might also offer a unique opportunity to stabilise low co-ordinate and low valent σ–aryl complexes of the transition metals. This chapter therefore describes attempts to prepare mononuclear base-free compounds with aryl substituents via straightforward metathetical routes for a range of transition metals (equation 2.1). The propensity for Ar^FLi to react with metal halides offers much scope for its incorporation into many different transition metal environments. It is anticipated that these products will display enhanced stability in much the same way as has been established for main group systems.

$$MCl_n + nAr^FLi \longrightarrow MAr^F_n + nLiX \quad (2.1)$$

$$n=1\text{-}3$$

The Ar^FLi salt is unstable in solution, and therefore has to be used swiftly upon its generation.[6] Several early transition metal complexes containing this ligand were successfully prepared and their syntheses and structures are described in the following sections.

2.2 Transition metal complexes of the Ar^F ligand

2.2.1 Synthesis of $Mo(N^tBu)_2(Ar^F)_2$

The hexavalent bis(imido) molybdenum complex **1** was obtained by treatment of $Mo(N^tBu)_2Cl_2(dme)$ with two equivalents of Ar^FLi, (equation 2.2).

$$Mo(N^tBu)_2Cl_2(dme) + 2Ar^FLi \xrightarrow[-dme]{-2LiCl} Mo(N^tBu)_2(Ar^F)_2 \qquad (2.2)$$

1

Compound **1** is relatively air-stable (days) and readily soluble in hydrocarbon solvents. The ^{19}F and ^1H NMR data indicate that the two Ar^F ligands are equivalent in solution though the *ortho*-CF_3 fluorines and *meta*-aryl hydrogens of each Ar^F are inequivalent at room temperature due to restricted rotation (figure 2.1). As the temperature is raised the resonances for the *ortho*-CF_3 fluorines coalesce in the ^{19}F NMR spectrum and *meta*-aryl hydrogens coalesce in the ^1H NMR spectrum (T_c = 323K), affording a free energy of activation ($\Delta G\ddagger$) of 64 $kJmol^{-1}$. This inequivalence at room temperature could be due to locking of the CF_3 groups through possible M···F interactions, a theory supported by the accompanying crystallographic data.

2.2.2 Molecular structure of $Mo(N^tBu)_2(Ar^F)_2$

Crystals of **1** suitable for X-Ray diffraction were grown by slow cooling of a pentane solution to -20°C. The molecular structure is shown in figure 2.2 and key bond distances and angles are given in table 2.1. Data were

collected and the structure was solved by Prof J.A.K. Howard and Mr. J.W. Yao of Durham University.

Complex **1** possesses a pseudo-tetrahedral geometry with N-Mo-N and C-Mo-C angles of 110.6(2)° and 138.3(2)° respectively. The latter is considerably larger than that observed for the mesityl analogue $[Mo(NBu^t)_2(2,4,6\text{-}Me_3\text{-}C_6H_2)_2]$ (122.6°),[14] a consequence of the larger size of the Ar^F group and possible F···F repulsions. Additionally, however, fluorines in two of the *ortho*-CF_3 groups lie in close contact with the molybdenum centre, with Mo···F distances of 2.467(3) and 2.476(3) Å. Such M···F interactions, though believed to be quite weak, are also observed widely throughout main group derivatives[1-4]; further discussion of this phenomenon will be deferred until later in this chapter. To minimise steric congestion and electrostatic F···F repulsions the two aromatic rings are twisted by 99.0(2)° relative to one another. For the imido groups the Mo=N distances, 1.724(5) and 1.729(4) Å lie within the range of bond lengths and angles found for 'linear' imido units in bis(imido)molybdenum compounds.[15]

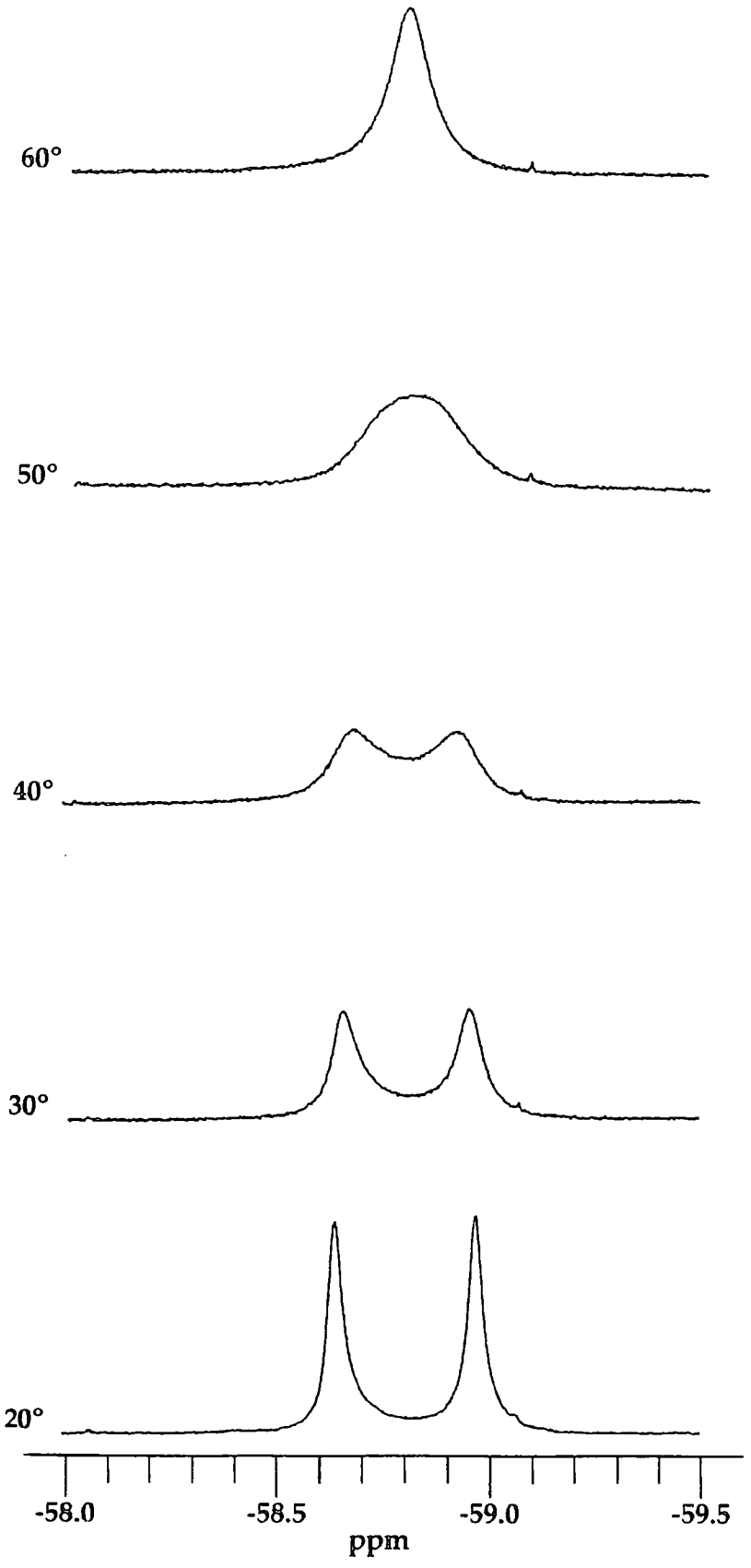

Figure 2.1: *Variable temperature ^{19}F NMR spectra for complex 1 (C_6D_6)*

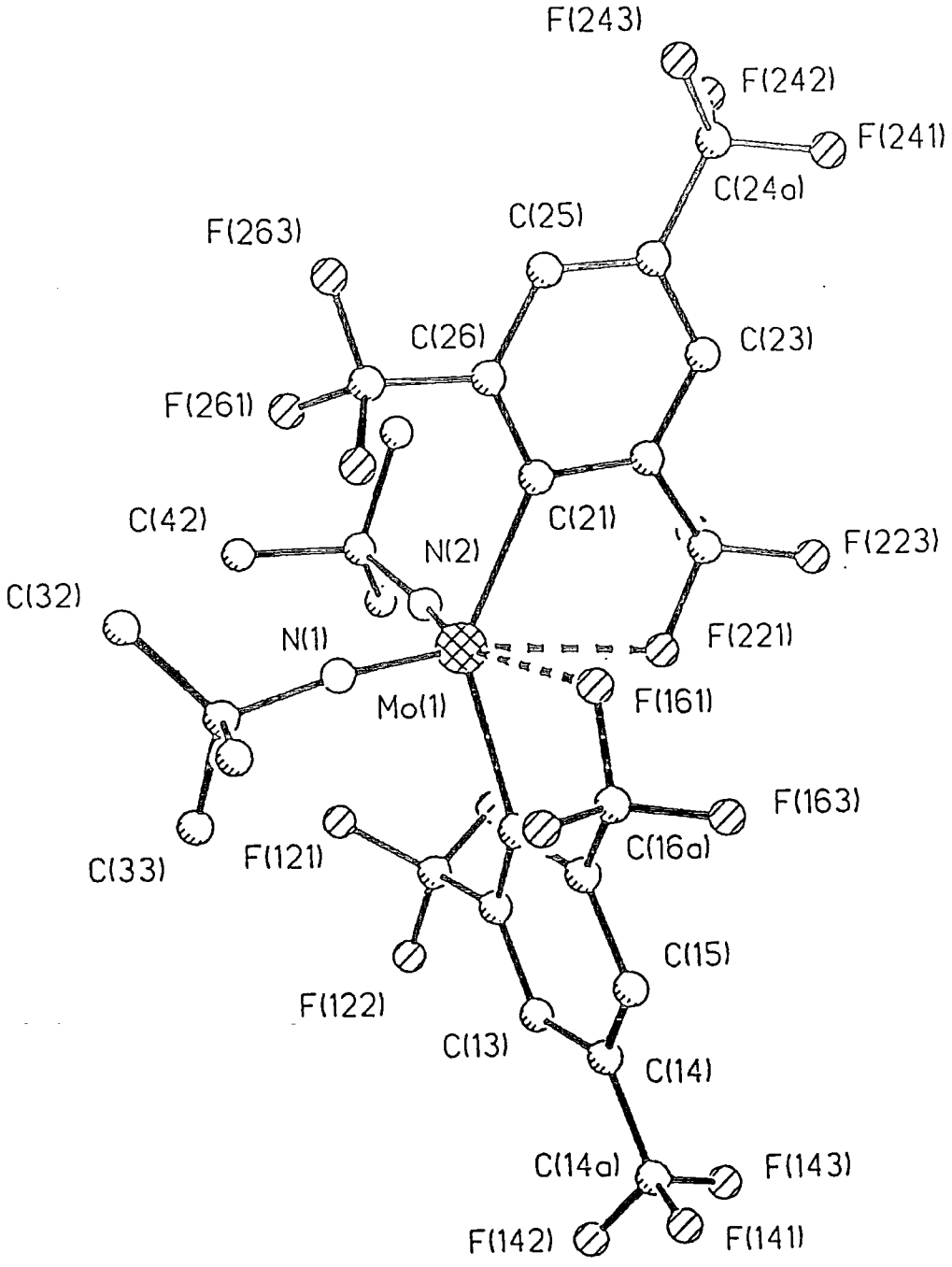

Figure 2.2: *The molecular structure of complex 1*

Mo(1)-N(1)	1.724(5)	Mo(1)-N(2)	1.729(4)
Mo(1)-C(11)	2.252(5)	Mo(1)-C(21)	2.241(5)
Mo(1)-F(161)	2.467(3)	Mo(1)-F(221)	2.476(3)
N(1)-C(3)	1.474(7)	N(2)-C(4)	1.476(7)
C(11)-C(12)	1.416(7)	C(12)-C(13)	1.385(8)
C(13)-C(14)	1.383(8)	C(14)-C(15)	1.390(8)
C(15)-C(16)	1.398(8)	C(16)-C(11)	1.392(7)
C(12)-C(12A)	1.505(8)	C(14)-C(14A)	1.501(8)
C(16)-C(16A)	1.480(8)	C(12A)-F(121)	1.346(6)
C(12A)-F(122)	1.349(6)	C(12A)-F(123)	1.337(6)
C(14A)-F(141)	1.22(2)	C(14A)-F(142)	1.27(2)
C(14A)-F(143)	1.351(9)	C(14A)-F(14A)	1.31(2)
C(14A)-F(14B)	1.27(2)	C(16A)-F(161)	1.362(6)
C(16A)-F(162)	1.323(7)	C(16A)-F(163)	1.322(7)
C(21)-C(22)	1.419(8)	C(22)-C(23)	1.382(9)
C(23)-C(24)	1.377(10)	C(24)-C(25)	1.380(10)
C(25)-C(26)	1.387(8)	C(26)-C(21)	1.411(8)
C(22)-C(22A)	1.473(9)	C(24)-C(24A)	1.498(9)
C(26)-C(26A)	1.497(9)	C(22A)-F(221)	1.362(7)
C(22A)-F(222)	1.350(9)	C(22A)-F(223)	1.307(8)
C(24A)-F(241)	1.344(11)	C(24A)-F(242)	1.283(10)
C(24A)-F(243)	1.315(10)	C(26A)-F(261)	1.340(7)
C(26A)-F(262)	1.342(7)	C(26A)-F(263)	1.343(7)
C(3)-C(31)	1.547(10)	C(3)-C(32)	1.498(9)
C(3)-C(33)	1.532(11)	C(4)-C(41)	1.523(9)
C(4)-C(42)	1.532(10)	C(4)-C(43)	1.522(9)
C(3)-H(13)	1.01(7)	C(15)-H(15)	0.91(7)
C(23)-H(23)	0.93(7)	C(25)-H(25)	0.81(7)
C(31)-H(311)	1.07(7)	C(31)-H(312)	1.09(7)
C(31)-H(313)	0.98(7)	C(32)-H(321)	1.01(7)
C(32)-H(323)	0.93(7)	C(33)-H(331)	0.59(8)
C(33-H(332)	1.04(7)	C(33)-H(333)	1.01(7)
C(41)-H(411)	1.01(7)	C(41)-H(412)	0.97(7)
C(41)-H(413)	1.03(7)	C(42)-H(421)	0.96(7)
C(42)-H(422)	0.99(7)	C(42)-H(423)	0.74(7)
C(43)-H(431)	0.95(7)	C(43)-H(432)	1.00(7)
C(43)-H(433)	0.97(7)		

N(1)-Mo(1)-N(2)	110.6(2)	N(1)-Mo(1)-C(11)	93.6(2)
N(1)-Mo(1)-C(21)	110.2(2)	N(2)-Mo(1)-C(11)	110.3(2)
N(2)-Mo(1)-C(21)	92.3(2)	C(11)-Mo(1)-C(21)	138.3(2)
N(1)-Mo(1)-F(161)	92.2(2)	N(2)-Mo(1)-F(161)	156.6(2)
N(1)-Mo(1)-F(221)	159.0(2)	N(2)-Mo(1)-F(221)	89.8(2)
C(11)-Mo(1)-F(161)	71.8(2)	C(21)-Mo(1)-F(161)	74.1(2)
C(11)-Mo(1)-F(221)	74.1(2)	C(21)-Mo(1)-F(221)	71.4(2)
F(161)-Mo(1)-F(221)	68.01(12)	Mo(1)-N(1)-C(3)	165.0(4)
Mo(1)-N(2)-C(4)	156.1(4)	Mo(1)-C(11)-C(12)	129.2(4)
Mo(1)-C(11)-C(16)	115.7(3)	C(12)-C(16)-C(11)	115.1(5)

C(11)-C(12)-C(13)	122.9(5)	C(12)-C(13)-C(14)	119.6(5)
C(13)-C(14)-C(15)	120.1(5)	C(14)-C(15)-C(16)	119.0(5)
C(11)-C(12)-C(12A)	121.3(5)	C(13)-C(12)-C(12A)	115.7(5)
C(13)-C(14)-C(14A)	119.5(5)	C(15)-C(14)-C(14A)	120.4(5)
C(11)-C(16)-C(15)	123.3(5)	C(11)-C(16)-C(16A)	122.5(5)
C(15)-C(16)-C(16A)	114.2(5)	F(121)-C(12A)-F(122)	105.6(5)
F(122)-C(12A)-F(123)	106.1(4)	F(121)-C(12A)-F(123)	106.7(4)
F(141)-C(14A)-F(142)	115(2)	F(142)-C(14A)-F(143)	86.4(12)
F(141)-C(14A)-F(143)	115(2)	F(143)-C(14A)-F(14A)	89.4(11)
F(143)-C(14A)-F(14B)	120(3)	F(161)-C(16A)-F(162)	104.8(5)
F(162)-C(16A)-F(163)	106.7(5)	F(161)-C(16A)-F(163)	105.6(5)
C(12)-C(12A)-F(121)	113.6(5)	C(12)-C(12A)-F(122)	112.5(4)
C(12)-C(12A)-F(123)	111.9(5)	C(14)-C(14A)-F(141)	115.1(9)
C(14)-C(14A)-F(142)	113.7(10)	C(14)-C(14A)-F(143)	109.7(6)
C(14)-C(14A)-F(14A)	113.2(10)	C(14)-C(14A)-F(14B)	113.8(10)
C(16)-C(16A)-F(161)	112.1(4)	C(16)-C(16A)-F(162)	113.3(5)
C(16)-C(16A)-F(163)	113.7(5)	C(16A)-F(161)-Mo(1)	113.7(3)
C(22)-C(21)-Mo(1)	116.3(4)	C(23)-C(22)-C(21)	123.3(6)
C(21)-C(22)-C(22A)	121.3(5)	C(23)-C(22)-C(22A)	115.4(6)
C(22)-C(23)-C(24)	120.4(7)	C(23)-C(24)-C(25)	119.1(6)
C(23)-C(24)-C(24A)	119.9(7)	C(25)-C(24)-C(24A)	121.0(7)
C(24)-C(25)-C(26)	120.2(6)	C(25)-C(26)-C(21)	123.5(6)
C(25)-C(26)-C(26A)	115.9(5)	C(21)-C(26)-C(26A)	120.7(5)
C(26)-C(21)-Mo(1)	130.0(4)	C(26)-C(21)-C(22)	113.6(5)
F(221)-C(22A)-F(222)	103.5(6)	F(221)-C(22A)-F(223)	105.4(6)
F(222)-C(22A)-F(223)	106.0(6)	C(22)-C(22A)-F(221)	112.8(5)
C(22)-C(22A)-F(222)	113.4(6)	C(22)-C(22A)-F(223)	114.8(7)
F(241)-C(24A)-F(242)	105.2(8)	F(241)-C(24A)-F(243)	101.2(8)
F(242)-C(24A)-F(243)	111.3(8)	C(24)-C(24A)-F(241)	112.1(7)
C(24)-C(24A)-F(242)	112.6(7)	C(24)-C(24A)-F(243)	113.5(7)
F(261)-C(26A)-F(262)	107.0(5)	F(261)-C(26A)-F(263)	105.9(5)
F(262)-C(26A)-F(263)	105.8(5)	C(26)-C(26A)-F(261)	111.9(5)
C(26)-C(26A)-F(262)	112.6(5)	C(26)-C(26A)-F(263)	113.0(5)
C(22A)-F(221)-Mo(1)	113.2(3)	N(1)-C(3)-C(31)	106.0(5)
N(1)-C(3)-C(32)	111.8(5)	N(1)-C(3)-C(33)	107.7(5)
C(31)-C(3)-C(32)	110.4(7)	C(31)-C(3)-C(33)	106.7(6)
C(32)-C(3)-C(33)	113.9(7)	N(2)-C(4)-C(41)	109.2(5)
N(2)-C(4)-C(42)	109.1(5)	N(2)-C(4)-C(43)	106.0(5)
C(41)-C(4)-C(42)	110.7(6)	C(41)-C(4)-C(43)	110.9(6)
C(42)-C(4)-C(43)	110.7(6)		

Table 2.1: *Bond lengths (Å) and angles (°) in* $Mo(N^tBu)_2(Ar^F)_2$. *Estimated standard deviations are in parentheses.*

2.2.3 Synthesis of $Cr(NAd)_2(Ar^F)_2$

The hexavalent bis(imido) chromium complex 2 was obtained in a similar fashion to the molybdenum analogue by treatment of $Cr(NAd)_2Cl_2$ with two equivalents of Ar^FLi, (equation 2.3).

$$Cr(NAd)_2Cl_2 + 2Ar^FLi \xrightarrow{-2LiCl} Cr(NAd)_2(Ar^F)_2 \quad (2.3)$$

2

The bis(*tert*-butylimido) chromium (VI) congener has also been prepared via this route and shows similar spectroscopic behaviour to 2. For example, both complexes show inequivalent *ortho*-CF_3 groups in their NMR spectra at room temperature suggesting that some form of metal-ligand interaction is present, as observed for complex 1.

2.2.4 Molecular structure of $Cr(NAd)_2(Ar^F)_2$

Bright red cubic crystals suitable for an X-ray study were grown from a pentane solution at -20°C. A crystal of dimensions 0.3 x 0.15 x 0.15mm was selected. The data were collected and solved by Prof. J.A.K. Howard and Dr. A. Batsanov within this department; the result is shown in figure 2.3 and the bond parameters are presented in table 2.2.

A crystal structure determination of $Cr(N^tBu)_2(Ar^F)_2$ has also been carried out. Unfortunately, although bond connectivity has been established the estimated standard deviations are too high to allow for an accurate assessment of the bond distances and angles (R factor = 8.8%). However, the structure of this complex is identical to that of 2 and it appears that both compounds contain weak metal-fluorine interactions.

As expected, the melting point of $Cr(N^tBu)_2(Ar^F)_2$ is 164°C, 18° higher than that of the mesityl analogue. Typically, fluorocarbon complexes of transition metals exhibit greater thermal stability than their hydrocarbon analogues. This improved stability is thought to be due, in part to the contraction of the metal orbitals by the electronegative fluorocarbon group, thus allowing greater overlap with the carbon atomic orbital.[16] This is evidenced by the metal carbon bond distance which is shorter in fluorocarbon-metal complexes than in the hydrocarbon metal complexes.

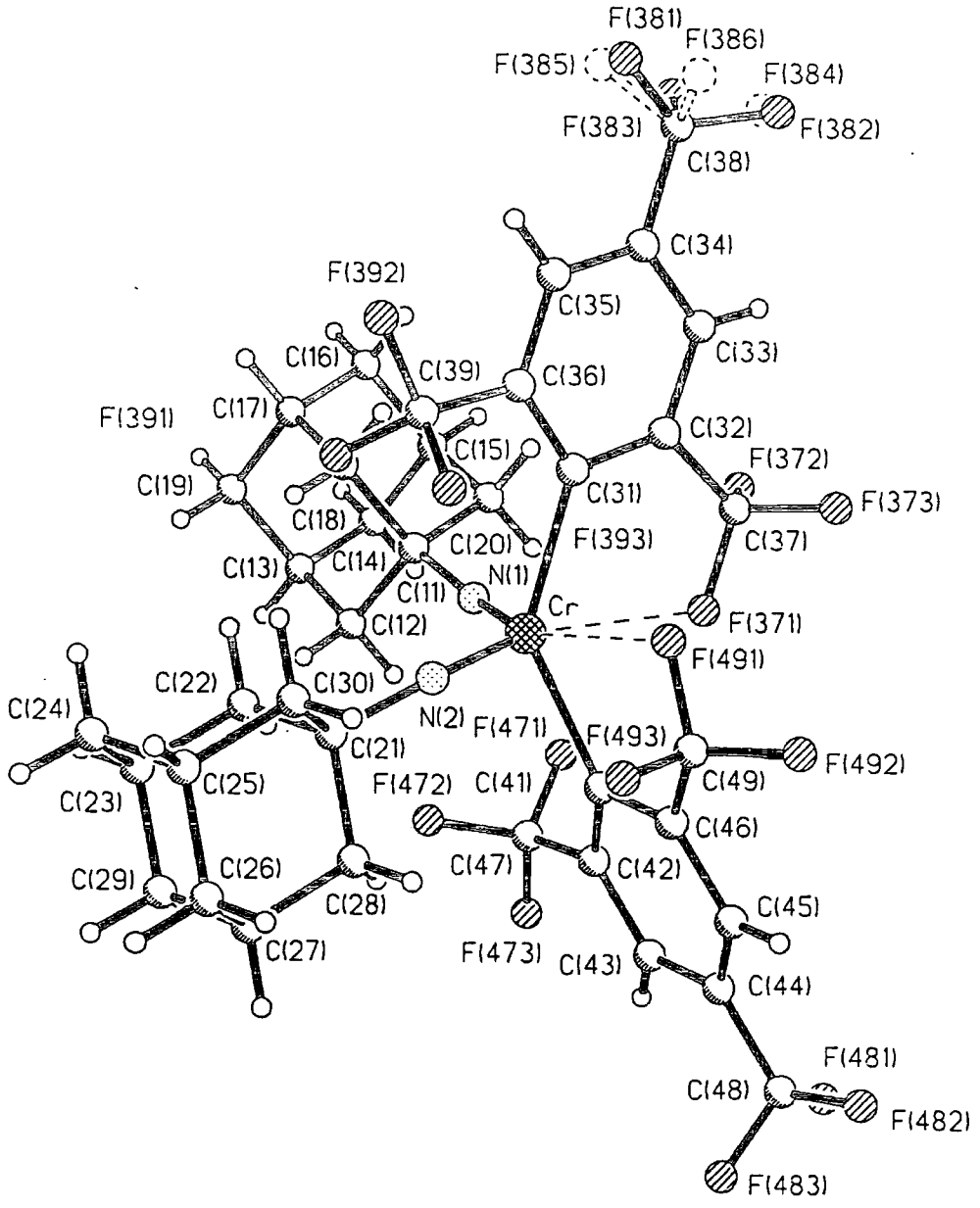

Figure 2.3: *The molecular structure of complex 2*

Cr(1)-N(1)	1.631(2)	Cr(1)-N(2)	1.644(2)
Cr(1)-C(31)	2.133(3)	Cr(1)-C(41)	2.133(3)
Cr(1)-F(371)	2.443(2)	Cr(1)-F(491)	2.462(2)
N(1)-C(11)	1.464(4)	N(2)-C(21)	1.454(3)
C(11)-C(12)	1.541(4)	C(11)-C(18)	1.541(4)
C(11)-C(20)	1.542(4)	C(13)-C(19)	1.522(4)
C(12)-C(13)	1.540(4)	C(14)-C(15)	1.522(4)
C(13)-C(14)	1.531(4)	C(15)-C(20)	1.540(4)
C(15)-C(16)	1.531(5)	C(17)-C(19)	1.527(5)
C(16)-C(17)	1.531(5)	C(21)-C(22)	1.530(4)
C(17)-C(18)	1.543(4)	C(21)-C(28)	1.555(4)
C(21)-C(30)	1.542(4)	C(23)-C(24)	1.534(4)
C(22)-C(23)	1.544(4)	C(24)-C(25)	1.538(4)
C(23)-C(29)	1.534(4)	C(25)-C(30)	1.540(4)
C(25)-C(26)	1.532(4)	C(27)-C(28)	1.541(4)
C(26)-C(27)	1.534(4)	C(31)-C(32)	1.411(4)
C(27)-C(29)	1.530(4)	C(32)-C(33)	1.390(4)
C(31)-C(36)	1.422(4)	C(33)-C(34)	1.379(4)
C(32)-C(37)	1.503(4)	C(34)-C(38)	1.512(4)
C(34)-C(35)	1.384(4)	C(36)-C(39)	1.504(4)
C(35)-C(36)	1.392(4)	C(37)-F(372)	1.335(4)
C(37)-F(371)	1.345(3)	C(38)-F(381)	1.258(8)
C(37)-F(373)	1.334(4)	C(38)-F(383)	1.242(7)
C(38)-F(382)	1.258(7)	C(38)-F(385)	1.281(7)
C(38)-F(384)	1.282(7)	C(39)-F(391)	1.345(3)
C(38)-F(386)	1.272(7)	C(39)-F(393)	1.342(3)
C(39)-F(392)	1.354(3)	C(41)-C(46)	1.409(4)
C(41)-C(42)	1.417(4)	C(42)-C(47)	1.499(4)
C(42)-C(43)	1.388(4)	C(44)-C(45)	1.385(5)
C(43)-C(44)	1.384(5)	C(45)-C(46)	1.393(4)
C(44)-C(48)	1.494(4)	C(47)-F(471)	1.342(3)
C(46)-C(49)	1.499(4)	C(47)-F(473)	1.357(3)
C(47)-F(472)	1.345(3)	C(48)-F(482)	1.283(5)
C(48)-F(481)	1.296(4)	C(49)-F(491)	1.359(4)
C(48)-F(483)	1.285(5)	C(49)-F(493)	1.347(4)
C(49)-F(492)	1.338(4)		

N(1)-Cr(1)-N(2)	112.29(11)	N(1)-Cr(1)-C(41)	111.67(11)
N(2)-Cr(1)-C(41)	92.20(11)	N(1)-Cr(1)-C(31)	90.97(11)
N(2)-Cr(1)-C(31)	111.38(11)	C(41)-Cr(1)-C(31)	138.52(10)
N(1)-Cr(1)-F(371)	89.37(9)	N(2)-Cr(1)-F(371)	157.16(9)
C(41)-Cr(1)-F(371)	72.25(8)	C(31)-Cr(1)-F(371)	73.82(9)
N(1)-Cr(1)-F(491)	157.00(9)	N(2)-Cr(1)-F(491)	89.25(9)
C(41)-Cr(1)-F(491)	73.81(9)	C(31)-Cr(1)-F(491)	72.95(8)
F(371)-Cr(1)-F(491)	70.66(6)	C(11)-N(1)-Cr(1)	163.2(2)
N(1)-C(11)-C(18)	110.4(2)	N(1)-C(11)-C(12)	112.1(2)
C(18)-C(11)-C(12)	109.1(2)	N(1)-C(11)-C(20)	106.8(2)
C(18)-C(11)-C(20)	109.0(2)	C(12)-C(11)-C(20)	109.4(2)

C(11)-C(12)-C(13)	109.5(2)	C(19)-C(13)-C(14)	109.7(3)
C(12)-C(13)-C(19)	109.5(2)	C(12)-C(13)-C(14)	109.0(2)
C(13)-C(14)-C(15)	110.2(2)	C(14)-C(15)-C(16)	110.1(3)
C(14)-C(15)-C(20)	108.9(2)	C(16)-C(15)-C(20)	109.1(2)
C(15)-C(16)-C(17)	109.2(2)	C(16)-C(17)-C(19)	110.1(3)
C(19)-C(17)-C(18)	109.6(3)	C(16)-C(17)-C(18)	109.6(3)
C(11)-C(18)-C(17)	109.1(2)	C(13)-C(19)-C(17)	109.6(3)
C(11)-C(20)-C(15)	109.8(2)	C(21)-N(2)-Cr(1)	155.2(2)
C(22)-C(21)-N(2)	112.3(2)	C(30)-C(21)-N(2)	109.3(2)
C(22)-C(21)-C(30)	109.7(2)	C(28)-C(21)-N(2)	107.1(2)
C(22)-C(21)-C(28)	109.6(2)	C(30)-C(21)-C(28)	108.6(2)
C(21)-C(22)-C(23)	109.3(2)	C(24)-C(23)-C(29)	109.7(2)
C(22)-C(23)-C(24)	109.5(2)	C(22)-C(23)-C(29)	109.4(2)
C(23)-C(24)-C(25)	109.4(2)	C(24)-C(25)-C(26)	110.0(2)
C(26)-C(25)-C(30)	109.9(2)	C(24)-C(25)-C(30)	108.6(2)
C(25)-C(26)-C(27)	109.5(2)	C(26)-C(27)-C(29)	109.4(2)
C(28)-C(27)-C(29)	109.4(2)	C(26)-C(27)-C(28)	109.6(2)
C(21)-C(28)-C(27)	109.3(2)	C(23)-C(29)-C(27)	109.9(2)
C(21)-C(30)-C(25)	109.7(2)	C(32)-C(31)-C(36)	113.6(2)
C(32)-C(31)-Cr(1)	116.6(2)	C(36)-C(31)-Cr(1)	129.7(2)
C(31)-C(32)-C(33)	124.1(3)	C(37)-C(32)-C(33)	114.4(2)
C(31)-C(32)-C(37)	121.4(2)	C(32)-C(33)-C(34)	119.7(3)
C(33)-C(34)-C(35)	119.1(3)	C(33)-C(34)-C(38)	120.7(3)
C(35)-C(34)-C(38)	120.1(3)	C(34)-C(35)-C(36)	120.6(3)
C(31)-C(36)-C(35)	122.7(3)	C(35)-C(36)-C(39)	116.4(2)
C(31)-C(36)-C(39)	120.8(2)	F(373)-C(37)-F(372)	106.0(2)
F(373)-C(37)-F(371)	105.5(2)	F(372)-C(37)-F(371)	106.3(2)
F(373)-C(37)-C(32)	112.1(2)	F(372)-C(37)-C(32)	113.5(3)
F(371)-C(37)-C(32)	112.8(2)	C(37)-F(371)-Cr(1)	113.6(2)
F(383)-C(38)-F(382)	103.2(7)	F(383)-C(38)-F(381)	111.0(8)
F(381)-C(38)-F(382)	104.7(9)	F(385)-C(38)-F(386)	101.4(7)
F(385)-C(38)-F(384)	107.8(8)	F(386)-C(38)-F(384)	104.9(8)
F(383)-C(38)-C(34)	113.2(4)	F(382)-C(38)-C(34)	110.8(4)
F(381)-C(38)-C(34)	113.1(4)	F(385)-C(38)-C(34)	113.2(4)
F(386)-C(38)-C(34)	113.1(5)	F(384)-C(38)-C(34)	115.3(4)
F(393)-C(39)-F(391)	107.3(2)	F(393)-C(39)-F(392)	105.7(2)
F(391)-C(39)-F(392)	105.4(2)	F(392)-C(39)-C(36)	112.2(2)
F(391)-C(39)-C(36)	113.4(2)	F(393)-C(39)-C(36)	112.2(2)
C(46)-C(41)-C(42)	113.6(3)	C(46)-C(41)-Cr(1)	116.3(2)
C(42)-C(41)-Cr(1)	130.0(2)	C(43)-C(42)-C(41)	123.0(3)
C(43)-C(42)-C(47)	116.5(3)	C(41)-C(42)-C(47)	120.5(3)
C(44)-C(43)-C(42)	120.8(3)	C(43)-C(44)-C(45)	118.8(3)
C(43)-C(44)-C(48)	119.6(3)	C(45)-C(44)-C(48)	121.6(3)
C(44)-C(45)-C(46)	119.7(3)	C(45)-C(46)-C(41)	124.1(3)
C(45)-C(46)-C(49)	115.2(3)	C(49)-C(46)-C(41)	120.8(3)
F(471)-C(47)-F(472)	107.8(2)	F(471)-C(47)-F(473)	105.7(2)
F(472)-C(47)-F(473)	105.1(2)	F(471)-C(47)-C(42)	113.0(2)
F(472)-C(47)-C(42)	112.4(2)	F(473)-C(47)-C(42)	112.4(2)
F(482)-C(48)-F(483)	105.9(4)	F(482)-C(48)-F(481)	105.0(4)

F(483)-C(48)-F(481)	105.1(4)	F(482)-C(48)-C(44)	113.5(3)
F(483)-C(48)-C(44)	113.3(3)	F(481)-C(48)-C(44)	113.2(3)
F(492)-C(49)-F(493)	106.5(3)	F(492)-C(49)-F(491)	105.8(3)
F(493)-C(49)-F(491)	105.8(3)	F(492)-C(49)-C(46)	113.1(3)
F(493)-C(49)-C(46)	113.3(3)	F(491)-C(49)-C(46)	111.7(2)
C(49)-F(491)-Cr(1)	109.4(2)		

Table 2.2: *Bond lengths (Å) and angles (°) in* $Cr(NAd)_2(Ar^F)_2$. *Estimated standard deviations are in parentheses.*

2.2.5 Synthesis of $[Mo(NAr)_2(Ar^F)Cl{\cdot}LiCl(dme)]_2$

The reaction of $Mo(NAr)_2Cl_2.dme$ with 2 equivalents of Ar^FLi did not give the expected product $Mo(NAr)_2(Ar^F)_2$ but instead, deep orange-red needle-like crystals of an air- and moisture-sensitive compound were obtained, which were structurally characterised as the dimolybdenum species $[Mo(NAr)_2(Ar^F)Cl{\cdot}LiCl(dme)]_2$.

The co-ordination of LiCl(dme) into the chloride-bridged dimolybdenum structure can be seen as resulting from the interaction of LiCl(dme) with the notional molybdenum mono-Ar^F fragment $Mo(NAr)_2Cl(Ar^F)$. Incorporation of LiCl has been observed on numerous occasions in metal alkoxide chemistry, *eg*. $[W\{NC_6H_4Me\text{-}4\}(OC_6H_{11})_5Li_2Cl(C_6H_{11}OH)\}_2].C_6H_{11}OH$ and $[\{ReO(OPr^i)_5Li_2Cl(thf)\}_2].2thf$.[17]

The ^{19}F NMR spectrum shows a sharp singlet at -63ppm for the *para*-CF_3 groups, although the signal for the *ortho*-CF_3 groups is broadened into the baseline.

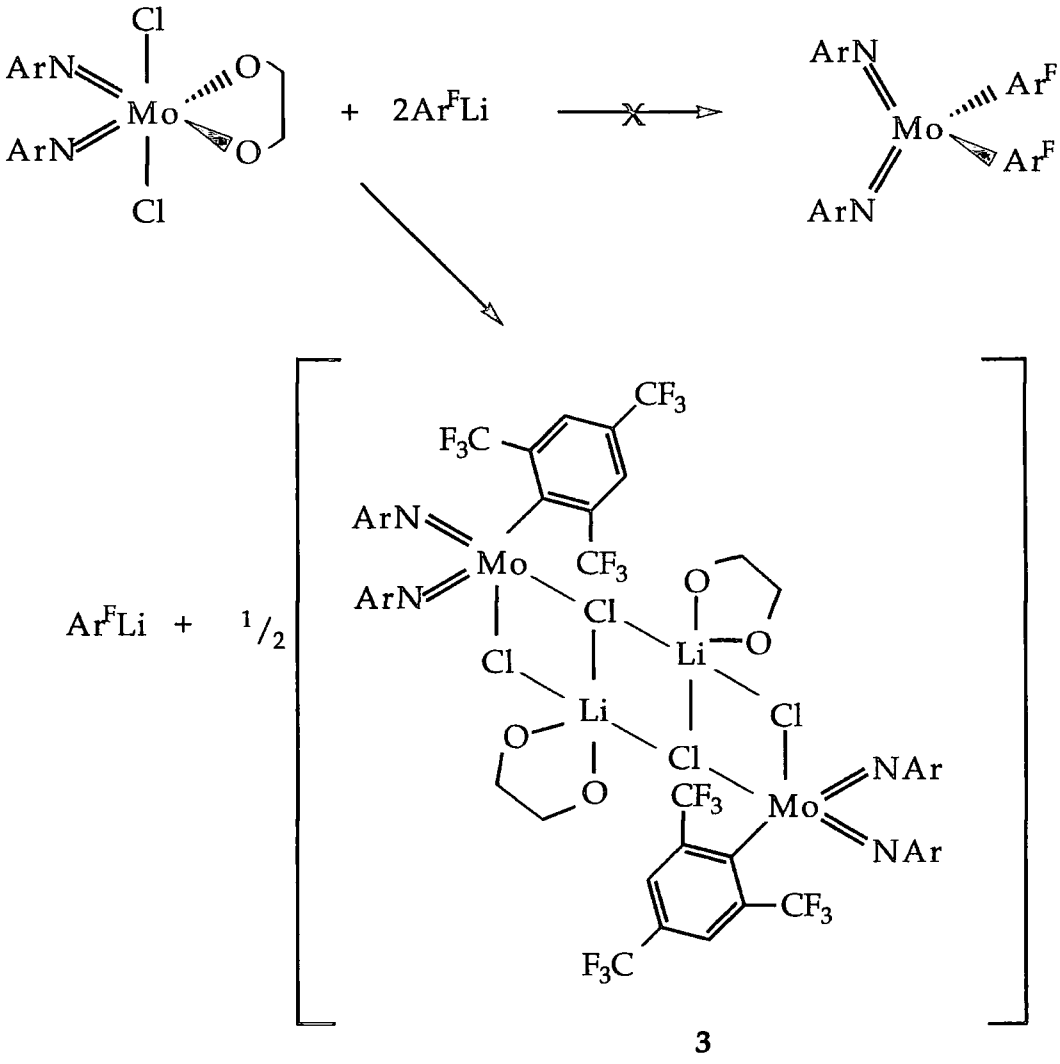

3

equation 2.4

2.2.6 Molecular structure of $[Mo(NAr)_2(Ar^F)Cl{\cdot}LiCl(dme)]_2$

Crystals of complex **3** suitable for X-ray analysis were obtained from a pentane solution at -20°C. The structure is shown in figure 2.4 and the bond data are summarised in table 2.3. The structure consists of a dimer of distorted octahedra linked by a $Mo_2Cl_4Li_2$ ladder arrangement. Each molybdenum centre reaches a co-ordination number of six via a weak interaction to one of the *ortho*-CF_3 fluorine atoms. The Mo···F distances are 2.526(7)Å and 2.556(6)Å and, although larger than those for the

bis(^{t}butyl)imido derivative, are still believed to be within the boundaries of a stabilising interaction.

The Mo-N-C bond angles 168.5(8) and 167.2(8)° lie within the range for "linear" imido units and the Mo=N bond distances 1.754(9) and 1.752(9)Å are typical for bis(imido)molybdenum complexes.[15]

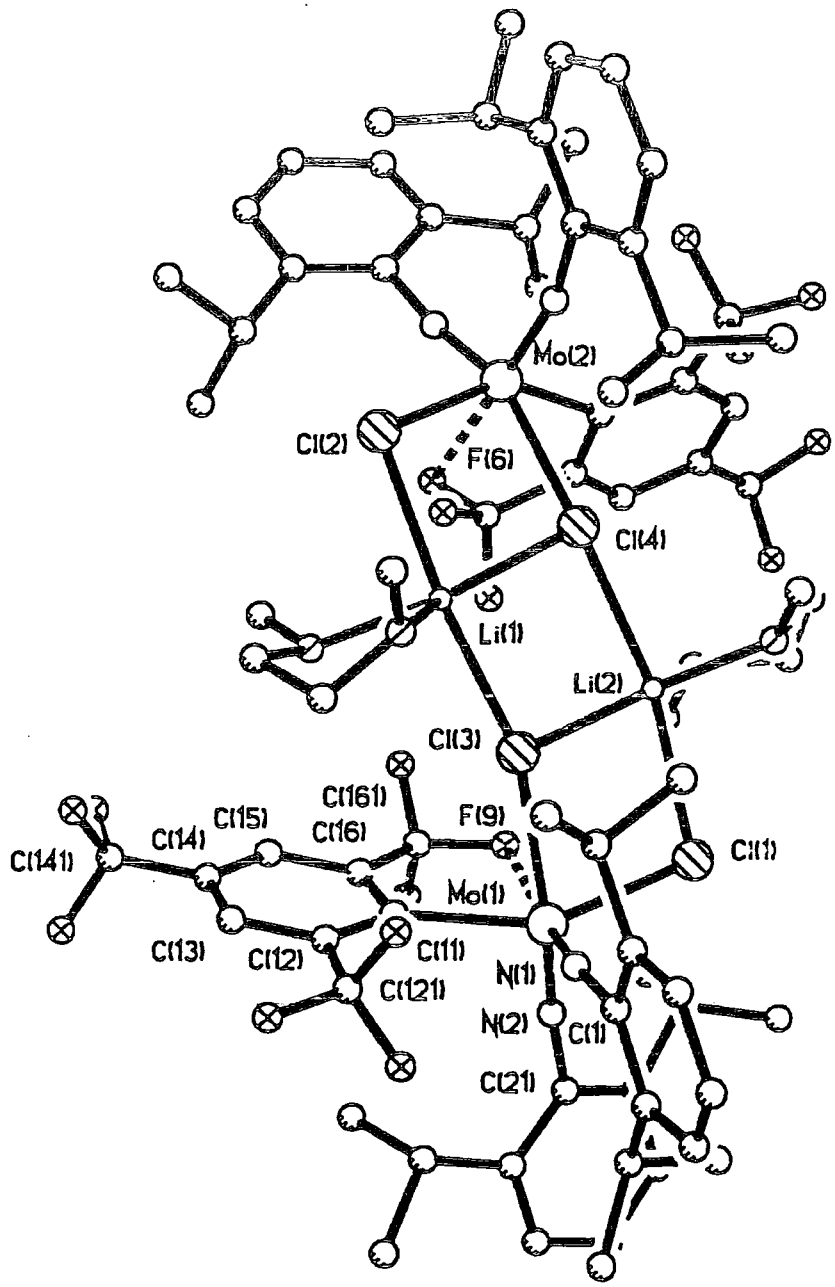

Figure 2.4: *The molecular structure of complex 3*

Mo(1)-N(1)	1.752(9)	Mo(1)-N(2)	1.754(9)
Mo(1)-C(11)	2.225(11)	Mo(1)-Cl(1)	2.432(3)
Mo(1)-F(9)	2.526(7)	Mo(1)-Cl(3)	2.614(3)
N(1)-C(1)	1.36(2)	N(2)-C(21)	1.399(14)
C(1)-C(2)	1.43(2)	C(2)-C(3)	1.36(2)
C(3)-C(4)	1.43(2)	C(4)-C(5)	1.37(2)
C(5)-C(6)	1.41(2)	C(6)-C(1)	1.42(2)
C(2)-C(2C)	1.54(2)	C(2C)-C(2A)	1.56(2)
C(2C)-C(2B)	1.55(2)	C(6)-C(61)	1.52(2)
C(61)-C(61A)	1.57(2)	C(61)-C(61B)	1.56(2)
C(11)-C(12)	1.41(2)	C(12)-C(121)	1.52(2)
C(12)-C(13)	1.40(2)	C(13)-C(141)	1.41(2)
C(14)-C(141)	1.50(2)	C(15)-C(141)	1.35(2)
C(15)-C(16)	1.42(2)	C(16)-C(161)	1.49(2)
C(16)-C(11)	1.43(2)	C(121)-F(11)	1.34(2)
C(121)-F(2)	1.343(14)	C(121)-F(3)	1.35(2)
C(14)-F(4)	1.32(2)	C(14)-F(5)	1.33(2)
C(14)-F(6)	1.33(2)	C(161)-F(7)	1.35(2)
C(161)-F(8)	1.314(14)	C(161)-F(9)	1.358(14)
C(21)-C(22)	1.42(2)	C(22)-C(23)	1.42(2)
C(23)-C(24)	1.40(2)	C(24)-C(25)	1.40(2)
C(25)-C(26)	1.41(2)	C(26)-C(21)	1.41(2)
C(22)-C(221)	1.52(2)	C(26)-C(261)	1.52(2)
C(221)-C(22A)	1.52(3)	C(221)-C(22B)	1.52(2)
C(261)-F(26A)	1.58(2)	C(261)-F(26B)	1.56(2)
Mo(2)-N(3)	1.741(10)	Mo(2)-N(4)	1.760(9)
Mo(2)-C(41)	2.208(11)	Mo(2)-Cl(2)	2.430(3)
Mo(2)-F(10)	2.556(7)	Mo(2)-Cl(4)	2.598(3)
N(3)-C(31)	1.397(14)	N(4)-C(51)	1.42(2)
C(31)-C(32)	1.43(2)	C(32)-C(33)	1.40(2)
C(33)-C(34)	1.35(2)	C(34)-C(35)	1.43(2)
C(35)-C(36)	1.42(2)	C(36)-C(31)	1.41(2)
C(32)-C(321)	1.49(2)	C(36)-C(361)	1.54(2)
C(321)-C(32A)	1.57(2)	C(321)-C(32B)	1.56(2)
C(361)-C(36A)	1.54(2)	C(361)-C(36B)	1.56(2)
C(41)-C(42)	1.43(2)	C(42)-C(43)	1.41(2)
C(43)-C(44)	1.39(2)	C(44)-C(45)	1.38(2)
C(45)-C(46)	1.41(2)	C(46)-C(41)	1.40(2)
C(42)-C(421)	1.49(2)	C(44)-C(441)	1.47(2)
C(46)-C(461)	1.49(2)	C(421)-F(13)	1.346(13)
C(421)-F(14)	1.359(12)	C(421)-F(15)	1.333(14)
C(441)-F(16)	1.30(2)	C(441)-F(17)	1.34(2)
C(441)-F(18)	1.27(2)	C(461)-F(10)	1.330(14)
C(461)-F(11)	1.343(14)	C(461)-F(13)	1.35(2)
C(51)-C(52)	1.44(2)	C(52)-C(53)	1.40(2)
C(53)-C(54)	1.43(2)	C(54)-C(55)	1.39(2)
C(55)-C(56)	1.43(2)	C(56)-C(51)	1.39(2)
C(52)-C(521)	1.49(2)	C(56)-C(561)	1.52(2)

C(521)-C(52A)	1.53(2)	C(521)-C(52B)	1.55(2)
C(561)-F(56A)	1.59(3)	C(561)-F(56B)	1.53(2)
O(1)-C(01)	1.43(2)	O(1)-C(02)	1.45(2)
O(1)-Li(2)	2.00(2)	O(2)-C(03)	1.45(2)
O(2)-C(04)	1.45(2)	O(2)-Li(2)	2.00(2)
O(3)-C(05)	1.36(2)	O(3)-C(06)	1.44(2)
O(3)-Li(1)	1.96(2)	O(4)-C(07)	1.46(2)
O(4)-C(08)	1.44(2)	O(4)-Li(1)	2.10(2)
C(02)-C(03)	1.56(2)	C(06)-C(07)	1.51(2)
Li(1)-Cl(2)#2	2.60(2)	Li(1)-Cl(4)#2	2.37(2)
Li(2)-Cl(4)#2	2.73(2)		

N(1)-Mo(1)-N(2)	109.0(4)	N(1)-Mo(1)-C(11)	105.5(4)
N(2)-Mo(1)-C(11)	94.9(4)	N(1)-Mo(1)-Cl(1)	95.0(3)
N(2)-Mo(1)-Cl(1)	98.3(3)	C(11)-Mo(1)-Cl(1)	150.5(3)
N(1)-Mo(1)-F(9)	170.9(3)	N(2)-Mo(1)-F(9)	80.1(3)
C(11)-Mo(1)-F(9)	73.0(3)	Cl(1)-Mo(1)-F(9)	83.3(2)
N(1)-Mo(1)-Cl(3)	98.5(3)	N(2)-Mo(1)-Cl(3)	152.5(3)
C(11)-Mo(1)-Cl(3)	77.2(3)	Cl(1)-Mo(1)-Cl(3)	78.92(10)
F(9)-Mo(1)-Cl(3)	72.4(2)	Mo(1)-Cl(1)-Li(2)	98.7(5)
Li(1)-Cl(3)-Li(2)	95.5(7)	Li(1)-Cl(3)-Mo(1)	163.2(5)
Li(2)-Cl(3)-Mo(1)	101.2(5)	C(161)-F(9)-Mo(1)	113.3(7)
C(1)-N(1)-Mo(1)	167.2(8)	C(21)-N(2)-Mo(1)	168.5(8)
N(1)-C(1)-C(2)	118.1(10)	N(1)-C(1)-C(6)	121.3(11)
C(1)-C(2)-C(3)	119.1(12)	C(2)-C(3)-C(4)	121.0(13)
C(3)-C(4)-C(5)	120.0(13)	C(4)-C(5)-C(6)	121.1(12)
C(5)-C(6)-C(1)	118.3(11)	C(6)-C(1)-C(2)	120.5(11)
C(1)-C(2)-C(2C)	119.4(11)	C(3)-C(2)-C(2C)	121.5(12)
C(1)-C(6)-C(61)	121.2(11)	C(5)-C(6)-C(61)	120.6(10)
C(2)-C(2C)-C(2A)	111.5(12)	C(2)-C(2C)-C(2B)	107.7(11)
C(2A)-C(2B)-C(2C)	110.4(12)	C(6)-C(61)-C(61A)	111.4(10)
C(6)-C(61)-C(61B)	108.0(10)	C(61A)-C(61)-C(61B)	110.7(11)
C(12)-C(11)-C(16)	113.7(10)	C(12)-C(11)-Mo(1)	130.7(8)
C(16)-C(11)-Mo(1)	115.5(8)	C(13)-C(12)-C(11)	124.3(11)
C(11)-C(12)-C(121)	121.6(10)	C(13)-C(12)-C(121)	114.0(11)
C(12)-C(13)-C(141)	117.8(11)	F(4)-C(14)-F(5)	104.8(12)
F(4)-C(14)-F(6)	106.4(12)	F(5)-C(14)-F(6)	105.8(11)
F(4)-C(14)-F(141)	113.8(11)	F(5)-C(14)-F(141)	112.6(13)
F(6)-C(14)-F(141)	112.7(12)	C(141)-C(15)-C(16)	118.8(11)
C(15)-C(16)-C(11)	123.3(10)	C(11)-C(16)-C(161)	123.8(10)
C(15)-C(16)-C(161)	112.9(10)	F(1)-C(121)-F(2)	107.3(10)
F(1)-C(121)-F(3)	105.2(11)	F(2)-C(121)-F(3)	106.2(10)
F(1)-C(121)-C(12)	112.2(11)	F(2)-C(121)-C(12)	113.7(11)
F(3)-C(121)-C(12)	111.6(10)	C(15)-C(141)-C(13)	122.0(11)
C(15)-C(141)-C(14)	122.4(13)	C(13)-C(141)-C(14)	115.5(12)
F(8)-C(161)-F(7)	107.5(11)	F(8)-C(161)-F(9)	105.3(10)
F(7)-C(161)-F(9)	104.2(10)	F(8)-C(61)-C(16)	114.1(10)
F(7)-C(161)-C(16)	111.5(10)	F(9)-C(161)-C(16)	113.4(10)
N(2)-C(21)-C(26)	121.7(11)	N(2)-C(21)-C(22)	116.7(11)

C(26)-C(21)-C(22)	121.5(11)	C(23)-C(22)-C(21)	117.7(12)
C(23)-C(22)-C(221)	120.5(12)	C(21)-C(22)-C(221)	121.7(12)
C(24)-C(23)-C(22)	120.8(13)	C(24)-C(25)-C(26)	121.0(13)
C(23)-C(24)-C(25)	120.3(13)	C(25)-C(26)-C(21)	118.6(12)
C(25)-C(26)-C(261)	122.1(11)	C(21)-C(26)-C(261)	119.1(11)
C(22A)-C(221)-C(22)	110.6(14)	C(22A)-C(221)-C(22B)	111(2)
C(22)-C(221)-C(22B)	111.9(14)	C(26)-C(261)-C(26B)	112.7(11)
C(26)-C(261)-C(26A)	107.6(11)	C(26B)-C(261)-C(26A)	107.4(11)
N(3)-Mo(2)-N(4)	108.8(4)	N(3)-Mo(2)-C(41)	105.7(4)
N(4)-Mo(2)-C(41)	92.0(4)	N(3)-Mo(2)-Cl(2)	98.0(3)
N(4)-Mo(2)-Cl(2)	98.5(3)	C(41)-Mo(2)-Cl(2)	149.4(3)
N(3)-Mo(2)-F(10)	170.7(3)	N(4)-Mo(2)-F(10)	80.5(3)
C(41)-Mo(2)-F(10)	71.9(3)	Cl(2)-Mo(2)-F(10)	81.5(2)
N(3)-Mo(2)-Cl(4)	98.2(3)	N(4)-Mo(2)-Cl(4)	152.9(3)
C(41)-Mo(2)-Cl(4)	77.6(3)	Cl(2)-Mo(2)-Cl(4)	80.13(11)
F(10)-Mo(2)-Cl(4)	72.5(2)	Mo(2)-Cl(2)-Li(1)#1	95.4(4)
Li(1)#1-Cl(4)-Mo(2)	97.0(5)	Li(1)#1-Cl(4)-Li(2)#1	91.5(6)
Mo(2)-Cl(4)-Li(2)#1	147.1(5)	C(461)-F(10)-Mo(2)	110.1(6)
C(31)-N(3)-Mo(2)	165.7(8)	C(51)-N(4)-Mo(2)	170.1(8)
N(3)-C(31)-C(36)	116.3(10)	N(3)-C(31)-C(32)	121.9(10)
C(36)-C(31)-C(32)	121.9(10)	C(31)-C(32)-C(33)	118.3(11)
C(33)-C(32)-C(321)	120.1(11)	C(31)-C(32)-C(321)	121.6(10)
C(32)-C(33)-C(34)	120.4(12)	C(33)-C(34)-C(35)	122.7(12)
C(34)-C(35)-C(36)	118.8(12)	C(31)-C(36)-C(35)	117.7(11)
C(31)-C(36)-C(361)	122.8(11)	C(35)-C(36)-C(361)	119.4(12)
C(32)-C(321)-C(32B)	114.7(11)	C(32)-C(321)-C(32A)	108.6(12)
C(32B)-C(321)-C(32A)	110.4(13)	C(36)-C(361)-C(36A)	109.9(11)
C(36A)-C(361)-C(36B)	113.0(14)	C(36)-C(361)-C(36B)	110.8(12)
C(42)-C(41)-Mo(2)	130.2(8)	C(46)-C(41)-Mo(2)	116.7(8)
C(46)-C(41)-C(42)	113.1(10)	C(41)-C(42)-C(43)	123.4(11)
C(42)-C(43)-C(44)	119.7(11)	C(43)-C(44)-C(45)	119.8(10)
C(44)-C(45)-C(46)	118.9(11)	C(43)-C(42)-C(421)	115.4(10)
C(41)-C(42)-C(421)	121.2(10)	C(43)-C(44)-C(441)	120.1(11)
C(45)-C(44)-C(441)	120.1(11)	C(41)-C(46)-C(461)	121.9(11)
C(45)-C(46)-C(461)	113.0(10)	F(15)-C(421)-F(13)	108.0(10)
F(15)-C(421)-F(14)	104.8(9)	F(13)-C(421)-F(14)	104.7(8)
F(15)-C(421)-C(422)	113.3(9)	F(13)-C(421)-C(422)	113.2(10)
F(14)-C(421)-C(422)	112.1(10)	F(18)-C(441)-F(16)	108.2(14)
F(18)-C(441)-F(17)	104.7(14)	F(16)-C(441)-F(17)	108(13)
F(18)-C(441)-C(44)	114.6(14)	F(16)-C(441)-C(44)	113.1(12)
F(17)-C(441)-C(44)	114.2(12)	F(10)-C(461)-F(11)	105.1(10)
F(10)-C(461)-F(12)	105.6(10)	F(11)-C(461)-F(12)	104.6(10)
F(10)-C(461)-C(46)	114.6(10)	F(11)-C(461)-C(46)	113.5(10)
F(12)-C(461)-C(46)	112.6(11)	C(56)-C(51)-N(4)	118.4(12)
C(56)-C(51)-C(52)	122.4(12)	N(4)-C(51)-C(52)	119.1(11)
C(53)-C(52)-C(51)	118.5(12)	C(53)-C(52)-C(521)	118.6(13)
C(51)-C(52)-C(521)	122.5(11)	C(52)-C(53)-C(54)	119(2)
C(53)-C(54)-C(55)	122(2)	C(54)-C(55)-C(56)	120(2)
C(51)-C(56)-C(55)	118(2)	C(51)-C(56)-C(561)	121.4(13)

C(55)-C(56)-C(561)	120.2(13)	C(52)-C(521)-C(52A)	110.5(12)
C(52)-C(521)-C(52B)	114.4(12)	C(52A)-C(521)-C(52B)	109.6(13)
C(56)-C(561)-C(56B)	111.2(13)	C(56)-C(561)-C(56A)	109(2)
C(56B)-C(561)-C(56A)	109(2)	C(01)-O(1)-C(02)	111.4(10)
C(01)-O(1)-Li(2)	127.9(10)	C(02)-O(1)-Li(2)	107.2(10)
C(03)-O(2)-C(04)	110.1(10)	C(03)-O(2)-Li(2)	108.6(10)
C(04)-O(2)-Li(2)	123.0(10)	C(05)-O(3)-C(06)	114.2(12)
C(05)-O(3)-Li(1)	127.1(11)	C(06)-O(3)-Li(1)	106.1(11)
C(08)-O(4)-C(07)	115.2(11)	C(08)-O(4)-Li(1)	124.9(10)
C(07)-O(4)-Li(1)	104.7(9)	O(1)-C(02)-C(03)	107.7(11)
O(2)-C(03)-C(02)	104.4(11)	O(3)-C(06)-C(07)	108.9(13)
O(4)-C(07)-C(06)	106.2(12)	O(3)-Li(1)-O(4)	85.3(9)
O(3)-Li(1)-Cl(4)#2	128.3(11)	O(4)-Li(1)-Cl(4)#2	146.2(10)
O(3)-Li(1)-Cl(3)	96.6(8)	O(4)-Li(1)-Cl(3)	91.8(8)
Cl(4)#2-Li(1)-Cl(3)	88.0(6)	O(3)-Li(1)-Cl(2)#2	99.7(7)
O(4)-Li(1)-Cl(2)#2	90.3(7)	Cl(4)#2-Li(1)-Cl(2)#2	81.2(6)
Cl(3)-Li(1)-Cl(2)#2	163.7(8)	O(1)-Li(2)-O(2)	85.2(9)
O(1)-Li(2)-Cl(3)	141.8(11)	O(2)-Li(2)-Cl(3)	132.9(10)
O(1)-Li(2)-Cl(1)	99.1(8)	O(2)-Li(2)-Cl(1)	92.1(8)
Cl(3)-Li(2)-Cl(1)	80.0(6)	O(1)-Li(2)-Cl(4)#2	88.3(7)
O(2)-Li(2)-Cl(4)#2	103.4(8)	Cl(3)-Li(2)-Cl(4)#2	84.9(7)
Cl(1)-Li(2)-Cl(4)#2	163.3(9)		

Table 2.3: *Bond lengths (Å) and angles (°) in the complex* $[Mo(NAr)_2(Ar^F)Cl.LiCl(dme)]_2$. *Estimated standard deviations are in parentheses.*

2.2.7 Synthesis of $V(Ar^F)_2Cl(thf)$

Given the precedent of trismesitylvanadium (III)[18], it was decided to target the analogous homoleptic Ar^F complex. While sigma-bonded homoleptic alkyl compounds of transition metals are now well-characterised and have been the focus of much study, the analogous aryl systems have received relatively little attention.[19] Early reports have described often poorly characterised species, although the synthesis and reaction chemistry of several examples have recently been reported and X-ray structural studies provided for their conclusive identification.[20]

Trismesitylvanadium was first reported by Seidel and Kreisel in 1974, prepared as shown in equation 2.5.

$$VCl_3(thf)_3 + 3mesMgBr \xrightarrow[-3thf]{-3MgClBr} V(mes)_3 \qquad (2.5)$$

However, reaction of 3 equivalents of Ar^FLi with $VCl_3(thf)_3$ affords the intense dark blue-black coloured $V(Ar^F)_2Cl(thf)$, **4**, rather than $V(Ar^F)_3$.

$$VCl_3(thf)_3 + 3Ar^FLi \xrightarrow{-2LiCl} V(Ar^F)_2Cl(thf) \qquad (2.6)$$

4

Complex **4** is paramagnetic and the EPR spectrum clearly shows 8 lines coupled to fluorine as expected for a vanadium (III) complex ($I=^7/_2$).

2.2.8 Molecular structure of $V(Ar^F)_2Cl(thf)$

Crystals of complex **4** were grown from a pentane solution at -20°C and the structure determined by Prof. W. Clegg. The structure is presented in figure 2.5. Pertinent bond lengths and angles are collated in table 2.4. The complex is pseudo-octahedral, with interactions between one of the fluorines on each Ar^F substituent and the vanadium centre. The V-C bond distances in complex **4** are 2.159(4) and 2.145(4) Å, slightly longer than those in $V(mes)_3(thf)$ (which range from 2.009(6) to 2.116(7)Å)[20]. The weak V···F interactions (2.306(2) and 2.378(2)Å) are also believed to contribute to the lengthening of the V-C bond, by compensating for the electron-deficient nature of the vanadium centre.

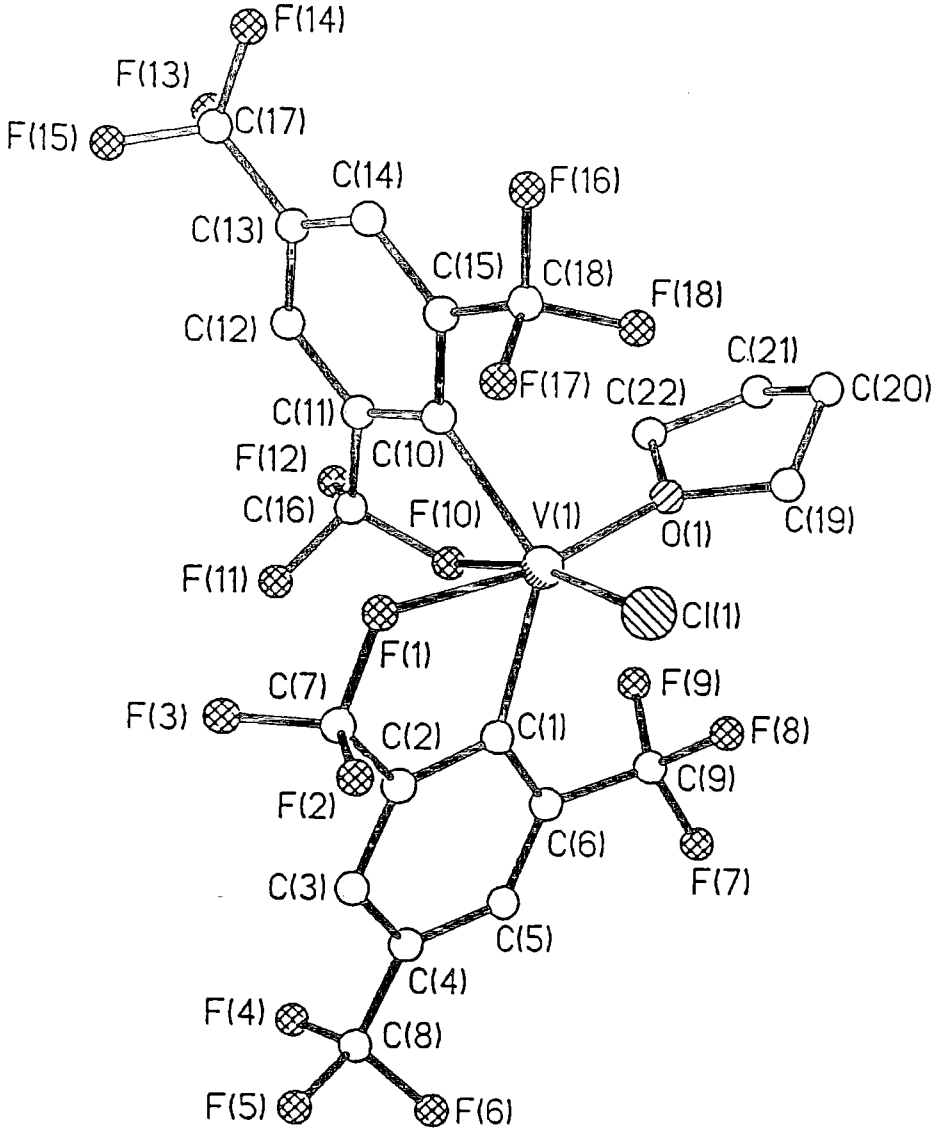

Figure 2.5: *The molecular structure of complex 4*

V(1)-O(1)	2.013(3)	V(1)-C(1)	2.145(4)
V(1)-C(10)	2.159(4)	V(1)-Cl(1)	2.2310(13)
V(1)-F(1)	2.306(2)	V(1)-F(10)	2.378(2)
C(1)-C(2)	1.394(6)	C(1)-C(6)	1.412(5)
C(2)-C(3)	1.393(6)	C(3)-C(4)	1.383(6)
C(4)-C(5)	1.382(6)	C(5)-C(6)	1.383(6)
C(2)-C(7)	1.503(6)	C(4)-C(8)	1.497(6)
C(6)-C(9)	1.499(6)	C(7)-F(1)	1.369(5)
C(7)-F(2)	1.335(5)	C(7)-F(3)	1.323(5)
C(8)-F(4)	1.333(5)	C(8)-F(5)	1.327(5)
C(8)-F(6)	1.345(5)	C(9)-F(7)	1.347(5)
C(9)-F(8)	1.334(5)	C(9)-F(9)	1.355(5)
C(10)-C(11)	1.401(5)	C(10)-C(15)	1.420(5)
C(11)-C(12)	1.395(5)	C(12)-C(13)	1.385(5)
C(13)-C(14)	1.376(5)	C(14)-F(15)	1.389(5)
C(11)-C(16)	1.491(6)	C(13)-C(17)	1.502(5)
C(15)-C(18)	1.493(5)	C(16)-F(10)	1.378(4)
C(16)-F(11)	1.334(5)	C(16)-F(12)	1.322(5)
C(17)-F(13)	1.301(6)	C(17)-F(14)	1.312(7)
C(17)-F(15)	1.292(7)	C(17)-F(13A)	1.302(13)
C(17)-F(14A)	1.27(2)	C(17)-F(15A)	1.271(13)
C(18)-F(16)	1.344(4)	C(18)-F(17)	1.354(5)
C(18)-F(18)	1.333(5)	O(1)-C(19)	1.480(5)
O(1)-C(22)	1.469(5)	C(19)-C(20)	1.475(7)
C(20)-C(21)	1.478(8)	C(21)-C(22)	1.477(7)

O(1)-V(1)-C(1)	118.33(14)	O(1)-V(1)-C(10)	94.01(13)
C(1)-V(1)-C(10)	128.7(2)	O(1)-V(1)-Cl(1)	96.72(94)
C(1)-V(1)-Cl(1)	95.66(11)	C(10)-V(1)-Cl(1)	120.39(11)
O(1)-V(1)-F(1)	167.72(10)	C(1)-V(1)-F(1)	73.28(12)
C(10)-V(1)-F(1)	74.60(12)	Cl(1)-V(1)-F(1)	85.49(8)
O(1)-V(1)-F(10)	84.80(10)	C(1)-V(1)-F(10)	72.97(12)
C(10)-V(1)-F(10)	71.62(11)	Cl(1)-V(1)-F(10)	167.60(7)
F(1)-V(1)-F(10)	95.63(9)	C(2)-C(1)-C(6)	113.6(4)
C(2)-C(1)-V(1)	118.1(3)	C(6)-C(1)-V(1)	128.0(3)
C(1)-C(2)-C(3)	124.3(4)	C(2)-C(3)-C(4)	119.3(4)
C(3)-C(4)-C(5)	118.9(4)	C(4)-C(5)-C(6)	120.3(4)
C(5)-C(6)-C(1)	123.4(4)	C(1)-C(2)-C(7)	118.5(4)
C(2)-C(3)-C(7)	117.0(4)	C(3)-C(4)-C(8)	120.6(4)
C(5)-C(4)-C(8)	120.5(4)	C(1)-C(6)-C(9)	118.5(4)
C(5)-C(6)-C(9)	118.1(4)	F(1)-C(7)-F(2)	105.7(3)
F(2)-C(7)-F(3)	106.8(4)	F(1)-C(7)-F(3)	106.2(3)
C(2)-C(7)-F(1)	110.1(4)	C(2)-C(7)-F(2)	113.1(3)
C(2)-C(7)-F(3)	114.4(4)	C(7)-F(1)-V(1)	118.3(2)
F(4)-C(8)-F(5)	106.9(4)	F(5)-C(8)-F(6)	106.4(4)
F(4)-C(8)-F(6)	105.8(4)	C(4)-C(8)-F(4)	112.4(4)
C(4)-C(8)-F(5)	112.9(4)	C(4)-C(8)-F(6)	111.9(4)
F(7)-C(9)-F(8)	106.8(3)	F(8)-C(9)-F(9)	105.7(3)

F(7)-C(9)-F(9)	105.7(3)	C(6)-C(9)-F(7)	113.0(4)
C(6)-C(9)-F(8)	112.4(4)	C(6)-C(9)-F(9)	112.7(3)
C(11)-C(10)-C(15)	113.2(3)	C(11)-C(10)-V(1)	118.4(3)
C(15)-C(10)-V(1)	128.4(3)	C(11)-C(10)-C(12)	125.2(4)
C(11)-C(12)-C(13)	118.0(4)	C(12)-C(13)-C(14)	120.4(3)
C(13)-C(14)-C(15)	120.0(3)	C(14)-C(15)-C(10)	123.2(3)
C(10)-C(10)-C(16)	117.8(3)	C(12)-C(11)-C(16)	117.0(3)
C(12)-C(13)-C(17)	119.5(3)	C(14)-C(13)-C(17)	120.2(3)
C(14)-C(15)-C(18)	117.0(3)	C(10)-C(15)-C(18)	119.8(3)
F(10)-C(16)-F(11)	114.8(3)	F(11)-C(16)-F(12)	107.2(3)
F(10)-C(16)-F(12)	105.7(3)	C(11)-C(16)-F(10)	109.6(3)
C(11)-C(16)-F(11)	113.7(4)	C(11)-C(16)-F(12)	115.0(3)
C(16)-F(10)-V(1)	112.7(2)	F(13)-C(17)-F(14)	106.9(6)
F(14)-C(17)-F(15)	107.4(7)	F(13)-C(17)-F(15)	105.8(5)
F(13A)-C(17)-F(14A)	101.7(13)	F(14A)-C(17)-F(15A)	105(2)
F(13A)-C(17)-F(15A)	105(2)	C(13)-C(17)-F(13)	103.0(4)
C(13)-C(17)-F(14)	112.2(4)	C(13)-C(17)-F(15)	111.1(4)
C(13)-C(17)-F(13A)	112.1(7)	C(13)-C(17)-F(14A)	114.3(8)
C(13)-C(17)-F(15A)	116.6(7)	F(16)-C(18)-F(17)	105.1(3)
F(17)-C(18)-F(18)	106.3(3)	F(16)-C(18)-F(18)	106.5(3)
C(15)-C(18)-F(16)	113.1(3)	C(15)-C(18)-F(17)	111.7(3)
C(15)-C(18)-F(18)	113.5(3)	C(22)-O(1)-C(19)	108.6(3)
C(22)-O(1)-V(1)	124.9(2)	C(19)-O(1)-V(1)	125.6(3)
C(20)-C(19)-O(1)	104.8(4)	C(19)-C(20)-C(21)	105.1(5)
C(20)-C(21)-C(22)	105.7(5)	C(21)-C(22)-O(1)	105.7(4)

Table 2.4: *Bond lengths (Å) and angles (°) in the compound* $V(Ar^F)_2Cl(thf)$. *Estimated standard deviations are in parentheses.*

2.2.9 Synthesis of $V(Ar^F)_3$-O-Li$(thf)_3$

Dr. C. Redshaw from our group has shown that when the same starting material, $VCl_3(thf)_3$, is reacted with a slight excess of three equivalents of Ar^FLi in thf, the light blue compound $V(Ar^F)_3$-O-Li$(thf)_3$, **5**, is obtained.

$$VCl_3(thf)_3 + 3Ar^FLi \xrightarrow{-3LiCl} V(Ar^F)_3\text{-O-Li}(thf)_3 \qquad (2.7)$$

5

Samples of complex **5** are EPR silent, either as solids or in toluene at room temperature; a similar situation has been reported for tetrabenzylvanadium.[21] The magnetic moment (Evans balance) of solid **5** (2.0 BM) is higher than the spin-only value, a feature previously observed for fluorinated derivatives of V(IV).[22] Given the oxophilic nature of vanadium, the formation of the V-O-Li moiety may be explained by assuming fragmentation of a thf or ether molecule in the presence of the lithium reagent; there are numerous examples of such an attack in the literature.[23]

2.2.10 Molecular structure of $V(Ar^F)_3$-O-Li$(thf)_3$

Turquoise hexagonal crystals of **5** suitable for a structural determination were obtained from a saturated solution of the reaction mother liquor. The structure was determined by Prof W. Clegg's group at Newcastle University.

The pertinent feature of the structure is the close approach of a single fluorine atom from each Ar^F ligand to the vanadium centre. As shown in

figures 2.6 and 2.7, complex **5** adopts a capped octahedral geometry, with the lithium-oxygen fragment capping the F-F-F face. A crystallographically-imposed threefold axis of symmetry runs through the Li-O(1)-V vector. It appears that the octahedral skeleton formed from the three fluorine and three carbon atoms is somewhat flattened, forming a chair-like arrangement with the vanadium atom occupying a position between the C(1)-C(1a)-C(1b) plane and the F(3)-F(3a)-F(3b) plane.

Complexes of vanadium (IV) normally contain the VO^{2+} ion.[24] In such compounds the V=O bonds are much shorter (1.55-1.68Å) than that observed in **5** (V-O(1) = 1.835(3)Å). Consistent with this there is no strong V=O stretching band in the IR spectrum of **5** between 950-1000cm^{-1}.

The V-C bond distances are 2.179(4)Å (table 2.5), again appreciably longer than in $V(mes)_3(thf)$[20]; the V···F distance is 2.668(2) Å (the V-F distance to the nearest non-interacting fluorine on the same substituent is 3.187Å). Although this is larger than the value in complex **4**, it could be attributed to the presence of three M···F interactions in complex **5** compared with only two such interactions in **4**.

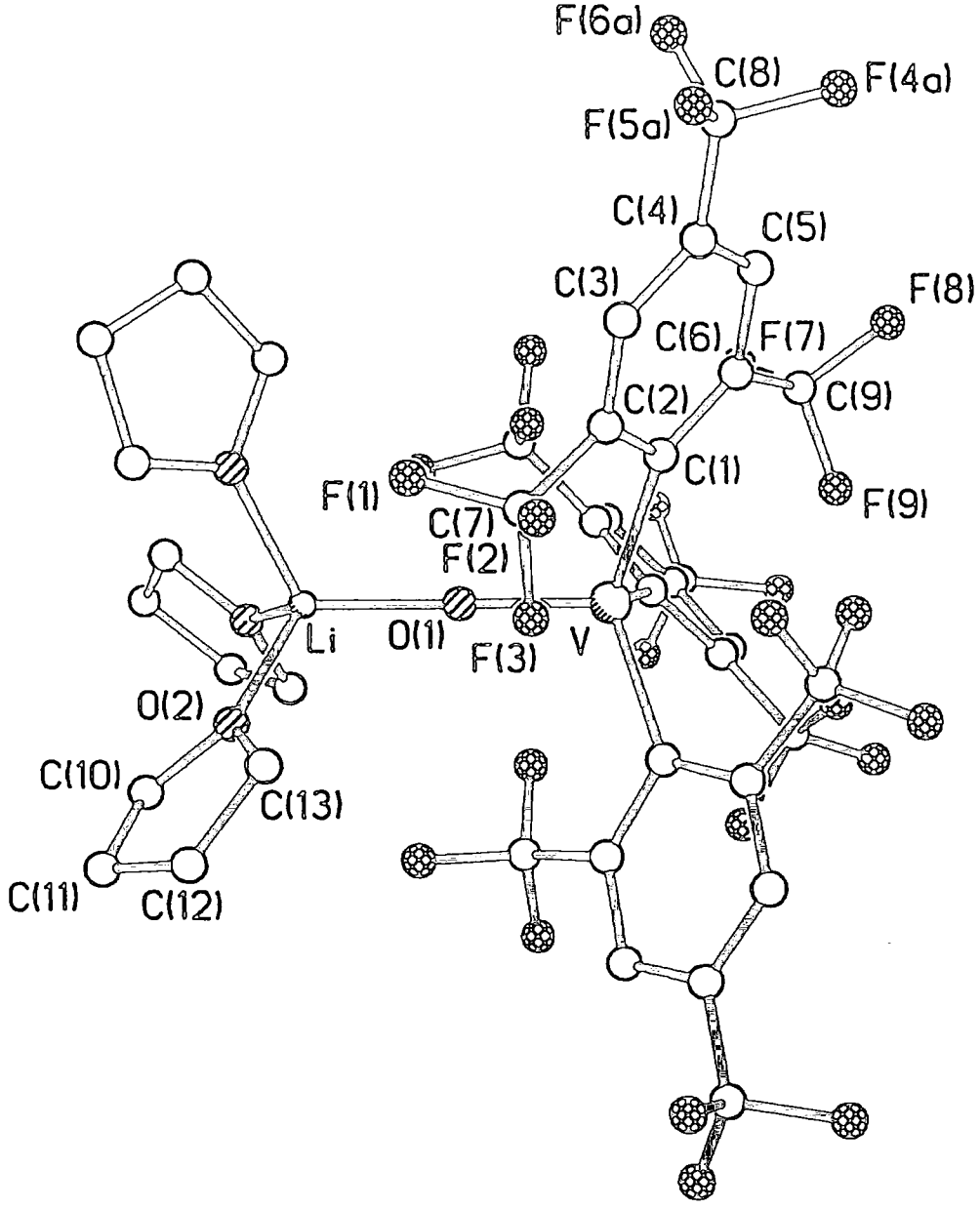

Figure 2.6: *The molecular structure of complex 5*

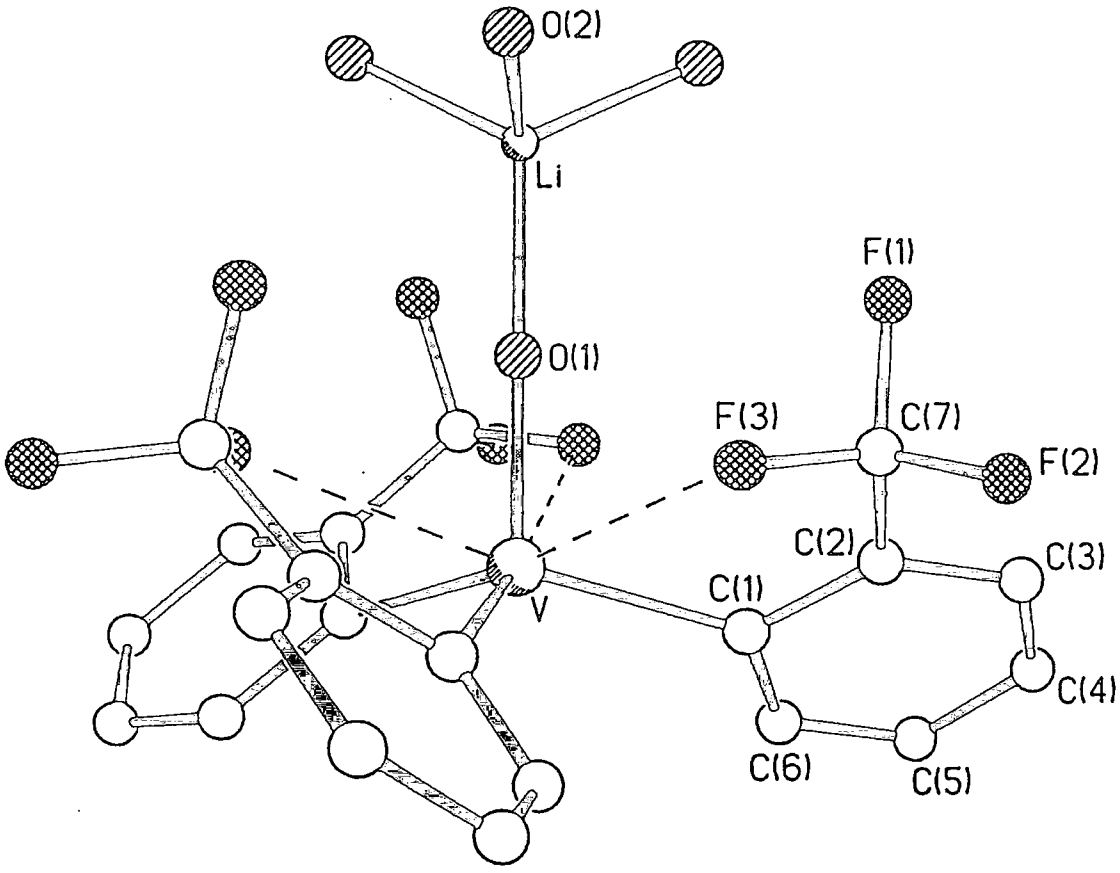

Figure 2.7: *Simplified view of the structure of complex 5*

V-O(1)	1.835(3)	V-C(1a)	2.179(4)
V-C(1)	2.179(4)	V-Cl(1b)	2.179(4)
C(1)-C(6)	1.411(5)	C(1)-C(2)	1.415(5)
C(2)-C(3)	1.373(7)	C(3)-C(4)	1.373(7)
C(4)-C(5)	1.368(6)	C(5)-C(6)	1.391(5)
C(2)-C(7)	1.504(5)	C(4)-C(8)	1.489(6)
C(6)-C(9)	1.510(6)	C(7)-F(1)	1.337(4)
C(7)-F(2)	1.345(5)	C(7)-F(3)	1.352(4)
C(8)-F(4A)	1.38(2)	C(8)-F(4B)	1.23(2)
C(8)-F(5A)	1.228(13)	C(8)-F(5B)	1.40(2)
C(8)-F(6A)	1.298(13)	C(8)-F(6B)	1.203(14)
C(9)-F(7)	1.344(4)	C(9)-F(8)	1.343(4)
C(9)-F(9)	1.335(5)	O(1)-Li	1.856(11)
Li-O(2a)	1.939(5)	Li-O(2b)	1.940(5)
Li-O(2)	1.939(5)	O(2)-C(10)	1.426(5)
O(2)-C(13)	1.427(6)	C(10)-C(11)	1.488(7)
C(11)-C(12)	1.453(9)	C(12)-C(13)	1.451(7)
V-F(3)	2.668(2)		

O(1)-V-C(1a)	105.46(9)	O(1)-V-C(1)	105.46(9)
O(1)-V-C(1b)	105.46(9)	C(1a)-V-C(1)	113.16(8)
C(1a)-V-C(1b)	113.16(8)	C(1)-V-C(1b)	113.17(8)
C(6)-C(1)-C(2)	112.3(3)	C(6)-C(1)-V	127.6(3)
C(2)-C(1)-V	119.8(3)	C(1)-C(2)-C(3)	124.4(4)
C(3)-C(2)-C(7)	113.9(3)	C(1)-C(2)-C(7)	121.7(3)
C(2)-C(3)-C(4)	119.9(4)	C(3)-C(4)-C(5)	119.0(4)
C(5)-C(4)-C(8)	120.5(5)	C(3)-C(4)-C(8)	120.5(5)
C(4)-C(5)-C(6)	120.4(4)	C(5)-C(6)-C(1)	123.9(4)
C(5)-C(6)-C(9)	115.0(4)	C(1)-C(6)-C(9)	121.1(3)
F(1)-C(7)-F(2)	105.7(3)	F(1)-C(7)-F(3)	106.0(3)
F(2)-C(7)-F(3)	105.7(3)	F(1)-C(7)-C(2)	113.6(3)
F(2)-C(7)-C(2)	112.3(3)	F(3)-C(7)-C(2)	112.9(3)
F(4A)-C(8)-F(5A)	103.9(13)	F(4A)-C(8)-F(6A)	101.3(11)
F(5A)-C(8)-F(6A)	110.7(14)	F(4B)-C(8)-F(5B)	100.4(12)
F(6B)-C(8)-F(4B)	112(2)	F(5B)-C(8)-F(6B)	103(2)
F(4A)-C(8)-C(4)	109.9(7)	F(5A)-C(8)-C(4)	117.4(7)
F(6A)-C(8)-C(4)	112.0(8)	F(4B)-C(8)-C(4)	111.9(9)
F(5B)-C(8)-C(4)	111.3(9)	F(6B)-C(8)-C(4)	116.5(8)

F(7)-C(9)-F(8)	104.9(3)	F(9)-C(9)-F(8)	106.1(3)
F(7)-C(9)-F(8)	106.7(3)	C(6)-C(9)-F(9)	113.2(3)
C(6)-C(9)-F(8)	112.7(3)	C(6)-C(9)-F(7)	112.6(3)
V-O(1)-Li	180.0	O(1)-Li-O(2a)	113.7(3)
O(1)-Li-O(2b)	113.7(3)	O(2a)-Li-O(2a)	104.9(3)
O(1)-Li-O(2)	113.7(3)	O(2a)-Li-O(2)	104.9(3)
O(2b)-Li-O(2)	104.9(3)	C(10)-O(2)-C(13)	109.7(3)
C(10)-O(2)-Li	123.9(3)	C(13)-O(2)-Li	126.1(3)
O(2)-C(10)-C(11)	106.4(4)	C(12)-C(11)-C(10)	106.1(5)
C(13)-C(12)-C(11)	107.7(5)	C(12)-C(13)-O(2)	107.7(4)

Table 2.5: *Bond lengths (Å) and angles (°) for the compound* $V(Ar^F)_3$-O-$Li(thf)_3$. *Estimated standard deviations are in parentheses.*

2.2.11 Synthesis of $Cr(Ar^F)_2(PMe_3)_2$

In work carried out in collaboration with Dr. C. Redshaw it was shown that $Cr(Ar^F)_2(PMe_3)_2$ may be isolated as an orange-red air- and moisture-sensitive compound in moderate yield (40-50% yield) upon treatment of $CrCl_2(thf)$ with two equivalents of Ar^FLi in the presence of excess PMe_3 (equation 2.8).

$$CrCl_2(thf) + 2Ar^FLi \xrightarrow[-2LiCl]{2PMe_3} Cr(PMe_3)_2(Ar^F)_2 \qquad (2.8)$$

6

The ^1H NMR spectrum of **6** shows broad contact-shifted resonances for the PMe_3 and aryl hydrogens at δ = -33.4 and 21.3 ppm respectively, which compare with the shifts of δ -26.2 and 33.8 for its protio-mesityl analogue.[25] In the ^{19}F NMR spectrum, the *para* $-CF_3$ group appears at δ -63 ppm while the *ortho*-CF_3 line is broadened into the base-line.

2.2.12 Molecular structure of $Cr(Ar^F)_2(PMe_3)_2$

Red prismatic crystals suitable for an X-ray crystallographic study were grown from a saturated pentane solution maintained at -20°C. A crystal of dimensions 0.34 x 0.35 x 0.20 mm was selected for study. The data were collected and solved by Prof. J.A.K. Howard and Mr. J. W. Yao within this department. The molecular structure is shown in figure 2.8 and selected bond distances and angles are collected in table 2.6.

The molecule possesses square planar geometry with the two bulky Ar^F groups positioned mutually *trans*. The Cr-C and Cr-P bond distances

[2.519(1)and 2.184(4) Å] are somewhat longer than those found in $[Cr(PMe_3)_2(2,4,6\text{-}Me_3C_6H_2)_2]$ [2.462(2)and 2.130(6) Å].[25] The metal-carbon bond is expected to be somewhat longer due to the increased electron-withdrawing nature of the fluorinated substituents. However, presumably electrostatic repulsions between the *ortho*-CF_3 groups force the two Ar^F ligands further apart and therefore reduce the volume of space available for the phosphine ligands (hence, the increased M-P distance). In most of the Ar^F main group compounds, structural analysis has also shown that the M-C bond distance is longer than in the mesityl analogues, reflecting the larger steric demands of the Ar^F substituent. The lengthening could also, as in $Sn(Ar^F)_2$, be due to repulsive interactions between the electropositive tin atom and the *ipso* carbon (as mentioned previously in section 1.1.1), which has been made electropositive due to the electron-withdrawing CF_3 groups.[2]

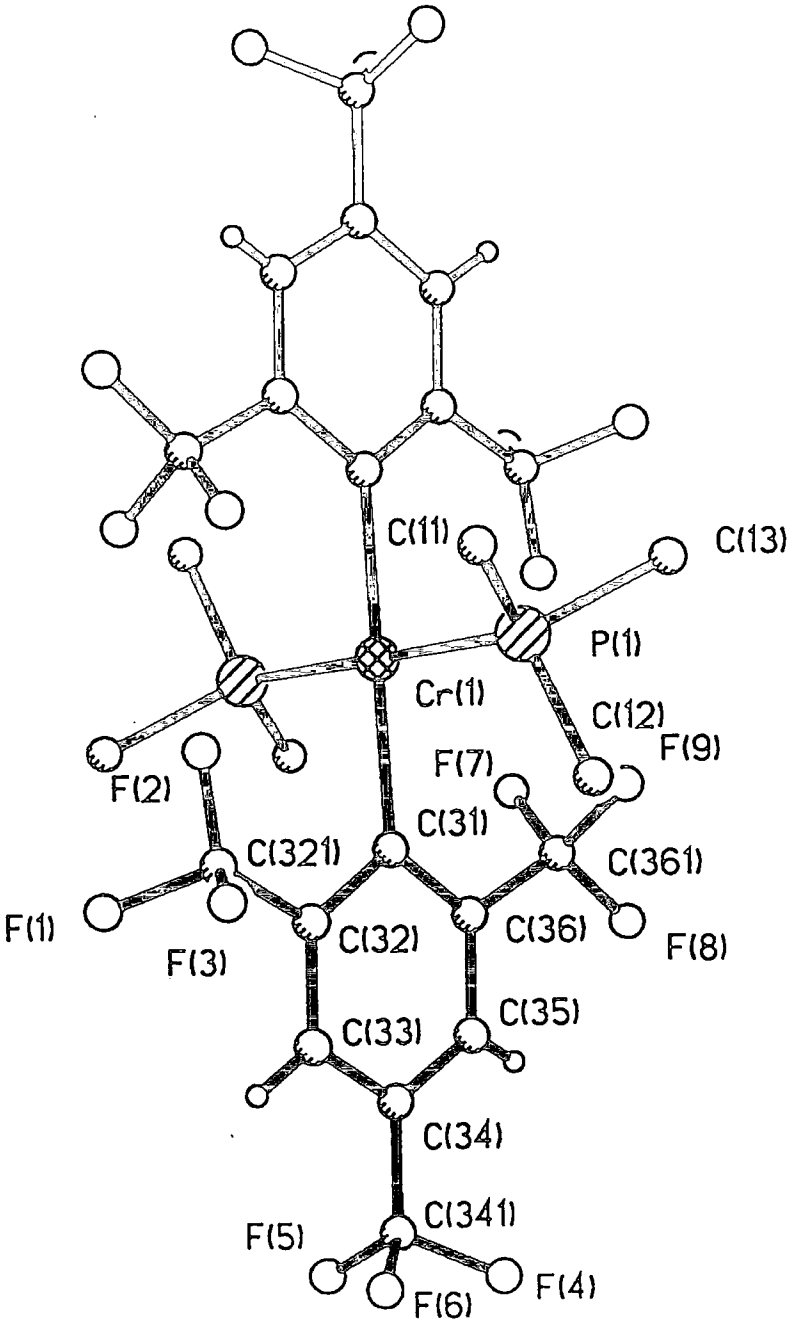

Figure 2.8: *The molecular structure of complex 6*

Cr(1)-C(31)	2.184(4)	Cr(1)-P(1)	2.5190(14)
P(1)-C(11)	1.782(9)	P(1)-C(12)	1.842(8)
P(1)-C(13)	1.872(8)	C(31)-C(36)	1.407(7)
C(31)-C(32)	1.414(6)	C(32)-C(33)	1.386(7)
C(33)-C(34)	1.369(8)	C(34)-C(35)	1.360(8)
C(35)-C(36)	1.392(7)	C(32)-C(321)	1.486(8)
C(321)-F(1)	1.393(12)	C(321)-F(2)	1.288(9)
C(321)-F(3)	1.304(12)	C(34)-C(341)	1.493(8)
C(341)-F(4)	1.311(12)	C(341)-F(5)	1.27(2)
C(341)-F(6)	1.358(9)	C(36)-C(361)	1.502(7)
C(361)-F(7)	1.338(7)	C(361)-F(8)	1.342(7)
C(361)-F(9)	1.324(7)		

C(31)#1-Cr(1)-C(31)	180.0	C(31)#1-Cr(1)-P(1)	89.42(12)
C(31)-Cr(1)-P(1)	90.58(12)	C(31)#1-Cr(1)-P(1)#1	90.58(12)
C(31)-Cr(1)-P(1)#1	89.42(12)	P(1)-Cr(1)-P(1)#1	180.0
C(11)-P(1)-C(12)	103.6(5)	C(11)-P(1)-C(13)	102.1(5)
C(12)-P(1)-C(13)	98.7(5)	C(11)-P(1)-Cr(1)	118.2(4)
C(12)-P(1)-Cr(1)	117.3(3)	C(13)-P(1)-Cr(1)	114.1(3)
C(11A)-P(1)-Cr(1)	112.4(8)	C(12A)-P(1)-Cr(1)	118.9(8)
C(13A)-P(1)-Cr(1)	114.4(8)	C(11A)-P(1)-C(12A)	104(2)
C(12A)-P(1)-C(13A)	104.9(14)	C(11A)-P(1)-C(13A)	100(2)
C(36)-C(31)-Cr(1)	124.8(3)	C(32)-C(31)-Cr(1)	122.7(3)
C(33)-C(32)-C(31)	124.1(5)	C(34)-C(33)-C(32)	119.8(5)
C(35)-C(34)-C(33)	119.4(5)	C(34)-C(35)-C(36)	120.4(5)
C(35)-C(36)-C(31)	127.3(5)	C(36)-C(31)-C(32)	112.5(4)
C(31)-C(32)-C(321)	120.4(4)	C(33)-C(32)-C(321)	115.4(5)
C(33)-C(34)-C(341)	120.6(6)	C(35)-C(34)-C(341)	120.0(6)
C(31)-C(36)-C(361)	119.3(4)	C(35)-C(36)-C(361)	117.0(5)
C(32)-C(33)-H(33)	122(3)	C(34)-C(33)-H(33)	119(3)
C(34)-C(35)-H(35)	123(4)	C(36)-C(35)-H(35)	117(4)
F(1)-C(321)-F(2)	101.7(8)	F(2)-C(321)-F(3)	112.7(10)
F(1)-C(321)-F(3)	101.9(9)	F(1A)-C(321)-F(2A)	105.9(12)
F(2A)-C(321)-F(3A)	104.2(12)	F(1A)-C(321)-F(3A)	103.4(12)
F(1)-C(321)-C(32)	109.2(7)	F(2)-C(321)-C(32)	117.2(5)
F(3)-C(321)-C(32)	112.4(7)	F(1A)-C(321)-C(32)	110.5(8)
F(2A)-C(321)-C(32)	112.7(7)	F(3A)-C(321)-C(32)	119.0(8)
F(4)-C(341)-F(5)	115.5(12)	F(5)-C(341)-F(6)	109.6(13)
F(4)-C(341)-F(6)	87.4(9)	F(4A)-C(341)-F(5A)	103(2)
F(5A)-C(341)-F(6)	83.3(14)	F(4A)-C(341)-F(6)	129(2)
F(4)-C(341)-C(34)	112.6(7)	F(5)-C(341)-C(34)	117.2(10)
F(4A)-C(341)-C(34)	113.8(9)	F(5A)-C(341)-C(34)	110.7(14)
C(341)-F(6)-F(5A)	46.5(10)	C(341)-F(5A)-F(6)	50.1(11)
F(6)-C(341)-C(34)	110.5(7)	F(7)-C(361)-F(8)	102.5(6)
F(8)-C(361)-F(9)	106.0(5)	F(7)-C(361)-F(9)	106.2(6)
F(7A)-C(361)-F(8A)	104(2)	F(8A)-C(361)-F(9A)	109(2)
F(7A)-C(361)-F(9A)	108(2)	F(7)-C(361)-C(36)	113.7(4)
F(8)-C(361)-C(36)	114.6(4)	F(9)-C(361)-C(36)	113.0(4)

F(7A)-C(361)-C(36)	113.4(7)	F(8A)-C(361)-C(36)	112.8(10)
F(9A)-C(361)-C(36)	109.2(9)		

Table 2.6: *Bond lengths (Å) and angles (°) in* $Cr(Ar^F)_2(PMe_3)_2$. *Estimated standard deviations are in parentheses.*

2.2.13 Attempts to synthesise other transition metal complexes

When reacted with the following metal substrates decomposition of the Ar^FLi was observed and no σ-Ar^F complexes could be isolated: $CrCl_3(thf)_3$, $TiCl_3(thf)_3$, $TiCl_4(thf)_2$, $ZrCl_4(thf)_2$, $TiCl_4$, $Re(O)Cl_3(PPh_3)_2$, $W(O)Cl_4$, $W(NPh)Cl_4$, WCl_6, $MoCl_5$, $TaCl_5$, $NbCl_5$, $CpNbCl_4$, $NbCl_3(dme)$ and $V(O)Cl_3$. It can be concluded that reaction has to occur immediately after addition of the Ar^FLi if it is to occur at all or perhaps that certain metal complexes catalyse its decomposition.

Attempts to use the softer organozinc reagent $Zn(Ar^F)_2$ and the Grignard with a selection of the above metal chlorides also failed to produce isolable complexes.

2.3 Discussion of M···F interactions in complexes 1-6

The synthetic and structural study described above firmly establishes the Ar^F ligand in transition metal co-ordination chemistry. An interesting feature of these compounds is the presence of weak metal-fluorine interactions, precedent for which had previously been established in main group systems. The nature of the M···F interactions will be examined in a little more detail in the following sections.

2.3.1 Main group Ar^F compounds

Interactions between the metal atom and the ortho fluorines have been proposed as a significant stabilising effect in main group chemistry. Evidence for these interactions is that the X-F distances (X = main group elements) lie between the sum of the Van der Waals radii and the covalent distance for the X-F bonds (table 2.7).

Compound	Covalent distance/ Å	Sum of Van der Waals Radii/Å (ref 26)	Distance in compound/Å
$Sn(Ar^F)_2$	2.12	1.47 + 2.17 = 3.64 (26a)	2.746(4)
$In(Ar^F)_3$	2.16	3.40 (26b)	2.762(7)
$[Li(Ar^F)\cdot Et_2O]_2$	1.95	1.47 + 1.82 = 3.29 (26a)	2.252(12)

Table 2.7: *Comparison of M···F Bond Distances in Main Group Ar^F Complexes to the M-F covalent Bond Distance and to the Sum of theVan der Waals radii.*

These weak interactions can sometimes be detected in solution by NMR. In $Sn(Ar^F)_2$ fluorine coupling can be observed in the ^{119}Sn NMR spectrum which is split into 13 lines by coupling to the fluorine atoms of the *ortho*-trifluoromethyl groups ($^1J_{Sn-F}$ 239.5Hz).[2] In $Bi(Ar^F)_3$ only one signal is seen for all of the fluorine atoms in the *ortho*-CF_3 groups at room temperature.[4] On cooling to -90° two signals are observed, indicating that rotation about the Bi-C bond is frozen out at this temperature. A barrier to rotation of 38.5 $kJmol^{-1}$ has been calculated.

2.3.2 Transition metal - fluorine interactions

Examples of C-F···M interactions in transition metal systems are rare and historically serendipitious. In many cases, it has not proved easy to establish without ambiguity the strength of the M···F interactions, due to the lack of Van der Waals radii values for the transition metals. In 1987, Crabtree and co-workers provided the first spectroscopic evidence of fluorocarbon co-ordination in solution with the observation of a significant upfield shift in the ^{19}F NMR spectrum for the 8-fluoroquinoline complex $\{IrH_2(PPh_3)_2L\}(SbF_6)$ (L=8-fluoroquinoline)[27] (figure 2.9). This evidence was further backed up by the crystal structure which confirms that the fluoroquinoline is chelated via a C-F bond. The F···Ir distance, 2.514(8)Å, is intermediate in length between the sum of the covalent radii (1.25 + 0.64 = 1.89Å) and the sum of the Van der Waals radii ($1.9_{estimate}$ + 1.35 = 3.25Å).

However, most examples in which metal-fluorine interactions have been postulated are less straightforward. For example in $[Ru\{SC_6F_4(F\text{-}2)\}(SC_6F_5)_2(PMe_2Ph)_2]$ an interaction between an ortho fluorine of one of the SC_6F_5 ligands and the metal was proposed, on the basis of a Ru-F distance of 2.489(6)Å compared to 2.7Å as the sum of F_{VdW} +$Ru_{atomic\ radius}$.[28] Interestingly, a few years earlier in a cobalt compound bearing the same ligand $Co(HB(3,5\text{-}Me_2pz)_3)(SC_6F_5)$,[29] the authors considered that the Co-F distance of 2.64(2)Å was not a bonding distance.

A C-F···M interaction has also been noted in the fluoroalkoxide compound $Ti(O\text{-}2,6\text{-}F_2C_6H_3)_3(O^iPr)$.[30] The proposed titanium fluorine interaction (2.704(5)Å) is longer than known Ti-F distances of titanium fluorides,[31] and is virtually the same as the sum of the Van der Waals radii of fluorine and octahedral Ti(IV) [1.35 + 1.36 = 2.72Å].[30]

Recently Caulton and co-workers have detected an intramolecular Zr···F-C interaction in $[Zr(OCH(CF_3)_2)_4]$ using ^{19}F NMR spectroscopy.[32] Although no changes in chemical shift were observed there was evidence of fluxional processes, which the authors speculated arose from interaction of a fluorine atom with the Zr(IV) metal centre, thereby restricting rotation of the CF_3 groups about the C-C single bond.

In another zirconium compound, $Cp^*_2ZrOB(C_6F_5)_3$ (figure 2.10), one of the pentafluorophenyl groups is oriented in such a way that one of the ortho fluorines approaches the zirconium atom so that the Zr···F contact is 2.346(3)Å.[33] This separation is about 0.1Å longer than the longest Zr-F covalent bonds found in 'simple' zirconium fluoroanions[34] and the authors believe that it represents a genuine Zr···F interaction. Significantly, the associated C-F bond is lengthened by 0.05Å relative to the average d(C-F).

At -88°C the ^{19}F NMR spectrum contains a resonance for the bridging fluorine at -190.3ppm, a shift of over 50ppm upfield from the region typical of *ortho*-C_6F_5 resonances. Analysis of the data shows that the free energy of activation for concomitant interconversion of all three C_6F_5 rings is 41.8 ± 0.2 $KJmol^{-1}$. It has been suggested that cleavage of the Zr···F bond is the primary contributor to the energy barrier. In other words the structure of $Cp^*_2ZrOB(C_6F_5)_3$ in solution is essentially that established for the solid state and therefore the unique C-F bond and Zr···F approach are not artefacts of crystal packing.

In most cases the evidence is less conclusive and it could be argued that these close M···F distances are not genuine interactions but are caused by crystal packing forces. However, it seems to be a general principle of structural chemistry that it is usually easier for bond angles to open up than for contacts to be substantially shorter than the sum of the Van der Waals radii.[27]

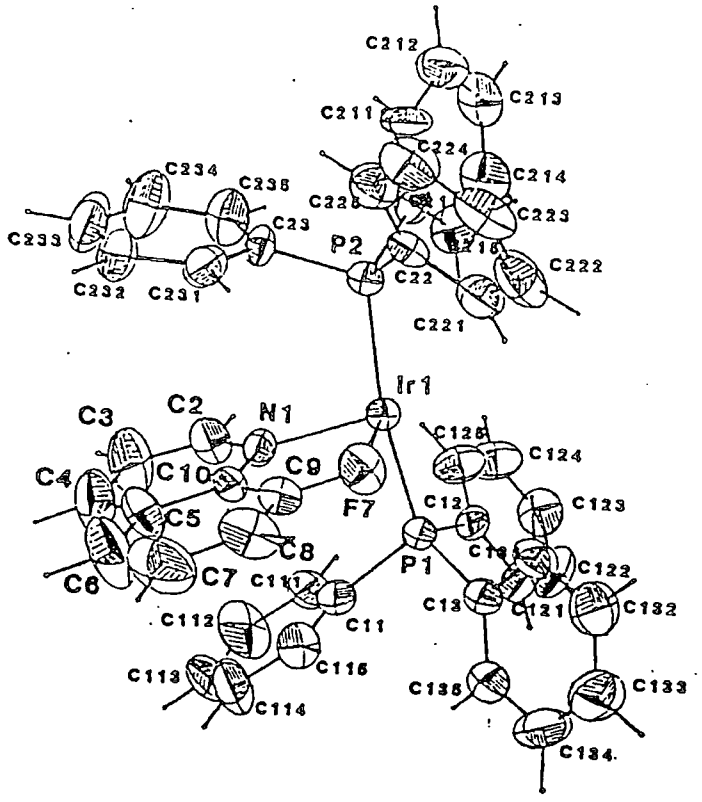

Figure 2.9: *The molecular structure of $IrH_2(PPh_3)_2L(SbF_6)$ (L = 8-fluoroquinoline) (ref 27)*

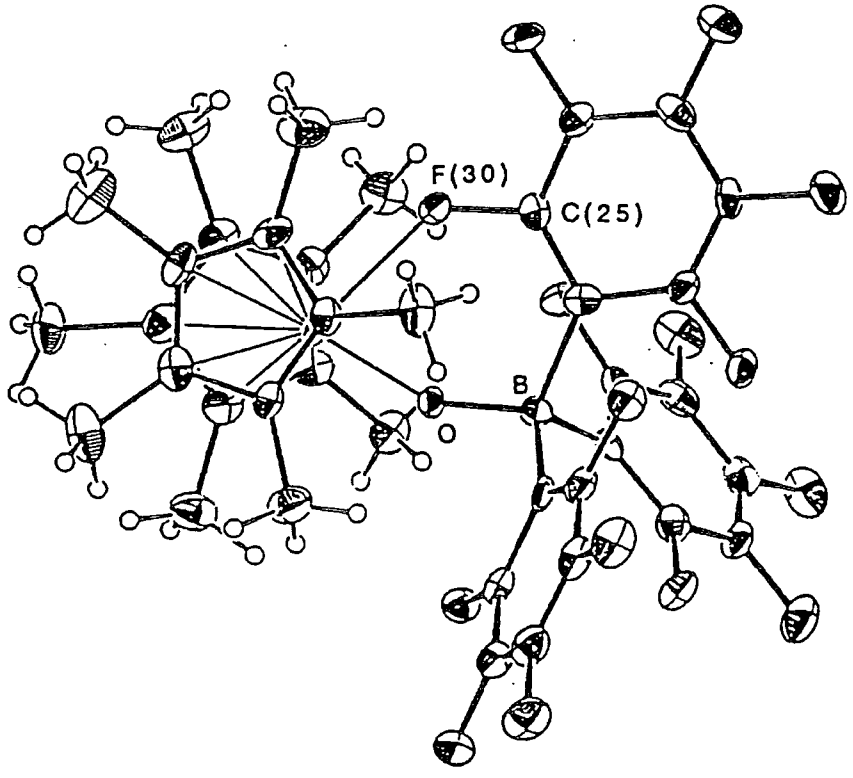

Figure 2.10: *The molecular structure of $Cp^*_2ZrOB(C_6F_5)_3$ (ref 33)*

Fluorocarbon-metal interactions, although weak, may be a common phenomenon in the co-ordination chemistry of ligands containing fluorine substituents, at least for co-ordinatively unsaturated metal centres. In addition to structural information, the ^{19}F chemical shift and in some cases coupling with the metal nucleus also seem to be useful spectroscopic criteria for interactions.

2.3.3 The M-F distance in complexes 1 - 6

By their very nature Van der Waals radii are difficult to calculate for transition metals. Literature examples of proposed metal-fluorine interactions have tended to calculate notional distances based on ionic, metallic or even atomic radii at the discretion of the authors. Indeed, there is even some ambiguity over the true Van der Waals radius of fluorine.[26]

Table 2.8 shows the calculated sum of the Van der Waals radius of fluorine[35] and the metallic radius of the transition metals[36] encountered in complexes **1 - 6**. The choice of metallic radius was made simply on the basis of availability of data. In all but one case the observed M···F distances are smaller than these values, thus implying that the complexes do indeed contain weak metal-fluorine interactions.

Complex	metallic radius (a) Å	radius F_{VdW} (b) Å	(a) + (b) Å	d(M···F) Å
Mo-F (1) (3)	1.36	1.35	2.71	2.467, 2.476 2.526, 2.556
Cr-F (2)	1.25	1.35	2.60	2.443, 2.462
V-F (5) (4)	1.31	1.35	2.66	2.668, 2.306, 2.378

Table 2.8: *A Comparison of the M···F Bond Distances in Complexes* ***1-5*** *to the sum of the Van der Waals radius of fluorine and the metallic radius of the respective metal*

2.3.4 Bond angles of the Ar^F ligand in complexes 1 - 6

Given the ambiguity of the true distance of a metal-fluorine interaction, attention is directed to other structural parameters of the complexes prepared in this study. In fact, this is the first such investigation in which a series of closely-related transition metal compounds containing close M···F approaches has been prepared, thus allowing the interactions to be probed without over-emphasising the importance of the M-F distance (*vide infra*).

The crystallographic data obtained on complexes **1** - **5** suggest that a single *ortho*-CF_3 fluorine atom of each Ar^F ligand closely approaches the metal centre. If such an interaction is a real effect then one might expect to observe repercussions in the bond angles and bond lengths of the Ar^F ligand. For example, if the interaction does occur in such an unsymmetric fashion, then the angle α shown below should be appreciably smaller than α'. In most main group Ar^F complexes, M-F interactions occur with both ortho-CF_3 groups on the aryl ring, so angle α is the same on each side.

From this table it can be seen that in all cases except complex **6** angle α is significantly reduced from 123°, reflecting the close approach of the fluorine to the metal centre on that side of the ring (angle $\alpha \approx 123°$ in compounds which show no M···F interactions as can be seen in complex **6**). This reduction is believed to be due to a metal-ligand interaction. The difference between α and α' is typically 10-15°. In complex **5**, however, the difference falls to 7.8(3)°, a reflection of the increased steric congestion and number of metal-fluorine interactions caused by the presence of a third Ar^F group in this complex.

Note that $\alpha + \alpha' + \delta \approx 360°$, so the planarity of the aryl ring is preserved. Angle β remains relatively unaffected.

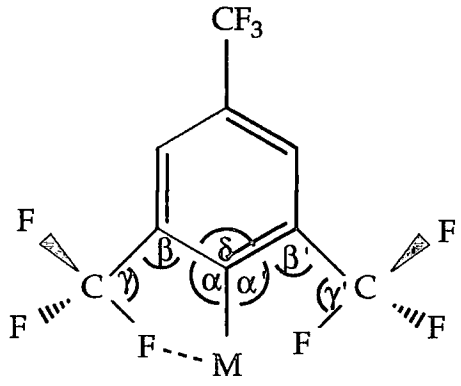

Compound	α	β	γ	α'	β'	γ'	δ
$Mo(N^tBu)_2(Ar^F)_2$ **1**	115.7(3)	122.5(5)	**112.1(4)** 113.3(5) 113.7(5)	129.2(4)	121.3(5)	111.9(5) 113.6(5) 112.5(4)	115.1(5)
$Mo(N^tBu)_2$(*o*-tolyl)$_2$	114.8(5)	121.5(6)	-	127.7(5)	121.4(7)	-	117.5(6)
$Cr(NAd)_2(Ar^F)_2$ **2**	116.3(2)	120.8(3)	**111.7(2)** 113.1(3) 113.3(3)	130.0(2)	120.5(3)	113.0(2) 112.4(2) 112.4(2)	113.6(3)
$Cr(N^tBu)_2$(mes)$_2$	114.4(4)	122.2(5)	-	127.7(4)	122.2(5)	-	117.7(5)
$[Mo(NAr)_2(Ar^F)LiCl.dme]_2$ **3**	115.5(8)	123.8 (10)	**113.4(10)** 111.4(10) 114.1(10)	130.7(8)	121.6 (10)	112.2(11) 111.6(10) 113.7(11)	113.7 (10)
$V(Ar^F)_2Cl$(thf) **4**	118.1(3)	118.5(4)	**110.1(4)** 114.4(4) 113.1(3)	128.0(3)	118.5(4)	112.7(3) 113.0(4) 112.4(4)	113.6(4)
$V(Ar^F)_3$-O-Li(thf)$_3$ **5**	119.8(3)	121.7(3)	**112.9(3)** 113.6(3) 112.3(3)	127.6(3)	121.1(3)	112.7(3) 113.2(3) 112.6(3)	112.3(3)
$Cr(Ar^F)_2(PMe_3)_2$ **6**	122.7(3)	120.4(4)	117.2(5) 112.4(7) 109.2(7)	124.8(3)	119.3(4)	113.7(4) 114.6(4) 113.0(4)	112.5(4)

Table 2.9: *Aryl Ring Bond Angles in Transition Metal Ar^F Complexes (°). (The figures in* ***Bold*** *indicate those which correspond to the interacting fluorine atom)*

2.3.5 Distortion of the aryl ring in complexes 1 - 6

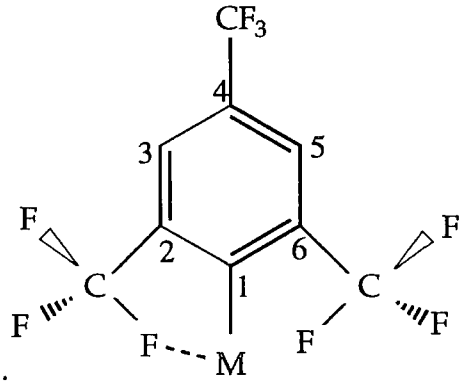

Compound	M-C_1	C_1-C_2	C_2-C_3	C_3-C_4	C_4-C_5	C_5-C_6	C_6-C_1
$Mo(N^tBu)_2(Ar^F)_2$ (1)	2.247 (av)	1.392(7)	1.398(8)	1.383(8)	1.390(8)	1.385(8)	1.416(7)
$Mo(N^tBu)_2$ (*o*-tolyl)$_2$	2.161(7)	1.418(8)	1.391(9)	1.382 (10)	1.358 (11)	1.368 (10)	1.404(9)
$Cr(NAd)_2(Ar^F)_2$ (2)	2.133 (3)	1.417(4)	1.388(4)	1.384(5)	1.385(5)	1.393(4)	1.409(4)
$Cr(N^tBu)_2$ (mes)$_2$	2.032(6)	1.404(6)	1.378(7)	1.366(7)	1.380(7)	1.375(7)	1.413(6)
[Mo(NAr)$_2$ (Ar^F)LiCl. dme]$_2$ (3)	2.225 (11)	1.41(2)	1.40(2)	1.41(2)	1.35(2)	1.42(2)	1.43(2)
$V(Ar^F)_2Cl$ (thf) (4)	2.152 (av)	1.394(6)	1.393(6)	1.383(6)	1.382(6)	1.383(6)	1.412(5)
$V(Ar^F)_3$-O-Li(thf)$_3$ (5)	2.179(4)	1.415(5)	1.387(5)	1.373(7)	1.368(6)	1.391(5)	1.411(5)
$Cr(Ar^F)_2(PMe_3)_2$ (6)	2.184(4)	1.407(7)	1.392(7)	1.360(8)	1.369(8)	1.368(7)	1.414(6)

Table 2.10: *M-C_{ipso} and Aryl Ring C-C Bond Lengths in Transition Metal Ar^F Complexes (Å)*

The effect of the proposed M···F interactions upon the C-C bond distances in the Ar^F aryl ring has also been investigated (table 2.10). In complexes **2** and **5** it appears that there is a slight lengthening in the C_{ipso}-C_{ortho} distances. However, it is difficult to rationalise the precise origin of this effect, especially given that a similar series of aryl ring bond lengths is also observed in complex **6**, in which no M···F interaction exists. On the whole the differences in bond lengths are not statistically significant and these parameters cannot be used to support conclusively the presence of weak M···F interactions.

2.3.6 C-F bond lengths: Comparison of C-F bond length of the interacting fluorine with the C-F bond lengths to non-interacting fluorine atoms.

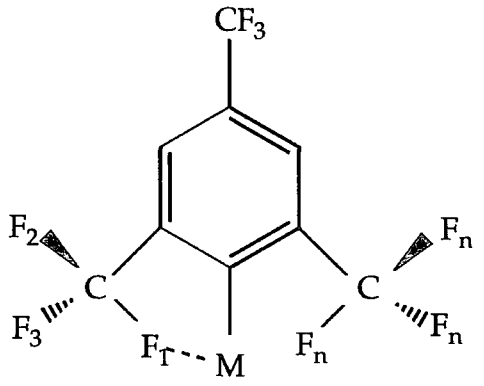

Compound	C----F_1	C----F_2/F_3 (av)	C----F_n (av)
$Mo(N^tBu)_2(Ar^F)_2$ **(1)**	1.362(7) 1.362(6)	1.325(8)	1.343(7)
$Cr(NAd)_2(Ar^F)_2$ **(2)**	1.345(3) 1.359(4)	1.338(4)	1.348(3)
$[Mo(NAr)_2(Ar^F)Cl.LiCl(dme)]_2$ **(3)**	1.358(14) 1.330(14)	1.339(14)	1.345(14)
$V(fmes)_2Cl(thf)$ **(4)**	1.369(5) 1.378(4)	1.328(5)	1.345(5)
$V(fmes)_3$-$OLi(thf)_3$ **(5)**	1.352(4)	1.341(4)	1.340(5)
Average C-F distance in complexes **1-5**	1.357	1.334	1.344

Table 2.11: *C-F Distances in Transition Metal Ar^F Complexes (Å)*

A general feature of metal-hydrogen agostic bonding is a slight lengthening in the carbon-hydrogen bond participating in the interaction relative to other non-interacting carbon-hydrogen bond distances on the same carbon.[37] An analogous effect is seen in complexes **1** - **5**; in most cases, the carbon-fluorine bond length to the interacting fluorine is 0.02-0.04Å longer than the bond lengths to either of the fluorine atoms on the same carbon atom and also longer than the average C-F bond distance (table 2.11). This has also been seen in all the main group compounds which had M···F interactions. This appears to be strong evidence supporting the existence of fluorine interactions with the metal centres in these complexes.

2.3.7 Solution State NMR

Despite the accumulation of several pieces of structural evidence for M···F interactions in early transition metal Ar^F complexes, as detailed in the preceding sections, the possibility that the M···F interactions actually arise through crystal packing effects must still be entertained. However, in complex **1** both ^1H and ^{19}F solution state NMR data indicate that the Ar^F group adopts a locked conformation (below 323K on the NMR timescale). Although variable temperature NMR experiments have not been carried out, we have observed a similar effect with complex **2** and its *tert*-butylimido equivalent. In all three cases we believe that this reflects the presence of metal-fluorine interactions in solution, thus supporting the observations for the solid state structure determinations.

2.3.8 The metal-based orbitals used in the M···F interactions

The presence of a secondary M···F bond implies that an empty low-lying orbital is located on the metal in the direction of the proposed interaction. This is entirely analogous to the situation found in complexes exhibiting M···H agostic interactions.[37] Consequently the M···F interactions in complexes **1** and **2** are in approximately the same positions as the M···H agostics in the related compound $Mo(NAr)(N^tBu)(CH_2CMe_3)_2$[38] (figure 2.11). Indeed the locations of the metal based orbitals (one above and one below the equatorial plane of the molecule) are seen in the isolobal complexes $CpNb(NAr)(CH_2CMe_3)_2$[39] and $Cr(NAd)_2(CH_2CMe_2Ph)_2$,[40] both of which also show multiple agostic interactions. This observation provides further evidence that the M···F interactions in complexes **1** and **2** are indeed genuine.

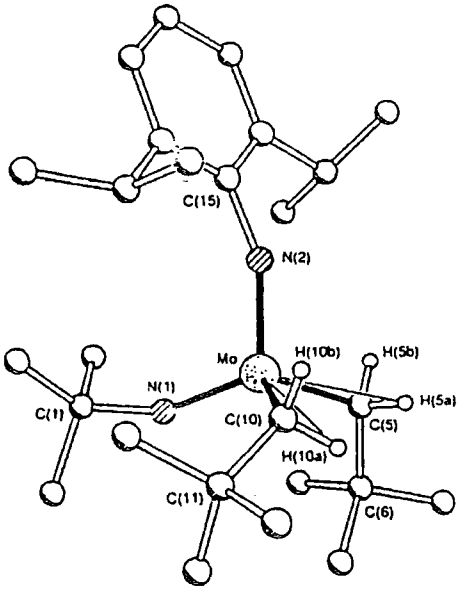

Figure 2.11: *The molecular structure of* $Mo(NAr)(N^tBu)(CH_2CMe_3)_2$ *(ref 38)*

Wilkinson also observed potential agostic interactions in the structurally characterised complex $Cr(N^tBu)_2(mes)_2$.[41] However, the failure of the crystallographic data to locate precisely the interacting protons means that a direct comparison cannot be made. However, the two closest methyl groups do approach the metal centre in a similar fashion, *ie.* one from above and one from below the equatorial binding plane.

C-F···M interactions could be regarded as being analagous to an end-on C-H···M agostic bond (figure 2.12a). However, it should be noted that whereas agostic interactions are normally viewed as arising from donation of the C-H bonding pair of electrons to the metal, C-F···M interactions clearly arise from fluorine lone pair donation (figure 2.12b).

(a) (b)

Figure 2.12: *Comparison of the end-on C-H···M agostic bond (a) to C-F···M fluorine lone pair donation (b)*

2.4 Conclusion

A variety of early transition metal complexes of the Ar^F ligand has successfully been synthesised and fully characterised. In five of the six examples structural evidence suggests the existence of weak metal-fluorine interactions. In all of these complexes the most informative structural parameters are the tilt of the aryl ring towards the interaction, and a lengthening in the C-F bond involved in the interaction. These two factors are far more conclusive than the oft quoted C-F···M bond distances, which, in the absence of accurate Van der Waals radii, at best provide only a very tentative indication for the presence of such interactions.

2.5 References

1 R.D. Schluter, A.H. Cowley, D.A. Atwood, R.A. Jones, M.R. Bond and C.J. Carrano, *J. Am. Chem. Soc.*, 1993, **115**, 2070; R.D. Schluter, H.S. Isom, A. H. Cowley, D.A. Atwood, R.A. Jones, F. Olbrich, S. Corbelin, and R.J. Lagow, *Organometallics*, 1994, **13**, 4058.

2 H. Grüzmacher, H. Pritzkow and F.T. Edelmann, *Organometallics*, 1991, **10**, 23.

3 S. Brooker, J-K. Buijink and F.T. Edelmann, *Organometallics*, 1991, **10**, 25.

4 K.H. Whitmire, D. Labahn, H.W. Roesky, M. Noltemeyer and G.M. Sheldrick, *J. Organomet. Chem.*, 1991, **402**, 55.

5 M. Scholtz, H.W. Roesky, D. Stalke, K. Keller, and F.T. Edelmann, *J. Organomet. Chem.*, 1989, **366**, 73.

6 J-K. Buijink, M. Noltemeyer and F.T. Edelmann, *J. Fluorine Chem.*, 1993, **61**, 51.

7 H.P. Goodwin, Thesis, University of Durham, 1990.

8 H.P. Goodwin, T.A. Straw, K.B. Dillon, and R.D. Chambers, Proc. Euchem. PSIBLOCS Conf., Paris, Palaiseau, 1988.

9 S. Brooker, N. Bertel, D. Stalke, M. Noltemeyer, H.W. Roesky, G.M. Sheldrick and F.T. Edelmann, *Organometallics*, 1992, **11**, 192.

10 G.E. Carr, R.D. Chambers, T.F. Holmes and D.G. Parker, *J. Organomet. Chem.*, 1987, **325**, 13.

11 M. Belay and F.T. Edelmann, *J. Organomet. Chem*, 1994, **479**, C21.

12 R.D. Schluter, D.A. Atwood, M.R. Bond, C.J. Carrano, R.A. Jones and A.H. Cowley, *J. Am. Chem. Soc.*, 1993, **115**, 2070.

13 P. v. R. Schleyer and, A.J. Kos, *Tetrahedron*, 1983, **39**, 1141.

14 A.C. Sullivan, G. Wilkinson, M. Motevalli and M.B. Hursthouse *J. Chem. Soc. Dalton Trans.*, 1988, 53.

15 A. Bell, W. Clegg, P.W. Dyer, M.R.J. Elsegood, V.C. Gibson and E.L Marshall, *J. Chem. Soc. Chem. Commun.*, 1994, 2247.

16 S.C. Cohen and A.G. Massey, *Advances in Fluorine Chemistry*, Eds. J.C. Tatlow, R.D. Peacock, H.H. Hyman and M. Stacey, Butterworths; London, Vol 8, 235-285.

17 W. Clegg, C. Redshaw and R.J. Errington, *J. Chem. Soc. Dalton Trans.*, 1992, 3189.

18 W. Seidel and G. Kreisel, *Z. Anorg. Allg. Chem.*, 1977, **435**, 146.

19 S.U. Koshmeider and G. Wilkinson, *Polyhedron*, 1991, **10**, 135-173 and references therein.

20 S. Gambarotta, C. Floriani, A. Chiesi-Villa and C. Guastini, *J. Chem. Soc. Chem. Commun.*, 1984, 886.

21 G.A. Razuvaev, V.N. Latyaeva, L.I. Vyshinskaja, A.N. Linyova, V.V. Drobotenko and V.K. Cherkasov, *J. Organomet. Chem.*, 1975, **93**, 113.

22 R.G. Cavell, E.D. Day, W. Byers and P.M. Watkins, *Inorg. Chem.*, 1972, **11**, 1591.

23 For example, see S. Gambarotta, J.J.H. Edema and R.K. Minhas, *J. Chem. Soc. Chem. Commun.*, 1993, 1503.

24 F.A. Cotton and G. Wilkinson, *Advanced Inorganic Chemistry*, Fifth Edition, J,Wiley, New York, 1988, Chapter 18.

25 A.R. Hermes, R.J. Morris and G.S. Girolami, *Organometallics*, 1988, **7**, 2732.

26 (a)A. Bondi, J. Phys. Chem., 1964, **68**, 441 **(b)**W.W. Porterfield, *Inorganic Chemistry. A Unified Approach*, Addison Wesley, 1983, p168.

27 R.J. Kulawiec, M. Lavin, E.M. Holt and R.H. Crabtree, *Inorg. Chem.*, 1987, **26**, 2559.

28 R.M. Catala, D. Cruz-Garritz, A. Hills, D.L. Hughes, R.L. Richards. P. Sosa and H. Torrens, *J. Chem. Soc. Chem. Commun.*, 1987, 261.

29 J.S. Thompson, T. Sorrell, T.J. Marks and J.A. Ibers, *J. Am. Chem. Soc.*, 1979, **101**, 4194.

30 C. Campbell, S. G. Bott, R. Larsen and W.G. Van der Sluys, *Inorg. Chem.*, 1994, **33**, 4950.

31 N.N. Greenwood and A. Earnshaw, *Chemistry of the Elements*; Pergamon, Oxford, 1984.

32 J.A. Samuels, E.B. Lobkovsky, W.E. Streib, K. Folting, J. C. Huffman, J.W. Zwanziger and K.G. Caulton, *J. Am. Chem. Soc.*, 1993, **115**, 5093.

33 (a)R.A. Newmark, W.M. Lamanna and A.R. Seidle, *Organometallics*, 1993, **12**, 1491. (b) A distance of 2.322(2)Å has been reported for a similar Zr···F interaction; J. Ruwwe, G. Erker and R. Fröhlich,*Angew. Chem. Int. Ed. Engl.*, 1996, **35**, 80.

34 D.R. Sears and J.H. Burns, *J. Chem. Phys.*, 1964, **41**, 3478; G. Brunton, *Acta Crystallogr.*, 1969, **B25**, 2164; J. Fischer and R. Weiss, *Acta Crystallogr.*, 1973, **B29**, 1955; M.A. Bush and G.A. Sim, *J. Chem. Soc.*, A, 1971, 2225.

35 L. Pauling, *The Nature of the Chemical Bond*, 3rd ed, Cornell Unversity Press, Ithaca, NewYork, 1960.

36 J.G. Stark and H.G. Wallace, *Chemistry Data Book*, S.I. Edition, Murray, 1975.

37 M.L.H. Green and M. Brookhart, *J. Organomet. Chem.*, 1983, **250**, 395.

38 A. Bell, W. Clegg, P.W. Dyer, M.R.J. Elsegood, V.C. Gibson and E.L Marshall, *J. Chem. Soc. Chem. Commun.*, 1994, 2547.

39 A. D. Poole, D.N. Williams, A.M. Kenwright, V.C. Gibson, W. Clegg, D.C.R. Hockless and P.A. O'Neil, *Organometallics*, 1993, **12**, 2549.

40 M. P. Coles and V. C. Gibson, *Unpublished Results.*

41 M.B. Hursthouse, M. Motevalli, A.C. Sullivan and G. Wilkinson, *J. Chem. Soc. Chem. Commun.*, 1986, 1398.

Chapter 3

Co-ordinaton of Diphosphenes to Transition Metals

3.1 Introduction

The classical double bond rule states that elements having a principal quantum number greater than two should not be able to form pπ-pπ bonds to themselves or other elements.[1] This is essentially correct for simple unprotected molecules such as HP=PH or $HP=CH_2$. However the pπ hybrid state can be stabilised using one of several approaches, for example incorporation into either a delocalised system or a charged system. Co-ordination to a metal centre can also be effective, as can steric protection by bulky groups.

This latter method was realised with the report of the first stable diphosphene Ar*P=PAr* in 1981,[2] since when bulky ligands such as mesityl ($C_6H_2(CH_3)_3$), 'super-mesityl' ($C_6H_2(Bu^t)_3$) and tris(trimethylsilyl)methyl have been widely used to stabilise unusually co-ordinated species, particularly those involving multiple bonds between main group elements.[3]

This chapter describes investigations into the co-ordination chemistry of diphosphenes stabilised by bulky aryl groups, in particular Ar^F. The transition metal co-ordination chemistry of these ligands is complicated by the potential for more than one bonding mode. Table 3.1 illustrates a variety of specific examples.

Table 3.1: *The co-ordination modes of diphosphenes. R' = C_6H_{11}, Et*

	ML_n	R	ref
η^2 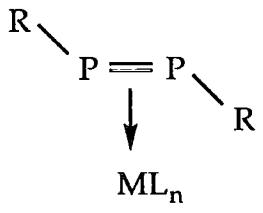	$Mo(\eta^5\text{-}C_5H_5)_2$	H	4
	$Pt(PPh_3)_2$	C_6F_5	4
	$Ni(PEt_3)_2$	$SiMe_3$	4
	$Pd(dppe)$	C_6H_5	4
	$Ni[R'_4P_2(CH_2)_2]$	Me, ^{t}Bu, Ph	5
	$Ni(^n Bu_3)_2$	Supermes, ^{t}BuN(H)	6
	$Ni(PMe_3)_2$, $Ni(PEt_3)_2$	$SiMe_3$, CMe_3, Ph, Me	7
	$TaCp_2H$	Ph	8
η^1 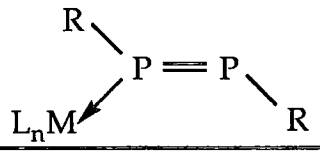	$Cr(CO)_5$	Supermes, mes,	9
		$(Me_3Si)_2CH$	10
	$Mo(CO)_5$	Supermes, mes	9
	$W(CO)_5$	Supermes, mes	9
	$Ni(CO)_3$	Supermes, RNH	6,11
	$Fe(CO)_4$	Supermes	11
bis-η^1 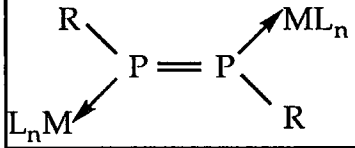	$Fe(CO)_4$	$(Me_3Si)_2CH$, Me_3Si_2N, mes	12
	$V(\eta^5\text{-}C_5H_5)(CO)_3$	mes	13
	$Cr(CO)_5$	Ph	14
bis-$\eta^1\eta^2$ 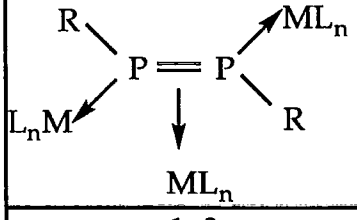	$Cr(CO)_5$	Ph, ^{t}Bu, ^{n}Bu	14 15,16
	$W(CO)_5$	Ph	15
$\eta^1\eta^2$ 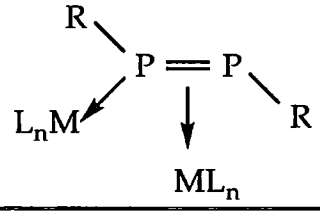	$Fe(CO)_4$	OSupermes,	10
		Ph,	17
		$Me_2C_2PN_2$	18
bis-η^2 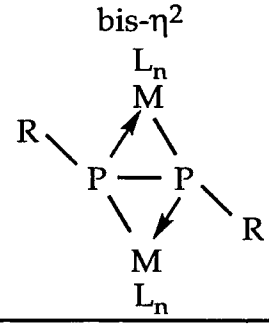	$Mo(CO)_2(\eta^5\text{-}C_5H_5)$	Ph,	19
	$^1/_2Fe_2(CO)_6$	$(Me_3Si)_2CH$	20
		^{t}Bu	21

3.2 Co-ordination of $Ar^FP{=}PAr^F$ to molybdenum

The diphosphene $Ar^FP{=}PAr^F$ is a surprisingly air- and moisture-stable solid at room temperature and binds less strongly to transition metals than its hydrocarbon analogues; for example, it does not form an adduct with vanadocene.[22] However, derivatives incorporating the following metal fragments have been synthesised, in which the diphosphene co-ordinates in an η^1 fashion: $[Mo(CO)_5]$, $[W(CO)_5]$ and $[Pt(PEt_3)Cl_2]$;[23] as illustrated in figure 3.1.

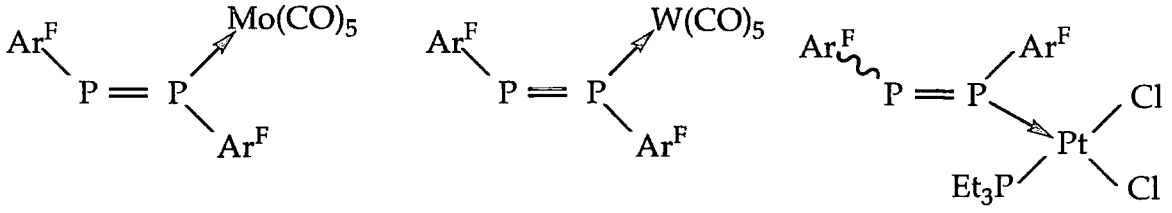

Figure 3.1: *Proposed configurations of η^1 co-ordinated complexes to molybdenum, tungsten and platinum*

3.2.1 Synthesis of $Mo(N^tBu)_2(PMe_3)(\eta^2\text{-}Ar^FP{=}PAr^F)$

Previous reactions carried out with the symmetrical diphosphene $Ar^FP{=}PAr^F$ have all resulted in η^1 co-ordination. In an attempt to obtain η^2 co-ordination the diphosphene was reacted with an η^2-bound olefin complex, namely $Mo(N^tBu)_2(PMe_3)(\eta^2\text{-}C_3H_6)$. (equation 3.1)

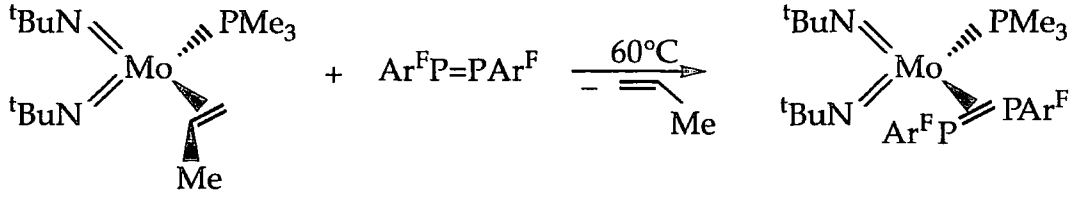

1 (3.1)

No reaction occurred after one week at room temperature. ^{31}P and ^{1}H NMR spectra showed that both starting materials remained totally uncomsumed and there were no new signals. However, after 36 hours at 60°C the solution had visibly darkened; solution NMR data indicated that complex **1** had formed in which the diphosphene is η^2-bound to the molybdenum centre. ^{31}P shifts for the diphosphene at -11.28 and -11.32 ppm lie in the range of other diphosphenes bound to transition metals in an η^2 fashion (^{31}P δ –70 to + 40ppm; cf. for η^1 350 - 450 ppm)[3]. The two ends of the diphosphene are inequivalent according to ^{31}P and ^{19}F NMR, implying that the P-P vector lies in the plane bisecting the two imido groups. The fact that there is no observable P-P coupling implies that the phosphorus centres are in extremely similar but not identical environments. The two minor, outer signals from the expected AB style doublet of doublets are presumably obscured due to PF coupling.

3.2.2 Molecular structure of $Mo(N^tBu)_2(PMe_3)(\eta^2\text{-}Ar^FP{=}PAr^F)$

Yellow prismatic crystals suitable for an X-ray determination were grown from a saturated diethyl ether solution at -20°C. A crystal of dimensions 0.80 x 0.75 x 0.40 mm was selected for study. The data were collected and solved by Prof. J.A.K. Howard and Mr. J. W. Yao within this department. The molecular structure is shown in figure 3.2. Bond distances and angles are collected in table 3.2.

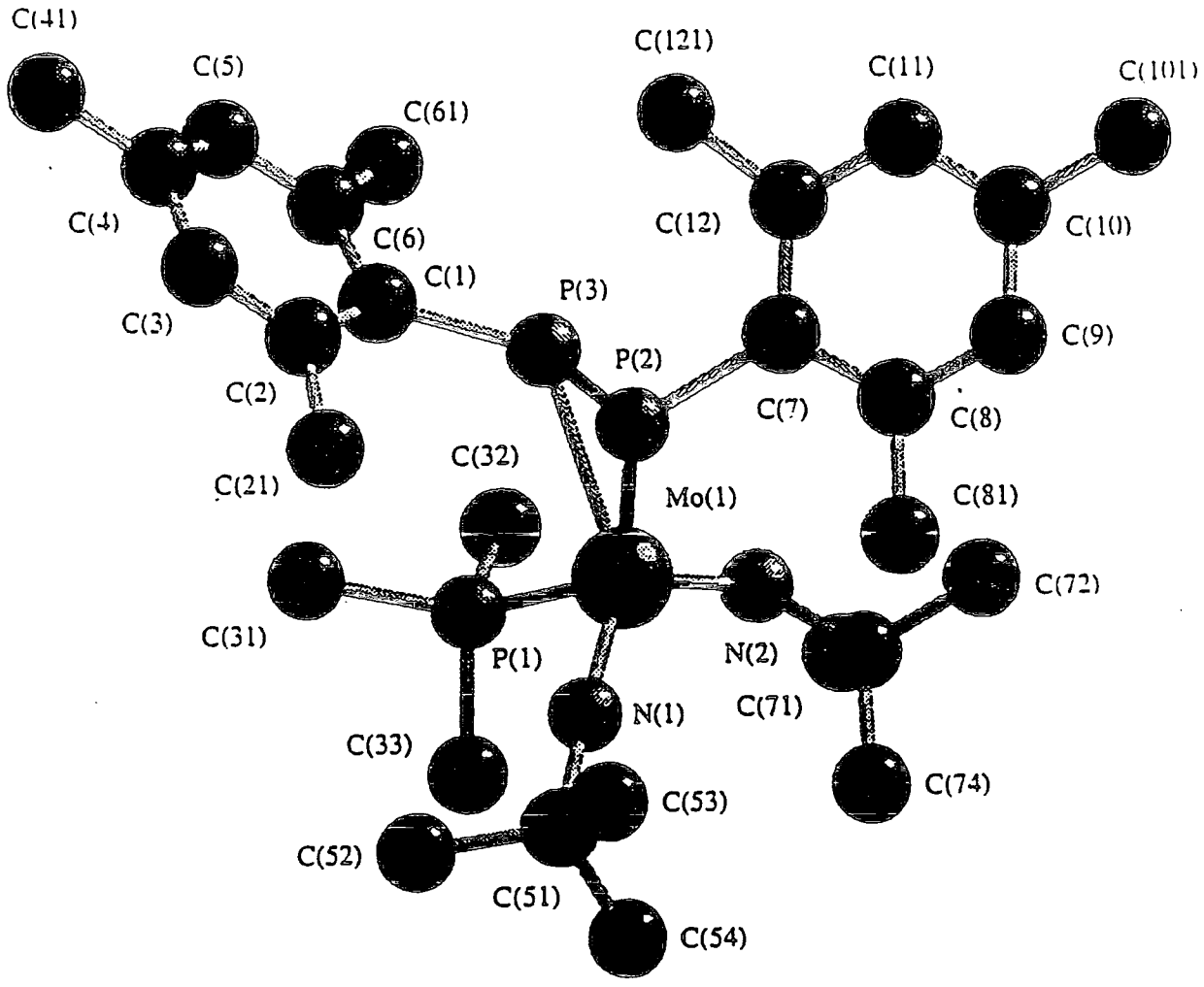

Figure 3.2: *The molecular structure of* $Mo(N^tBu)_2(PMe_3)(\eta^2\text{-}Ar^FP{=}PAr^F)$

Mo(1)-N(1)	1.757(3)	Mo(1)-N(2)	1.763(3)
Mo(1)-P(1)	2.475(2)	Mo(1)-P(2)	2.538(2)
Mo(1)-P(3)	2.588(2)	P(1)-C(31)	1.812(4)
P(1)-C(32)	1.818(3)	P(1)-C(33)	1.820(3)
P(2)-C(7)	1.862(3)	P(2)-P(3)	2.160(2)
P(3)-C(1)	1.878(3)	N(2)-C(71)	1.467(4)
N(1)-C(51)	1.461(4)	F(121)-C(21)	1.353(4)
F(122)-C(21)	1.335(4)	F(123)-C(21)	1.344(4)
F(21)-C(21)	1.335(4)	F(22)-C(21)	1.338(4)
F(23)-C(21)	1.356(4)	F(61)-C(61)	1.346(4)
F(62)-C(61)	1.352(4)	F(63)-C(61)	1.335(4)
F(81)-C(81)	1.343(4)	F(82)-C(81)	1.334(4)
F(83)-C(81)	1.338(4)	C(101)-F(103)	1.295(4)
C(101)-F(102)	1.307(4)	C(101)-F(101)	1.329(5)
C(101)-C(10)	1.496(4)	C(1)-C(2)	1.416(4)
C(1)-C(6)	1.436(4)	C(2)-C(3)	1.389(4)
C(2)-C(21)	1.520(4)	C(3)-C(4)	1.378(5)
C(4)-C(5)	1.385(5)	C(4)-C(41)	1.500(5)
C(41)-F(41)	1.279(5)	C(41)-F(43)	1.323(5)
C(41)-F(42)	1.350(5)	C(5)-C(6)	1.384(4)
C(6)-C(61)	1.516(4)	C(7)-C(12)	1.419(4)
C(7)-C(8)	1.422(4)	C(8)-C(9)	1.386(4)
C(8)-C(81)	1.519(4)	C(9)-C(10)	1.386(4)
C(10)-C(11)	1.374(4)	C(11)-C(12)	1.392(4)
C(12)-C(121)	1.520(4)	C(51)-C(54)	1.526(5)
C(51)-C(52)	1.528(5)	C(51)-C(53)	1.530(5)
C(71)-C(74)	1.528(4)	C(71)-C(72)	1.533(5)
C(71)-C(73)	1.535(4)		

N(1)-Mo(1)-N(2)	115.90(12)	N(1)-Mo(1)-P(1)	95.99(9)
N(2)-Mo(1)-P(1)	95.58(9)	N(1)-Mo(1)-P(2)	99.53(9)
N(2)-Mo(1)-P(2)	116.01(9)	N(1)-Mo(1)-P(2)	133.17(4)
N(1)-Mo(1)-P(3)	132.85(9)	N(2)-Mo(1)-P(3)	110.33(9)
P(1)-Mo(1)-P(3)	88.19(5)	P(2)-Mo(1)-P(3)	49.82(4)
C(31)-P(1)-C(32)	105.4(2)	C(31)-P(1)-C(33)	104.1(2)
C(32)-P(1)-C(33)	102.9(2)	C(31)-P(1)-Mo(1)	116.26(12)
C(32)-P(1)-Mo(1)	115.57(12)	C(33)-P(1)-Mo(1)	111.18(12)
C(7)-P(2)-P(3)	103.93(10)	C(7)-P(2)-Mo(1)	115.13(10)
P(3)-P(2)-Mo(1)	66.29(4)	C(1)-P(3)-P(2)	108.78(11)
C(1)-P(3)-Mo(1)	125.11(10)	P(2)-P(3)-Mo(1)	63.89(5)
C(71)-N(2)-Mo(1)	154.1(2)	C(51)-N(1)-Mo(1)	177.1(2)
F(103)-C(101)-F(102)	107.4(3)	F(103)-C(101)-F(101)	104.2(3)
F(102)-C(101)-F(101)	103.8(3)	F(103)-C(101)-C(10)	114.1(3)
F(102)-C(101)-C(10)	114.0(3)	F(101)-C(101)-C(10)	112.5(3)
C(2)-C(1)-C(6)	114.1(3)	C(2)-C(1)-P(3)	130.0(2)
C(6)-C(1)-P(3)	115.3(2)	C(3)-C(2)-C(1)	122.2(3)
C(3)-C(2)-C(21)	113.1(3)	C(1)-C(2)-C(21)	124.6(3)

F(21)-C(21)-F(22)	108.4(2)	F(21)-C(21)-F(23)	105.3(2)
F(22)-C(21)-F(23)	105.2(2)	F(21)-C(21)-C(2)	113.8(2)
F(22)-C(21)-C(2)	113.3(3)	F(23)-C(21)-C(2)	110.3(2)
C(4)-C(3)-C(2)	121.1(3)	C(3)-C(4)-C(5)	119.1(3)
C(3)-C(4)-C(41)	120.9(3)	C(5)-C(4)-C(41)	119.9(3)
F(41)-C(41)-F(43)	107.3(4)	F(41)-C(41)-F(42)	109.0(4)
F(43)-C(41)-F(42)	101.4(3)	F(41)-C(41)-C(4)	114.1(3)
F(42)-C(41)-C(4)	111.4(4)	F(43)-C(41)-C(4)	113.0(3)
C(6)-C(5)-C(4)	120.1(3)	C(5)-C(6)-C(1)	122.9(3)
C(5)-C(6)-C(61)	114.9(3)	C(1)-C(6)-C(61)	122.3(3)
F(63)-C(61)-F(61)	107.0(3)	F(63)-C(61)-F(62)	105.7(3)
F(61)-C(61)-F(62)	104.9(3)	F(63)-C(61)-C(6)	114.5(3)
F(61)-C(61)-C(6)	112.3(3)	F(62)-C(61)-C(6)	111.7(3)
C(12)-C(7)-C(8)	115.2(3)	C(12)-C(7)-P(2)	124.2(2)
C(8)-C(7)-P(2)	120.1(2)	C(9)-C(8)-C(7)	121.7(3)
C(9)-C(8)-C(81)	116.1(3)	C(7)-C(8)-C(81)	122.0(3)
F(82)-C(81)-F(83)	105.6(2)	F(82)-C(81)-F(81)	106.3(2)
F(83)-C(81)-F(81)	105.9(2)	F(82)-C(81)-C(8)	112.1(3)
F(83)-C(81)-C(8)	114.9(2)	F(81)-C(81)-C(8)	111.4(3)
C(8)-C(9)-C(10)	120.5(3)	C(11)-C(10)-C(9)	119.3(3)
C(11)-C(10)-C(101)	119.4(3)	C(9)-C(10)-C(101)	121.2(3)
C(10)-C(11)-C(12)	120.6(3)	C(11)-C(12)-C(7)	121.6(3)
C(11)-C(12)-C(121)	113.9(3)	C(7)-C(12)-C(121)	124.4(3)
F(122)-C(121)-F(123)	107.5(2)	F(122)-C(121)-F(121)	105.4(3)
F(123)-C(121)-F(121)	150.0(2)	F(122)-C(121)-C(12)	114.8(3)
F(123)-C(121)-C(12)	113.3(3)	F(121)-C(121)-C(12)	110.1(2)
N(1)-C(51)-C(54)	110.0(3)	N(1)-C(51)-C(52)	109.1(3)
C(54)-C(51)-C(52)	110.0(3)	N(1)-C(51)-C(53)	106.2(2)
C(54)-C(51)-C(53)	111.2(3)	C(52)-C(51)-C(53)	110.2(3)
N(2)-C(71)-C(74)	109.5(3)	N(2)-C(71)-C(72)	108.2(3)
C(74)-C(71)-C(72)	111.1(3)	N(2)-C(71)-C(73)	108.7(3)
C(74)-C(71)-C(73)	109.7(3)	C(72)-C(71)-C(73)	109.6(3)

Table 3.2: *Selected bond distances (Å) and angles(°) for* $Mo(N^tBu)_2(PMe_3)(\eta^2$-$Ar^FP{=}PAr^F)$ ***(1)*** *with estimated standard deviations in parentheses.*

The P=P bond distance of 2.160(2)Å is slightly longer than in the free diphosphene (2.022(2)Å)[24] and is in the normal range for an η^2-bonded diphosphene, (most values lie between 2.11Å and 2.19Å).[4,25] It is interesting to compare the structure of this compound with that of the bis(imido)molybdenum alkene complex from which it is prepared.[26] The bulkier diphosphene ligand forces the other bond angles around molybdenum to contract such that angle P(1)-Mo-N(1) is 101.9(1)° in the alkene and 95.99(9)° in the diphosphene complex. Angle P(1)-Mo-N(2) contracts from 99.4(1)° to 95.58(9)° and angle N(1)-Mo-N(2) from 123.0(2)° to 115.90(12)°. The molybdenum nitrogen bonds are slightly shorter in the diphosphene complex Mo-N(1) 1.757(3)Å, Mo-N(2) 1.763(4)Å compared with its alkene analogue Mo-N(1) 1.771(3)Å, Mo-N(2) 1.772(4)Å, whereas the bond from the PMe_3 ligand to the metal is slightly longer (2.475(2)Å and 2.446(1)Å respectively).

These bond length variations are minor, however, in comparison to the differences which occur in the angles at the imido nitrogens. In the olefin complex the Mo-N-C angles are quite similar, 162.9(3)° and 168.2(3)°, whereas in the diphosphene complex the corresponding angles are 177.1(2)° and 154.1(2)°, the smaller angle possibly arising from unfavourable steric interactions between an Ar^F substituent and the t-butyl group attached to N(2).

It is also interesting to note that the C-P-P angles of 103.93(10)° and 108.78(11)° are larger than in the free diphosphene where the C-P-P angle is only 97.8(1)°. Thus just as metal-olefin complexes may be described as metallacyclopropanes, in complex **1** the diphosphene phosphorus atoms may be regarded as sp^3 hybridised as the ligand approaches a metallacyclophosphane description. It also appears that the aryl groups bend away from the metal centre, thus reducing steric interactions. A similar effect has been seen previously in the structure of $[NEt_4]^+[Cp_2Zr(\eta^2$-PhP=PPh)(Br)].[27] Furthermore, theoretical calculations on HP=PH[28] have demonstrated that the P-P π^* molecular orbital is the LUMO of this molecule

and therefore should be readily accessible for metal electron back-bonding. The co-ordinated diphosphene differs substantially from the symmetrical free species, especially in the P-C_{ipso}-C_{ortho} angles (table 3.3). The Ar^F substituent at P(3) shows a marked deviation from the near symmetrical situation observed at P(2), with P(3)-C(1)-C(2) opening up to 130.0(2)° in order to accomodate the steric bulk of the PMe_3 ligand.

	Free diphosphene	Bound diphosphene
P - P	2.022(2)	2.160(2)
P - C_{ipso}	1.860(4)	1.862(3), 1.878(3)
C_{ipso} -P - P	97.8(1)	103.93(10), 108.78(11)
C_{ortho} - C_{ipso} - P	121.6(3) 121.6(3)	130.0(2), 115.3(2) 120.1(2), 124.2(2)
C_{ortho} - C_{ipso} - C_{ortho}	117.0(3)	114.1(3), 115.2(3)

Table 3.3: *Comparison of bond lengths and angles in the free diphosphene and the bound diphosphene.*

3.2.3 Synthesis of $Mo(NAr)_2(PMe_3)(\eta^2\text{-}Ar^FP{=}PAr^F)$

In an attempt to synthesise a five co-ordinate species η^2-diphosphene complex, the diphosphene was reacted with one equivalent of the five co-ordinate $Mo(NAr)_2(PMe_3)_2(\eta^2\text{-}C_2H_4)$ at 60°C.

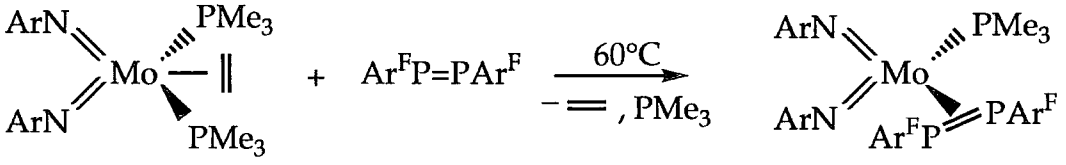

2 (3.2)

Upon work-up a bright orange crystalline solid was isolated. However, both ^1H and ^{31}P NMR studies indicated that the four co-ordinate complex $Mo(NAr)_2(PMe_3)(\eta^2\text{-}Ar^FP{=}PAr^F)$, **2**, had been formed with the loss of one PMe_3 ligand. This is not surprising since attempted direct replacement of the ethene ligand by propene results in a propene adduct which is unstable to vacuum.[29] The stability of the five co-ordinate olefin complexes is therefore dependent on the size of the co-ordinated olefin. Thus, due to the steric bulk of the diphosphene the four co-ordinate complex is formed exclusively. The bis(arylimido)molybdenum therefore reacts in a similar fashion to $Mo(N^tBu)_2(PMe_3)(\eta^2\text{-}C_3H_6)$. Solution NMR data indicate that **2** has a structure closely related to $Mo(N^tBu)_2(PMe_3)(\eta^2\text{-}Ar^FP{=}PAr^F)$ in which the diphosphene is η^2-bonded to the molybdenum centre (^{31}P δ +3.6, broad).

3.2.4 Attempted synthesis of $Mo(N^tBu)_2(PMe_3)(\eta^2\text{-}Ar^{F'}P{=}PAr^{F'})$

Given that the expected reactivity of the diphosphene $Ar^{F'}P{=}PAr^{F'}$ should be very similar to that of $Ar^FP{=}PAr^F$, it too was reacted with $Mo(N^tBu)_2(PMe_3)(\eta^2\text{-}C_2H_4)$.

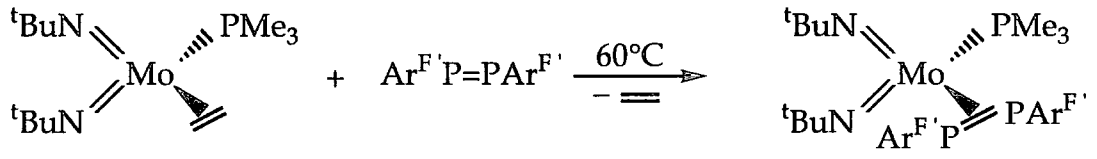

3 (3.3)

After warming to 60°C for 4 days the solution had changed colour from pale orange to orange/red. The ^{31}P NMR spectrum showed that the reaction had not reached completion, and that only about 50% of the diphosphene had reacted. The ^1H NMR spectrum showed that the remaining $Mo(N^tBu)_2(PMe_3)(\eta^2\text{-}C_2H_4)$ had decomposed. ^{31}P NMR values for the new complex **3** occur at -10 and -13 ppm for the co-ordinated diphosphene. These values are very similar to those for complex **1** and again lie within the range for η^2-co-ordinated diphosphenes. This observation indicates that subtle effects in a diphosphene's substituents can play a decisive role in its reactivity.

3.2.5 Attempted synthesis of $Mo(N^tBu)_2(PMe_3)(\eta^2\text{-}Ar^*P{=}PAr^*)$

The reaction of $Mo(N^tBu)_2(PMe_3)(\eta^2\text{-}C_2H_4)$ with Ar*P=PAr* was carried out in an attempt to synthesise the analogous η^2-bonded complex to **1**.

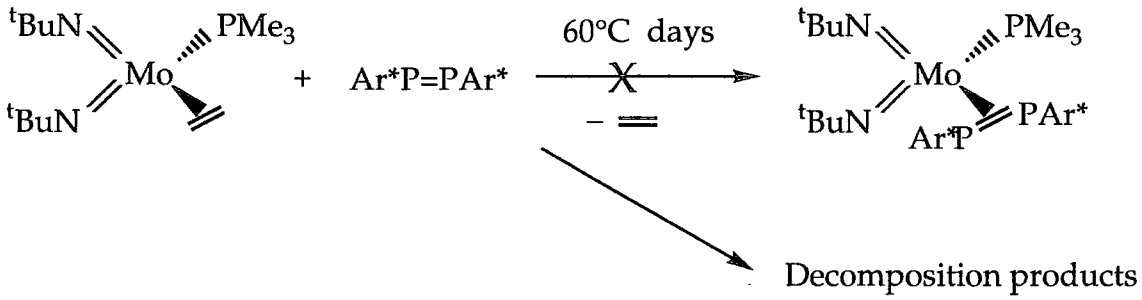

(3.4)

Solution NMR data showed that no reaction had taken place after 4 days, at room temperature. The reaction was warmed to 60°C for 4 days after which time ^{31}P and ^1H NMR spectra indicated that the $Mo(N^tBu)_2(PMe_3)(\eta^2\text{-}C_2H_4)$ had decomposed and the diphosphene remained unreacted.

t-Butyl groups are spatially much larger than CF_3 groups and as a consequence of this, Ar*P=PAr* is more bulky than $Ar^FP{=}PAr^F$. A possible explanation for the observed reactivity is that due to the increased steric bulk of Ar*P=PAr* the diphosphene cannot fit around the already sterically crowded metal centre.

3.2.6 Attempted synthesis of $Mo(N^tBu)_2(PMe_3)(\eta^2\text{-}Ar^FP{=}PAr^*)$

The previous reaction was also carried out using the unsymmetrical diphosphene $Ar^FP{=}PAr^*$.

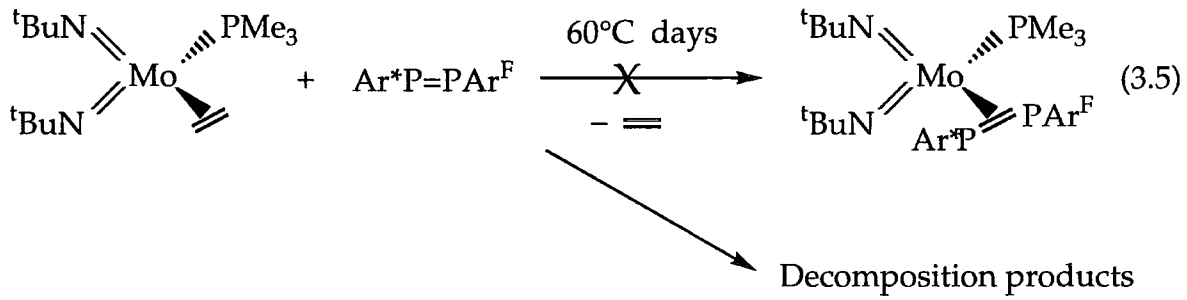

(3.5)

However, after maintaining the reaction at 60°C for 4 days, the same decomposition products were observed for $Mo(N^tBu)_2(PMe_3)(\eta^2\text{-}C_2H_4)$, and, as in the previous reaction, the diphosphene remained unreacted.

3.3 Co-ordination to platinum

Platinum-phosphine complexes, in particular analogues of *cis*-platin[TM], may have exciting applications as anti-tumour agents.[30] It has been suggested that the subtle σ-donor and π-acceptor properties of fluorophosphines within these systems may enhance anti-tumour properties.[31] In work previously carried out the compounds $[PtCl_2(PEt_3)(Ar^FPCl_2)]$,[32] $[PtCl_2(PEt_3)(Ar^FP{=}CHPh)]$,[33] $[PtCl_2(PEt_3)(\eta^1\text{-}Ar^FP{=}PAr^F)]$[23] and other related compounds have been isolated. All of these compounds are square planar with η^1-co-ordinated modes for the Ar^FP moiety and with the phosphine ligands *cis* orientated. In the first two examples the *trans* isomer is favoured kinetically and over time converts to the *cis*. In the third case, only the thermodynamically more stable *cis* isomer is observed. The observed stability is attributed to the more effective overlap of the d-orbital at the metal centre in the *cis* configuration than the *trans*.

The remainder of this chapter discusses further studies in this area, with Ar^F, non-fluorinated and mixed diphosphenes.

3.3.1 Reaction of $[Pt(PEt_3)Cl_2]_2$ with Ar*P=PAr*

The platinum dimer $[Pt(PEt_3)Cl_2]_2$ was reacted stoichiometrically with the symmetrical diphosphene Ar*P=PAr* and the unsymmetrical diphosphene $Ar^*P{=}PAr^F$ in an attempt to form analogous complexes to the previously synthesised $(PEt_3)PtCl_2(\eta^1\text{-}Ar^FP{=}PAr^F)$.

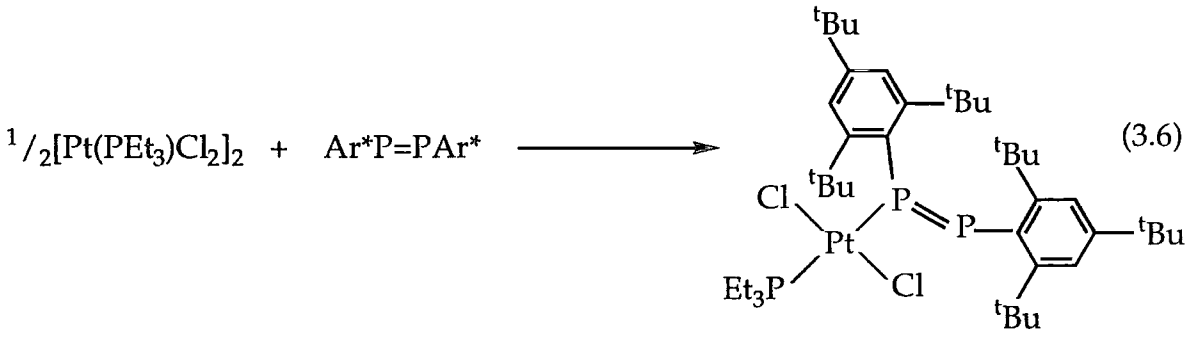

(3.6)

In the reaction of Ar*P=PAr* with $[Pt(PEt_3)Cl_2]_2$, after a few hours at room temperature, although there was no apparent colour change the ^{31}P NMR spectrum revealed that some of the starting material had been consumed (figure 3.3) and signals corresponding to new material were observed between 330 and 390ppm (figure 3.4). Close examination of the product region reveals a doublet at 380ppm ($^1J_{PP}$ = 548Hz) and a set of resonances made up of 12 lines between 335 and 370ppm. These resonances arise from η^1-bound diphosphene (δ ^{31}P for η^2 –70 to + 40ppm cf. for η^1 350 - 450 ppm)[2] shown in figure 3.5 ($^1J_{P_BPt}$ = 2200Hz, $^1J_{P_AP_B}$ = 548Hz, $^2J_{P_BPEt_3}$ = 487 Hz).

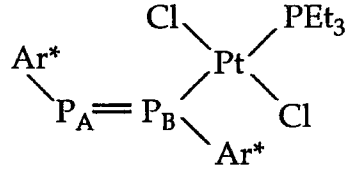

Figure 3.5: *The product formed in reaction 3.6*

It is not possible to infer from the ^{31}P NMR spectrum whether the diphosphene adopts a *cis* or *trans* configuration, but the coupling constants show that the diphosphene must be *trans* to the PEt_3 ligand since $^2J_{P_BPEt_3}$ has a significant value.

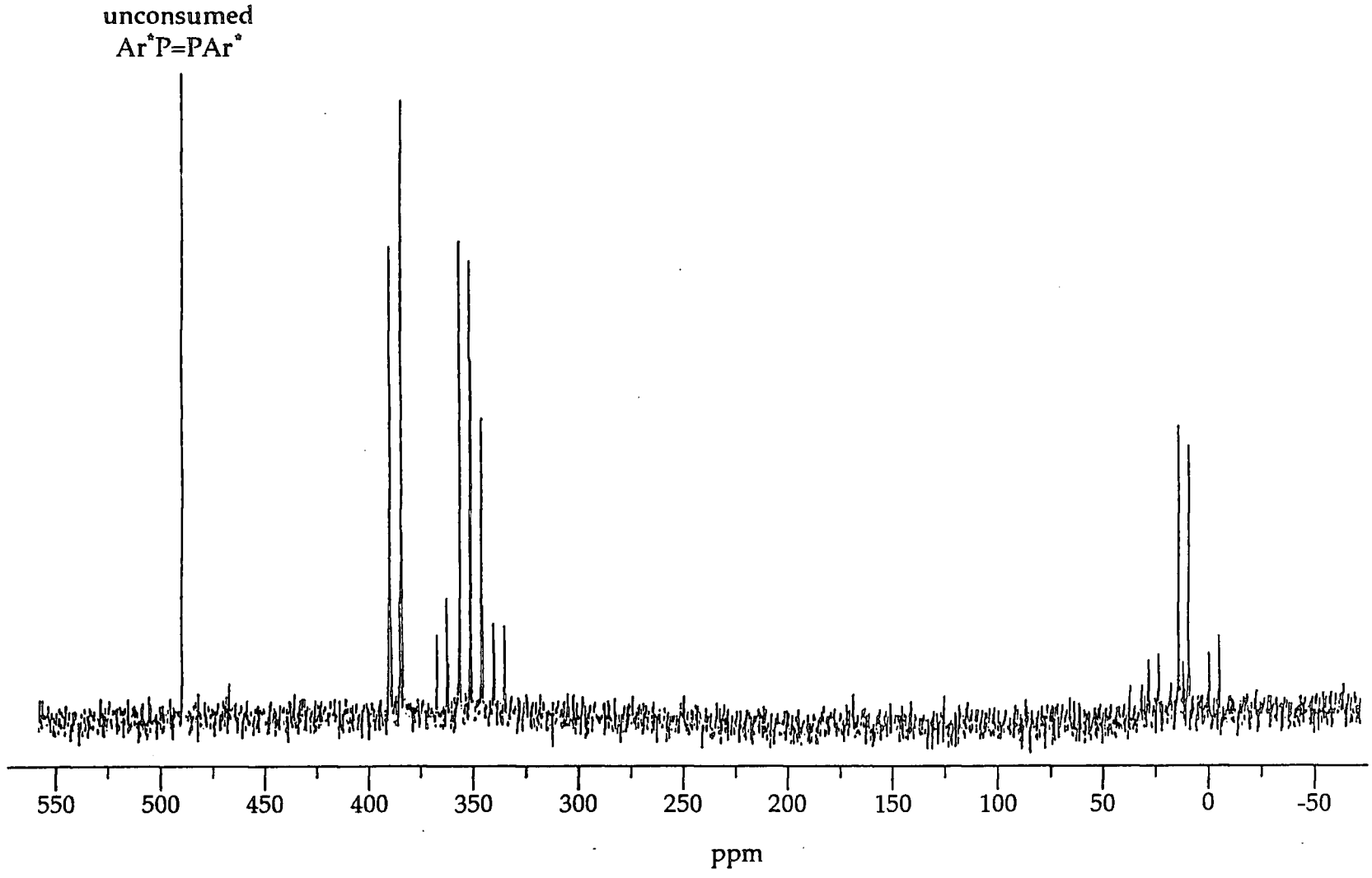

Figure 3.3: ^{31}P *NMR spectrum of the reaction of* $^1/_2[Pt(PEt_3)Cl_2]_2$ *with* $Ar^*P{=}PAr^*$

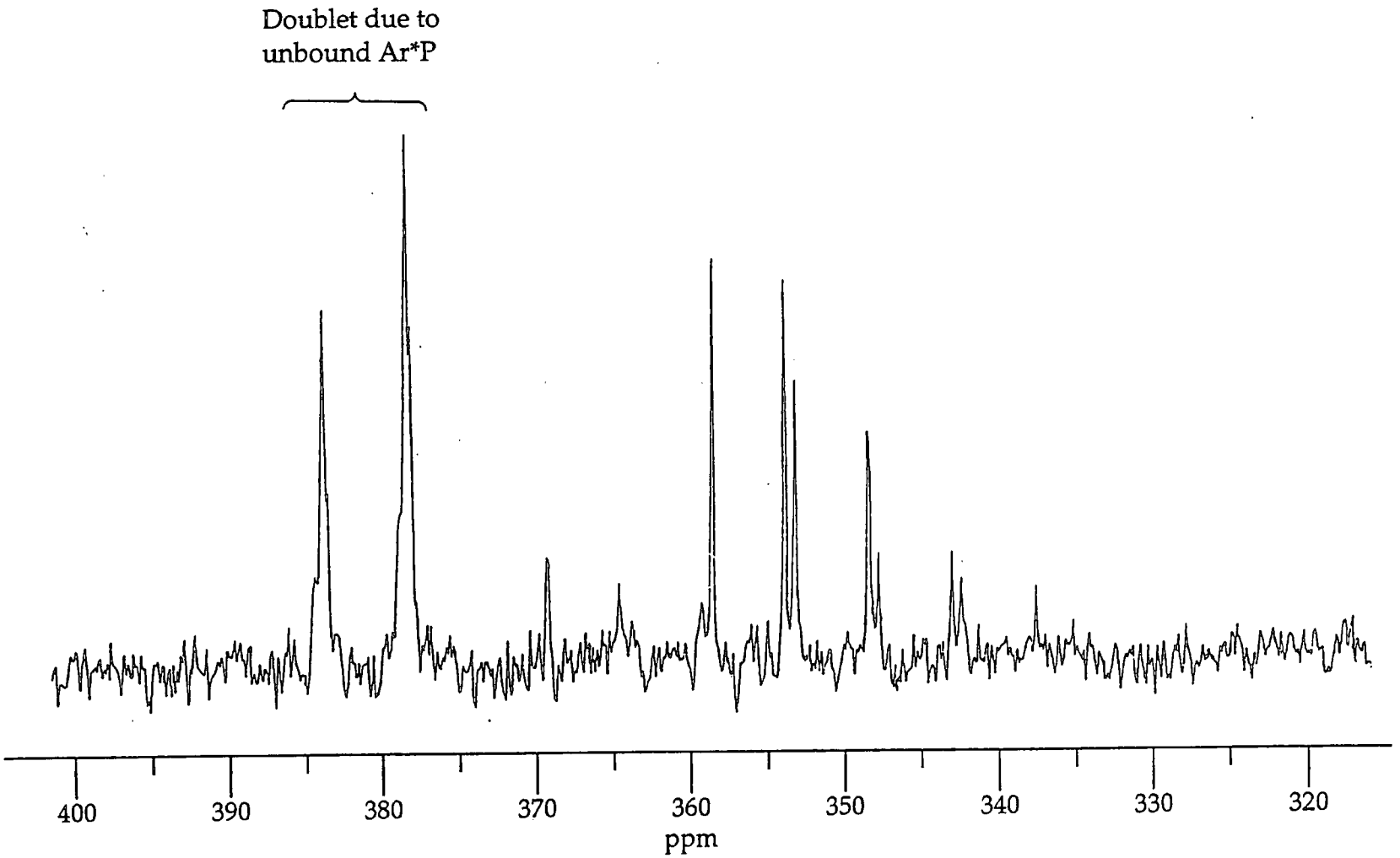

Figure 3.4: *Region of the ^{31}P NMR spectrum of the reaction of $^1/_2[Pt(PEt_3)Cl_2]_2$ with $Ar^*P{=}PAr^*$*

3.3.2 Reaction of $[Pt(PEt_3)Cl_2]_2$ with $Ar^*P{=}PAr^F$

$$^1/_2[Pt(PEt_3)Cl_2]_2 + Ar^*P{=}PAr^F \longrightarrow PtCl_2(PEt_3)(\eta^1\text{-}Ar^FP{=}PAr^*) \quad (3.7)$$

In the case of the unsymmetrical diphosphene $Ar^FP{=}PAr^*$, although as previously there is no colour change, the ^{31}P NMR spectrum of the reaction indicates that there are two separate species in solution. The products are again believed to be the simple η^1 bound diphosphene complexes shown in figure 3.6.

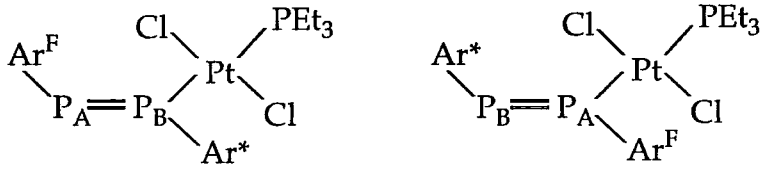

(i) (ii)

Figure 3.6: *The two possible products of equation 3.7*

After 1 hour at 60°C the ^{31}P NMR spectrum confirms the presence of a small amount of unconsumed $Ar^FP{=}PAr^*$ and also contains two distinct product regions, 380 - 420ppm and 300 - 335 ppm (figure 3.7). The downfield region is believed to arise from Ar*P resonances and the upfield signals from Ar^FP; this assignment is made on the basis of the relative shifts of the unco-ordinated ligand and also by comparison with the complexes $[PtCl_2(PEt_3)(\eta^1\text{-}Ar^FP{=}PAr^F)]$and $[PtCl_2(PEt_3)(\eta^1\text{-}Ar^*P{=}PAr^*)]$.

An expansion of the first product region 300-335 ppm is shown in figure 3.8. As predicted the region contains twelve lines, (similar to those observed in section 3.3.1) corresponding to the Ar^F substituted phosphorus atom in (ii) ($^1J_{P_AP_B}$ = 552Hz, $^1J_{P_A\text{-}Pt}$ = 2406Hz, $^2J_{P_APEt_3}$ = 521Hz). The remaining doublet at 308 ppm ($^1J_{P_AP_B}$= 537Hz) is attributed to the unco-ordinated phosphorus in complex (i).

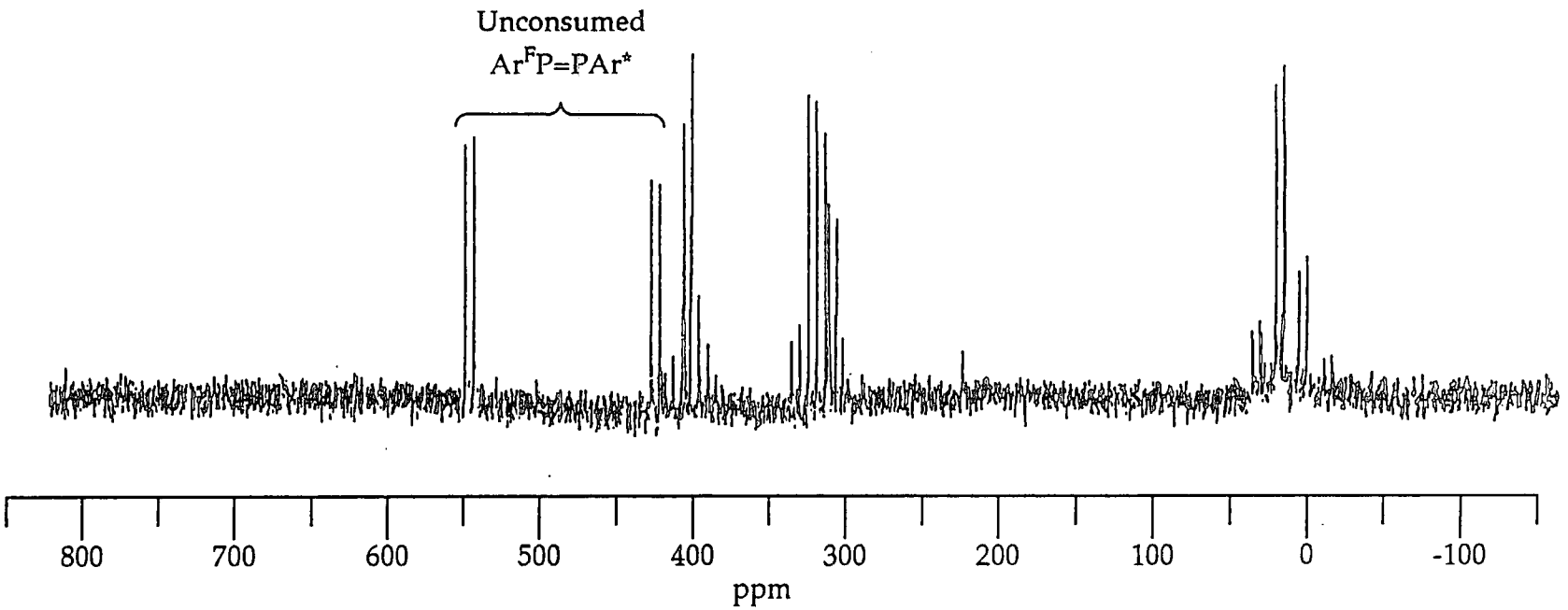

Figure 3.7: *^{31}P NMR spectrum of the reaction of $^1/_2[Pt(PEt_3)Cl_2]_2$ with $Ar^*P{=}PAr^F$*

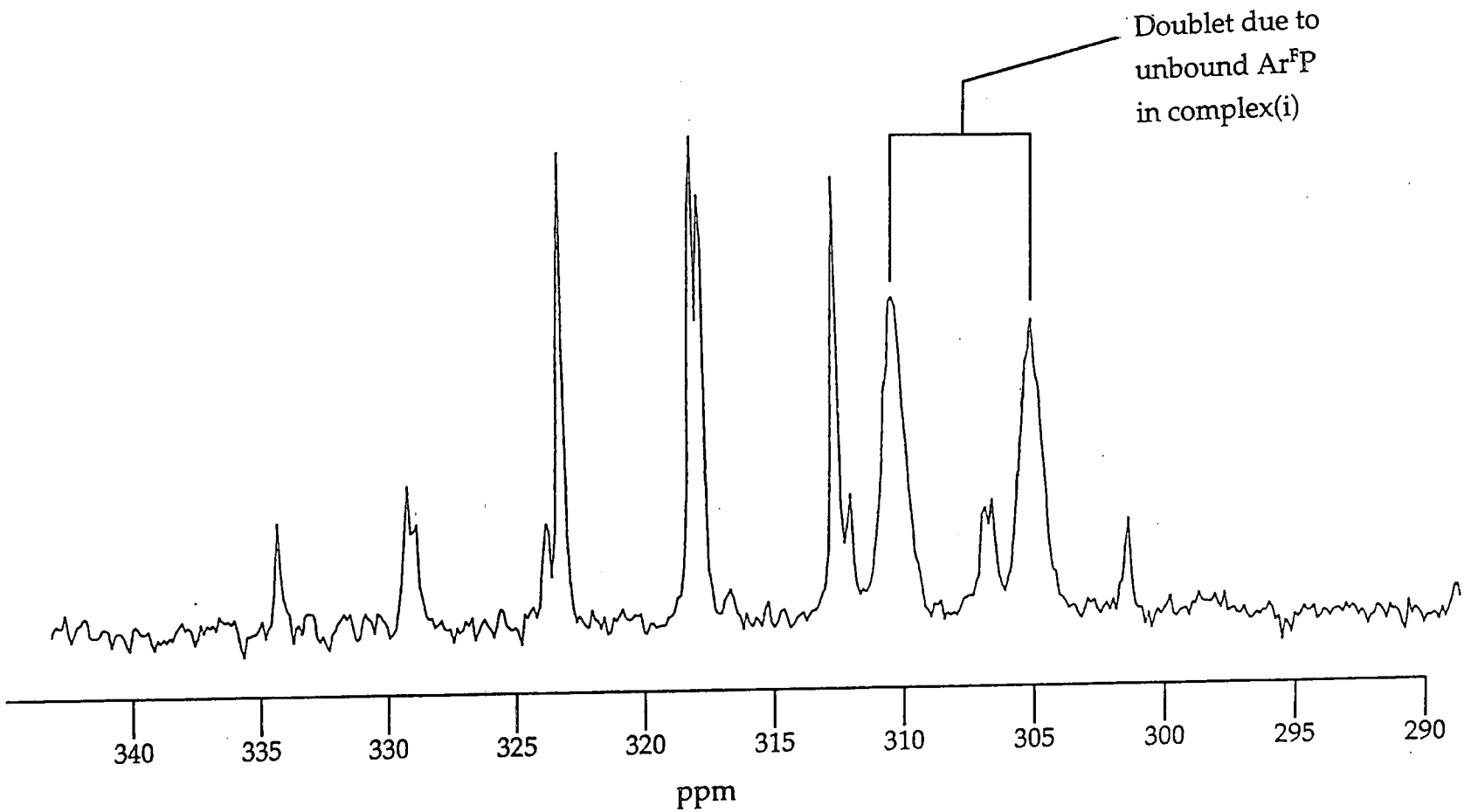

Figure 3.8: *Upfield region of the ^{31}P NMR spectrum of the reaction of $^{1}/_{2}[Pt(PEt_3)Cl_2]_2$ with $Ar^*P{=}PAr^F$*

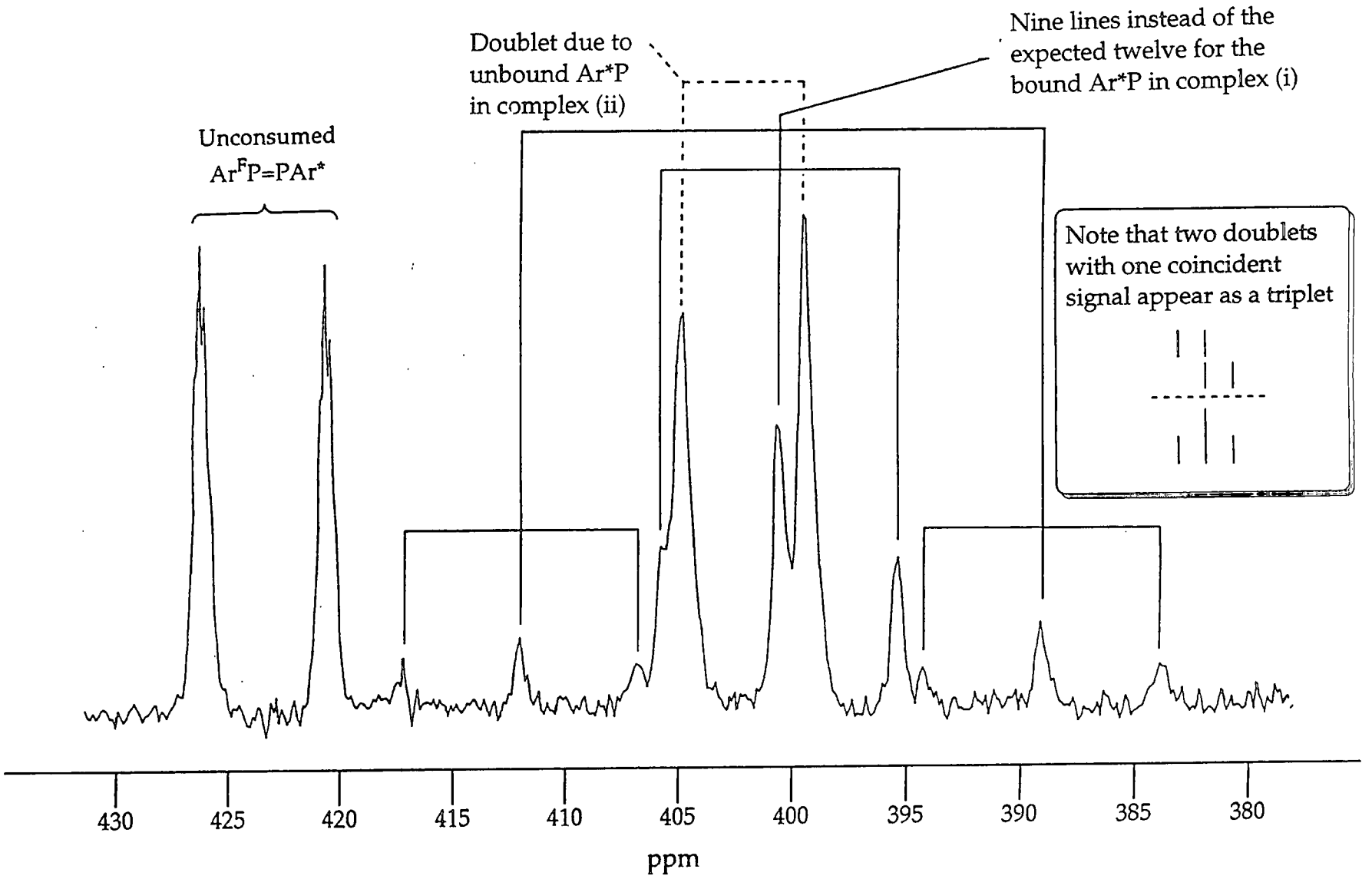

Figure 3.9: *Downfield region of the ^{31}P NMR spectrum of the reaction of $^1/_2[Pt(PEt_3)Cl_2]_2$ with $Ar^*P{=}PAr^F$*

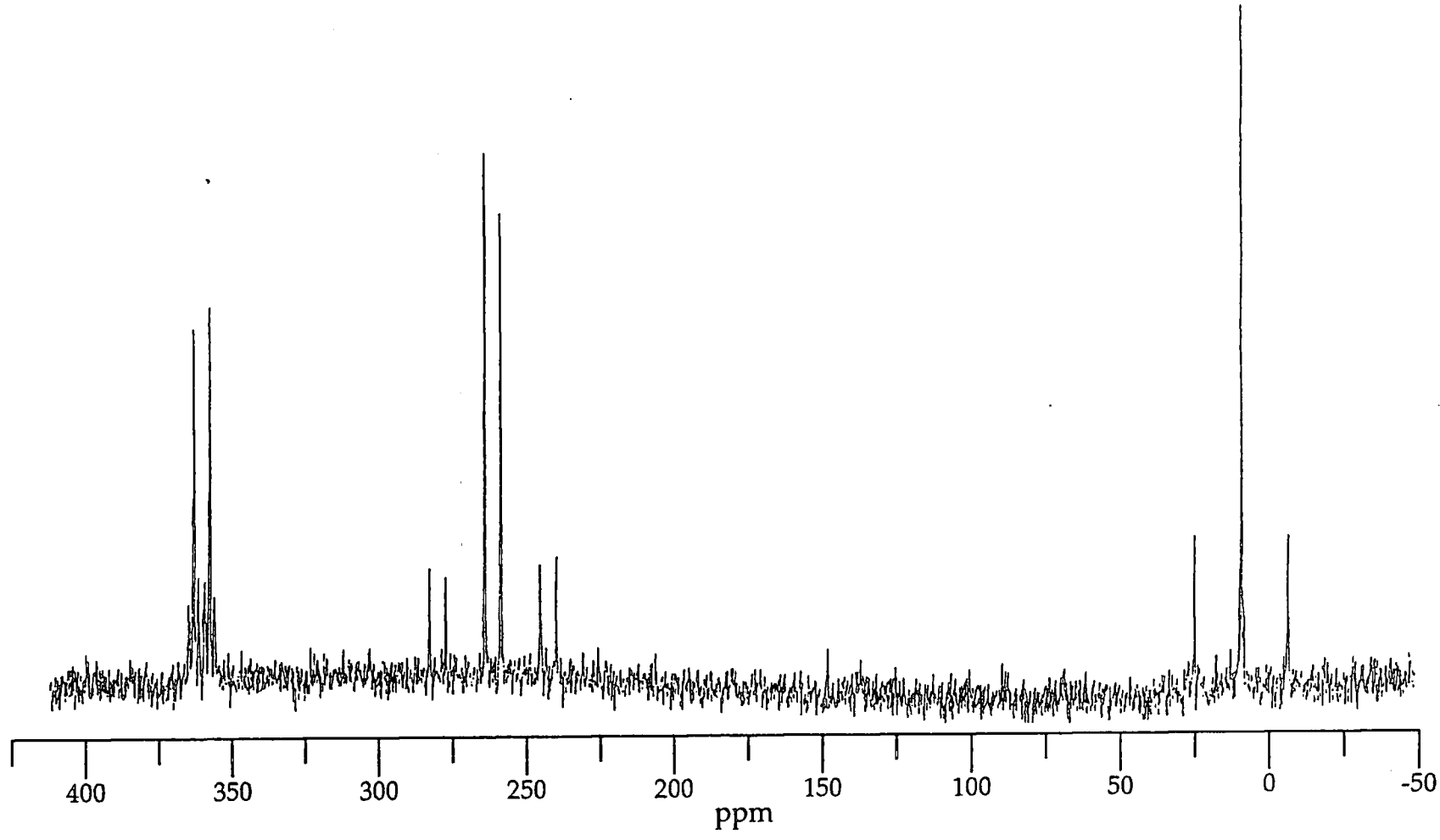

Figure 3.10: *^{31}P NMR spectrum of isolated complex (iv)*

In the Ar*P region, the coincident $^1J_{P_AP_B}$ and $^2J_{P_BPEt_3}$ coupling constants result in 9 lines instead of the expected 12 lines for complex (i) (figure 3.9) ($^1J_{P_AP_B}$ = 528Hz, $^1J_{P_B\text{-}Pt}$ = 2328Hz, $^2J_{P_BPEt_3}$ = 528Hz). There is also a doublet arising from complex (ii) at 402ppm ($^1J_{PP}$ = 548Hz). In both of these complexes, as previously, the diphosphene is inferred to be *trans* to the PEt_3 ligand due to the significant $^2J_{PPEt_3}$ values.

It has not yet proved possible to isolate either of the above products when the reaction was repeated on a larger scale. Unfortunately, although less air-sensitive than the previous product mixture, the complexes decomposed when passed through a silica column. Strangely, when a ^{31}P NMR spectrum was obtained of the scaled-up reaction mixture, signals for a third complex were observed in addition to (i) and (ii) at 260 and 358ppm (figure 3.10). Although a very small amount of this complex was isolated, not enough was obtained for any further characterisation. However, as shown in figure 3.11 complex (iii) would appear to be related to (ii); it is therefore believed that in complex (iii) the diphosphene is *cis* to the PEt_3 ligand. ($^1J_{P_APt}$ = 3732 Hz, $^1J_{P_AP_B}$ = 549 Hz, $^2J_{P_BPt}$ = 343 Hz, $^1J_{PtPEt_3}$ = 3174 Hz, $^2J_{P_APEt_3}$ is not observed).

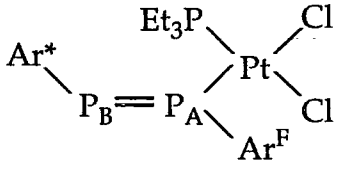

(iii)

Figure 3.11

From this it can be inferred that although the kinetic products of this reaction are the *trans* isomers bound through either of the phosphorus atoms, the thermodynamic product is possibly the *cis* isomer in which the diphosphene is bound through the phosphorus atom attached to the Ar^F group.

A summary of the NMR data for all of these complexes is presented below in table 3.4.

Compound	$^1J_{P(bound)Pt}$ Hz	$^1J_{P_AP_B}$ Hz	$^2J_{PPEt_3}$ Hz	$^1J_{PtPEt_3}$ Hz	δ ^{31}P ppm	
					P_A	P_B
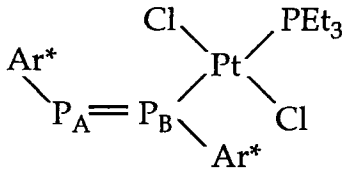	2200	548	487	2917	380	353
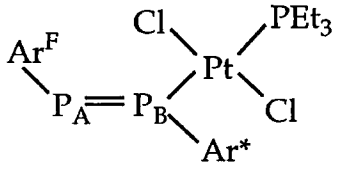	2328	529	528	3000	308	400
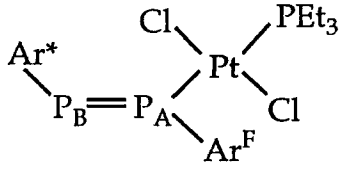	2406	552	521	3139	317	402
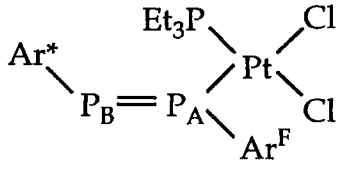	3732	549	-	3174	258	360

Table 3.4: *Summary of NMR data for the proposed complexes formed in reactions 3.6 and 3.7*

3.4 Conclusion

Previous transition metal complexes of the diphosphene $Ar^FP=PAr^F$ have all shown η^1 co-ordination and none has been structurally characterised using X-ray crystallography. In this chapter we have synthesised the first η^2 complexes of $Ar^FP=PAr^F$ on co-ordinatedly unsaturated molybdenum centres and obtained an X-ray structure of one of these complexes.

Complexation to platinum was more complicated, as a number of closely related complexes were formed in the same reaction which made the products of the reaction difficult to separate. However, some insight into the nature of these products was possible from the available NMR data. There is clearly much scope for further research in this field.

3.5 References

1 K.S. Pitzer, *J. Am. Chem. Soc.*, 1948, **70**, 2140. R.S. Mulliken, *J. Am. Chem. Soc.*, 1950, **72**, 4493.

2 M. Yoshifuji, I. Shima, and N. Inamoto, *J. Am. Chem. Soc.*, 1981, **103**, 4587.

3 A.H. Cowley and N.C. Norman, *Progr. Inorg. Chem.*, 1986, **31**, 1 and references therein.

4 O. J. Scherer, *Angew. Chem., Int. Ed. Engl.*, 1985, **24**, 924 and references therein.

5 H. Schäfer and D. Binder, *Z. Anorg. Allg. Chem.*, 1988, **557**, 45. H. Schäfer, D. Binder and D. Fenske, *Angew. Chem., Int. Ed. Engl.*, 1985, **24**, 522. H. Schäfer, D. Binder B. Deppisch and G. Mattern, *Z. Anorg. Allg. Chem.*, 1987, **546**, 799.

6 E. Niecke, B. Kramer and M. Nieger, *Angew. Chem., Int. Ed. Engl.*, 1989, **28**, 215.

7 H. Schäfer and D. Binder, *Z. Anorg. Allg. Chem.*, 1987, **546**, 55.

8 J.C. Leblanc and C. Moïse, *J. Organomet. Chem.*, 1989, **364**, C3-C4.

9 M. Yoshifuji, T. Hashida, K. Shibayama and N. Inamoto, *Chem. Lett.*, 1985, 287.

10 K.M. Flynn, H. Hope, B. D. Murray, M.M. Olmstead and P.P. Power, *J. Am. Chem. Soc.*, 1983, **105**, 7750.

11 A.H. Cowley, J.E. Kilduff, J.G. Lasch N.C. Norman, M. Pakulski, F. Ando and T.C. Wright, *J. Am. Chem. Soc.*, 1983, **105**, 7751.

12 R.A. Bartlett, H.V.R. Dias, K.M. Flynn, M.M. Olmstead and P.P. Power, *J. Am. Chem. Soc.*, 1987, **109**, 5699.

13 R.A. Bartlett, H.V.R. Dias and P.P. Power, *J. Organomet. Chem.*, 1989, **362**, 87.

14 A-M. Caminade, C. Couret, J. Escudié, and M. Koenig, *J. Chem. Soc., Chem. Commun.*, 1984, 1622.

15 G. Huttner, J. Borm and L. Zsolnai, *J. Organomet. Chem.*, 1986, **304**, 309.

16 G. Huttner, J. Borm and L. Zsolnai, *Angew. Chem., Int. Ed. Engl.*, 1985, **24**, 1069.

17 A-M. Caminade, J-P. Majoral, M. Sanchez, R. Mathieu, S. Attali and A. Grand, *Organometallics*, 1987, **6**, 1459.

18 A.G. del Pozo, A-M. Caminade, F. Dahan, J-P. Majoral and R. Mathieu, *J. Chem. Soc., Chem. Commun.*, 1988, 574.

19 D. Fenske and K. Merzweiler, *Angew. Chem., Int. Ed. Engl.*, 1986, **25**, 338.

20 A.H. Cowley, D.M. Giolando, C.M. Nunn, M. Pakulski, D. Westmoreland, and N. C. Norman, *J. Chem. Soc., Dalton. Trans.*, 1988, 2127.

21 H. Vahrenkamp and D. Wolters, *Angew. Chem., Int. Ed. Engl.*, 1983, **22**, 154.

22 M. Scholtz, H.W. Roesky, D. Stalke, K.Keller and F.T.Edelmann, *J. Organomet. Chem.*, 1989, **366**, 73.

23 K.B. Dillon and H.P. Goodwin, *J. Organomet. Chem.*, 1992, **429**, 169 and references therein.

24 T. Lübben, H.W. Roesky, H. Gornitzka, A. Steiner, and D. Stalke, *Eur. J. Solid State Inorg. Chem.* 1995, **32**, 121.

25 R.A. Jones, M.H. Seeberger and B.R. Whittlesey, *J. Am. Chem. Soc.*, 1985, **107**, 6424.

26 P.W. Dyer, V.C. Gibson, J.A.K. Howard, B. Whittle and C. Wilson, *Polyhedron*, 1995, **14**, 103.

27 J. Ho, T.L. Breen, A. Ozarowski and D.W. Stephan, *Inorg. Chem.*, 1994, **33**, 865.

28 M. Yoshifuji, K. Shibayama, N. Inamoto, T. Matsushita and K. Nishimoto, *J. Am. Chem. Soc.*, 1983, **105**, 2495. J.G. Lee, A.H. Cowley and J.E. Boggs, *Inorg. Chim. Acta*, 1983, **77**, L61. V. Galasso, *Chem. Phys.*, 1984, **83**, 407. T.K. Ha, M.T. Nguyan and P. Ruelle, *Chem. Phys.*, 1984, **87**, 23.

29 P.W. Dyer, V.C. Gibson and W. Clegg, *J. Chem. Soc., Dalton Trans.*, 1995, 3313.

30 F.W. Bennett, H.J. Emeleus and R.N. Haszeldine, *J. Chem. Soc.*, 1953, 1565.

31 M. Fild, Z. *Naturforsch*, 1968, **23(b)**, 604.

32 H.P. Goodwin, *Ph.D Thesis*, University of Durham, 1990.

33 K.B. Dillon and H.P. Goodwin, *J. Organomet. Chem.*, 1994, **469**, 125.

Chapter 4

Transition Metal Catalysed Metathesis of Phosphorus-Phosphorus Double Bonds

4.1 Introduction

The two most widely employed routes to symmetrical diphosphenes (RP=PR') involve either treatment of the $RPCl_2$ species with the primary phosphine RPH_2 in the presence of base, typically 1,8-diazabicyclo[5,4,0]undec-7-ene (DBU), (equation 4.1)[1] or the reaction of $RPCl_2$ with a chloride-abstracting agent such as elemental magnesium or bisimidazolidine base (equation 4.2).[2]

$$RPCl_2 + RPH_2 \xrightarrow[-2DBU.HCl]{2DBU} RP{=}PR \qquad (4.1)$$

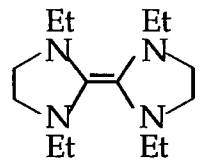

$$2RPCl_2 \longrightarrow RP{=}PR \qquad (4.2)$$

Although the first method can be used to synthesise both symmetrical and unsymmetrical diphosphenes (the latter by using $RPCl_2$ and $R'PH_2$), the second route has, so far, only proved synthetically useful for the formation of symmetrical diphosphenes.

In view of the highly reducing nature and labile co-ordination sphere of the zerovalent tungsten complex $W(PMe_3)_6$[3] it was envisaged that this species would also act as an efficient chloride ion abstractor as in equation 4.3.

$$2RPCl_2 + W(PMe_3)_6 \xrightarrow{-3\ PMe_3} RP{=}PR + WCl_4(PMe_3)_3 \qquad (4.3)$$

This chapter will show that this reaction occurs as anticipated, and in a manner highly reminiscent of the metal-carbene catalysed olefin metathesis reaction.[4]

4.2 Diphosphene metathesis

4.2.1 Reaction of Ar^FPCl_2 with $W(PMe_3)_6$

Initial reactions were carried out with the Ar^F substituted compound, simply on the basis of the stability of the postulated diphosphene product (equation 4.4).

$$2Ar^FPCl_2 + W(PMe_3)_6 \xrightarrow{-3\ PMe_3} Ar^FP{=}PAr^F + WCl_4(PMe_3)_3 \quad (4.4)$$

When a solution of $W(PMe_3)_6$ was treated with 2 equivalents of Ar^FPCl_2 in benzene-d_6 at room temperature the solution immediately changed colour from orange/yellow to deep red. The reaction proceeded smoothly over several hours to give the diphosphene $Ar^FP{=}PAr^F$ in virtually quantitative yield (^{31}P NMR) along with the tungsten(IV) by-product $WCl_4(PMe_3)_3$, which is clearly evident in the ^1H NMR spectrum as a paramagnetic contact-shifted resonance at -8.5ppm.[5]

A possible mechanism for the formation of the symmetrical diphosphene is shown in scheme 4.1. The key intermediate proposed in this mechanism is the tungsten-phosphinidene complex. Doubly bonded transition metal phosphorus compounds are relatively rare, although a few have been structurally characterised.[6-10] Complexes such as $W(=X)Cl_2(PMe_3)_3$ where X = oxo,[11] sulfido[12] and phenylimido[13] demonstrate the ability of the $[WCl_2(PMe_3)_3]$ fragment to stabilise multiply-bonded ligands. However, despite the potential stabilising properties of the Ar^F ligand, no resonance was observed for a phosphinidene complex in the ^{31}P NMR spectrum [^{31}P NMR shifts of metal phosphinidenes can occur over a wide frequency range *e.g* δ 666-800 for $(\eta\text{-}C_5H_5)_2Mo(=PR)$[6] to δ 175-230 for $(N_3N)Ta(=PR)$[7], $(N_3N=(Me_3SiN(CH_2)_2)_3N)$].

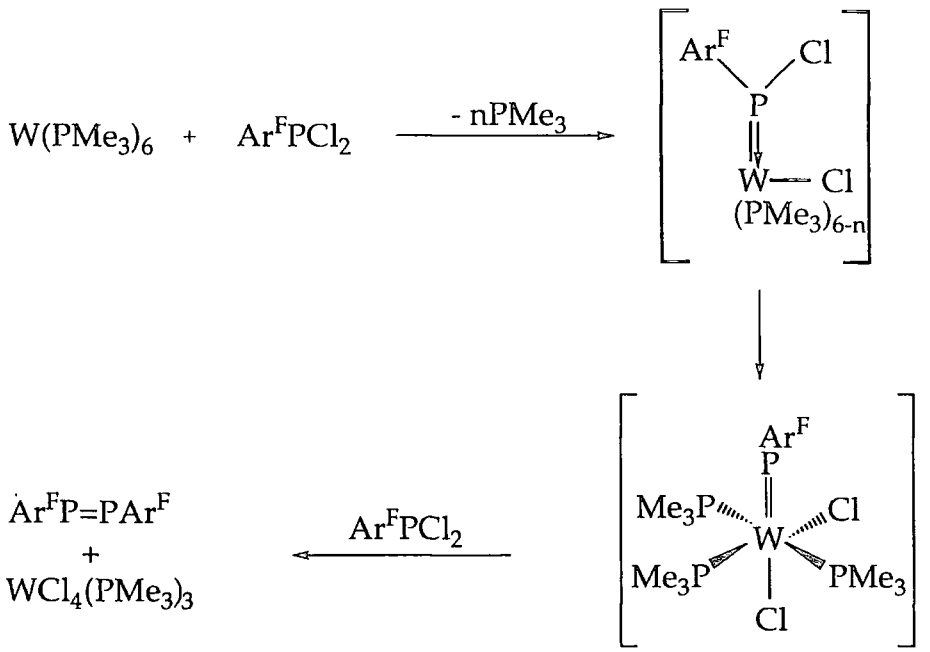

Scheme 4.1

When the reaction was scaled up, the symmetrical diphosphene could be isolated simply by removal of the solvent and subsequent sublimation of the diphosphene (80°, 5 x 10^{-2} Torr) from the reaction mixture (85% yield).

The reaction has also been carried out using other closely-related precursors Ar*PCl_2 and $Ar^{F'}PCl_2$ to afford the diphosphenes Ar*P=PAr* and $Ar^{F'}P=PAr^{F'}$ in good yield.

4.2.2 Synthesis of the unsymmetrical diphosphene $Ar^FP=PAr^*$

Unsymmetrical diphosphenes have previously been prepared via the analogous route to that outlined in equation 4.1; however, these syntheses proceed only in low yield and often give product mixtures of the symmetrical and unsymmetrical diphosphenes.[14] In an attempt to synthesise the unsymmetrical diphosphene, $Ar^FP=PAr^*$, $W(PMe_3)_6$ was reacted with a 1:1 mixture of Ar^FPCl_2 and Ar^*PCl_2 (equation 4.5).

$$Ar^FPCl_2 + Ar^*PCl_2 + W(PMe_3)_6 \xrightarrow{-3\ PMe_3} Ar^FP=PAr^* + WCl_4(PMe_3)_3 \quad (4.5)$$

As in the previous reactions, the solution immediately changed colour from orange/yellow to deep red and ^{31}P NMR spectroscopy indicted that the unsymmetrical diphosphene $Ar^FP=PAr^*$ was generated in >95% yield (figure 4.1). $Ar^FP=PAr^*$ gives rise to two doublet resonances at 536ppm (Ar^*P, $^1J_{PP}$=570 Hz) and 417ppm (Ar^FP, $^1J_{PP}$=570 Hz). * and Δ indicate resonances due to the symmetrical diphosphenes; note that Δ is broadened due to PF coupling ($^4J_{PF}$ = 22Hz), an effect also seen on the Ar^FP signals of the major product. During formation it could be seen that the symmetrical diphosphene $Ar^FP=PAr^F$ formed first, which then converted to $Ar^FP=PAr^*$ with the Ar^*PCl_2 over a few hours.

Somewhat surprisingly, when the reaction was scaled up, upon removal of the reaction solvent the symmetrical diphosphenes were precipitated as shown by the resultant ^{31}P NMR spectrum (figure 4.2), indicating the presence of a species in solution that is capable of rapidly catalysing the exchange of the diphosphene PR end groups (Scheme 4.2).

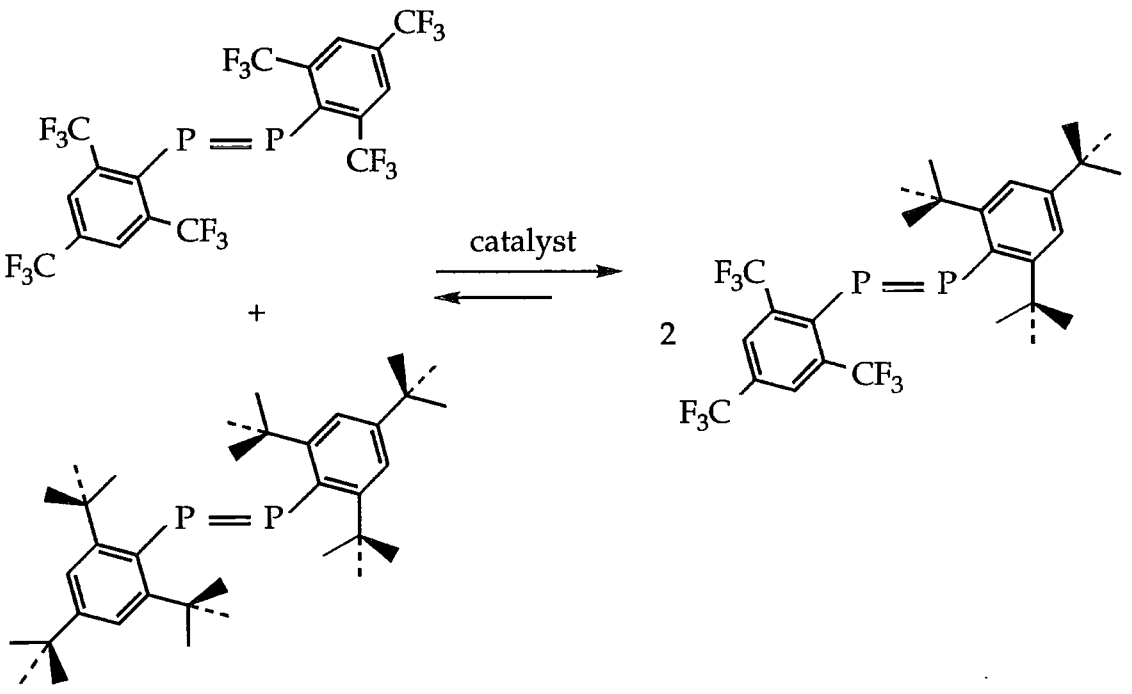

Scheme 4.2

That the exchange does not occur in the absence of the tungsten species was shown by stirring a mixture of the two symmetrical diphosphenes in benzene solution at room temperature; none of the symmetrical diphosphene is formed under these conditions. However, when a trace amount of a solution derived from the $W(PMe_3)_6/Ar^FPCl_2$ mixture is added to this solution, exchange of the PR end groups occurs to establish the same (equilibrium) mixture of the symmetrical and unsymmetrical diphosphene species.

In order to isolate the unsymmetrical diphosphene it is first necessary to destroy the catalytic metal phosphinidene species. A convenient method involves treating the solution mixture with benzaldehyde, a procedure analogous to that used to terminate well-defined alkylidene olefin metathesis catalysts and one which generates the phosphaalkene species $Ar^FP{=}C(H)Ph$[15] and $Ar^*P{=}C(H)Ph$.[16] These could be identified by their characteristic ^{31}P NMR resonances at 218.1 and 257.4ppm (figure 4.3); together they lend strong support for metal-phosphinidene species of the type [M]=PR

being present in the catalyst solution. Schrock and co-workers, for example, have shown that the isolable tantalum phosphinidene compound $(N_3N)Ta{=}PR$ [N_3N= $(Me_3SiN(CH_2)_2)_3N$][7] reacts with benzaldehyde to generate RP=CHPh and the oxo complex $(N_3N)Ta{=}O$.

Although it has not yet been possible to detect a phosphinidene species directly (as mentioned earlier M=PR chemical shifts cover a wide range of values), a possible mechanism for the reaction could be PR end-group exchange that involves the intermediacy of M=PR species, a mechanism that is attractive in its close resemblance to the metal-alkylidene catalysed exchange of CHR end-groups in olefin metathesis (Scheme 4.3).

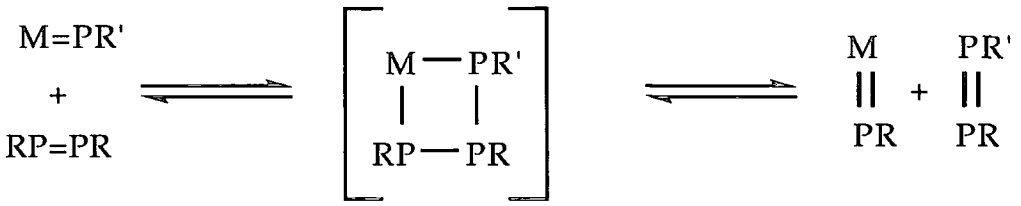

Scheme 4.3

When the reaction was scaled up, the reaction solution was filtered prior to the addition of benzaldehyde and the filtrate was stirred at room temperature. The solution was then filtered again and Et_2O added. This solution was left standing in the fridge overnight, after which time further tungsten oxo species had precipitated. The remaining solution was then filtered again, the solvent was removed *in vacuo* and the unsymmetrical diphosphene purified as a viscous oil by passing it down a silica column (yield 50%). Crystals precipitated slowly over several days from this viscous material upon prolonged standing at room temperature.

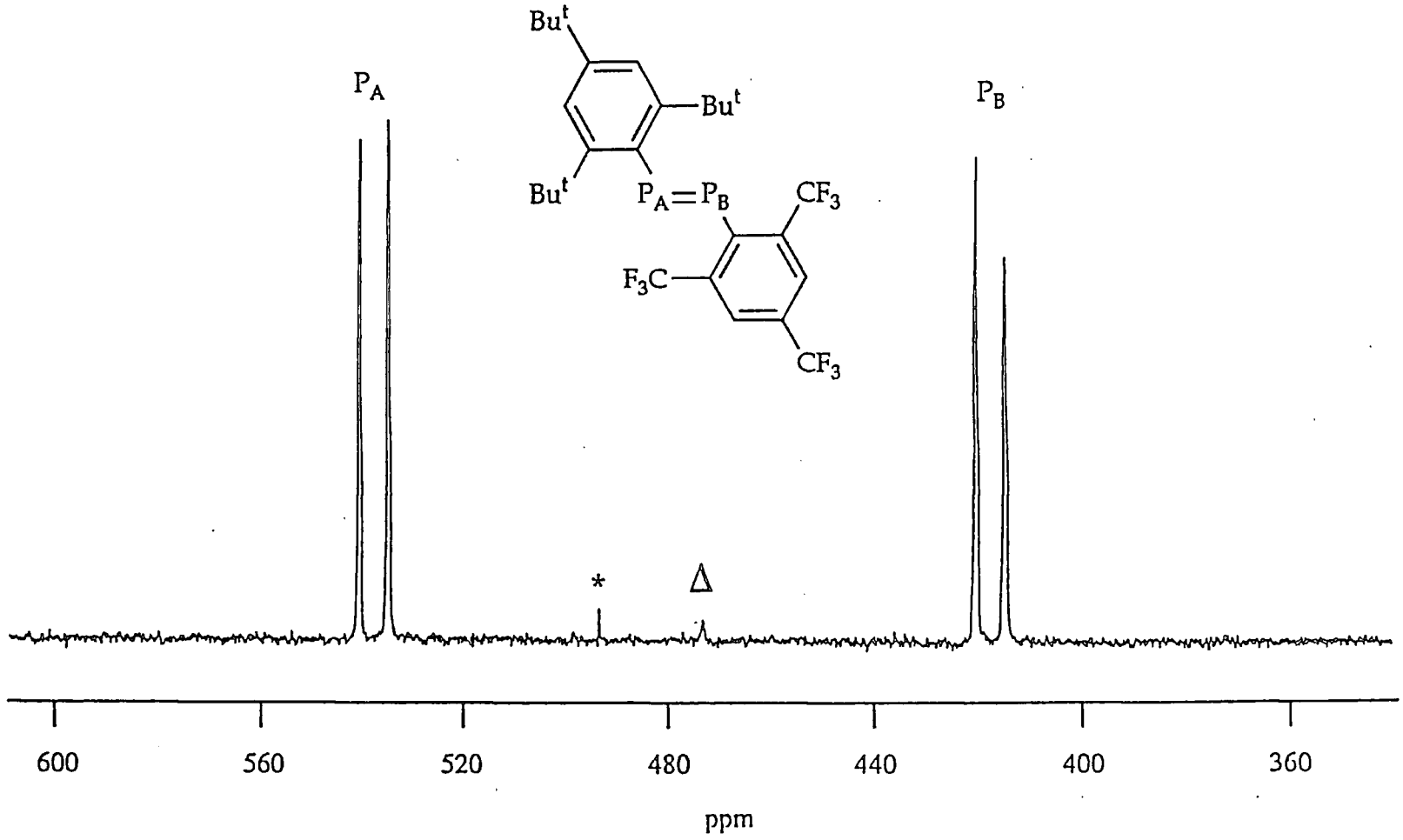

Figure 4.1: *^{31}P NMR spectrum of $Ar^FP{=}PAr^*$ generated upon treatment of a 1:1 mixture of Ar^FPCl_2 and Ar^*PCl_2 with $W(PMe_3)_6$ in benzene*
(and Δ indicate resonances due to the symmetrical diphosphenes, $Ar^FP{=}PAr^F$ and $Ar^*P{=}PAr^*$ respectively)*

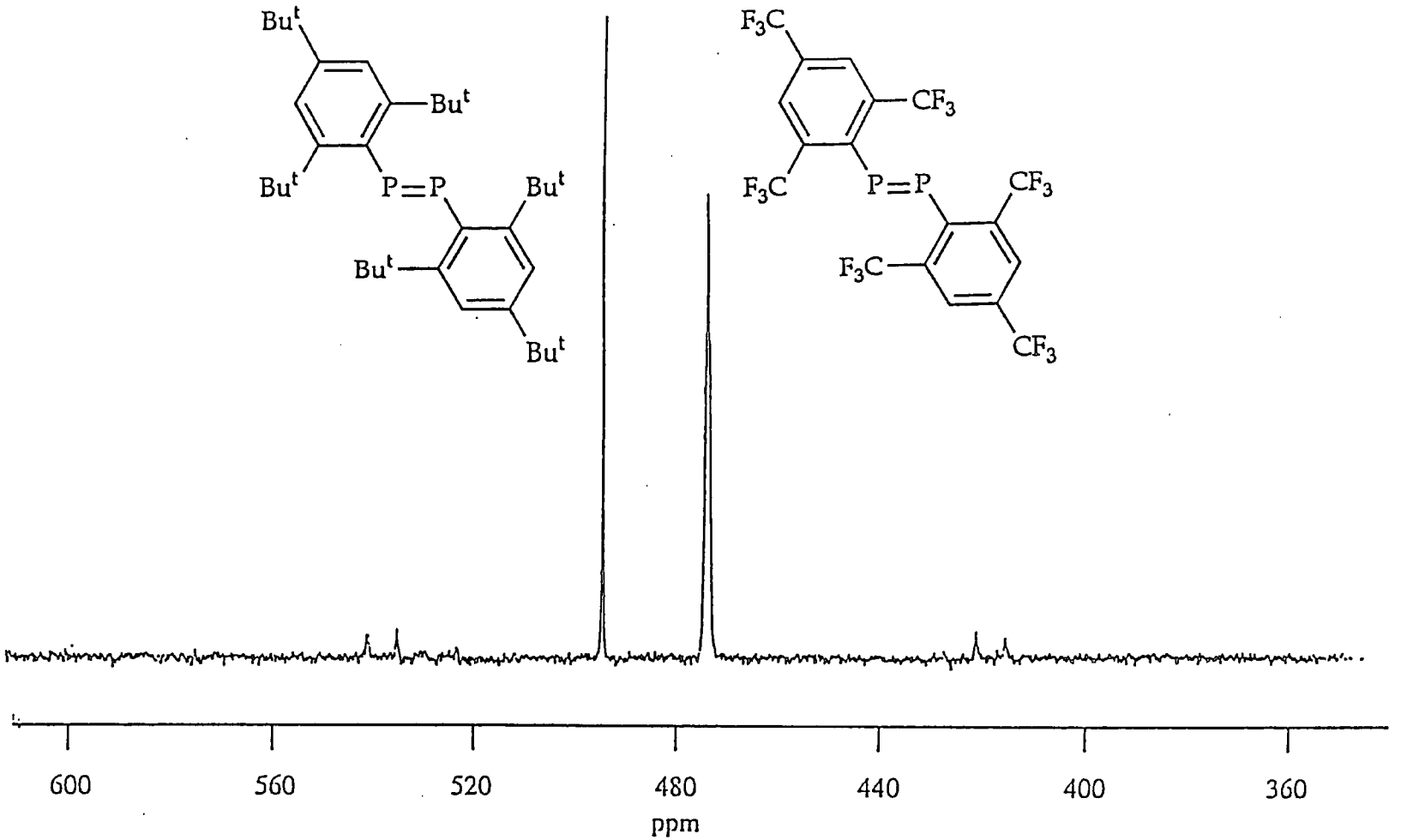

Figure 4.2: *^{31}P NMR spectrum of the precipitated solids from the reaction of a 1:1 mixture of Ar^FPCl_2 and Ar^*PCl_2 with $W(PMe_3)_6$ in benzene*

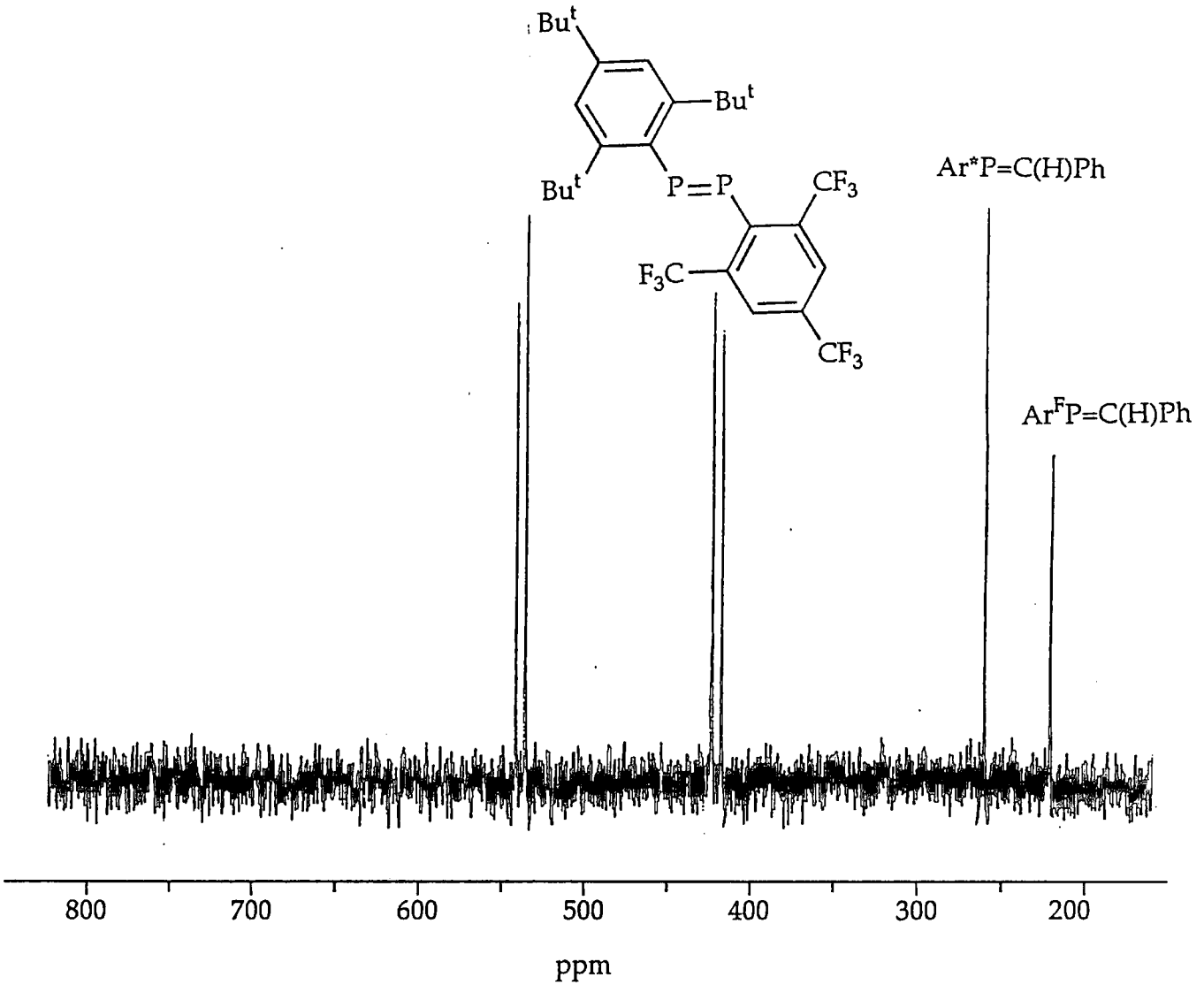

Figure 4.3: *^{31}P NMR spectrum of the $Ar^FPCl_2/Ar^*PCl_2/W(PMe_3)_6$ mixture following the addition of benzaldehyde*

4.3 Tricyclophosphane synthesis

4.3.1 Reaction of (trip)PCl_2 with $W(PMe_3)_6$

The reaction was carried out using a precursor bearing the slightly smaller substituent, 2,4,6-tri-*iso*propylphenyl (trip), to see whether the system could be extended to other diphosphenes (equation 4.6). Treatment of $W(PMe_3)_6$ with (trip)PCl_2 initially affords the symmetrical diphosphene (trip)P=P(trip) (^{31}P δ 517). However, this is gradually consumed over a period of 8 hours to give the tricyclophosphane $P_3(trip)_3$ which displays characteristic doublet and triplet resonances at δ -99 and -133 (J_{PP} = 180Hz) in its ^{31}P NMR spectrum[17] (figure 4.4).

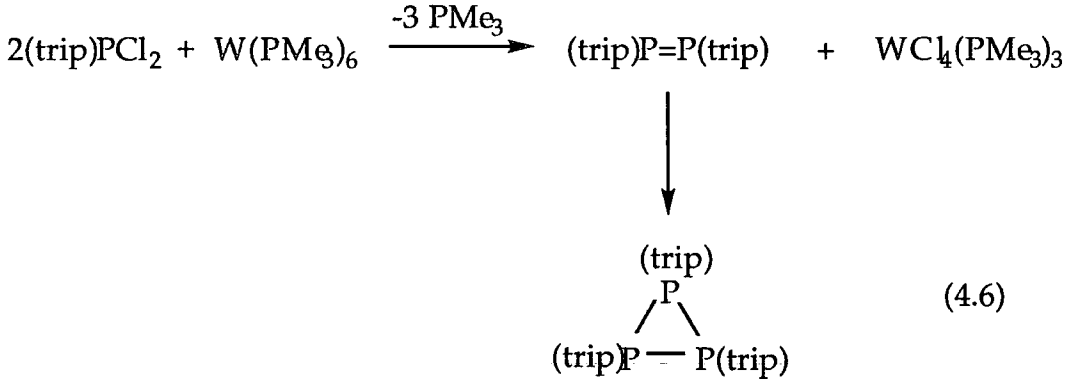

(4.6)

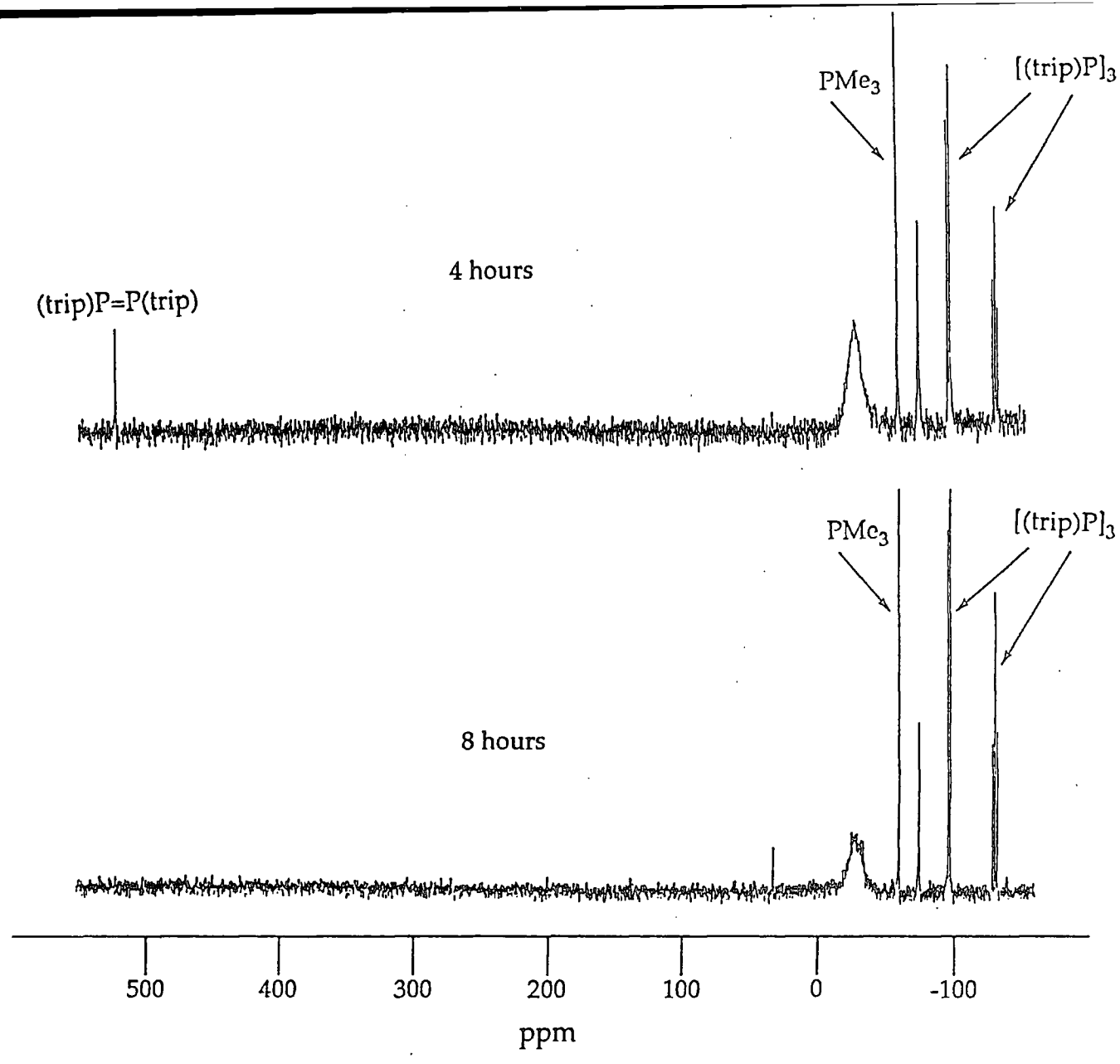

Figure 4.4: *The ^{31}P NMR spectrum of a mixture of $W(PMe_3)_6$ and (trip)PCl_2 after 4 hours (top) and 8 hours (bottom)*

4.3.2 Reaction of $(mes)PCl_2$ with $W(PMe_3)_6$

When the size of the substituents is further reduced to mesityl (mes) the diphosphene is no longer observed [(mes)P=P(mes) is unstable[17]] and the sole product is $P_3(mes)_3$ (δ -109 and -143, J_{PP}= 184Hz).[18]

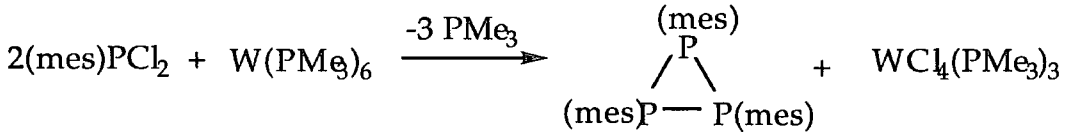

(4.7)

This cyclotrimerisation of PR groups parallels the cyclopropanation reaction observed in reactions of certain metal carbenes with alkenes.[19a] For example, $[CpFe(CO)_2(=CMe_2)]^+[BF_4]^-$ reacts with styrene to afford 1,1-dimethyl-2-phenylcyclopropane.[19b] This further reinforces the analogy between hydrocarbon and phosphorus systems (Scheme 4.4).

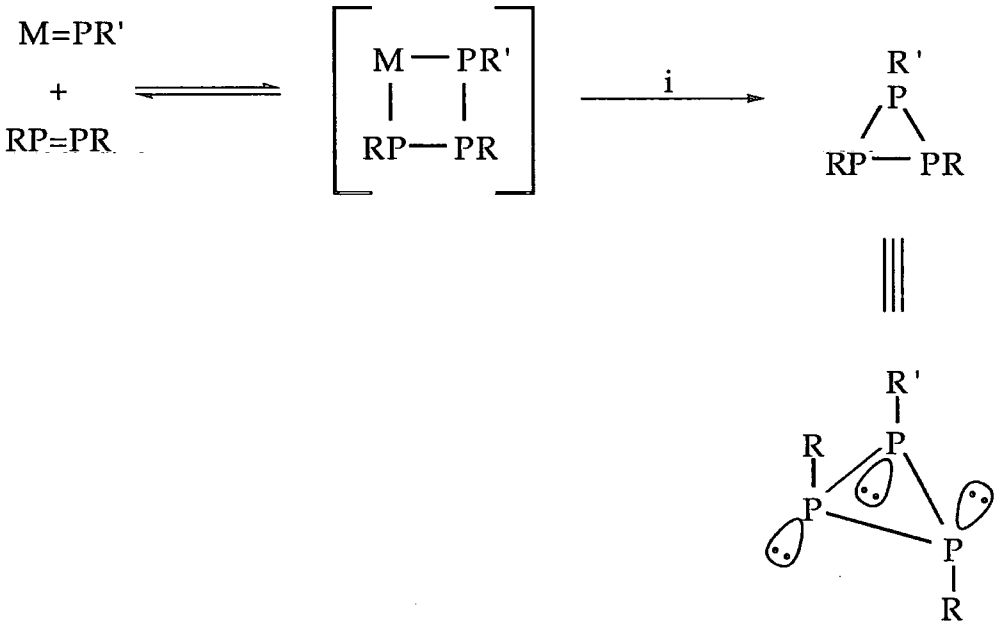

Scheme 4.4: i, R,R' = $C_6H_2Me_3$-2,4,6 or $C_6H_2Pr^i$-2,4,6

These observations are in line with previous reports in which it has been noted that in the cases of alkyl- and aryl-substituted monocyclophosphanes, each substituent favours a certain ring size corresponding to the compound with the highest thermodynamic stability. When sufficient kinetic stabilisation is present, however, other oligomers with different ring sizes can also be observed and can be prepared by special synthetic methods, hence the observation of the diphosphene (trip)P=P(trip) in the previous reaction.

A general synthetic route for the synthesis of tricyclophosphanes is the dehalogenation of an organodihalophosphane by a metal (table 4.1). However, using this method a mixture of oligomers of various ring sizes is always obtained, which has to be separated by fractional distillation or crystallisation. It is therefore interesting to note that conversion to the tricyclophosphane appears to be quantitative for both the mesityl and triisopropyl substituents (^{31}P NMR). This reaction may therefore hold promise as a new synthetic strategy for such compounds, and warrants further study.

Tricyclophosphane	Reducing agent	yield %	ref
$(PCy)_3$	Na	18	20
$(PBu^s)_3$	Mg	24	21
$(PPr^i)_3$	Mg	38	22
$(PBu^t)_3$	Mg	35-60	23
$(PC_3F_7{}^i)_3$	Hg	100	23
$(PC_3F_7{}^n)_3$	Hg	-	24
$(PC_2F_5)_3$	Hg	-	24, 25

Table 4.1: *Comparison of reducing agents and yields in the synthesis of various tricyclophosphanes*

4.4 Attempted metathesis with other doubly bonded species

4.4.1 Reaction of Ar^FPCl_2 with *cis* - stilbene and azobenzene

The ability of the proposed [W]=PAr^F species to undergo heteroatom metathesis was investigated by reacting the *in situ* diphosphene metathesis mixture with *cis*-stilbene and azobenzene. The proposed products, a phosphaalkene and a phospha-imine are shown in equations 4.8 and 4.9 respectively.

$$2Ar^FPCl_2 + PhHC{=}CHPh \xrightarrow{W(PMe_3)_6} 2Ar^FP{=}CHPh \quad (4.8)$$

$$2Ar^FPCl_2 + PhN{=}NPh \xrightarrow{W(PMe_3)_6} 2Ar^FP{=}NPh \quad (4.9)$$

In both cases, upon mixing the reagents in benzene-d_6 at room temperature ^{31}P NMR spectroscopy revealed that only the diphosphene $Ar^FP{=}PAr^F$ had formed. The *cis*-stilbene and the azobenzene remained completely unconsumed. Presumably this is due to the thermodynamic stability of the diphosphene.

4.5 Attempted isolation of a stable phosphinidene

In an attempt to synthesise a stable phosphinidene using the Ar^F group as a substituent, a reaction analogous to the one used by Lappert *et al* in the isolation of the phosphinidene $Cp_2Mo{=}PAr^*$ was carried out (equation 4.10).

$$Cp_2MoHLi + Ar^FPCl_2 \longrightarrow Cp_2Mo{=}PAr^F + LiCl + HCl \qquad (4.10)$$

The reaction was monitored by ^{31}P NMR spectroscopy. A reaction took place immediately; the solution changed colour to bright yellow and a large quantity of a pale solid precipitated. There was no evidence of a phosphinidene species; the only signal observed was that of the diphosphene $Ar^FP{=}PAr^F$.

This can be seen as further evidence that a phosphinidene bearing the Ar^F substituent is far too reactive to be isolated and will react further to form the extremely stable diphosphene.

4.6 Discussion

Historically, the first mononuclear terminal phosphinidene complexes were studied by Mathey *et al*, who showed that the thermal decomposition of 7-phosphanorbornadiene complexes of $M(CO)_5$ (M = Cr, Mo, W) led to the *in situ* formation of $RP{=}M(CO)_5$.[26] These complexes are only transiently stable and their highly reactive nature has been utilised in a rich and varied derivative chemistry characteristic of an electrophilic phosphorus centre (fig 4.5).

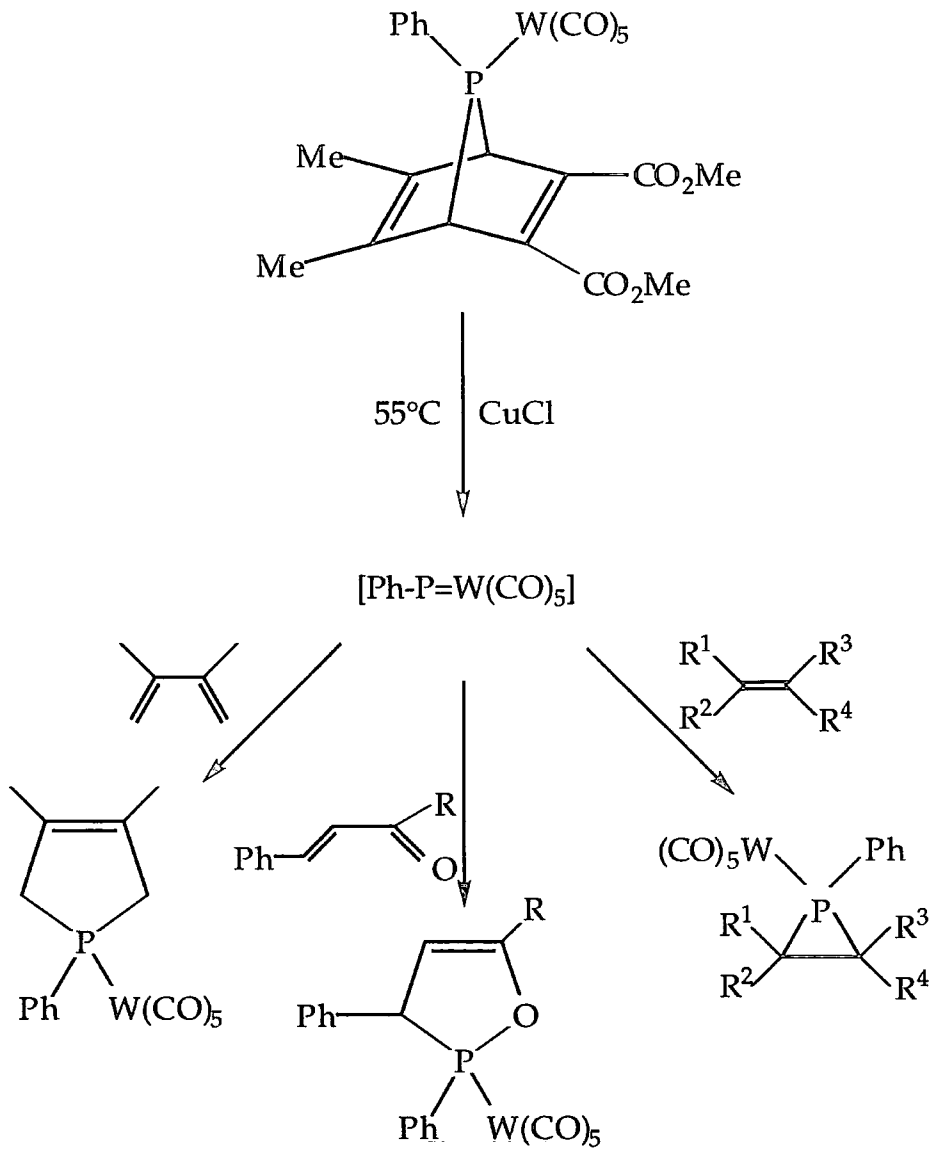

Figure 4.5: *The carbene-like behaviour of the transient phosphinidene PhP=W(CO)$_5$ towards olefins (ref 27)*

The first isolable transition metal phosphinidene complexes were originally reported by Lappert ($Cp_2Mo{=}PAr^*$)[6] and Cowley ($(CO)(PMe_2Ph)_2Cl_2W{=}PAr^*$).[8] The stability of these compounds arises from the bulky nature of the phosphorus substituent.

However, in recent years a new class of nucleophilic phosphinidene complexes has come to light, with the report by Schrock[7] of $(N_3N)Ta{=}PR$

where R=Ph, Cy, or ^{t}Bu, by Wolczanski[10] of (^{t}Bu$_3$SiO)$_3$Ta=PPh, and by Stephan[9] of Cp$_2$Zr(=PAr*)(PMe$_3$). These electron-rich phosphinidenes are believed to be analogous to Schrock-type carbenes and distinct from the transient phosphinidene complexes of low valent transition metals.

Aldehydes react smoothly with (N$_3$N)Ta=PR to provide the stable oxo tantalum complex (N$_3$N)Ta=O and the coresponding phosphaalkene; similar reactivity has been reported for the zirconocene phosphinidene also. Similar observations with our system lead us to believe that the phosphinidene intermediate generated is also nucleophilic. Its transient nature is ascribed to the strong thermodynamic stability of the diphosphene product.

Interestingly, Stephan and co-workers have observed the formation of the η^2-diphosphene adduct Cp*$_2$Zr{η^2-(mes)P=P(mes)} from the postulated phosphinidene intermediate Cp*$_2$Zr=P(mes).[9] However, the potential of this system for diphosphene metathesis has not been explored.

4.7 Conclusion

$W(PMe_3)_6$ can be used to metathesise catalytically P=P double bonds. By analogy to olefin metathesis chemistry, (phosphorus is diagonally related to carbon), a transition metal phosphinidene is the proposed active intermediate. The driving force for the reaction is the thermodynamic stability of the diphosphene or tricyclophosphane products, which in turn is dependent upon the phosphorus substituent. This is believed to be the first reported example of a second row element heteroatom metathesis reaction.

4.8 References

1 A.H. Cowley and N.C. Norman, *Prog. Inorg. Chem.*, 1986, **34**, 1.

2 M. Yoshifuji, *Multiple Bonds and Low Coordination in Phosphorus Chemistry*, ed. M. Regitz and O.J. Scherer, Thieme, Stuggart, 1991.

3 D. Rabinovich, R. Zelman and G. Parkin, *J. Am. Chem. Soc.*, 1992, **114**, 4611.

4 K.J. Ivin, *Olefin Metathesis*, Academic Press, New York, 1983.

5 V.C. Gibson, C.E. Graimann, P.M. Hare, M.L.H. Green, J.A. Bandy, P.D. Grebenik and K. Prout, *J. Chem. Soc., Dalton Trans.*, 1985, 2025.

6 P.B. Hitchcock, M. F. Lappert and W.P. Leung, *J. Chem. Soc., Chem. Commun.*, 1987, 1282.

7 C.C. Cummins, R.R. Schrock and W.M. Davis, *Angew. Chem., Int. Ed. Engl.* 1993, **32**, 756.

8 A.H. Cowley, C. Pellerin, J.L. Atwood and S.G. Bott, *J. Am. Chem. Soc..*, 1990, **112**, 6734.

9 Z. Hou, T.L. Breen and D.W. Stephan, *Organometallics*, 1993, **12**, 3158.

10 J.B. Bonanno, P.T. Wolczanski and E.B. Lobtovsky, *J. Am. Chem. Soc.*, 1994, **116**, 11159.

11 K.W. Chiu, D. Lyons, G. Wilkinson, M. Thornton-Pett and M.B. Hursthouse, *Polyhedron*, 1983, **2**, 803.

12 K.A. Hall and J.M. Mayer, *J. Am. Chem. Soc.*, 1992, **114**, 10402.

13 D.C. Bradley, M.B. Hursthouse, K.M.A. Malik, A.J. Nielson and R.L. Short, *J. Chem. Soc., Dalton Trans.*, 1983, 2651.

14 L. Weber, *Chem. Rev.*, 1992, **92**, 1839 and references therein.

15 K.B. Dillon and H.P. Goodwin, *J. Organomet. Chem.*, 1994, **469**, 125.

16 M. Yoshifuji, K. Toyota, K. Shibayama and N. Inamoto, *Chem. Lett.*, 1983, 1153.

17 F. Bicklehaupt, C.N. Smit, and Th.A. Van der Knapp, *Tetrahedron Lett.*, 1983, 24, 2031.

18 V. Saboonchian, A.A. Danopoulos, A. Gutierrez, G. Wilkinson and D.J. Williams, *Polyhedron*, 1991, 10, 2241.

19 (a) M. Brookhart and W.B. Studabaker, *Chem Rev*, 1987, 87,411
(b) C.P Casey, W.H. Miles, H. Tukada and J.M. O'Connor, *J. Am. Chem. Soc.*, 1982, **104**, 3761.

20 M. Baudler, C. Pinner, C. Gruner, J. Hellmann, M. Schwamborn and B. Kloth, *Z. Naturforsch*, 1977, **32b**, 1244.

21 M. Baudler, G. Furstenberg, H. Suchomel and J. Hahn, *Z. Anorg. Allg. Chem.*, 1983, **498**, 57.

22 M. Baudler and C. Gruner, *Z. Naturforsch*, 1977, **31b**, 1311, M. Baudler and J. Hellmann, *Z. Anorg. Allg. Chem.*, 1981, **480**, 129.

23 R.A. Wolcott and J.L. Mills, *Inorg. Chim. Acta*, 1978, **30**, L331.

24 L.R. Smith and J.L. Mills, *J. Am. Chem. Soc.*, 1976, **98**, 3852. H.G. Ang, M.E. Redwood and B.O. West, *Aust. J. Chem.*, 1972, **25**, 493.

25 A.H. Cowley, T.A. Furtsch and D.S. Dierdorf, *J. Chem. Soc., Chem. Commun.*, 1970, 523.

26 A. Marinetti, F. Mathey, J. Fischer and A. Mitschler, *J. Chem. Soc., Chem. Commun.*, 192, 667.

27 A. Marinetti and F. Mathey, *Organometallics*, 1984, **3**, 456.

Chapter 5

Metal Vapour Synthesis of π-Bound 1,3,5-Tris(trifluoromethyl)benzene Complexes

5.1 Introduction

5.1.1 Metal vapour synthesis

Metal vapour synthesis (MVS) is historically one of the more important synthetic developments in the field of organometallic chemistry, particularly for the preparation of low oxidation state metal complexes, such as d^0 bis(η-arene)s. The other major synthetic route for compounds of this type, the reductive Fischer - Hafner method[1], is somewhat more time-consuming and not viable for several classes of compounds (*vide infra*).

Over thirty years have passed since Pimentel[2] demonstrated that radicals and other highly reactive species could be trapped, and thus studied, within the matrix of an inert gas at extremely low temperatures. Skell[3] modified the technique by employing reactive matrix species co-condensed with carbon vapour. On warming to room temperature, the two reacted together, forming new organic compounds. The process was finally adapted to involve metal atoms by Timms[4] in the late 1960's, when he succeeded in producing $[Cr(\eta\text{-}C_6H_6)_2]$ in high yield by co-condensing chromium atoms with benzene, and elaborated with great effect by Cloke, Green and their co-workers.[5]

The MVS technique involves the low temperature co-condensation of thermally generated metal atoms with molecules of a suitable ligand in an evacuated reaction chamber. The procedure is attractive since atomic metal is far more reactive than bulk metal, as there is considerably greater surface area for collisions and lattice forces are absent. If one considers figure 5.1, the activation energy for the gas phase reaction, $\Delta G_g^{\dagger}$, is much lower than that for the standard state reaction, $\Delta G_s^{\dagger}$. Thus kinetically, MVS has an important advantage over conventional syntheses.

MVS also has thermodynamic advantages. For a favourable process, ΔG, the change in Gibbs' free energy on going from reactants to products, must be negative. From the diagram, the value of ΔG_g for the gas phase reaction will obviously be larger than ΔG_s for the standard state reaction. The possibility also occurs that for certain processes, ΔG_s will actually be positive. In this situation, the reaction will only proceed in the gas phase.

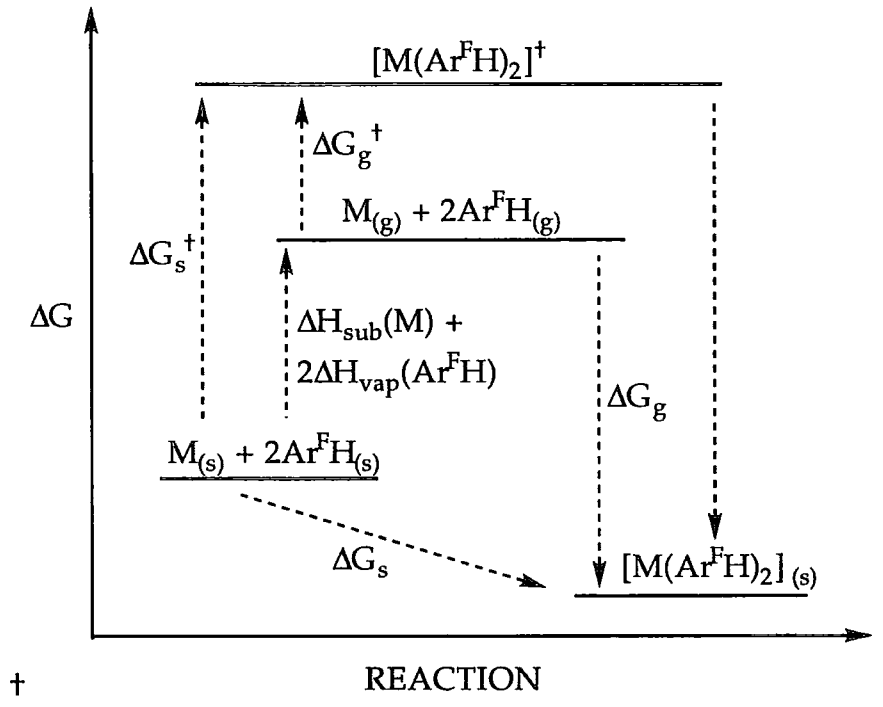

Figure 5.1

As mentioned above, although the Fischer-Hafner route can be used to synthesise several bis(η-arene) metal compounds such as $[Cr(\eta\text{-}C_6H_6)_2]$ (equations 5.1 and 5.2), it is by no means a universal process.

$$CrCl_3 + AlCl_3 + Al + C_6H_6 \longrightarrow [Cr(\eta\text{-}C_6H_6)_2]^+ \qquad (5.1)$$

$$[Cr(\eta\text{-}C_6H_6)_2]^+ + S_2O_4^{2-} \longrightarrow [Cr(\eta\text{-}C_6H_6)_2] \qquad (5.2)$$

This is because it is essentially a Friedel-Crafts type process in which a metal chloride co-ordinates to $AlCl_3$ *via* a lone pair on one of the chlorine atoms. The resultant increased positive dipole of the metal centre then leaves it susceptible to nucleophilic attack by two successive benzene molecules. However, replacement of the benzene by a ligand containing a Lewis base function, *e.g.* acetophenone, inhibits the desired reaction *via* increased competition for the Lewis acidic metal centre. In such cases, the only viable route for the production of M(η-arene)$_2$ compounds is MVS.[6]

The limitations of the Fischer-Hafner route are exemplified by unsuccessful attempts to prepare 16-electron bis(η-arene) titanium or 17-electron bis(η-arene) niobium species. The reason lies in the inability of aluminium to reduce titanium or niobium from higher oxidation states to the zerovalent state under the conditions of the Fischer-Hafner method. The only species which has been obtained from the reaction of $TiCl_4$ with Al/$AlCl_3$ and benzene (or substituted arenes) was a half-sandwich Ti(II) species with co-ordinated $AlCl_3$[7] [fig 5.2(i)]. Similarly, one of the few reported Nb(η-arene) compounds[8] with a dimeric structure and anionic Cl ligands [fig 5.2(ii)], was also prepared *via* Al/$AlCl_3$ reduction.

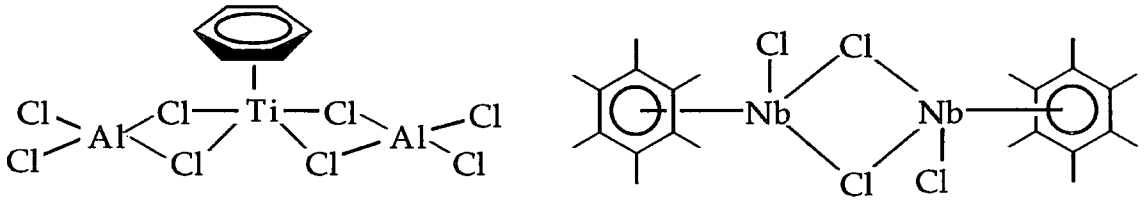

(i) (ii)

Fig 5.2

Subsequent use of MVS by Green *et al* enabled the production of zerovalent Ti and Nb bis(η-arene) species[8,10]. Interestingly, Calderazzo *et al* have recently reported the preparation of bis(η-1,3,5-trimethylbenzene)niobium using the reductive Fischer-Hafner route, in which further reduction of the initial Nb(II) product is facilitated by the addition of thf or dme to the reaction mixture at 258K[11].

5.1.2 The MVS apparatus

The study described in this chapter was carried out in collaboration with Prof. F.G.N. Cloke at the University of Sussex on apparatus based on a machine built at Oxford by Green and Cloke[12]. A schematic representation is given in figure 5.3. Timms' apparatus[13] employed an alumina crucible wound with tungsten wire which was resistively heated. This method only has a useful range up to the melting point of the crucible, (*ca* 1700°C). The reduction by certain metals, *e.g.* the lanthanides, of the crucible at such elevated temperatures is also a problem. Refinements made by Cloke and Green included the development of an electron beam furnace. This consists of a resistively heated tungsten filament which encircles a water-cooled copper hearth. The metal sample is located on the hearth. Originally[14], a 1.4 kW power source was used, with the hearth at earth potential. As the filament is heated, it becomes a thermionic emitter and the beam of electrons is focused onto the metal sample by a stainless steel shield. The metal surface is heated by transfer of kinetic energy, resulting in the production of metal atoms. However, this original design was found to be unable to vaporise certain metals (*e.g.* zirconium, tungsten) and at high potentials, stray electrons were suspected to be the cause of decomposition of ligand and products. Cloke and Green[12] modified the apparatus to employ a hearth at positive potential, in which much higher energies could be employed (3.5

kW), enabling vaporisation of even zirconium and tungsten with little risk of stray electrons. Neither of the above methods, however, is suitable for the vaporisation of aluminium. In order to obtain aluminium atoms, the sample must be placed in a resistively heated $(BN)_x$ crucible.

One of the major criteria for efficient MVS is a high vacuum. In earlier apparatus, a cryogenic pumping system was used, but this was replaced in the Sussex machine by a more efficient system using a two-stage rotary pump and a turbo-molecular pump. This enables an ultimate pressure of 1×10^{-7} mbar to be achieved and a pressure of *ca.* 1×10^{-5} mbar to be maintained during the course of the co-condensation.

There are two types of ligand inlet system, depending on the ambient state of the ligand. The 'solid ligand' system consists of a 250 ml round-bottomed flask with a single elongated neck terminating in a glass to metal seal. This is connected to the ligand delivery line by a coupling with a vacuum-tight perfluorinated silicone rubber seal. The flask is located in a heating mantle which is regulated from the main control panel of the machine. The rate of sublimation into the reaction vessel is controlled by a stainless steel bellows valve.

For volatile, liquid ligands, a glass dropping funnel, incorporating a capillary flow meter, is used. Rate of entrance to the reaction vessel is controlled by a bellows sealed needle valve. In both ligand inlet systems, their delivery lines into the machine and the gas ring can be uniformly heated to maintain a constant flow and to prevent blockage through condensation of the ligand.

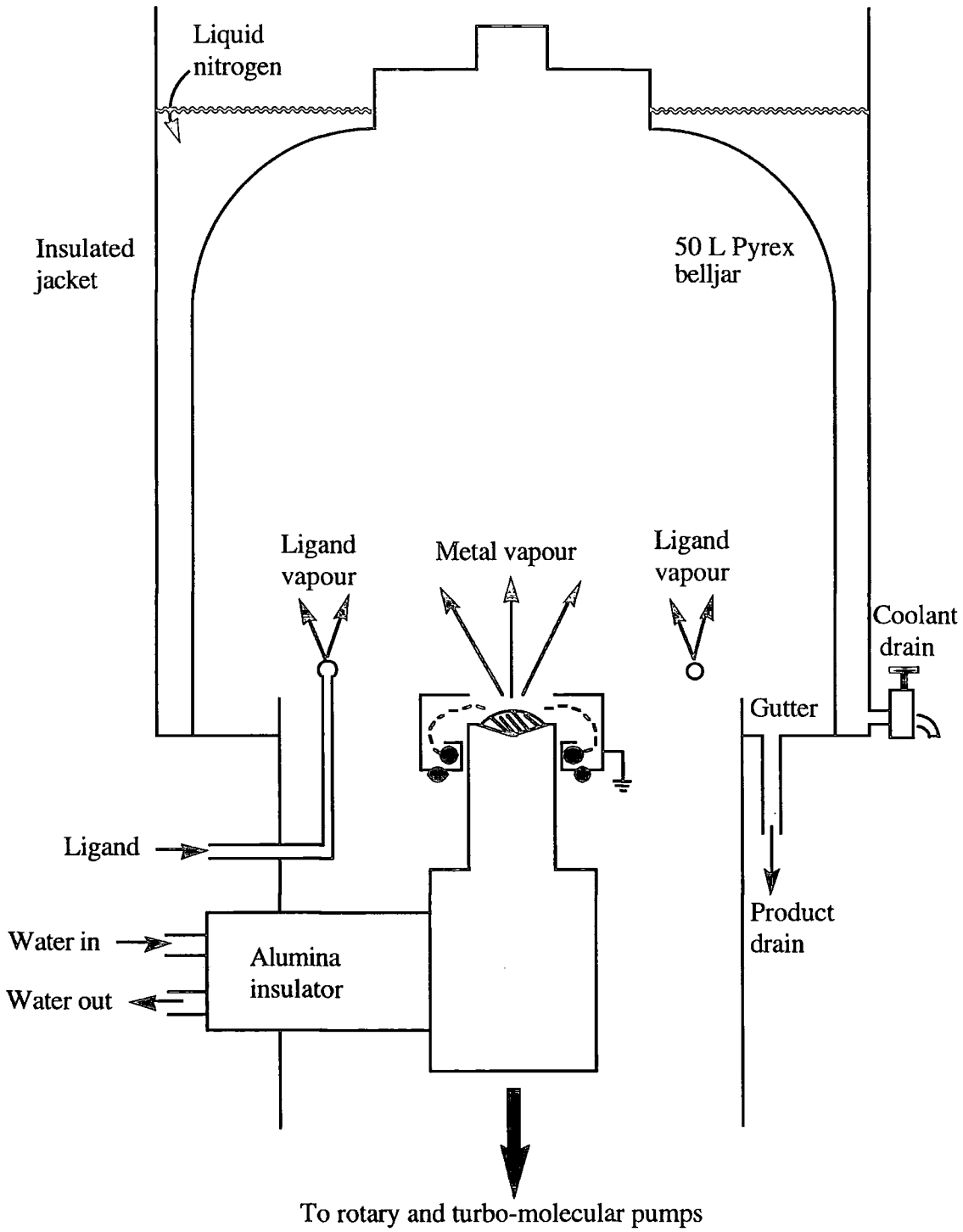

Fig 5.3: MVS Apparatus used at Sussex

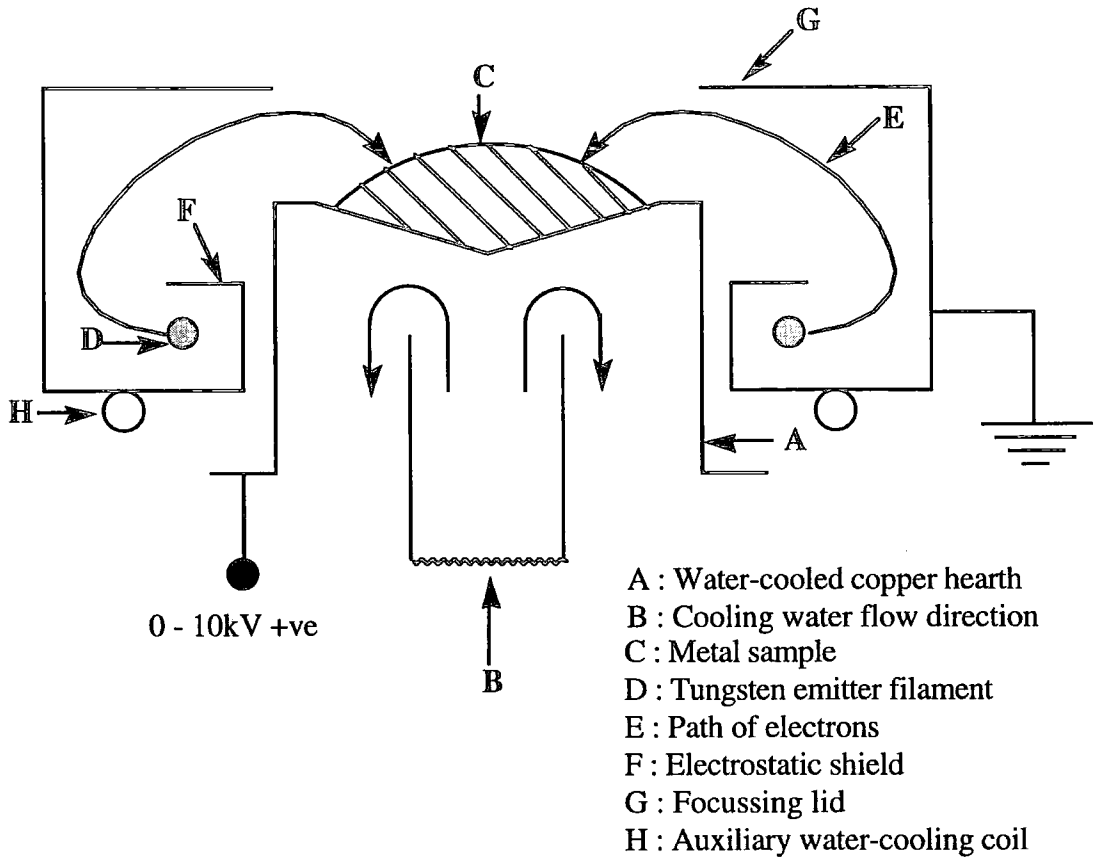

Fig. 5.4: Electron Beam Furnace Cross Section

The reaction vessel is a Pyrex belljar of either 5 or 50 litres capacity, depending on the desired scale. The base of the belljar is fitted with a viton 'O' ring, which acts as a vacuum seal. The bottom of the belljar is also fitted with a heating coil to prevent freezing of the 'O' ring, as it is in close proximity to the cooling jacket. The insulated jacket surrounds the belljar to a level *ca.* 3 cms. from the base and is filled with a suitable coolant during the course of the reaction. The coolant is normally liquid nitrogen, but may be acetone / solid CO_2. In co-condensation at a higher temperature, the reactants may have more kinetic energy for productive collisions, *e.g.* bond-breaking processes.

5.1.3 Description of the MVS technique

Although the actual MVS apparatus has evolved considerably over the years, the basic technique remains the same. The reactants must be vaporised into an evacuated chamber, where they co-condense onto the walls of the chamber, which are cooled to 77K by liquid nitrogen. The low temperature and high vacuum in the chamber serve a number of purposes:

(i) the cooled surface provides a co-condensation and reaction site.

(ii)The high vacuum aids vaporisation of the metal and provides a long mean-free path to discourage gas phase reactions.

(iii)The low temperature keeps the vapour pressure of the ligand to a minimum within the chamber, thus maintaining the high vacuum.

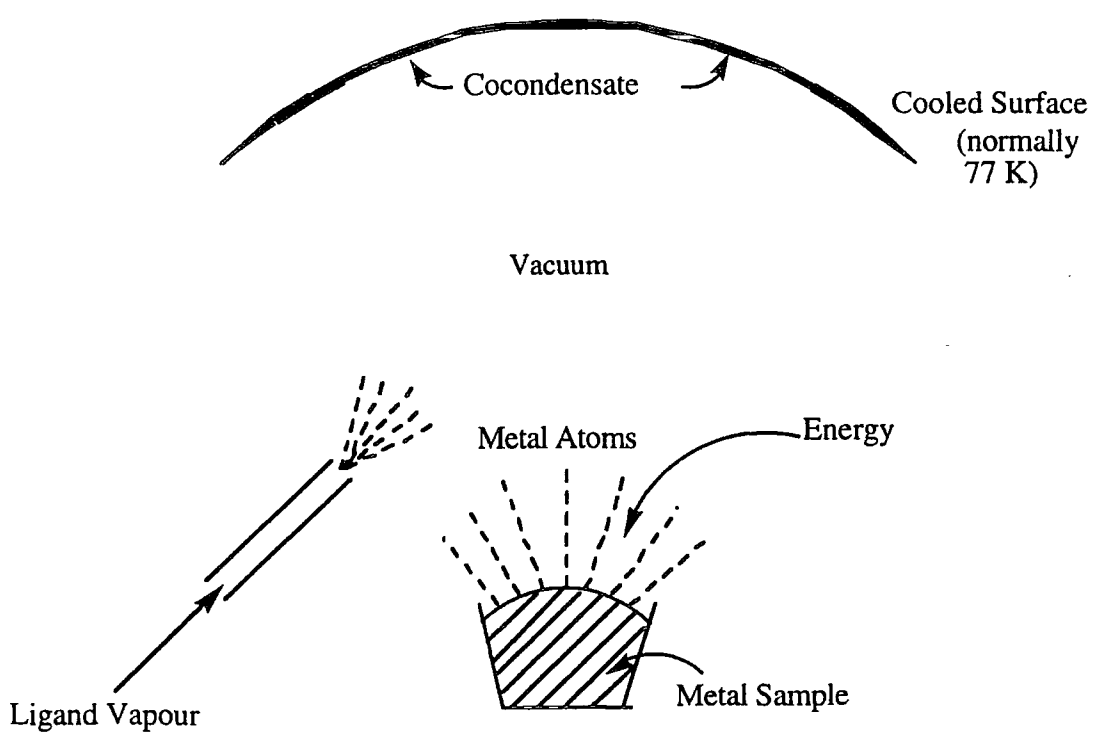

Fig 5.5: Basics of the MVS Technique

The walls of the reaction bell jar are initially coated with a thin layer of the ligand, onto which the metal atoms and further ligand are subsequently vaporised. This ensures that each metal atom is surrounded by an excess of ligand molecules, increasing the likelihood of reaction and lowering the possibility of metal atom recombinations. To this end, the normal ligand-metal excess is approximately tenfold. The coating of ligand on the bell jar also assists in the product removal step since a layer of metal is very difficult to remove with solvent. Thereafter, both metal and ligand are simultaneously vaporised at a rate sufficient to maintain a vacuum of *ca.* $1x10^{-5}$ mbar. After the required quantity of ligand has been vaporised, evaporation of the metal is halted and the coolant is removed from the insulated jacket. The reaction chamber is isolated from the pumping system and filled with nitrogen or argon. A mercury bubbler fitted to the apparatus allows for the expansion of the gas on warming to ambient temperature. The products are subsequently washed from the chamber using a suitable solvent, usually 40-60° petroleum ether or toluene. The resulting solution is filtered to remove colloidal metal, which can lead to product degradation. The solvent / ligand is removed under reduced pressure, or relatively involatile excess ligands may be removed by *in vacuo* sublimation onto a glass finger cooled to 77K. Work-up then follows conventional Schlenk techniques, terminating in product purification by recrystallisation, sublimation or chromatography.

5.2 Synthesis of $M(\eta\text{-}Ar^FH)_2$ complexes using the MVS technique.

5.2.1 Synthesis of $Cr(\eta\text{-}Ar^FH)_2$

Due to the ease with which chromium can be vaporised, it is not surprising that it is the most widely studied metal for MVS. Several zerovalent chromium bis(η-arene) metal complexes have been synthesised and structurally characterised. These include $[Cr(\eta\text{-}C_6H_6)_2]$,[15] $Cr[(\eta\text{-}p\text{-}C_6H_4(CF_3)_2]_2$,[16] $Cr[(\eta\text{-}m\text{-}C_6H_4(CF_3)]_2$,[16] $Cr(\eta\text{-mesitylene})_2$[17] and $Cr(\eta\text{-}C_6F_6)(\eta\text{-}C_6H_6)$.[18] Most of them show planar and parallel aromatic rings which adopt an eclipsed conformation both for benzene and alkylbenzene complexes. The triple decker sandwich complex $Cr_2(\eta^6\text{-mesitylene})_2(\mu\text{-}\eta^6\text{:}\eta^6\text{-mesitylene})$ has also been synthesised.[17] This is the first homoleptic complex of this type containing all arene ligands.

Co-condensation of chromium metal atoms generated by electron beam evaporation with an excess of Ar^FH and heptane at 77K gave a yellow/brown matrix. Room temperature extraction of the products from the reactor with 40-60° petroleum ether and removal of the excess Ar^FH and heptane by distallation under reduced pressure gave the dark yellow 18-electron compound $Cr(\eta\text{-}Ar^FH)_2$ (equation 5.3). The overall isolated yield of the product was 8%, not unreasonable for a metal vapour synthesis experiment.

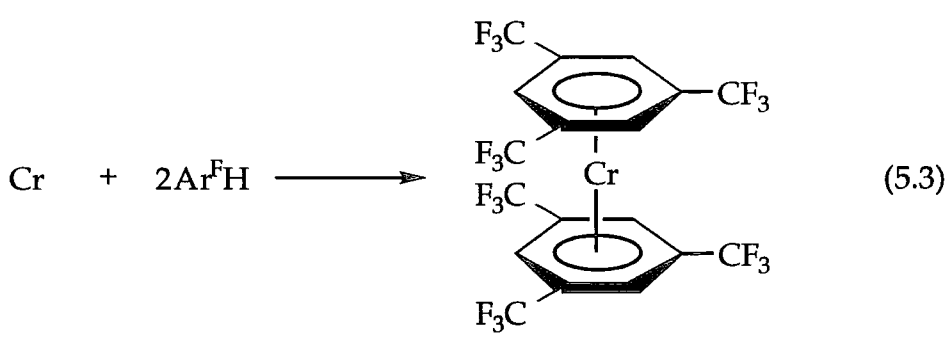

(5.3)

The compound is very soluble in hydrocarbon solvents and is air-stable, as are the previously synthesised Cr[η-*m*-$C_6H_4(CF_3)_2]_2$[16] and Cr[η-*p*-$C_6H_4(CF_3)_2]_2$.[16] This behaviour contrasts sharply with that of other bis(η-arene) chromium complexes which undergo facile one-electron oxidation to Cr^+ species.[18] Electron-withdrawing arene substituents therefore impart kinetic stabilisation to the low valent chromium centre.[16] $Cr(\eta\text{-}Ar^F)_2$ is also fairly volatile; it sublimes at 80°C (1 x 10^{-3} torr). This compares well with other chromium compounds, for example, $Cr(\eta^6\text{-mesityl})_2$ sublimes at 65-70°C (1 x 10^{-3} Torr).[17]

Elemental analysis is consistent with an empirical formula of $C_{18}H_6F_{18}Cr$. The mass spectrum of the compound exhibits a parent ion at 616 (^{52}Cr), and fragments corresponding to $Cr(\eta\text{-}Ar^FH)$ and Ar^FH (334 and 282 respectively) are also observed.

The ^1H NMR spectrum (cyclohexane-d_{12}) shows a sharp singlet at 5.29ppm, and the ^{19}F NMR spectrum shows a sharp singlet at -61.4ppm. These shifts relative to those of the free ligand (^1H δ 7.59, ^{19}F δ -63.3) are characteristic of η-arene transition metal complexes.[19] The ^{13}C NMR spectrum is also consistent with the postulated formula $Cr(\eta\text{-}Ar^FH)_2$.

Cyclic voltammetry was also performed on the compound (figure 5.6). There is a well defined reversible oxidation at +0.46V (*vs.* ferrocene). This rather high value is presumably a reflection of the electron-deficient nature of the complex. $Cr(C_6H_6)_2$ has a reversible oxidation at -0.80V (vs. NCE, -0.12V vs ferrocene)[20] whereas $Cr(C_6H_5F)_2$ has an reversible oxidation at -0.425V (vs. NCE, +0.255V vs ferrocene).[20] These data are in agreement with the theory that electron-donating alkyl substituents facilitate the oxidation and shift the potentials to more negative values.[20] There is also an irreversible reduction at -2.27V (*vs.* ferrocene)

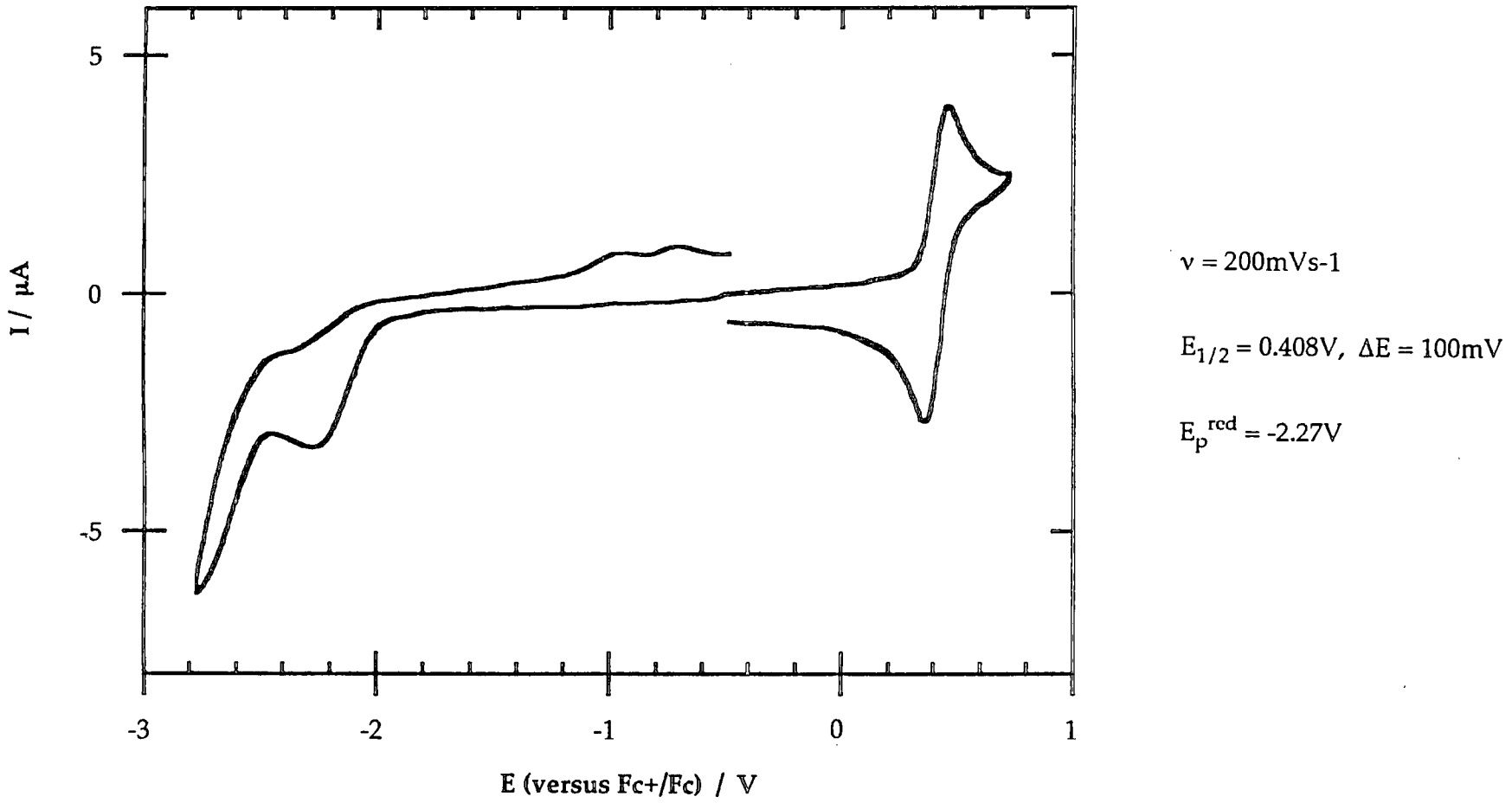

Figure 5.6: *Cyclic Voltammetry trace of $Cr(Ar^FH)_2$ in acetonitrile*

5.2.2 Synthesis of $V(\eta\text{-}Ar^FH)_2$

The first report of $V(\eta^6\text{-arene})_2$ derivatives describes the synthesis of $V(\eta^6\text{-}C_6H_6)_2$ by reaction of VCl_4 with $Al/AlCl_3$ in benzene, followed by the treatment of the reaction mixture with an alkaline aqueous solution of $Na_2S_2O_4$.[21] Some years later bis(mesityl)vanadium was also obtained in a similar way, from VCl_3 with $Al/AlCl_3$ and mesitylene.[22] It was the first $V(\eta^6\text{-arene})_2$ to be structurally characterised.

$[V(\eta\text{-}p\text{-}C_6H_4F_2)_2]$[23], $[V(\eta\text{-}P_3C_2{}^tBu_2)(\eta\text{-}P_2C_3{}^tBu_3)]$[24] and $[V(\eta\text{-}1,4\text{-}Bu^t{}_2C_2H_4)_2]$[25] have been formed using MVS techniques.

When vanadium atoms were co-condensed with an excess of Ar^FH/ heptane on the walls of the reaction vessel which were cooled to 77K, a deep red matrix was observed. Room temperature extraction with 40-60° petroleum ether gave the burgundy red 17 electron compound $V(\eta\text{-}Ar^FH)_2$ (equation 5.4) which is extremely air-sensitive.

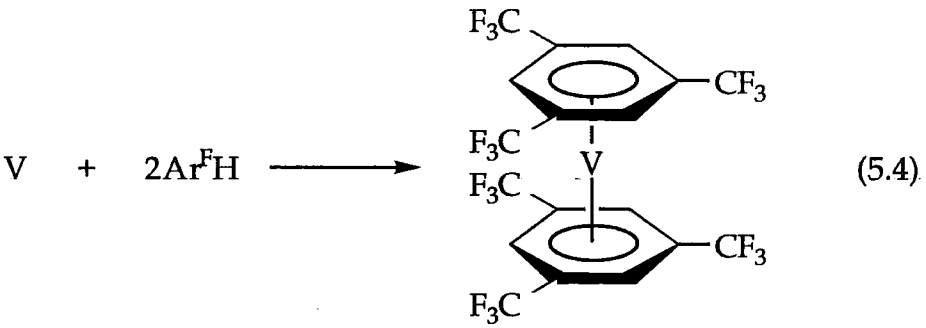

(5.4)

Both mass spectral data (parent ion at 615) and elemental analysis support the proposed product formula. The paramagnetic nature of the compound has been investigated by EPR. The resultant trace (Fig 5.7) clearly shows vanadium hyperfine coupling with 8 lines centred around 3341G (g= 2.011), as would be expected for a V(0) compound (^{51}V, $I=^7/_2$, 99.75% isotopic abundance).

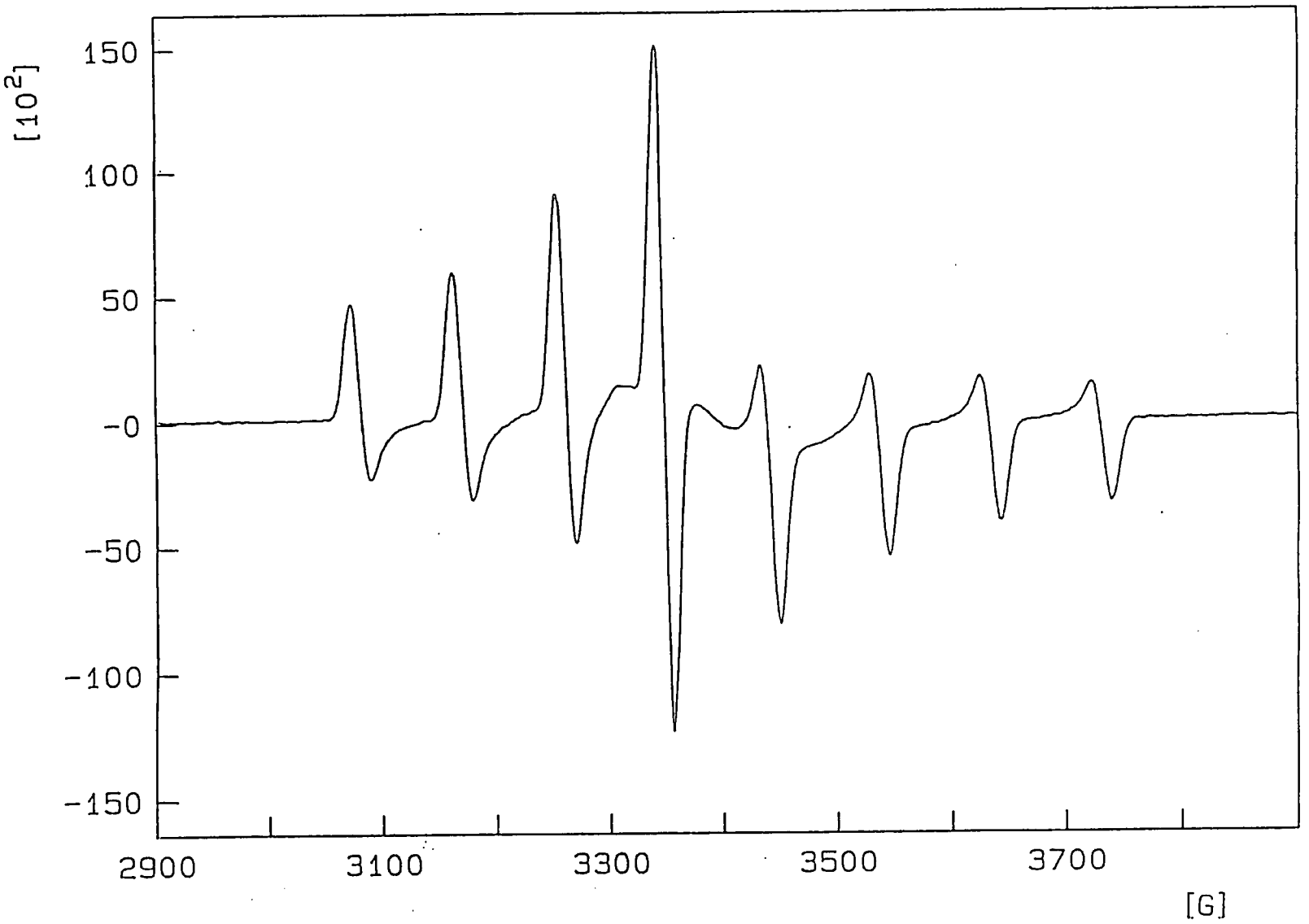

Figure 5.7: *EPR spectrum of $V(Ar^FH)_2$ in acetonitrile*

In comparison, the EPR spectrum of a dilute solution of [V(η-1,4-$Bu^t_2C_6H_4)_2$][25] in toluene at room temperature reveals a well-resolved isotropic octet, indicating coupling to a single ^{51}V nucleus (g = 1.957). In both cases, no proton hyperfine coupling was observed. The EPR spectrum of V(η-$C_6H_6)_2$[26,27] has also been studied and reveals an eight line spectrum centred around 3360G (g = 1.986). In this case, proton hyperfine coupling was resolved under matrix conditions, ($a(^1H)$ = 4.3G).

The complex has also been studied using electrochemistry. In acetonitrile it undergoes a *quasi*-reversible one-electron reduction at -1.74V (vs ferrocene) presumably to the $[V(Ar^FH)_2]^-$ monoanion (Figure 5.8). A cyclovoltammetric study of the redox behaviour of V(η-$C_6H_6)_2$ revealed both a reversible one-electron oxidation (-0.31V *vs* SCE, +0.33V*vs* ferrocene) and a reversible one-electron reduction (-2.71V *vs* SCE, -2.07V *vs* ferrocene). For the V(η-$C_6H_6)_2$/$[V(\eta\text{-}C_6H_6)_2]^+$ couple, an irreversible oxidation to the dication was also observed at 0.35V (*vs* SCE, +0.99V *vs* ferrocene). These data are consistent with the idea that the electron-withdrawing π-bound Ar^FH ligand renders the complex more susceptible to electron gain, and is therefore less likely to undergo oxidation than its electron-rich π-benzene counterparts.

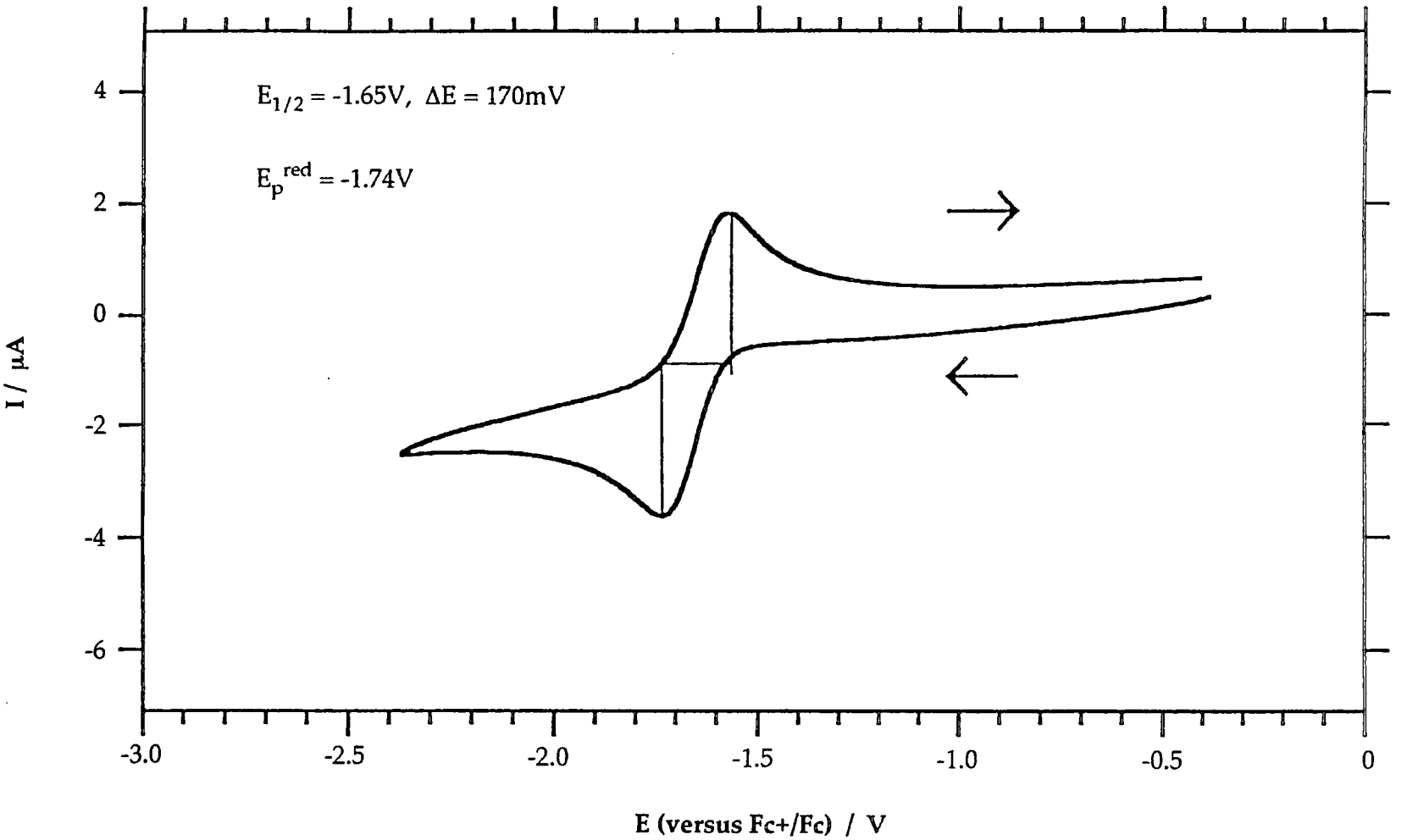

Figure 5.8: *Cyclic Voltammetry trace of $V(Ar^FH)_2$ in acetonitrile*

5.2.3 Synthesis of $Nb(\eta\text{-}Ar^FH)_2$

Organometallic compounds of niobium in which the metal is in an oxidation state ≤ 1 are uncommon. However, several 17 electron bis(arene) derivatives have been prepared using metal vapour synthesis techniques. These include $[Nb(C_6H_6)_2]$,[5] $[Nb(C_6H_5Me)_2]$[5] and [Nb(mesitylene)$_2$].[5] Of these only the [Nb(mesitylene)$_2$] has been structurally characterised, in which the niobium atom is bound to two almost parallel and planar mesitylene rings.[28] The methyl substituents are in an eclipsed conformation. Other characterising data obtained on these three compounds include elemental analyses, mass spectral data, matrix isolation IR spectra and EPR studies.

Co-condensation at 77K of niobium atoms with an excess of Ar^FH / heptane onto the walls of the reaction vessel (equation 5.5) afforded a deep red matrix which was extracted with 40-60° petroleum ether at room temperature to give $Nb(Ar^FH)_2$. The paramagnetic 17 electron product is a highly air-sensitive red compound, which can be recrystallised from *n*-pentane at -30°C.

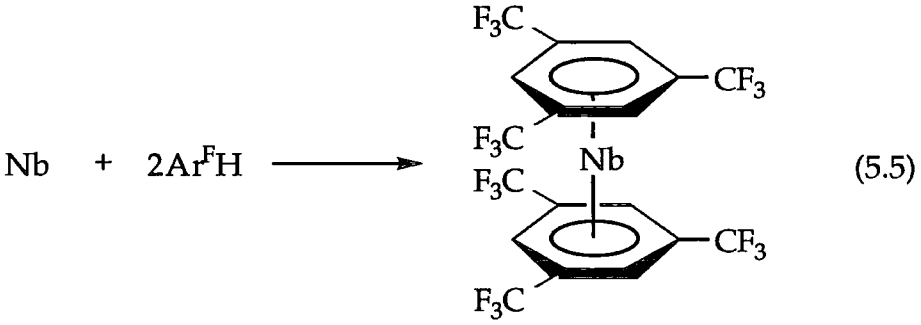

(5.5)

The mass spectrum shows a peak at 657 for the parent ion. Further evidence for the postulated product was obtained by elemental analysis [Observed (calculated) for $C_{18}H_6F_{18}Nb$: C 32.50% (32.90%), H 0.86% (0.92%)].

Slow evaporation of solvent from a saturated heptane solution yielded small dark pink crystals which have been submitted for X-Ray analysis.

Cloke and Green[5] have previously reported that [Nb(η-arene)$_2$] complexes exhibit low first ionisation potentials, indicative of "high energy" electron-rich molecules. The η-toluene and η-mesityl compounds give rise to EPR spectra which contain 10 lines each, as expected for 17 electron d^5 niobium complexes (I = $^9/_2$) with a single unpaired electron: (Nb(η-toluene)$_2$: A_{iso} = 4.59mT, g = 1.992; Nb(η-mesityl)$_2$: A_{iso} = 7.74mT, g = 2.009). An EPR spectrum of Nb(η-Ar^{F}H)$_2$ was obtained in toluene at room temperature. An isotopic singlet exhibiting no hyperfine splitting was observed, centred at 3421G (g = 1.9941).

A cyclic voltammetry study on Nb(η-Ar^{F}H)$_2$ was carried out in acetonitrile (fig. 5.9). It showed a very broad irreversible reduction at -2.52V (*vs.* ferrocene). The irreversible nature of this reduction appears to suggest that the [Nb(η-Ar^{F}H)$_2$]$^-$ anion decomposes and is surprisingly less stable than the anions of the non-fluorinated bis(arene) compounds previously reported. For example, cyclic voltammetry of [Nb(η-C$_6$H$_5$Me)$_2$][29] in tetrahydrofuran shows two fully reversible one-electron waves at chemically accessible potentials: an oxidation at -0.90V (vs SCE, -0.26V *vs* ferrocene) and a reduction at -2.46V (*vs.* SCE, -1.82V *vs* ferrocene).

The ability of [Nb(η-C$_6$H$_5$Me)$_2$] to accommodate an electron implies that it possesses a low lying unoccupied non-bonding orbital. We therefore postulate that the analogous LUMO of [Nb(η-Ar^{F}H)$_2$] is antibonding, and hence reduction leads to facile decomposition. This instability may therefore be due to loss of the arene ring. An alternative explanation is that the fluorinated Ar^{F}H ring decomposes via loss of a fluoride ion, a situation well-documented in organic trifluoromethyl chemistry.[30]

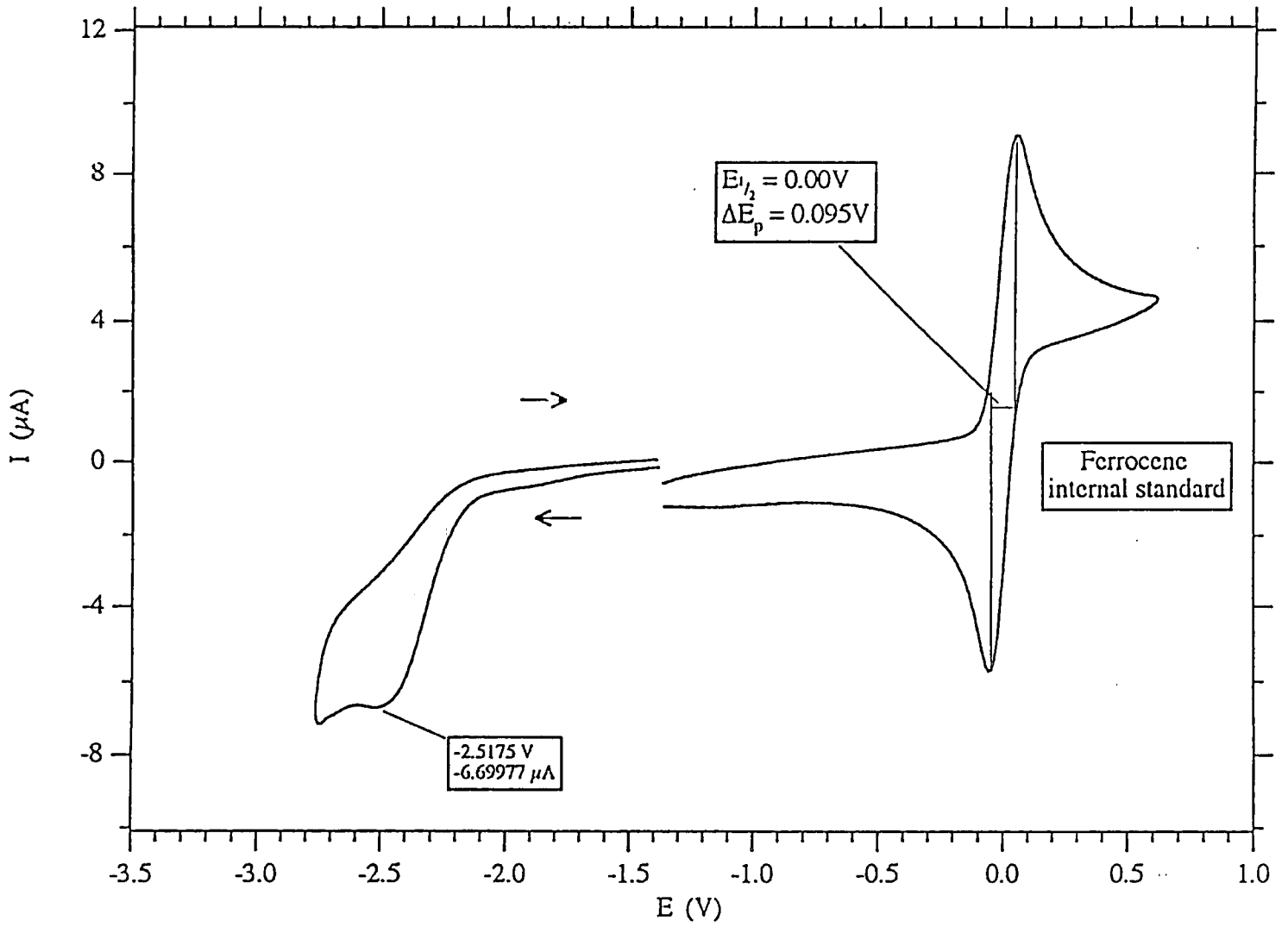

Figure 5.9: *Cyclic Voltammetry trace of $Nb(Ar^FH)_2$ in acetonitrile*

5.2.4 Attempted synthesis of $Ru(\eta\text{-}Ar^F)_2$

In 1994, Timms *et al* synthesised the $[M(\eta^6\text{-arene})(\eta^4\text{-}C_6F_6)]$ complexes (M = Ru, Os, arene = $C_6H_3Me_3$-1,3,5, $C_6H_4Me_2$-1,3 or C_6H_6).[31] The η^6,η^4 co-ordination of these compounds is often observed in the arene chemistry of the Group 8 metals. For example, both $Ru(\eta^6\text{-}C_6H_6)(\eta^4\text{-}C_6H_6)$,[32] which is unstable above -30°C, and thermally stable $Os(\eta^6\text{-}C_6H_6)(\eta^4\text{-}C_6H_6)$ have previously been prepared via the MVS technique.[33] Thermally stable $Ru(\eta^6\text{-}C_6Me_6)(\eta^4\text{-}C_6Me_6)$[34] has also been reported, being prepared *via* the two-electron reduction of $[Ru(\eta^6\text{-}C_6Me_6)_2]^{2+}$. An MVS experiment using the Ar^FH ligand with ruthenium vapour was therefore carried out in an attempt to prepare the analogous 18 electron $Ru(\eta^6\text{-}Ar^FH)(\eta^4\text{-}Ar^FH)$ compound (equation 5.6).

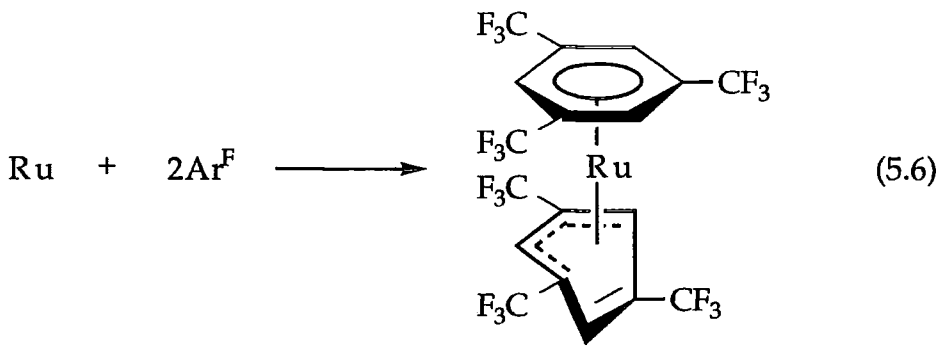

(5.6)

The reaction was carried out following a procedure analogous to that described for Cr, V, and Nb to give a small quantity of a red/brown compound. The extremely low yield of the reaction precluded full characterisation of the product. Nonetheless, mass spectroscopy revealed the parent ion at 666 (^{102}Ru), consistent with the postulated $Ru(\eta^6\text{-}Ar^FH)(\eta^4\text{-}Ar^FH)$ species and fragment ions were also observed for the free Ar^FH ligand, and $Ru(Ar^FH)$, (282 and 384 respectively). Unfortunately, attempts to obtain

NMR spectra of the product were hampered due to apparent decomposition in solution at room temperature.

5.2.5 Attempted synthesis of $Ti(\eta\text{-}Ar^FH)_2$

Despite the relatively rich synthetic history of titanium complexes via the MVS[35] technique, the co-condensation of titanium atoms with the Ar^FH ligand did not afford a tractable product.

5.3 Conclusion

This study has demonstrated the ability of the Ar^FH ligand to bind to metals in an η^6-arene fashion. Despite the lack of structural data to date, this would therefore appear to be an area worthy of further study.

5.4 References

1. E.O. Fischer, F. Scherer and H.O. Stahl, *Chem. Ber.*, 1960, **93**, 2665 ; E.O. Fischer, *Inorg. Synth.*, 1960, **6**, 132.
2. G.C. Pimentel, *Spectrochim. Acta*, 1958, **12**, 94 ; *Pure Appl. Chem.*, 1962,**4**, 61.
3. P.S. Skell, *J. Am. Chem. Soc.*, 1963, **85**, 1023; P.S. Skell, L.D. Wescott, J.P.Goldstein and R.R. Engel, *J. Am. Chem. Soc.*, 1965, **87**, 2829; P.S. Skell and R.R. Engel, *J. Am. Chem. Soc.*, 1966, **88**, 3749 and 4883.
4. P.L. Timms, *Endeavour*, 1968, 27, 133; P.L. Timms, *J. Chem. Soc., Chem. Commun.* , 1969, 1033.
5 F.G.N. Cloke and M.L.H.Green, *J. Chem. Soc., Dalton Trans.*, 1981, 1938
6 P.L. Timms and T.W. Turney, *Adv. Organomet. Chem.*, 1977, **15**, 53.
7 G. Natta, G. Mazzanti and G. Pregaglia, *Tetrahedron*, 1960, **8**, 86; H. Martin and F. Vohwinkel, *Chem. Ber.*, 1961, **94**, 2416; F. Osterle and U. Thewalt, *J. Organomet. Chem.*, 1979, **172**, 317; F. Stallmeier and U. Thewalt, *J. Organomet. Chem.*, 1982, **228**, 149.
8 E.O. Fischer and F. Röhrscheid, *J. Organomet. Chem.*, 1966, **6**, 53.
9 M.T. Anthony, M.L.H. Green and D. Young, *J. Chem. Soc., Dalton Trans.*, 1975, 1419; F.W. Benfield, M.L.H. Green, J.S. Ogden and D. Young, *J. Chem. Soc., Chem. Commun.*, 1973, 866; F.G.N. Cloke, M.F. Lappert, G.A. Lawless and A.C. Swain,*J. Chem. Soc., Chem. Commun.*, 1987, 1667; A.C. Swain, *D. Phil. Thesis*, University of Sussex, 1990.
10 F.G.N. Cloke and M.L.H. Green, *J. Chem. Soc., Dalton Trans.*, 1981, 1938.
11 F. Calderazzo, G. Pampaloni, L. Rocchi, J. Strähle and K. Wurst,*Angew. Chem. Int. Ed. Engl.*, 1991, **30**, 102.
12 F.G.N. Cloke, *D. Phil. Thesis.*, University of Oxford, 1978.

13 R.E. MacKenzie and P.L. Timms, *J. Chem. Soc., Chem. Commun.*, 1974, 650.

14 D. Young, *D. Phil. Thesis*, University of Oxford, 1974.

15 P.L. Timms, *J. Chem. Soc., Chem. Commun.*, 1969, 1033.

16 K.J. Klabunde and H.W. Efner, *Inorg. Chem.*, 1975, **14**, 789.

17 W.M. Lamanna and W.B. Gleason., *Organometallics*, 1987, **6**, 1593.

18 P.L. Timms, Advan. *Inorg. Radiochem.*, 1972, **14**, 121. E.O. Fischer and H.P. Fritz, *Angew. Chem.*, 1961, **73**, 353.

19 P.S. Skell, D.L. Williams-Smith and M.J. McGlinchey, *J. Am. Chem, Soc.*, 1973, **95**, 3337.

20 L.P. Yur'Eva, S.M. Peregudova, L.N. Nekrasov, A.P. Korotkov, N.N. Zaitseva, N.V. Zakurin and A.Yu. Vasil'Kov, *J. Organomet. Chem.*, 1981, **219**, 43.

21 E.O. Fischer and H.P. Kögler, *Chem. Ber.*, 1957, **90**, 250.

22 F. Calderazzo, *Inorg. Chem.*, 1964, **3**, 810.

23 K.J. Klabunde and H.W. Efner, *Inorg. Chem.*, 1975, **14**, 789.

24 F.G.N. Cloke, K.R. Flower, P.B. Hitchcock and J.F. Nixon, *J. Chem. Soc., Chem. Commun.*, 1995, 1659.

25 F.G.N. Cloke and A. McCamley, *J. Chem. Soc., Chem. Commun.*, 1991, 1470.

26 E. Rytter and D.M. Gruen, *Spectrochim. Acta*, 1979, Part A, **35A**, 199.

27 M. P. Andrews, S.M. Mattar and G.A. Ozin, *J. Phys. Chem.*, 1986, **90**, 744.

28 F. Calderazzo, F. Gingl, G. Pampaloni, L. Rocchi and J. Strähle, *Chem. Ber.*, 1992, **125**, 1005.

29 J.A. Bandy, K. Prout, F.G.N. Cloke, H.C.deLemos and J.M. Wallis, *J. Chem. Soc., Dalton Trans.*, 1988, 475.

30 M.W. Briscoe, R.D. Chambers, S.J. Mullins, T. Nakamura, J.F.S. Vaughan and F.G. Drakesmith, *J. Chem. Soc., Perkin Trans.*, 1994, 3115

31 A. Martin, A.G. Orpen, A.J. Seeley and P.L. Timms, *J. Chem. Soc., Dalton Trans.*, 1994, 2251.

32 D. Minitti and P.L. Timms, *J. Chem. Soc., Chem. Commun.*, 1978, 898

33 J.A. Bandy, M.L.H. Green and D. O'Hare, *J. Chem. Soc., Dalton Trans.*, 1986, 2477.

34 E.O. Fischer and C. Elschenbroich, *Chem. Ber.*, 1970, **103**, 162.

35 J.R. Blackborow, D. Young., *Metal Vapour Synthesis in Organometallic Chemistry*, Springer-Verlag, New York, 1979, p124

Chapter 6

Experimental

6.1 General

6.1.1 Experimental techniques, solvents and reagents for chapters 2-5

All manipulations of air- and/or moisture-sensitive compounds were performed on a conventional vacuum/inert atmosphere (nitrogen) line using standard Schlenk and cannula techniques, or in an inert atmosphere (nitrogen) filled dry box.

The following solvents were dried by prolonged reflux over a suitable drying agent, freshly distilled and deoxygenated prior to use (drying agent in parentheses); toluene (sodium metal), pentane (lithium aluminium hydride), heptane (lithium aluminium hydride), benzene (calcium hydride), petroleum ether (40-60°C, lithium aluminium hydride), tetrahydrofuran (sodium benzophenone ketyl), diethylether (lithium aluminium hydride), 1,2-dimethoxyethane (potassium metal) and acetonitrile (calcium hydride).

NMR solvents were dried by vacuum distillation from a suitable drying agent (in parentheses) and stored under nitrogen or vacuum prior to use); d_6-benzene (phosphorus (V) oxide) and d_1-chloroform (phosphorus (V) oxide).

Elemental analyses were performed by the microanalytical services within this department.

Infrared spectra were recorded on Perkin-Elmer 577 and 457 grating spectrophotometers or a Perkin-Elmer 1600 FTIR spectrometer, and are quoted in cm^{-1}. They were recorded between CsI plates, either with the sample neat or in a Nujol mull. Absorptions are abbreviated as: s (singlet), d (doublet), m (multiplet), br (broad), w(weak).

Mass Spectra were recorded on a VG 7070E Organic Mass Spectrometer and performed by Dr M. Jones and Miss L.M. Turner.

NMR spectra were recorded on the following machines at the frequencies listed unless otherwise stated: Bruker AC250, ^{1}H (250.13 MHz), ^{13}C (62.90 MHz), ^{31}P (101.26 MHz), ^{19}F (235.36 MHz); Varian VXR400, ^{1}H (399.95 MHz), ^{31}C (100.58 MHz), ^{31}P (161.90 MHz), ^{19}F (376.32 MHz). The following abbreviations have been used for band multiplicities: s (singlet), d (doublet), t (triplet), q (quartet), sept (septet), m (multiplet). Chemical shifts are quoted as δ in ppm with respect to the following unless otherwise stated: ^{31}P (85% H_3PO_4, 0 ppm); ^{13}C (C_6D_6, 128.0ppm; $CDCl_3$, 77.0 ppm), ^{1}H (C_6D_6, 7.15ppm; $CDCl_3$, 7.26ppm), ^{19}F (external $CFCl_3$, 0 ppm). ^{1}H and ^{13}C spectra are referenced downfield of tetramethylsilane.

Cyclic Voltammetry was performed by Dr. Peter Scott (University of Sussex) using a MacLab Potentiostat and EChem software on the Apple Macintosh. The single compartment airtight cell comprised a Pt disk working electrode, Pt wire auxiliary electrode and Ag wire pseudo reference electrode. Potentials were calibrated by the method of Gagné[1] and are quoted versus the potential of the ferrocenium/ferrocene couple. No compensation for the resistance of the cell was applied. The sample was a dilute solution in 0.1M tetrabutylammonium hexafluorophosphate/acetonitrile at 22°C.

EPR spectra were recorded by Dr. K. Flower using a Varian 104A spectrometer.

The following chemicals were prepared using previously published procedures: 1,3,5-tris(trifluoromethyl)benzene (Ar^FH),[2] 2,4,6-tris (trifluoromethyl)phenyllithium (Ar^FLi),[3] Ar^FPCl_2,[4] Ar^FPH_2,[4] 1,1′,3,3′-tetraethyl-2,2′-bis(imidazolidine),[5] PMe_3,[6] $W(PMe_3)_6$,[7] $Mo(N^tBu)_2(PMe_3)(\eta^2\text{-}C_2H_4)$.[8]

The $CrCl_2$ and $VCl_3(thf)_3$ used in chapter 2 were provided by Dr. C. Redshaw. The $Mo(NAr)_2Cl_2$.dme used in chapter 2 was provided by M. Giles. The $Mo(N^tBu)_2Cl_2$.dme, $Cr(NAd)_2Cl_2$ and $Cr(N^tBu)_2Cl_2$ used in chapter 2 were provided by M.P. Coles. The $Mo(N^tBu)_2(PMe_3)(\eta^2\text{-}C_3H_6)$ and $Mo(NAr)_2(PMe_3)_2(\eta^2\text{-}C_2H_4)$ used in chapter 3 were provided by Dr. P.W. Dyer. All other chemicals were obtained commercially, and used as received unless otherwise stated.

6.2 Experimental details to chapter 2

6.2.1 Synthesis of $Mo(N^tBu)_2(Ar^F)_2$

To $Mo(N^tBu)_2Cl_2$.dme (500mg, 1.25mmols) in Et_2O (20ml) were added 2.4 equivalents of Ar^FLi (3.00mmols) in Et_2O (20ml) at -78°C. This solution was allowed to warm to room temperature and stirred overnight. After removal of solvent the residue was extracted with pentane (3 x 40ml) which was reduced in volume (to *ca.* 25ml) and cooled to -78°C to give pale yellow crystals. Yield: 600mg, *ca.* 75%.

Elemental Analysis for $C_{26}H_{22}N_2F_{18}Mo$: Found: C, 38.71%; H, 2.86%; N, 3.62%. Required C, 39.00%; H, 2.75%; N, 3.50%.

Mass Spectral data m/e ^{98}Mo; 802 $[M]^+$

Infrared data (Nujol, CsI, cm^{-1}): 1621(s), 1567(s), 1280(m), 1125(m), 908(d), 842(d), 805(d), 740(d), 684(s), 434(s).

^{1}H NMR data (C_6D_6, 400MHz, 298K): δ 8.00 (s, 2H, *m*-ArH), 7.68 (s, 2H, *m*-ArH), 1.13 (18H, s, $NCMe_3$).

^{19}F NMR data (C_6D_6, 376.32MHz, 298K): δ -68.6 (s, 6F, *o*-CF_3), -59.0 (s, 6F, *o*-CF_3), -62.8 (s, 6F, *p*-CF_3).

$^{13}C\{^1H\}$ NMR data (C_6D_6, 100.582MHz, 298K): δ 172.7 (br, *ipso*-C), 140.7 (broad unresolved multiplet, *o*-CF_3), 137.5 (broad unresolved multiplet, *o*-CF_3), 130.3 (q, $^2J_{CF}$ 34Hz, CCF_3) 123.4 (q, $^1J_{CF}$ 272Hz, *p*-CF_3), 124.8, 125.1 (s (br), *m*-C), 73.8 (s, $NCMe_3$), 31.0 (s, $NCMe_3$). Accurate assignment of all other resonances hampered due to overlapping signals.

6.2.2 Synthesis of $Cr(NAd)_2(Ar^F)_2$

To $Cr(NAd)_2Cl_2$ (250mg, 0.59mmols) in Et_2O (20ml) were added 2 equivalents of Ar^FLi (1.20mmols) in Et_2O (20ml) at -78°C. This solution was allowed to warm to room temperature and stirred overnight. After removal of solvent the residue was extracted with pentane (3 x 40ml) which was reduced in volume (to *ca.* 25ml) and cooled to -78°C to give deep red crystals. Yield: 400mg, *ca.* 75%. (M.p 158-160°C)

Elemental Analysis for $C_{38}H_{34}N_2F_{18}Cr$: Found: C, 50.25%; H, 3.87%; N, 3.49%. Required C, 50.01%; H, 3.75%; N, 3.06%

Mass Spectral data m/e ; 913 $[M]^+$

Infrared data (Nujol, CsI, cm^{-1}): 1619(s), 1568(s), 1386(s) 1288(d), 1259(s), 1102(s), 1137(br), 1079(s), 1009(s), 909(d), 843(d), 684(s),

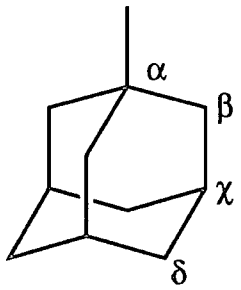

^{1}H NMR data ($CDCl_3$, 400MHz, 298K): δ 8.05 (s, 1H, *m*-ArH), 7.82 (s, 1H, *m*-ArH), 2.02 (s, 3H, Ad-H_γ), 1.88 (6H, s, Ad-H_δ), 1.54 (6H, s, Ad-H_β).

^{19}F NMR data ($CDCl_3$, 376.32MHz, 298K): δ -56.8 (s, 6F, *o*-CF_3), -59.1 (s, 6F, *o*-CF_3), -62.9 (s, 6F, *p*-CF_3).

^{13}C{^{1}H} NMR data ($CDCl_3$, 100.582MHz, 298K): δ 175.8 (br, *ipso*-C), 138.5 (q, $^2J_{CF}$ 30Hz, *o*-CCF_3), 137.2 (q, $^2J_{CF}$ 30Hz, *o*-CCF_3), 128.7 (q, $^2J_{CF}$ 34Hz, *p*-CCF_3), 126.7 (q, $^1J_{CF}$ 275Hz, *p*-CF_3), 123.9 (q, $^1J_{CF}$ 273Hz, *o*-CF_3), 123.2 (q, $^1J_{CF}$ 272Hz, *o*-CF_3), 125.0, 124.8 (s(br), *m*-C), 82.8 (s, Ad-C_α), 43.7 (s, Ad-C_β) 35.6 (s, Ad-C_δ), 29.5 (s, Ad-C_γ)

6.2.3 Synthesis of $Cr(N^tBu)_2(Ar^F)_2$

To $Cr(N^tBu)_2Cl_2$ (400mg, 1.51mmols) in Et_2O (20ml) were added 2 equivalents of Ar^FLi (3.0mmols) in Et_2O (20ml) at -78°C. This solution was allowed to warm to room temperature and stirred overnight. After removal of solvent the residue was extracted with pentane (3 x 40ml) which was reduced in volume (to *ca.* 25ml) and cooled to -78°C to give deep red crystals. Yield: 635mg, *ca.* 84%. (M.p 163-165°C)

Elemental Analysis for $C_{26}H_{22}N_2F_{18}Cr$: Found: C, 41.28%; H, 2.99%; N, 3.83%. Required C, 41.28%; H, 2.93%; N, 3.70%

Mass Spectral data: m/e ; 757 $[M]^+$, 476 $[M\text{-}Ar^F]^+$

Infrared data (Nujol, CsI, cm^{-1}): 1620(s), 1569(s), 1290(d), 1257(s), 1187(s), 1123(br), 1080(s), 1010(s), 909(d), 843(d), 685(s), 435(s).

^{1}H NMR data (C_6D_6, 400MHz, 298K): δ 8.00 (s, 2H, *m*-ArH), 7.74 (s, 2H, *m*-ArH), 1.06 (18H, s, $NCMe_3$).

^{19}F NMR data (C_6D_6, 376.32MHz, 298K): δ -57.0 (s, 6F, *o*-CF_3), -59.3 (s, 6F, *o*-CF_3), -62.7 (s, 6F, *p*-CF_3).

$^{13}C\{^1H\}$NMR data (C_6D_6, 100.582MHz, 298K): δ 176.0 (br, *ipso*-C), 138.7 (q, $^2J_{CF}$ 30Hz, *o*-CCF_3), 137.4 (q, $^2J_{CF}$ 32Hz, *o*-CCF_3), 129.5 (q, $^2J_{CF}$ 34Hz, *p*-CCF_3), 127.4 (q, $^1J_{CF}$ 275Hz, *p*-CF_3), 124.4 (q, $^1J_{CF}$ 273Hz, *o*-CF_3), 123.6 (q, $^1J_{CF}$ 272Hz, *o*-CF_3), 125.5, 125.1 (s(br), *m*-C), 80.5 (s, $NCMe_3$), 31.1 (s, $NCMe_3$).

6.2.4 Synthesis of $Mo(NAr)_2(Ar^F)Cl{\cdot}LiCldme$

To $Mo(NAr)_2Cl_2$.dme (1.0g, 1.66mmols) in Et_2O (20 ml) were added 2.0 equivalents of Ar^FLi (3.32mmols) in Et_2O (20 ml) at -78°C. This solution was allowed to warm to room temperature and stirred overnight. After removal of solvent, the residue was extracted with pentane (3 x 40 ml) which was reduced in volume (to *ca.* 25 ml) and cooled to -78°C to give orange/red crystals. Yield: 950mg, *ca.* 63%.

Elemental analysis for $C_{37}H_{46}N_2O_2F_9Cl_2LiMo$: Found: C, 49.51%; H, 5.19%; N, 3.56%. Required C, 49.62%; H, 5.17%; N, 3.13%

Mass Spectral data *m/e* ^{98}Mo: 763 $[Mo(NAr)_2(Ar^F)Cl]^+$

Infrared data (Nujol, CsI, cm^{-1}): 1619(s), 1567(s), 1278(m), 1188(s), 1150(d) 1090(m), 908(s), 842(weak), 802(s), 745(d), 684(s), 466(s), 399(s)

^{1}H NMR data ($CDCl_3$, 400 MHz, 298K): δ 8.09 (2H, s, Ar^FH), 7.09 - 7.02 (6H, m,*m,p*-C_6H_3), 3.9 (2H, sept, C*H*Me_2), 3.7 (6H, s, *Me*OCH_2CH_2O*Me*), 3.5 (4H, s, MeOCH_2CH_2OMe), 2.9 (2H, sept, $^3J_{CH}$=6.8Hz, C*H*Me_2), 1.26 (12H, d, CH*Me*$_2$), 1.03 (12H, d, CH*Me*$_2$).

^{19}F NMR data ($CDCl_3$, 376.32MHz, 298K): δ -63.6 (*p*-CF_3).

^{13}C{^{1}H}NMR data ($CDCl_3$, 100.582MHz, 298K): δ 155-118 Accurate assignment of aryl resonances in this region hampered due to poor resolution and overlapping nature of signals, 71.2(s, MeOCH_2CH_2OMe), 60.0(q, s, *Me*OCH_2CH_2O*Me*), 28.40(s(br), $CHMe_2$), 24.6 (s, CH*Me*$_2$).

6.2.5 Synthesis of $V(Ar^F)_2Cl(thf)$

To $VCl_3(thf)_3$ (0.85g, 2.36mmols) in Et_2O (20ml) were added 2.5 equivalents of Ar^FLi (6 mmols) in Et_2O at -78°C. The solution was allowed to warm to room temperature and left stirring overnight. After removal of solvent the residue was extracted into pentane and reduced in volume (to ca. 50ml). Cooling of this solution to 4°C afforded deep blue/green crystals. (0.8g, 47%)

Elemental analysis for $C_{22}H_{12}ClF_{18}OV$: Found: C, 36.29%; H, 1.79%. Required C, 36.66%; H, 1.68%

Infrared data (Nujol, CsI, cm^{-1}): 1618(s), 1269(m), 1188(s), 1092(m), 1017(s), 801(s), 721(d), 684(s)

E.P.R The compound was found to be EPR active as discussed in section 2.2.7

6.2.6 Synthesis of $V(Ar^F)_3$-O-$Li(thf)_3$

This compound was synthesised using the following method by Dr. C. Redshaw from our group.

To $VCl_3(thf)_3$ (0.85g, 2.36mmols) in Et_2O (20ml) were added 3.5 equivalents of Ar^FLi (8.26 mmols) in Et_2O at -78°C. The solution was allowed to warm to room temperature and left stirring overnight. After removal of solvent the residue was extracted into pentane and reduced in volume (to ca. 50ml). Cooling of this solution to 4°C afforded turquoise crystals. (1.1g, 41%)

Elemental analysis for $C_{39}H_{30}F_{27}O_4LiV$: Found: C, 41.00%; H, 2.55%. Required C, 41.28%; H, 2.64%

Infrared data (Nujol, CsI, cm^{-1}): 1621(s), 1281(m), 1184(s), 1141(s), 1110(s), 1062(d),910(s), 800(s), 721(m), 687(s), 587(d), 433(s)

E.P.R The compound was found to be EPR silent as discussed in section 2.2.8

6.2.7 Synthesis of $Cr(Ar^F)_2(PMe_3)_2$

This compound was synthesised using the following method by Dr. C. Redshaw from our group.

To $CrCl_2$.thf (0.85g, 4.36mmols) in Et_2O (30 ml) was added PMe_3 (0.69g, 9.07mmols), to give a deep blue solution. Ar^FLi (9.15mmol) in Et_2O (20 ml)was then added. After stirring for three hours, the solution was filtered and reduced in volume (to *ca.* 30ml). Cooling of this solution to *ca.* -20°C afforded large red prisms. Yield: 1.43g, *ca.* 43%.

Elemental analysis for $C_{24}H_{22}P_2F_{18}Cr$: Found: C, 37.70%; H, 2.92%. Required C, 37.61%; H, 2.89%

^{1}H NMR data (C_6D_6, 400MHz, 298K): δ 21.3 (s, br, $\upsilon_{1/2}$ *ca.* 500 Hz, 4H, *m*-ArH), -33.4 (s, br, $\upsilon_{1/2}$ *ca.* 1600Hz, 18H, PMe_3).

^{19}F NMR data (C_6D_6, 376.32MHz, 298K): δ -63.0 (s, 6F, *p*-CF_3).

6.3 Experimental details to chapter 3

6.3.1 Synthesis of $Mo(N^tBu)_2(PMe_3)(\eta^2\text{-}Ar^FP{=}PAr^F)$

$Mo(N^tBu)_2PMe_3(\eta^2\text{-}C_3H_6)$ (100mg, 0.28mmols) in heptane (15ml) was added dropwise over 5 minutes to $Ar^FP{=}PAr^F$ (170mg, 0.27mmols) in heptane (15ml) at room temperature. The pale brown solution was warmed to 60°C and stirred at this temperature for 3 days. During this time the solution changed colour to yellow/orange. The solvent was removed *in vacuo* and the remaining solid extracted with diethyl ether (20ml). On cooling this solution to -78°C yellow/orange crystals were obtained. Yield: 150mg, *ca.* 58%. (M.p = 215-217°C)

Elemental analysis for $C_{29}H_{31}N_2P_3F_{18}Mo$: Found: C, 37.00%; H, 3.38%; N, 2.75%. Required C, 36.83%; H, 3.30%; N, 2.95%

Mass Spectral data *m/e* ^{98}Mo: 940 [M^+], 310 [Ar^FP], 279 [Ar^F], 77 [PMe_3], 57 [t-butyl].

Infrared data (Nujol, CsI, cm^{-1}): 2722(weak), 1619(s), 1564(s), 1282(m), 1175(d), 1126(d) 1071(s), 911(s), 828(weak), 737(d), 685(s)

^1H NMR data (C_6D_6, 400MHz, 298K): δ +7.94 (s, 2H, Ar^FH), 7.80 (s, 2H, Ar^FH), +1.39 (s, 9H, $NC(Me)_3$), +0.94 (d, $^2J_{PH}$=9.6Hz, 9H, PMe_3), +0.74 (s, 9H, $NCMe_3$).

^{31}P NMR data (C_6D_6, 101.26MHz, 298K): δ -11.38 (sept, 1P, Ar^FP, $^4J_{PF}$ 39Hz), -11.32 (sept, 1P, Ar^FP, $^4J_{PF}$ 39Hz), +11.58 (s, 1P, P Me_3).

^{19}F NMR data (C_6D_6, 376.32MHz, 298K): δ -51.89 (t, $^4J_{PF}$ 35.3Hz, 6F, *o*-CF_3), -53.67 (t, $^4J_{PF}$ 42.1Hz, 6F, *o*-CF_3), -62.83 (s, 3F, *p*-CF_3), -62.95 (s, 3F, *p*-CF_3).

^{13}C{^{1}H}NMR data (C_6D_6, 100.582MHz, 298K): δ 160.5, 155.3(m, broad, *ipso* Ar^F, $^1J_{PC}+^2J_{PC}$=43Hz), 139.1,137.1(qd, *p*C-CF_3, $^2J_{CF}$=30Hz, $^4J_{PC}$=11Hz), 126.1(*o*-C-CF_3), 125.6(*m*-Ar^F), 124.4, 124.1(q, *o*-C-CF_3 , $^1J_{CF}$=275Hz), 123.7, 123.4(q, p-C-CF_3, $^1J_{CF}$=272Hz), 70.09(s, $NCMe_3$), 69.2(s, $NCMe_3$), 65.87(Et_2O), 32.3(q, $NCMe_3$), 31.5(q, $NCMe_3$), 19.3(d, PMe_3, $^2J_{PC}$=31Hz), 15.55(s, Et_2O).

6.3.2 Synthesis of $Mo(NAr)_2(PMe_3)(\eta^2\text{-}Ar^FP{=}PAr^F)$

$Mo(NAr)_2(PMe_3)_2(\eta^2\text{-}C_2H_4)$, (135mg, 0.24mmols) in heptane (15ml) was added dropwise over 5 minutes to $Ar^FP{=}PAr^F$ (153mg, 0.24mmols) in heptane (20ml) at room temperature. The purple solution was warmed to 60°C and stirred at this temperature for 3 days. During this time the solution changed colour to orange. The solvent was removed *in vacuo* and the remaining solid extracted with diethyl ether (3 x 20 ml). On cooling this solution to -78°C bright orange crystals were obtained. Yield : 210mg, *ca.* 76%. (M.p 225-226°C)

Elemental analysis for $C_{45}H_{47}N_2P_3F_{18}Mo$: Found: C, 47.00%; H, 4.16%; N, 2.61%. Required C, 47.12%; H,4.10%; N, 2.44%)

Infrared data (KBr pellet, cm^{-1}): 2870(s), 1620(s), 1566(s), 1439(d), 1364(s), 1279(s), 1190(s), 1145(s) 1076(s), 959(s), 911(s), 856(s), 800(s), 747(s), 685(s)

^{1}H NMR data (400MHz, C_6D_6, 298K): δ +7.9 (s, 2H, Ar^F*H*), 7.7 (s, 2H, Ar^F*H*), 7.07-7.02 (m, 3H, *m,p*-C_6H_3), 6.85-6.80 (m, 3H, *m,p*-C_6H_3), 3.84(sept, $^{3}J_{CH}$=6.4Hz, 2H, C*H*Me_2), 3.59(sept, $^{3}J_{CH}$=6.4Hz, 2H, C*H*Me_2), 1.28(d, 6H, CH*Me*$_3$), 1.16(d, 6H, CH*Me*$_3$), 1.06(d, 6H, CH*Me*$_3$), 1.01 (d, $^{2}J_{PH}$=10Hz, 9H, P*Me*$_3$), 0.59(d, 6H, CH*Me*$_3$).

^{31}P NMR data (C_6D_6, 161.90MHz, 298K): δ 7.82 (s, 1P,PMe_3), 3.62 (broad multiplet, 2P, Ar^FP).

^{19}F NMR data (C_6D_6, 376.32MHz, 298K): δ -53.14 (t, $^{4}J_{PF}$ 30.7Hz, 6F, *o-CF*$_3$) -53.82 (t, $^{4}J_{PF}$ 36.5Hz, 6F, *o-CF*$_3$) -62.9 (s, 3F, *p-CF*$_3$), -63.1 (s, 3F, *p-CF*$_3$).

^{13}C{^{1}H}NMR data (C_6D_6, 100.582MHz, 298K): δ 153.7, 152.8(*ipso* NAr), 147.1, 141.8(*p*-NAr), 140.4 (unresolved multiplet ,*p*C-CF_3), 138.2, 137.8 (unresolved multiplet, *o*-CCF_3), 129.2(*m*-NAr), 126.8, 126.6(*m*-Ar^F), 125.6(*m*-NAr), 123.2,122,8(s, *o*-NAr), 28.59, 28.24($CHMe_2$), 24.6, 23.8, 23.7, 23.6(CH*Me*$_2$), 16.25(d, P*Me3*, $^{1}J_{PC}$=30Hz). Unresolved CF_3 groups and Ar^F *ipso*C.

6.3.3 NMR reactions of $Mo(N^tBu)_2(PMe_3)(\eta^2\text{-}C_2H_4)$ with $Ar^{F'}P{=}PAr^{F'}$, $Ar^*P{=}PAr^*$ and $Ar^FP{=}PAr^*$

Each of the diphosphenes was reacted with $Mo(N^tBu)_2(PMe_3)(\eta^2\text{-}C_2H_4)$ *in vacuo* in C_6D_6 (840µl) at room temperature and then warmed to 60°C in a sealed NMR tube (Table 6.1). A discussion of the NMR data is given in section 3.2.

Diphosphene	No. of moles of diphosphene	No. of moles of $Mo(N^tBu)_2(PMe_3)(\eta^2\text{-}C_2H_4)$	^{31}P NMR data
$Ar^{F'}P{=}PAr^{F'}$	0.028	0.028	9.6ppm (s, 1P) -10ppm (m, 1P) -13ppm (m, 1P)
$Ar^*P{=}PAr^*$	0.041	0.041	No reaction
$Ar^FP{=}PAr^*$	0.041	0.041	No reaction

Table 6.1

6.3.4 NMR reactions of $[Pt(PEt_3)Cl_2]_2$ with $Ar^*P{=}PAr^*$ and $Ar^*P{=}PAr^F$

Both diphosphenes were reacted seperately with $[Pt(PEt_3)Cl_2]_2$ *in vacuo* in C_6D_6 (840µl) at room temperature in a sealed NMR tube (Table 6.2). A discussion of the NMR data is given in section 3.3.

Diphosphene	No. of moles of diphosphene	No. of moles of $[Pt(PEt_3)Cl_2]_2$	^{31}P NMR data
$Ar^*P{=}PAr^*$	0.052	0.026	See section 3.3.1
$Ar^*P{=}PAr^F$	0.052	0.026	See section 3.3.2

Table 6.2

6.4 Experimental details to chapter 4

6.4.1 Synthesis of $Ar^FP{=}PAr^F$ by dechlorination using $W(PMe_3)_6$

$W(PMe_3)_6$ (0.500g, 0.77mmols) and Ar^FPCl_2 (0.585g, 1.53mmols) were placed in an ampoule and benzene (30 ml) was condensed into the vessel at -196°C; the reaction mixture was then allowed to warm to room temperature under vacuum. This mixture was stirred at room temperature for 24 hours. During this time the solution changed colour from yellow/gold to deep red, with some precipitation of a pale solid. ^{31}P NMR indicated that the reaction had reached completion.

The solution was then filtered and the benzene was removed *in vacuo*. $Ar^FP{=}PAr^F$ was sublimed out of this crude mixture (80°, 5 x 10^{-2} Torr). Further diphospene could be extracted from the filtrate by washing with toluene at 60°C. These fractions were combined and the diphosphene recrystallised from toluene at 4°C (Yield 0.400g, 85%). The diphosphene was identified by its characteristic low field ^{31}P NMR shift (septet δ +474, $^4J_{PF}$ = 45Hz)

6.4.2 Synthesis of Ar*P=PAr* by dechlorination using $W(PMe_3)_6$

$W(PMe_3)_6$ (0.500g, 0.77mmols) and Ar^*PCl_2 (0.520g, 1.5mmols) were placed in an ampoule and benzene (30 ml) was condensed into the vessel at -196°C; the reaction mixture was then allowed to warm to room temperature under vacuum. This mixture was stirred at room temperature for 36 hours. During this time the solution changed colour from yellow/gold to orange. ^{31}P NMR indicated that all of the Ar^*PCl_2 had been consumed and that the reaction had reached completion.

The solution was transferred to a schlenk and the benzene was removed *in vacuo*. The residue was extracted with pentane (3 x 15ml). The solution was reduced in volume (to *ca.* 20ml) and cooled to -78°C to give a bright orange crystalline product. (Yield 100mg, 80%). The product was identified by its characteristic ^{31}P NMR resonance (δ +494).

6.4.3 Synthesis of $Ar^{F'}P=PAr^{F'}$ by dechlorination using $W(PMe_3)_6$

A similar procedure to that used in the previous section was used to react $Ar^{F'}PCl_2$ (0.473g, 1.50mmols) with $W(PMe_3)_6$ (0.500g, 0.77mmols) in benzene. $Ar^{F'}P=PAr^{F'}$ was extracted by sublimation from the crude mixture (75°, 5 x 10^{-2} Torr) and recrystallised from toluene at 4°C. (Yield 250mg, 68%). The product was identified by its characteristic ^{31}P NMR resonance (δ +472).

6.4.4 Synthesis of $Ar^*P=PAr^F$ by dechlorination using $W(PMe_3)_6$

$W(PMe_3)_6$ (0.300g, 0.46mmols), Ar^*PCl_2 (0.156g, 0.45mmols) and Ar^FPCl_2 (0.175g, 0.45mmols) were placed in an ampoule and benzene (30 ml) was condensed into the vessel at -196°C. The reaction mixture was then allowed to warm to room temperature under vacuum. This mixture was stirred at room temperature for 36 hours, during which time the solution changed colour from yellow/gold to bright red with some precipitation of a pale solid. After this time ^{31}P NMR indicated that the reaction had reached completion.

The solution was filtered and benzaldehyde (5ml, 5.22g 49 mmols) was added to the filtrate. This mixture was stirred at room temperature for 48 hours, during which time much pale solid was precipitated; ^{31}P NMR indicated that this pale solid contained no diphosphene and was comprised of $Ar^*P=CHPh$, $Ar^FP=CHPh$, and tungsten oxo species. After further

filtration, Et_2O (15ml) was added and the solution cooled to 4°C for 48 hours. During this time further solid had precipitated (^{31}P NMR indicated that this pale solid was more tungsten oxo species and some $O=PMe_3$). This solution was filtered, and the benzene and Et_2O were removed *in vacuo*. ^{31}P NMR of the resultant orange oil indicated that the diphosphene was 90% pure. The residue was passed down a silica column using CH_2Cl_2 as eluant. Removal of the solvent *in vacuo* afforded the pure unsymmetrical diphosphene $Ar^*P=PAr^F$ as an orange oil. After standing at room temperature for a few days the diphosphene can be seen to crystallise as small florets. (Yield 185mg, *ca.* 70%).

Elemental analysis for $C_{27}H_{31}P_2F_9$: Found: C, 55.12%; H, 5.30%. Required C, 55.10%; H, 5.31%)

Mass Spectral data: *m/e* : 588 $[M^+]$, 307 $[M^+]$-Ar^F,

Infrared data (Nujol, CsI, cm^{-1}): 2726(s), 1716(br). 1624(s), 1592(s), 1278(s), 1194(s), 1147(s) 1086(s), 1022(s), 959(s), 914(s), 860(s), 802(s), 723(s), 694(d)

^1H NMR data (400MHz, C_6D_6, 298K): δ 8.25 (s, 2H, Ar^FH), 7.63 (s, 2H, Ar^*H), 1.62 (s, 18H, *o*-^{t}Bu), 1.51, (s, 9H, *p*-^{t}Bu)

^{31}P NMR data ($CDCl_3$, 101.26MHz, 298K): δ 536 (d, 1P, Ar^*P, $^1J_{PP}$=570 Hz), 417 (1P, $^1J_{PP}$=570 Hz, $^4J_{PF}$ = 22Hz).

^{19}F NMR data (C_6D_6, 235.342MHz, 298K): δ -56.83 (t, $^4J_{PF}$ 20.0Hz, 6F, *o*-CF_3) - 63.7 (s, 3F, *p*-CF_3).

$^{13}C\{^{1}H\}$NMR data ($CDCl_3$ 100.582MHz, 298K): δ 160.3(br, *ipso* Ar^FP) , 159.9(br, ipso Ar*P) 154.5(d, $^4J_{PC}$ 8Hz, C_6H_2-C_{para}), 150.1(d, $^2J_{PC}$ 10.5Hz, C_6H_2-C_{ortho}), 135.0(m, *p*C-CF_3), 131.1(q, $^2J_{CF}$ 35Hz,*o*-C-CF_3), 126.6(s(br),*m*-CH Ar^FP), 123.1 (q, $^1J_{CF}$ 275Hz, *o*-CCF_3), 122.8(m-ArH Ar*), unresolved *p*-CCF_3., 38.6 (s, *o*-$C(CH_3)_3$), 34.8 (s, *p*-$C(CH_3)_3$), 33.7(s(br), *o*-$C(CH_3)_3$, 31.3(s(br), *p*-$C(CH_3)_3$)

6.4.5 NMR reactions of $(trip)PCl_2$ and $(mes)PCl_2$ with $W(PMe_3)_6$

Each of the dichlorophosphines was reacted *in vacuo* with $W(PMe_3)_6$ in C_6D_6 (840 μl) at room temperature, in a sealed NMR tube (Table 6.3). A discussion of the NMR data is given in section 4.3.

Dichloro-phosphine	No. of moles of dichloro-phosphine	No. of moles of $W(PMe_3)_6$	^{31}P NMR data
$(trip)PCl_2$	0.035	0.070	See section 4.3.1
$(mes)PCl_2$	0.035	0.070	See section 4.3.2

Table 6.3

6.5 Experimental details to chapter 5

6.5.1 Synthesis of $Cr(Ar^FH)_2$ using MVS

The pre-melted and pre-weighed chromium ingot was placed on an Al_2O_3 crucible on the copper hearth and the apparatus assembled as described in chapter 5. The Ar^FH was placed in a thick-walled ampoule and degassed. This ampoule and an identical ampoule containing degassed heptane were connected to the ligand inlet system. The entire apparatus was subsequently evacuated to 5×10^{-7} mbar for approximately 12 hours before the start of the reaction.

The insulated jacket was filled with liquid nitrogen and the flange heater switched on. The ligand mantle and delivery line were also heated to a temperature slightly higher than the boiling point of the ligand. The ligand manifold was then opened to the reaction chamber, allowing a thin layer of heptane and then a thin layer of ligand to condense on the walls of the bell-jar. A voltage was then applied to heat resistively the tungsten wire around the crucible, causing the metal to evaporate at the appropriate voltage. The rates of metal evaporation and ligand sublimation were regulated to maintain a vacuum of 1×10^{-5} mbar.

Co-condensation of chromium (0.78g, 15.29mmols) and Ar^FH was continued for 2 hours, until the majority of the ligand had been sublimed. A gradual build up of a yellow/brown matrix was observed.

At the end of the experiment, all heating systems were switched off (except the vacuum seal flange) and the liquid nitrogen drained from the jacket. The pumps were then shut off, the reaction chamber filled with nitrogen and the apparatus allowed to achieve ambient temperature (a mercury bubbler fitted to the apparatus allows for the expansion of the gas). The product was washed from the walls of the reaction chamber with dry,

degassed 40-60° petroleum ether (ca. 1500 ml), to yield a yellow solution. The solution was filtered through anhydrous celite to remove any excess metal and the residue washed with more 40-60° petroleum ether (ca. 150 mls). The petroleum ether, heptane and excess ligand were subsequently removed *in vacuo*, leaving a yellow-brown solid. The solid was sublimed (60°C, 1 x 10^{-3} mm Hg) to give a pure yellow/brown microcrystalline solid. Despite repeated crystallisation attempts, crystals of X-Ray quality could not be obtained.

Mass chromium vaporised	=	0.78g
Mass ligand sublimed	=	20g
Voltage (W wire)	=	10-20V
Delivery line temperature	=	323K
Ligand ring temperature	=	353K

Yield (based on metal): 750mg (8%)

Mass Spectral data: *m/e* : 616 [M^+], 334 [M-Ar^FH]

Elemental analysis for $C_{18}H_6F_{18}Cr$: Found: C, 35.28%; H, 1.05%. Required C, 35.01%; H, 0.98%)

^{1}H NMR data (400MHz, C_6D_6, 298K): δ 5.29 (s, Ar^FH)

^{19}F NMR data (C_6D_6, 235.342MHz, 298K): δ-61.4 (s, CF_3).

$^{13}C\{^1H\}$NMR data (C_6D_{12}, 100.582MHz, 298K): δ 125.8 (q, CF_3 $^1J_{CF}$ = 274.5Hz), 87.3 (q, CCF_3, $^2J_{CF}$ = 39.1Hz), 76.3 (s, CH)

6.5.2 Synthesis of $V(Ar^FH)_2$ using MVS

Co-condensation of vanadium metal (0.450 g, 8.82 mmols) with Ar^FH (20 g, 0.709 mols) using the procedure outlined above, yielded a deep red matrix, which dissolved in 40-60 petroleum ether (1500 ml) to give a red solution. Work-up of this solution in the normal manner produced a burgundy red solid. After analysis there was not enough solid left to attempt the growth of X-Ray quality crystals.

Mass vanadium vaporised	=	0.450g
Mass ligand sublimed	=	20g
Voltage (W wire)	=	10-20V
Delivery line temperature	=	323K
Ligand ring temperature	=	353K

Yield (based on metal): 80mg (1.5%)

Mass Spectral data: *m/e* : 615 [M^+], 333 [M-Ar^FH]

Elemental analysis for $C_{18}H_6F_{18}V$: Found: C, 35.24%; H, 0.96%. Required C, 35.12%; H, 0.98%)

EPR The compound was found to be EPR active as discussed in section 5.2.2

6.5.3 Synthesis of $Nb(Ar^FH)_2$ using MVS

Co-condensation of niobium metal (350 g, 3.77 mmols) with Ar^FH (20 g, 0.709 mols) using the procedure outlined above, yielded a pale red matrix, which dissolved in 40-60°C petroleum ether to give a red/pink solution. Work-up of this solution in the normal manner produced a dark pink solid. X-Ray quality crystals were obtained by slow evaporation of heptane from a saturated solution at room temperature in a nitrogen-filled glove box and have been submitted for structural analysis.

Mass niobium vaporised	=	0.350g
Mass ligand sublimed	=	20g
Voltage (W wire)	=	18-25V
Delivery line temperature	=	323K
Ligand ring temperature	=	353K

Yield (based on metal): 300 mg (12%)

Mass Spectral data: *m/e* : 657 [M^+].

Elemental analysis for $C_{18}H_6F_{18}Nb$: Found: C, 32.50%; H, 0.86%. Required C, 32.90%; H, 0.92%)

EPR The compound was found to be EPR active, as discussed in section 5.2.3

6.5.4 Attempted Synthesis of $Ru(Ar^FH)_2$ using MVS

Co-condensation of ruthenium metal (0.150 g, 1.48 mmols) with Ar^FH (20 g, 0.709 mols) using the procedure outlined above, yielded a pale brown matrix, which dissolved in 40-60°C petroleum ether to give a red/pink solution. Work-up of this solution in the normal manner produced a pale brown solid. Unfortunately, there was only enough of this compound to get mass spectral analysis.

Mass ruthenium vaporised	=	0.150g
Mass ligand sublimed	=	20g
Voltage (W wire)	=	20-25V
Delivery line temperature	=	323K
Ligand ring temperature	=	353K

Mass Spectral data: *m/e* : 666 [M^+], 384 [M-Ar^FH]

6.5.5 Attempted Synthesis of $Ti(Ar^FH)_2$ using MVS

Co-condensation of titanium metal (0.350 g, 7.00 mmols) with Ar^FH (20 g, 0.709 mols) using the procedure outlined above, did not result in the observation of a matrix. The ligand was washed off the sides of the reaction vessel with 40-60 petroleum ether. The sides of the bell jar were then washed with isopropyl alcohol under an atmosphere of nitrogen to destroy any finely divided pyrophoric titanium metal before the apparatus was dismantled.

6.6 References

1 R.R. Gagné, C.A. Koval and G. C. Lisensky, Inorg. Chem., 1980, **19**, 2854.

2 M. Scholz, H.W. Roesky, D. Stalke, K. Keller and F.T. Edelmann, J. *Organomet. Chem.*, 1989, **366**, 73.

3 G.E. Carr, R.D. Chambers, T.F. Holmes and D.G. Parker, *J. Organomet. Chem.*, 1987, **325**, 13.

4 H.P. Goodwin, Thesis, University of Durham, 1990.

5 H. Goldwhite, J. Kaminski, G. Millhauser, J. Ortiz, M.Vargas, L. Vertal, M.F. Lappert and S.J. Smith, *J. Organomet. Chem.*, 1986, **310**, 21

6 W. Wolfsberger, H. Schmidbaur, *Synth. React. Inorg. Metal-Org. Chem.*, 1974, **4**, 149.

7 D. Rabinovich, R. Zelman and G. Parkin, *J. Am. Chem. Soc.*, 1992, **114**, 4611

8 P.W. Dyer, V.C. Gibson, J.A.K. Howard, B. Whittle and C. Wilson, *Polyhedron*, 1995, **14**, 103.

Appendices

Appendix 1: X-Ray Crystallographic Data

The structural determinations described in this thesis were performed on Rigaku AFC65 and Siemens SMART CCD diffractometers by:

[a]Prof. J.A.K. Howard, [b]J.-W. Yao, [c]Dr. A. Batsanov (University of Durham),

[d]Prof. W. Clegg, [e]Dr M.R.J. Elsegood (University of Newcastle).

Appendix 1A: Crystal data for $Cr(Ar^F)_2(PMe_3)_2$ [a,b]

$C_{21}H_{22}CrF_{18}P_2$:	730.33
Crystal system:	Monoclinic
Space group:	P2(1)/c
Unit cell dimensions:	a = 10.674(2)Å
	b = 14.493(2)Å
	c = 10.2410(10)Å
	α = 90°
	β = 98.130(10)°
	γ = 90°
	V = 1568.3(4)Å^3
	Z = 2
	D_c = 1.547gcm^{-3}
Final R-value:	0.0468 (wR = 0.1148)

Appendix 1B: Crystal data for $Mo(N^tBu)_2(Ar^F)_2$ [a,b]

$C_{26}H_{22}F_{18}MoN_2$:	800.40
Crystal system:	Monoclinic
Space group:	C2/c
Unit cell dimensions:	a = 18.721(7)Å
	b = 18.622(8)Å
	c = 17.652(6)Å
	α = 90°
	β = 92.66(3)°
	γ = 90°
	V = 6147(4)Å^3
	Z = 8
	D_c = 1.730gcm^{-3}
Final R-value:	0.0438 (wR = 0.1121)

Appendix 1C: Crystal data for $Cr(NAd)_2(Ar^F)_2$[a,c]

$C_{38}H_{34}CrF_{18}N_2$:	912.67
Crystal system:	Triclinic
Space group:	P-1
Unit cell dimensions:	a = 12.099(1)Å
	b = 12.818(1)Å
	c = 14.466(1)Å
	α = 97.57(1)°
	β = 113.49(1)°
	γ = 106.36(1)°
	V = 1896.8(3)Å^3
	Z = 2
	D_c = 1.598gcm^{-3}
Final R-value:	0.0438 (wR = 0.1015)

Appendix 1D: Crystal data for $[Mo(NAr)_2(Ar^F)Cl{\cdot}LiCl(dme)]_2$ [a,b]

$C_{74}H_{84}Cl_4F_{18}Li_2Mo_2N_4O_4$:	1783.00
Crystal system:	Triclinic
Space group:	P(-1)
Unit cell dimensions:	a = 16.127(3)Å
	b = 18.186(4)Å
	c = 18.347(4)Å
	α = 118.80(3)°
	β = 104.26(3)°
	γ = 92.78(3)°
	V = 4481(2)Å^3
	Z = 2
	D_c = 1.322gcm^{-3}
Final R-value:	0.0812 (wR = 0.2046)

Appendix 1E: Crystal data for $V(Ar^F)_2Cl(thf)$ [d,e]

$C_{22}H_{12}ClF_{18}OV$:	720.21
Crystal system:	Monoclinic
Space group:	$P2_1/c$
Unit cell dimensions:	a = 16.531(2)Å
	b = 8.8360(10)Å
	c = 17.711(2)Å
	α = 90°
	β = 102.424(3)°
	γ = 90°
	V = 2526.5(5)Å^3
	Z = 4
	D_c = 1.895gcm^{-3}
Final R-value:	0.0553 (wR = 0.1014)

One CF_3 group is disordered with 73(3)% occupancy F(13),F(14),F(15) and 27(3)% F(13A),F(14A),F(15A).

Appendix 1F: Crystal data for $V(Ar^F)_3$-O-$Li(thf)_3$ [d,e]

$C_{39}H_{30}F_{27}LiO_4V$:	1133.51
Crystal system:	Trigonal
Space group:	P3c1
Unit cell dimensions:	a = 15.4005(14)Å
	b = 15.4005(14)Å
	c = 22.559(5)Å
	α = 90°
	β = 90°
	γ = 120°
	V = 4633.6(12)Å^3
	Z = 4
	D_c = 1.625gcm^{-3}
Final R-value:	0.0574 (wR = 0.1413)

V, O(1) and Li are on special positions along the three fold axis.

The *para*-CF_3 group is disordered with 53(2)% occupancy F(4a),F(5a),F(6a) and 47(2)% F(4B),F(5B),F(6B).

Appendix 1G: Crystal data for $Cr(N^tBu)_2(Ar^F)_2$ [a,b]

$C_{26}H_{22}F_{18}CrN_2$:	756.46
Crystal system:	Monoclinic
Space group:	P2(1)/n
Unit cell dimensions:	a = 12.760(5)Å
	b = 9.451(7)Å
	c = 25.330(8)Å
	α = 90°
	β = 99.10(3)°
	γ = 90°
	V = 3016.2(11)Å^3
	Z = 4
	D_c = 1.666gcm^{-3}
Final R-value:	0.0883 (wR = 0.2279)

Appendix 1H: Bond lengths (Å) and angles (°) for $Cr(N^tBu)_2(Ar^F)_2$

Cr(1)-N(1)	1.609(10)	Cr(1)-N(2)	1.617(10)
Cr(1)-C(11)	2.148(12)	Cr(1)-C(21)	2.126(11)
Cr(1)-F(121)	2.415(7)	Cr(1)-F(221)	2.464(7)
N(1)-C(1N)	1.49(2)	N(2)-C(2N)	1.46(2)
C(11)-C(12)	1.41(2)	C(12)-C(13)	1.41(2)
C(13)-C(14)	1.36(2)	C(14)-C(15)	1.39(2)
C(15)-C(16)	1.42(2)	C(16)-C(11)	1.38(2)
C(12)-C(12A)	1.46(2)	C(14)-C(14A)	1.50(2)
C(16)-C(16A)	1.50(2)	C(12A)-F(121)	1.39(2)
C(12A)-F(122)	1.33(2)	C(12A)-F(123)	1.32(2)
C(14A)-F(141)	1.30(2)	C(14A)-F(142)	1.28(2)
C(14A)-F(143)	1.30(2)	C(16A)-F(161)	1.346(14)
C(16A)-F(162)	1.356(14)	C(16A)-F(163)	1.316(14)
C(21)-C(22)	1.39(2)	C(22)-C(23)	1.39(2)
C(23)-C(24)	1.38(2)	C(24)-C(25)	1.37(2)
C(25)-C(26)	1.38(2)	C(26)-C(21)	1.42(2)
C(22)-C(22A)	1.54(2)	C(24)-C(24A)	1.49(2)
C(26)-C(26A)	1.52(2)	C(22A)-F(221)	1.32(2)
C(22A)-F(222)	1.32(2)	C(22A)-F(223)	1.34(2)
C(24A)-F(241)	1.35(2)	C(24A)-F(242)	1.30(2)
C(24A)-F(243)	1.30(2)	C(26A)-F(261)	1.342(13)
C(26A)-F(262)	1.332(13)	C(26A)-F(263)	1.351(13)
C(1N)-C(1N1)	1.51(2)	C(1N)-C(1N2)	1.53(2)
C(1N)-C(1N3)	1.58(2)	C(2N)-C(2N1)	1.53(2)
C(2N)-C(2N2)	1.58(2)	C(2N)-C(2N3)	1.56(2)

N(1)-Cr(1)-N(2)	111.9(5)	N(1)-Cr(1)-C(11)	110.3(5)
N(1)-Cr(1)-C(21)	89.8(5)	N(2)-Cr(1)-C(11)	92.6(4)
N(2)-Cr(1)-C(21)	112.0(5)	C(11)-Cr(1)-C(21)	140.1(4)
N(1)-Cr(1)-F(121)	156.1(4)	N(2)-Cr(1)-F(121)	90.9(4)
N(1)-Cr(1)-F(221)	89.2(4)	N(2)-Cr(1)-F(221)	157.7(4)
C(11)-Cr(1)-F(121)	74.3(4)	C(21)-Cr(1)-F(121)	74.4(3)

C(11)-Cr(1)-F(221)	72.7(3)	C(21)-Cr(1)-F(221)	73.6(4)
F(121)-Cr(1)-F(221)	69.4(3)	Cr(1)-N(1)-C(1N)	163.9(9)
Cr(1)-N(2)-C(2N)	155.4(9)	Cr(1)-C(11)-C(12)	113.8(9)
Cr(1)-C(11)-C(16)	130.1(10)	C(12)-C(16)-C(11)	116.1(11)
C(11)-C(12)-C(13)	122.5(11)	C(12)-C(13)-C(14)	117.6(12)
C(13)-C(14)-C(15)	124.1(11)	C(14)-C(15)-C(16)	115.6(12)
C(11)-C(12)-C(12A)	124.2(11)	C(13)-C(12)-C(12A)	113.3(12)
C(13)-C(14)-C(14A)	120.3(14)	C(15)-C(14)-C(14A)	115.5(14)
C(11)-C(16)-C(15)	123.9(12)	C(11)-C(16)-C(16A)	122.4(12)
C(15)-C(16)-C(16A)	113.7(12)	F(121)-C(12A)-F(122)	103.4(11)
F(122)-C(12A)-F(123)	107.3(14)	F(121)-C(12A)-F(123)	105.5(13)
F(141)-C(14A)-F(142)	105(2)	F(142)-C(14A)-F(143)	105.5(14)
F(141)-C(14A)-F(143)	101.8(14)	F(161)-C(16A)-F(162)	105.4(10)
F(162)-C(16A)-F(163)	105.9(11)	F(161)-C(16A)-F(163)	106.6(11)
C(12)-C(12A)-F(121)	110.2(13)	C(12)-C(12A)-F(122)	115.6(14)
C(12)-C(12A)-F(123)	113.9(12)	C(14)-C(14A)-F(141)	113.0(11)
C(14)-C(14A)-F(142)	116.8(14)	C(14)-C(14A)-F(143)	113.8(13)
C(16)-C(16A)-F(161)	113.0(11)	C(16)-C(16A)-F(162)	110.7(10)
C(16)-C(16A)-F(163)	114.6(11)	C(12A)-F(121)-Cr(1)	110.7(8)
C(22)-C(21)-Cr(1)	117.8(9)	C(23)-C(22)-C(21)	124.7(11)
C(21)-C(22)-C(22A)	121.2(11)	C(23)-C(22)-C(22A)	114.0(11)
C(22)-C(23)-C(24)	118.8(12)	C(23)-C(24)-C(25)	120.3(11)
C(23)-C(24)-C(24A)	118.0(13)	C(25)-C(24)-C(24A)	121.6(13)
C(24)-C(25)-C(26)	119.0(12)	C(25)-C(26)-C(21)	123.9(11)
C(25)-C(26)-C(26A)	115.0(11)	C(21)-C(26)-C(26A)	121.0(11)
C(26)-C(21)-Cr(1)	129.0(9)	C(26)-C(21)-C(22)	113.1(10)
F(221)-C(22A)-F(222)	108.0(13)	F(221)-C(22A)-F(223)	107.3(11)
F(222)-C(22A)-F(223)	106.7(12)	C(22)-C(22A)-F(221)	112.3(11)
C(22)-C(22A)-F(222)	111.4(12)	C(22)-C(22A)-F(223)	110.9(12)
F(241)-C(24A)-F(242)	103.6(13)	F(241)-C(24A)-F(243)	106.6(13)
F(242)-C(24A)-F(243)	105.6(13)	C(24)-C(24A)-F(241)	112.4(13)
C(24)-C(24A)-F(242)	113.8(13)	C(24)-C(24A)-F(243)	114.0(13)
F(261)-C(26A)-F(262)	106.0(10)	F(261)-C(26A)-F(263)	106.6(10)
F(262)-C(26A)-F(263)	107.3(9)	C(26)-C(26A)-F(261)	112.1(10)
C(26)-C(26A)-F(262)	113.3(10)	C(26)-C(26A)-F(263)	111.3(10)
C(22A)-F(221)-Cr(1)	113.9(7)	N(1)-C(1N)-C(1N1)	109.7(10)

N(1)-C(1N)-C(1N2)	106.7(10)	N(1)-C(1N)-C(1N3)	109.9(10)
C(1N1)-C(1N)-C(1N2)	111.1(12)	C(1N1)-C(1N)-C(1N3)	110.2(11)
C(1N2)-C(1N)-C(1N3)	101.1(11)	N(2)-C(2N)-C(2N1)	111.4(11)
N(2)-C(2N)-C(2N2)	105.5(10)	N(2)-C(3N)-C(2N3)	109.8(10)
C(2N1)-C(2N)-C(2N2)	109.2(12)	C(2N1)-C(2N)-C(2N3)	111.9(12)
C(2N2)-C(2N)-C(2N3)	108.8(12)		

Appendix 1I: Crystal data for $Mo(N^tBu)_2(PMe_3)(\eta^2\text{-}Ar^FP{=}PAr^F)$ [a,b]

$C_{29}H_{31}F_{18}MoN_2P_3$:	938.41
Crystal system:	Triclinic
Space group:	$P\bar{1}$
Unit cell dimensions:	a = 12.265(6)Å
	b = 12.448(8)Å
	c = 14.760(7)Å
	α = 66.45(4)°
	β = 88.01(4)°
	γ = 66.37(4)°
	V = 1871(2)Å^3
	Z = 2
	D_c = 1.665 gcm^{-3}
Final R-value:	0.0303 (wR = 0.0799)

Appendix 2: Courses Attended

Appendix 2A: First Year Induction Courses: October 1992

The course consists of a series of one hour lectures on the services available in the department.

1. Departmental Safety
2. Safety Matters
3. Electrical Appliances and Infrared Spectroscopy
4. Chromatography and Elemental Analysis
5. Atomic Absorption and Inorganic Analysis
6 Library Facilities
7. Mass Spectroscopy
8. Nuclear Magnetic Resonance
9. Glassblowing Techniques

Appendix 2B: Examined Lecture Courses: October 1992 - April 1993

Three courses were attended consisting of 6 one hour lectures followed by a written examination in each.

" Synthetic Methodology in Organometallic and Coordination Chemistry" , 3 lectures Prof V.C. Gibson and 3 lectures Prof D. Parker.

"Diffraction Techniques" 4 lectures Prof J.A.K. Howard and 2 lectures Prof R.W. Richards.

"Crystallography" 6 lectures Prof J.A.K. Howard.

Appendix 3. Colloquia, Lectures and Seminars Organised by the Department of Chemistry 1992 - 1995

(* - Indicates Colloquia attended by the author).

1992

*October 15	Dr. M. Glazer & Dr. S. Tarling, Oxford University & Birkbeck College, London *It Pays to be British! - The Chemist's Role as an Expert Witness in Patent Litigation*
*October 20	Dr. H.E. Bryndza, Du Pont Central Research *Synthesis, Reactions and Thermochemistry of Metal (Alkyl) Cyanide Complexes and Their Impact on Olefin Hydrocyanation Catalysis*
*October 22	Prof. A. Davies, University College, London *The Ingold-Albert Lecture: The Behaviour of Hydrogen as a Pseudometal*
*October 28	Dr. J.K. Cockcroft, University of Durham *Recent Developments in Powder Diffraction*
*October 29	Dr. J. Emsley, Imperial College, London *The Shocking History of Phosphorus*
*November 4	Dr. T.P. Kee, University of Leeds *Synthesis and Coordination Chemistry of Silylated Phosphites*
*November 5	Dr. C.J. Ludman, University of Durham *Explosions, A Demonstration Lecture*
November 11	Prof. D. Robins, Glasgow University *Pyrrolizidine Alkaloids: Biological Activity, Biosynthesis and Benefits*
November 12	Prof. M.R. Truter, University College, London *Luck and Logic in Host-Guest Chemistry*
*November 18	Dr. R. Nix, Queen Mary College, London *Characterisation of Heterogeneous Catalysts*
November 25	Prof. Y. Vallee, University of Caen *Reactive Thiocarbonyl Compounds*
*November 25	Prof. L.D. Quin, University of Massachusetts, Amherst *Fragmentation of Phosphorus Heterocycles as a Route to Phosphoryl Species with Uncommon Bonding*

November 26 Dr. D. Humber, Glaxo, Greenford
AIDS - The Development of a Novel Series of Inhibitors of HIV

*December 2 Prof. A.F. Hegarty, University College, Dublin
Highly Reactive Enols Stabilised by Steric Protection

December 2 Dr. R.A. Aitken, University of St. Andrews
The Versatile Cycloaddition Chemistry of $Bu_3P.CS_2$

*December 3 Prof. P. Edwards, Birmingham University
The SCI Lecture: What is Metal?

December 9 Dr. A.N. Burgess, ICI Runcorn
The Structure of Perfluorinated Ionomer Membranes

1993

January 20 Dr. D.C. Clary, University of Cambridge
Energy Flow in Chemical Reactions

January 21 Prof. L. Hall, Cambridge
NMR - Window to the Human Body

January 27 Dr. W. Kerr, University of Strathclyde
Development of the Pauson-Khand Annulation Reaction: Organocobalt Mediated Synthesis of Natural and Unnatural Products

*January 28 Prof. J. Mann, University of Reading
Murder, Magic and Medicine

February 3 Prof. S.M. Roberts, University of Exeter
Enzymes in Organic Synthesis

February 10 Dr. D. Gillies, University of Surrey
NMR and Molecular Motion in Solution

*February 11 Prof. S. Knox, Bristol University
The Tilden lecture: Organic Chemistry at Polynuclear Metal Centres

February 17 Dr. R. W. Kemmitt, University of Leicester
Oxotrimethylenemethane Metal Complexes

February 18 Dr. I. Fraser, ICI Wilton
Reactive Processing of Composite Materials

February 22 Prof. D.M. Grant, University of Utah
Single Crystals, Molecular Structure and Chemical-Shift Anisotropy

February 24	Prof. C.J.M. Stirling, University of Sheffield *Chemistry on the Flat-Reactivity of Ordered Systems*
*March 10	Dr. P.K. Baker, University College of North Wales, Bangor *Chemistry of Highly Versatile 7-Coordinate Complexes*
*March 11	Dr. R.A.Y. Jones, University of East Anglia *The Chemistry of Wine-Making*
March 17	Dr. R.J.K. Taylor, University of East Anglia *Adventures in Natural Product Synthesis*
March 24	Prof. I.O. Sutherland, University of Liverpool *Chromogenic Reagents for Cations*
*May 13	Prof. J.A. Pople, Carnegie-Mellon University, Pittsburgh *The Boys-Rahman Lecture: Applications of Molecular Orbital Theory*
*May 21	Prof. L. Weber, University of Bielefeld *Metallo-phospha Alkenes as Synthons in Organometallic Chemistry*
June 1	Prof. J.P. Konopelski, University of California, Santa Cruz *Synthetic Adventures with Enantiomerically Pure Acetals*
*June 2	Prof. F. Ciardelli, University of Pisa *Chiral Discrimination in the Stereospecific Polymerisation of Alpha Olefins*
June 7	Prof. R.S. Stein, University of Massachusetts *Scattering Studies of Crystalline and Liquid Crystalline Polymers*
June 16	Prof. A. K. Covington, University of Newcastle *Use of Ion Selective Electrodes as Detectors in Ion Chromatography*
June 17	Prof. O.F. Nielsen, H.C. Arsted Institute, University of Copenhagen *Low-Frequency IR and Raman Studies of Hydrogen Bonded Liquids*
*September 13	Prof. A.D. Schlüter, Freie Universität Berlin, Germany *Synthesis and Characterisation of Molecular Rods and Ribbons*
September 13	Prof. K.J. Wynne, Office of Naval Research, Washington, USA *Polymer Surface Design for Minimal Adhesion*

*September 14	Prof. J.M. DeSimone, University of North Carolina, Chapel Hill, USA *Homogenous and Heterogenous Polymersiations in Environmentally Responsible Carbon Dioxide*
September 28	Prof. H. Ila, North Eastern University, India *Synthetic Strategies for Cyclopentanoids via OxoKetene Dithiaacetals*
*October 4	Prof. F.J. Feher, University of California at Irvine *Bridging the Gap Between Surfaces and Solution with Sessilquioxanes*
*October 14	Dr. P. Hubberstey, University of Nottingham *Alkali Metals: Alchemist's Nightmare, Biochemist's Puzzle and Technologist's Dream*
*October 20	Dr. P. Quayle, University of Manchester *Aspects of Aqueous ROMP Chemistry*
*October 23	Prof. R. Adams, University of South Carolina *The Chemistry of Metal Carbonyl Cluster Complexes Containing Platinum and Iron, Ruthenium or Osmium and the Development of a Cluster Based Alkyne Hydrogenating Catalyst*
October 27	Dr. R.A.L. Jones, Cavendish Laboratory *Perambulating polymers*
November 10	Prof. M.N.R. Ashfold, University of Bristol *High-Resolution Photofragment Translational Spectroscopy: A New Way to Watch Photodissociation*
November 17	Dr. A. Parker, Laser Support Facility *Applications of Time Resolved Resonance Raman Spectroscopy to Chemical and Biochemical Problems*
*November 24	Dr. P.G. Bruce, University of St. Andrews *Synthesis and Applications of Inorganic Materials*
*November 25	Dr. R.P. Wayne, University of Oxford *The Origin and Evolution of the Atmosphere*
*December 1	Prof M.A. McKervey, Queens University, Belfast *Functionalised Calixarenes*
December 8	Prof. O. Meth-Cohen, Sunderland University *Friedel's Folly Revisited*
December 16	Prof. R.F. Hudson, University of Kent *Close Encounters of the Second Kind*

1994

*January 26	Prof. J. Evans, University of Southampton *Shining Light on Catalysts*
February 2	Dr. A. Masters, University of Manchester *Modelling Water Without Using Pair Potentials*
February 9	Prof. D. Young, University of Sussex *Chemical and Biological Studies on the Coenzyme Tetrahydrofolic Acid*
*February 16	Prof. K.H. Theopold, University of Delaware, USA *Paramagnetic Chromium Alkyls: Synthesis and Reactivity*
*February 23	Prof. P.M. Maitlis, University of Sheffield *Why Rhodium in Homogenous Catalysis*
March 2	Dr. C. Hunter, University of Sheffield *Non Covalent Interactions between Aromatic Molecules*
March 9	Prof. F. Wilkinson, Loughborough University of Technology *Nanosecond and Picosecond Laser Flash Photolysis*
*March 10	Prof. S.V. Ley, University of Cambridge *New Methods for Organic Synthesis*
*March 25	Dr. J. Dilworth, University of Essex *Technetium and Rhenium Compounds with Applications as Imaging Agents*
*April 28	Prof. R.J. Gillespie, McMaster University, Canada *The Molecular Structure of some Metal Fluorides and Oxo Fluorides: Apparent exceptions to the VSEPR model*
May 12	Prof. D.A. Humphreys, McMaster University, Canada *Bringing Knowledge to Life*
*October 5	Prof. N.L. Owen, Brigham Young University, Utah, USA *Determining Molecular Structure - the INADEQUATE NMR way*
*October 19	Prof. N. Bartlett, University of California *Some Aspects of Ag(II) and Ag(III) Chemistry*
*November 2	Dr. P.G. Edwards, University of Wales, Cardiff *The Manipulation of Electronic and Structural Diversity in Metal Complexes - New Ligands*
*November 3	Prof. B.F.G. Johnson, Edinburgh University *Arene - Metal Clusters - DUCS Lecture*

November 9 Dr. J.P.S. Badyal, University of Durham
Chemistry at Surfaces, A Demonstration Lecture

*November 9 Dr. G. Hogarth, University College, London
New Vistas in Metal Imido Chemistry

November 10 Dr. M. Block, Zeneca Pharmaceuticals, Macclesfield
Large Scale manufacture of the Thromboxane Antagonist Synthase Inhibitor ZD 1542

November 16 Prof. M. Page, University of Huddesfield
Four Membered Rings and β-Lactamase

November 23 Dr. J.M.J. Williams, University of Loughborough
New Approaches to Asymmetric Catalysis

December 7 Prof. D. Briggs, ICI and University of Durham
Surface Mass Spectrometry

1995

January 11 Prof. P. Parsons, University of Reading
Applications of Tandem Reactions in Organic Synthesis

January 18 Dr. G. Rumbles, Imperial College, London
Real or Imaginary 3rd Order Non-Linear Optical Materials

January 25 Dr. D.A. Roberts, Zeneca Pharmaceuticals
The Design and Synthesis of Inhibitors of the Renin-Angiotension System

February 1 Dr. T. Cosgrove, Bristol University
Polymers do it at Interfaces

*February 8 Dr. D. O'Hare, Oxford University
Synthesis and Solid State Properties of Poly-, Oligo- and Multidecker Metallocenes

February 22 Prof. E. Schaumann, University of Claustal
Silicon and Sulphur Mediated Ring-Opening Reactions of Epoxide

*March 1 Dr. M. Rosseinsky, Oxford University
Fullerene Intercalation Chemistry

*March 22 Dr. M. Taylor, University of Auckland, New Zealand
Structural Methods in Main Group Chemistry

April 26 Dr. M. Schroder, University of Edinburgh
Redox Active Macrocyclic Complexes: Rings, Stacks and Liquid Crystals

May 3	Prof. E.W. Randall, Queen Mary and Westfield College *New Perspectives in NMR Imaging*
May 4	Prof. A.J. Kresge, University of Toronto *The Ingold Lecture - Reactive Intermediates: Carboxylic Acid Enols and Other Unstable Species*

Appendix 4. Conferences and Symposia Attended

(* denotes poster presentation)

1. "Sixth Firth Symposium"

University of Sheffield, April 1994

2.* The XVIth International Conference of Organometallic Chemistry

University of Sussex, July 1994

3.* The 11th International Symposium on Olefin Metathesis and Related Chemistry (ISOM)

University of Durham, July 1995

Appendix 5. Publications

Transition-metal catalysed metathesis of phosphorus-phosphorus double-bonds

K.B. Dillon, V.C. Gibson and L.J. Sequeira

J. Chem. Soc., Chem. Commun., 1995, 2429

Bis(imido)molybdenum (IV) complexes containing η^2-diphosphene ligands

K.B. Dillon, V.C. Gibson, J.A.K. Howard, L.J. Sequeira and J.W. Yao

In press

Transition-metal complexes containing the σ-bonded 2,4,6-tris(trifluoromethyl) phenyl ligand.

K.B. Dillon, V.C. Gibson, J.A.K. Howard, C. Redshaw, L.J. Sequeira and J.W. Yao

Manuscript in preparation

Monomeric vananium (III) and (IV) complexes containing the 2,4,6-tris(trifluoromethyl) phenyl ligand.

V.C. Gibson, C. Redshaw, L.J. Sequeira, W. Clegg and M.R.J. Elsegood

Manuscript in preparation